Glycomic markers of inflammatory bowel disease and IgA nephropathy

Clerc, F.

Glycomic Markers of Inflammatory Bowel Disease and IgA Nephropathy

Florent Clerc

ISBN 978-94-6534-094-4

The work presented in this thesis was performed at the Center for Proteomics and Metabolomics (CPM), Leiden University Medical Center (LUMC), The Netherlands.

This work was supported by the IBD-BIOM project (FP7 HEALTH Grant No. 305479).

Printing ProefschriftMaken | proefschriftmaken.nl

Glycomic Markers of Inflammatory Bowel Disease and IgA Nephropathy

---

Proefschrift

ter verkrijging van

de graad van doctor aan de Universiteit Leiden,

op gezag van rector magnificus prof.dr. S. de Rijcke,

volgens besluit van het college voor Promoties

te verdedigen op woensdag 9 september 2026

klokke 10:00 uur

door

Florent Clerc

geboren te Genève

in 1988

Promotor

Prof. dr. M. Wuhrer

Co-Promotor

Dr. V. Dotz

Johnson and Johnson Innovative Medicine, Leiden, the Netherlands

Leden promotiecommissie

Prof. dr. C. van Kooten Secretary

Dr. L. R. Ruhaak Member

Prof. dr. S. Pinho Member
Instituto de Investigação e Inovação em Saúde, Porto, Portugal

Dr. Y. Rombouts Member
Institut de Pharmacologie et de Biologie Structurale, Toulouse, France

Table of Contents

Chapter 1

INTRODUCTION

Introduction

1.1. Definition

Glycosylation, a word formed from the Greek *glyco-*, meaning sweet/sugar, *-yl-* meaning "wood/material/from which something is made of", and from the Latin suffix *-ation*, a process, the action of doing something. The process of adding a derivative of sugar (the glycosyl) to something.

1.2. Background

Glycosylation is a post translational modification (PTM) of proteins, lipids or other molecules where a sugar moiety composed of building blocks called carbohydrates, monosaccharides, or glycans, are enzymatically attached to a peptide backbone *i.e.* of a human protein, thus creating a glycoprotein[1]. Glycosylation is not to be confused with glycation, which is a non-enzymatic direct chemical reaction[2]. Glycosylation is the most abundant protein PTM and more than half of the human proteins are glycosylated[3, 4]. The glycan part of a glycoprotein can be composed of only a few monosaccharides and be small in comparison to the size of the naked protein, but it can also be much larger and become a big part of the total mass of the protein in the case where multiple glycans are attached at different places of the molecule[5-7].

Glycosylation can affect the physical properties and biological activities of proteins and has been associated with health and disease[8, 9]. It is also becoming of growing importance for medical diagnosis and biopharmaceutical treatments[10-14].

The research presented in this thesis aims to expand the knowledge about human protein glycosylation in health and disease as the understanding of glycosylation patterns in disease can help elucidate pathological mechanisms and provide new basis for the development of techniques using glycans as biomarkers for early disease detection, stratification of patients and for better targeted medication.

1.3. Monosaccharides

There are seven major types of monosaccharides found in the glycosylation of human proteins: Glucose (Glc), galactose (Gal), mannose (Man), fucose (Fuc), *N*-acetylglucosamine (GlcNAc), *N*-acetylgalactosamine (GalNAc) and *N*-acetylneuraminic acid[15]. Glucoses, galactoses and mannoses are hexose sugars with different stereochemical configuration of the alcohol groups on carbon two and four, while *N*- acetylglucosamine and *N*-acetylgalactosamine are their homologues where an *N*-acetyl group is replacing the alcohol on the second carbon of their respective hexose base, creating an amide bond (**Figure 1**). Fucose is based on a hexose sugar but the alcohol group of the 6th carbon of hexoses is replaced by a hydrogen atom. *N*-Acetylneuraminic acid is a complex sugar with a 9-carbon atom backbone and belongs to the family of sialic acids (SA). Other monosaccharides like xylose are

present in glycan structures of plants while *N*-glycolylneuraminic acid is mostly found in non-human mammals (not shown). Human ancestors were able to produce *N*-glycolylneuraminic acid until a mutation of the gene encoding the CMP-*N*-acetylneuraminic acid hydroxylase occurred[16].

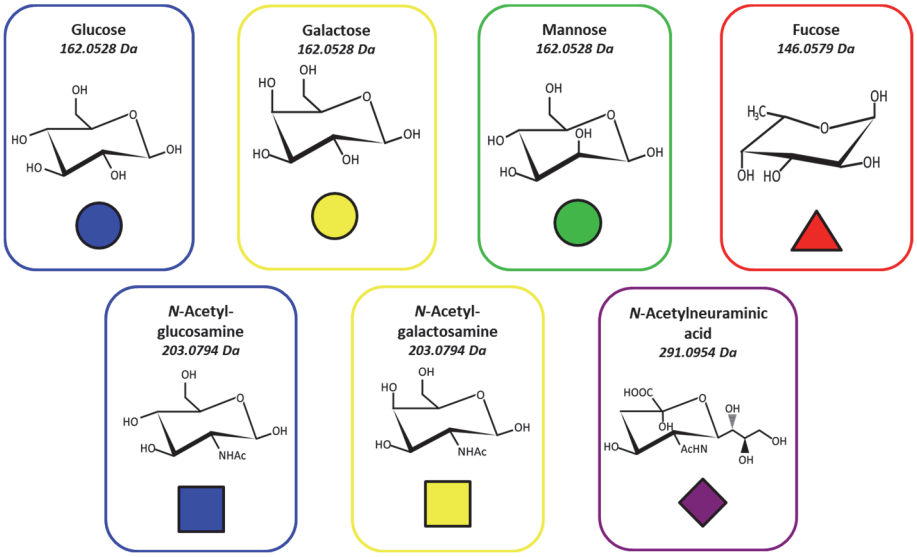

Figure 1: Monosaccharides. *The structure and graphical representation of the monosaccharides presents in human plasma, according to definition by the Consortium of Functional Glycomics*[17]

To simplify the nomenclature of these sugars, they are often referred to with H for hexoses, N for *N*-acetylhexosamines, F for fucoses and S for sialic acids. In this thesis, the sialic acids are sometimes differentiated on the basis of their linkage reflected in differential chemical derivatization are then abbreviated with E and L if they are respectively α2,3- or α2,6- linked[18].

1.4. Biosynthetic pathways

The monosaccharides are used as building blocks and can be added and removed during the synthesis of complex glycan structures by the various enzymes found in the endoplasmic reticulum (ER) and the Golgi apparatus[19, 20]. These carbohydrates are most often arranged in complex branched structures, unlike DNA and amino acids sequences which are built linearly.

This biosynthetic pathway of glycosylation does not follow an exact template but more depends on genetic regulation, on the availability of the nucleotide sugars, the time spent in the endoplasmic reticulum (ER) and in the Golgi apparatus[21]. It also highly depends on the activity of the specific glycosidases and glycosyltransferases responsible for the cutting and transfer of building blocks during the synthesis. This biosynthetic pathway can also be affected by diseases and some environmental factors which will be discussed in a later part of this thesis. By having an extensive knowledge of the synthetic pathway, hypotheses can be formed about the root cause of certain types of defects in glycosylation patterns depending on which step of the trimming or building shows abnormal activity[22, 23].

1.5. *N*-glycosylation

A prevalent type of glycosylation is called "*N*-" glycosylation, because the carbohydrate chain is linked to the amide nitrogen of an Asparagine - abbreviated Asn or "N" - in the amino acid sequence Asparagine-X-Serine/Threonine (Asn-X-Ser/Thr). As exception, the X in this sequence cannot be a Proline (Pro) because of the steric hindering of its sidechain which would block enzymes from getting close enough to the glycosylation site to attach glycans on the neighboring Asparagine. In rare cases, *N*-glycosylation has also been reported in other sequence *i.e.* Asn-X-Cys[24]. With the help of protein sequencing tools, databases and advances in computational biochemistry, it is possible to predict the potential glycosylation sites of a protein[25-28]. These glycosylation sites must also be accessible by being at the surface of the protein, otherwise the glycosyltransferases are not able to reach the suitable location to transfer the precursor oligosaccharide. On the glycan moiety, the glycosylation bond is created on the *N*-acetylglucosamine (GlcNAc) reducing end on carbon one of the precursor oligosaccharide.

The biosynthetic pathway of such branched glycan structures can be divided in three major steps. The first step begins in the endoplasmic reticulum (ER) where a precursor of glycan structure is formed on a lipid donor called dolichol which is a polymeric chain composed of 14 to 21 open isoprene units[29, 30]. At first, the hydrophobic part of the dolichol donor is fixed in the membrane of the ER while the hydrophilic part with the glycan precursor is facing the cytoplasm side of the membrane. Glycosyltransferase enzymes will attach GlcNAc and mannose sugars to the dolichol. When the precursor glycan reaches a size of 7 sugars ($Man_5GlcNAc_2$), the whole precursor flips in the membrane and the glycan part switches to the lumen side of the membrane where additional sugars are added until the complete precursor glycan reaches a size of fourteen sugars ($Glc_3Man_9GlcNAc_2$)[20].

Once the precursor glycan has reached its final size, the second part of the process takes place where the precursor glycan is transferred *en-bloc*, meaning at once, from

the dolichol donor to the glycosylation site of the receiving protein by an oligosaccharyltransferase in the rough ER. The released dolichol donor will then flip back in the membrane where it will be able to start a new cycle[20, 30].

The third part of the glycan synthesis starts when the newly created glycoprotein undergoes folding quality control and migrates from the ER to the Golgi apparatus while a succession of glycosidases (glucosidases and mannosidases) start to trim down the precursor glycan. Additionally, a succession of various glycosyltransferases like GlcNAc transferase I and II, galactosyl transferases and sialyl-transferases start to attach new monosaccharides on the non-reducing termini side of the terminal sugars to build elaborate glycan branches. In some cases, the trimming process will not happen or stay incomplete, leading to what is called oligomannose (M) glycoforms, with the composition of the branched glycan remaining with nine to five mannoses[20].

In humans, there are three *N*-glycan types called high-mannose (M), hybrid (Hy) or of the complex (C) type. They share a common core composed of two successive GlcNAcs, three mannoses and the later composition of the antennas determines the type of glycan category (**Figure 2**). The antennas of high-mannose glycans are composed exclusively of mannoses, complex-type antennas contain GlcNAc, galactoses or sialic acids bound in specific order and hybrid glycans contain a mix of high-mannose and complex antennas. Complex glycans can have up to four antennas. The two branching mannoses are either α1-3- or α1-6-linked to the GlcNAc-linked mannose and give the names to the respective 1-3 arm and 1-6 arm of the glycan. Fucoses can be found in different places on the glycan linked to a GlcNAc either on the antenna or on the first core GlcNAc and are respectively called antenna and core fucoses.

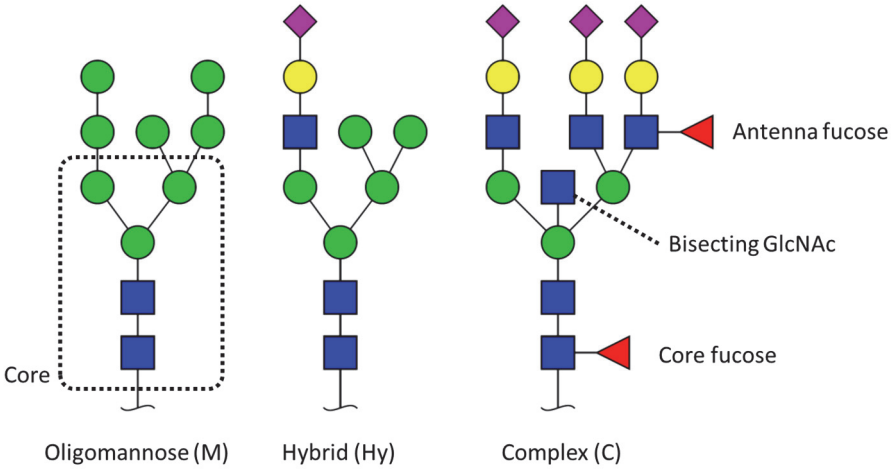

Figure 2: Schematic representation of *N*-glycans types. *The common part to oligomannose-, hybrid- and complex-type glycans called the core is composed of two N-acetylglucosamine (GlcNAc) and three mannoses. Fucoses are differentiated whether they are linked to a GlcNAc in the core of the glycan or on the side of an antenna and are respectively called core and antenna fucoses. In complex type glycans, there is the possibility to have GlcNAc linked β1,4 to the first core mannose which is called bisecting GlcNAc.*

It is not uncommon to have variations of the glycan present, for example when a third GlcNAc is added on the fourth position of the innermost core mannose sugar which is called a bisecting GlcNAc[29].

In other organisms like yeasts including *Saccharomyces cerevisiae*, much bigger structures can be found with elongated hyper mannosylated antennae[31]. Insects also have glycosylated proteins with different fucosylation and elongated structures[32]. Plants also have glycosylation that differs from humans by having a monosaccharide not present in humans, xylose, in the sidechain of some glycan structures[33].

Knowing about glycans biosynthetic pathways can lead to educated hypotheses about the root cause of misformed glycans[22, 23]. For example, observing a high percentage of oligomannose glycoforms with 8 or 9 mannoses on a protein (or in the total plasma *N*-glycome) could indicate a deficiency in the activity or in the genes coding for mannosidases while an elevated percentage of glycoforms with five mannoses could make one think about a lack of activity of the GlcNAc I transferase. Because the building process of the glycan branches happens in a quite ordered sequence, if one specific step fails, the following steps are unlikely to occur. There are also intermediate situations where the trimming of one arm of the precursor is

incomplete while the building of the other arm follows a normal path which leads to hybrid structures.

1.6. *O*-glycosylation

Another type of protein glycosylation present in humans is called "*O*-"glycosylation because the glycans are attached to the -OH residue of amino-acids serine or threonine (Ser/Thr)[34]. The *O*-glycans are generally smaller and of simpler structure (less branching but sometimes elongated repetitive sequences of glycans) compared to the *N*-glycans. The building blocks of the *O*-glycans are the same as in the *N*-glycans, however their biosynthetic pathway differs on multiple points. The *O*-glycosylation doesn't require a specific amino-acid sequence pattern like the *N*-glycans (Asn-X-Ser/Thr) to be possible and the post-translational transfer of the glycan precursor occurs in the Golgi apparatus instead of in the ER for the *N*-glycans. While the start of the *N*-glycosylation process depends on a single oligosaccharyltransferase, *O*-glycosylation on a serine or threonine can be carried out by numerous different enzymes. This multiplicity of enzymes that can be part of the *O*-glycosylation leads to less specificity needs for the glycosylation sites, and the reaction is less likely to be blocked by the steric hindrance of the glycosylation sites than for the *N*-glycans, meaning that *O*-glycans can be added even in parts of the protein that are not directly at its surface. The most common type of O-glycosylation is mucine-type *O*-glycosylation, featuring a GalNAc as the innermost monosaccharide.

O-glycans are built based on core structures like the *N*-glycans and their glycan chains can be elongated with repetitive sequence and can contain fucoses and sialic acids (**Figure 3**). Due to their relatively small size, it is not uncommon to find multiple *O*-glycosylation sites in close vicinity. This close vicinity of the sites complicates the analysis of the specific site's glycosylation and often, only a total glycosylation of a glycopeptide can be determined without the micro-heterogeneity information (cf **§ 1.7**). The relative high content of terminal sialic acids in the *O*-glycans makes that portion of the protein quite hydrophilic and creates charges that can attract water[34].

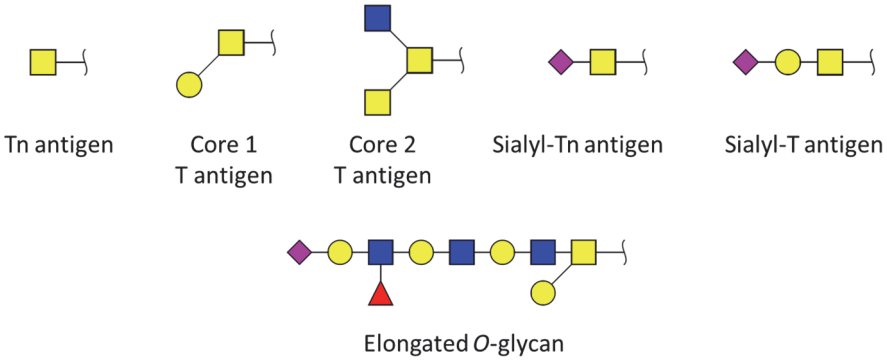

Figure 3: Examples of *O*-glycans cores. *The Tn antigen core O-glycan is composed of one GalNAc, the core 1 (also called T antigen) is composed of one GalNAc and one galactose, the core 2 (T antigen) contains two GalNAc and one GlcNAc, the sialyl-Tn antigen is composed of one sialic acid and one GalNAc and the Sialyl-T antigen is a core 1 with an additional sialic acid.*

One of the most well known biological effect of *O*-glycosylation in human immune response is the different type of blood types (A,B, AB, O and others) where different *O*-glycans are present at the surface of red blood cells (RBC) **Figure 4**. The immune response between the donor's blood and the acceptor's plasma antibodies during the transfusion will depend on the antigens present at the surface of their RBCs[35]. A mismatch of blood compatibility between the donor and acceptor can have fatal outcomes and the discovery of the compatibility matrix between blood types for transfusion is probably the first personalized treatment involving glycosylation.

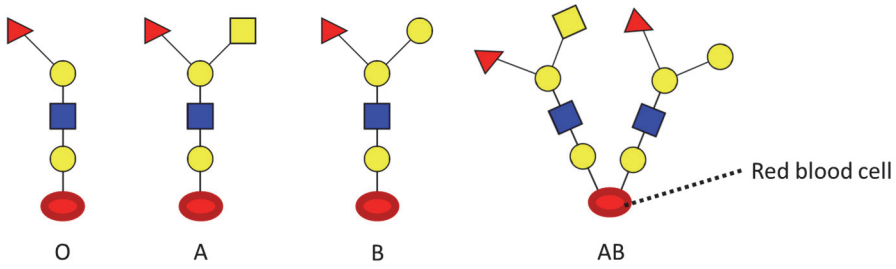

Figure 4: Example of blood type and *O*-glycan structures. *The different O-glycan structures of the blood types A, B, AB and O are linked to the surface of red blood cells.*

Like mammalians, insects have GalNAc *O*-glycans linked to serine and threonine. Plants also possess GalNAc *O*-glycans on threonine and serine residues. These *O*-glycan structures are abundantly found in the cell walls and contain arabinose or

galactose residues attached to hydroxyproline. Yeasts often contain mannose-based *O*-glycosylation.

In humans, O-glycosylation is highly abundant in large mucus proteins known as mucins. Mucins are widespread at the surface of body parts and secreted body fluids that are exposed to the environment like the digestive system, in the lungs and in genital organs. These proteins are found in many body fluids and are of interest for targeted analysis because of their readily availability and presence on body surfaces that can be damaged by diseases. The affinity for water created by the presence of the negatively charged sialic acids in mucins confers them their viscous and sticky aspect and helps them stay at the surface e.g. of the intestinal tract. The stickiness of the mucus is a first barrier against microbes that either get physically trapped in it or that are recognized by the antibodies in the mucus layer as part of the immune response mechanism.

Overall, *O*-glycosylation has received less research attention than *N*-glycosylation, primarily due to analytical challenges such as the complex prediction of glycosylation sites resulting from diverse initiating enzymes, the presence of clustered *O*-glycosylation sites on large and difficult-to-digest peptides, and the lack of efficient enzymatic labelling or release methods. However, recent advances in glycoproteomic platforms and analytical technologies now allow the simultaneous characterization of both *O*- and *N*-glycosylation within a single workflow, renewing scientific interest in the analysis of *O*-glycans in large patient groups[36, 37].

1.7. Macro- and micro-heterogeneity

In both *N*- and *O*-glycosylation, when a protein contains one or several potential glycosylation sites predicted from its amino acid sequence, the extent to which these sites are occupied is referred to as macro-heterogeneity. On a site-specific level, the variety of glycan structures that can be attached to this site is called micro-heterogeneity (**Figure 5**).

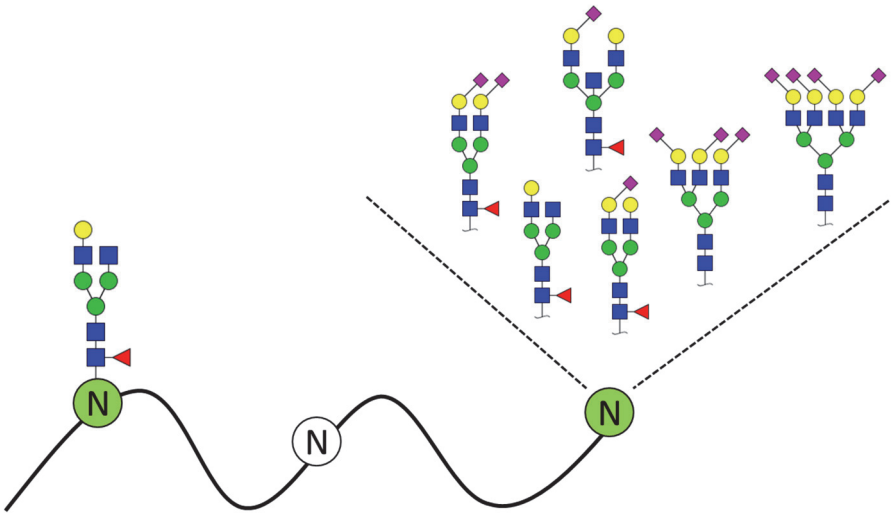

Figure 5: Micro- and Macro-heterogeneity of *N*-glycosylation sites on protein backbone. *The rate of site occupancy, the macroheterogeneity, is represented by the green and white balls for the occupied and respectively unoccupied predicted N-glycosylation sites while the microheterogeneity is represented on the right glycosylation site where different glycans can occupy this site.*

1.8. Biological roles of glycosylation

Glycans can have a great variety of effects on their conjugate. They can influence physical properties such as thermodynamic stability by preventing protein aggregation during thermal stress[38-40]. Glycans may also protect against freezing damage by forming a barrier at ice-nucleation points, thereby isolating them from the surrounding environment[41]. In addition, glycosylation can affect protein folding by promoting disulfide-bond formation, preventing aggregation of unfolded intermediates, and marking misfolded proteins for degradation[42, 43].

Glycans can also influence protein structure by protecting or exposing hydrophobic parts of the protein surface[44, 45], influence their secretion process by modulating their binding with transport proteins[46-48], and also modify the half-life of proteins by protecting them from clearance[40, 49, 50]. Sometimes, the glycosylation has an impact on the protein even before it is released in the circulation by acting as a quality control agent *e.g.* by ensuring proper protein folding during the synthesis and blocking the secretion of malformed proteins and tagging them for elimination[51, 52]. The glycans can also influence the functions of the protein, the recognition with its ligand, a binding site or pathogens[7, 53-55].

Considering all the possible effects of glycosylation on protein properties and interactions with its receptors, it becomes clear that glycans can play a major role in shaping protein behavior in healthy individuals and it is easy to imagine that any deviations from the intended function of one or multiple proteins can lead to severe diseases and/or be affected and may reflect such changes. The knowledge of whether the changes in glycosylation are due to mutations in the genes encoding the proteins and enzymes involved in the synthesis of the glycoproteins or during the refining of the glycans post transfer can give very specific information about the failure mode, and help elucidate unknown disease mechanisms.

1.9. Glycosylation in healthy individuals

In healthy individuals, glycosylation traits have been associated with age, sex and lifestyle. The most common change of glycosylation that has been associated with age is the decrease of terminal galactosylation and sialylation in immunoglobulins such as IgG and an increase in bisecting GlcNAc[56-58]. There are even some researches specialized on individual with exceptional longevity trying to reveal the secret of long life[59]. Glycosylation patterns have also been shown to differ significantly between males and females, for example in the fucosylation of triantennary glycans. In addition, interactions between age and sex have been reported, with certain glycosylation changes occurring exclusively in females and coinciding with hormone-related transitions such as menopause[60].

There is a high variability in the glycosylation of healthy individuals and there is a genetic and hereditary component to human glycosylation which has been demonstrated by analyzing the plasma of isolated populations, for example living on islands[61]. Certain protein polymorphisms, e.g. in haptoglobin, have been shown to vary across different ethnic groups, and distinct glycosylation patterns have also been observed between these polymorphic forms[3, 62-64]. In healthy individuals, a change in the protein sequence causing an allotype can occur exactly at the position of a glycosylation site, and cause the addition or the deletion of a glycoside, like in the allotype A2M of IgA2, without necessarily causing a disease[65].

Sometime, lifestyle can be traceable by its effect on the glycosylation. The serotransferrin glycosylation pattern has been reported to be affected by alcohol usage while smoking was also reported to have an effect on protein levels and glycosylation patterns[66-69]. Protein glycosylation has also been associated with medication in healthy individuals, for example with the intake of contraceptive pills[70].

1.10. Glycosylation changes in diseases

It is known that glycosylation significantly influences protein folding, stability, and function, affecting processes like cell-cell interaction, immune response, and molecular recognition. Glycosylation is involved in the quality control of protein folding within the endoplasmic reticulum[71]. Misfolded glycoproteins are often degraded, preventing the accumulation of dysfunctional proteins or other deviations of the intended function. Glycosylation of antibodies influences their efficacy and interactions with immune cells, affecting immune responses and therapeutic antibody design. Glycans are involved in biomolecular interactions, such as those between pathogens and host cells[72]. Glycosylation modulates receptor activity on cell surfaces, impacting signal transduction pathways[73]. This regulation is critical in processes like growth, differentiation, and apoptosis. Glycans mediate cell adhesion processes, crucial for tissue formation and repair, as well as metastasis in cancer biology.

Understanding protein glycosylation helps explain disease pathogenesis. The research reported in this thesis helps researchers understand disease mechanisms and identify new intervention points for early diagnosis and monitoring disease progression. One step further than explaining disease pathogenesis, understanding glycosylation pathways can lead to the development of new therapeutic strategies. For instance, targeting specific glycan structures can modulate immune responses in diseases like cancer and chronic inflammation[74, 75]. In the future, glycomic data will be used to design personalized treatment plans based on individual glycosylation patterns, leading to more effective and tailored therapies with personalized medicine[76].

Glycosylation patterns on viral proteins are key in vaccine design. For example, the efficacy of influenza and HIV vaccines is influenced by glycosylation, affecting antigen recognition by the immune system[77]. Biopharmaceuticals, such as monoclonal antibodies, require specific glycosylation patterns for optimal efficacy and reduced immunogenicity. Ensuring correct glycosylation is vital in biopharmaceutical manufacturing[78]. Understanding protein glycosylation thus provides comprehensive insights into health, disease, and therapeutic development, highlighting its critical role in modern biomedical research.

Considering the complexity of the glycosylation pathway, the number of genes, enzymes and environmental factors that can have an impact on the glycans and the proteins they are bound to, it is likely that at some point, on top of the changes occurring in healthy individuals, something deviates from the intended path and leads to harmful outcomes. As the glycosylation is already varied in healthy individuals due to heredity, sex, age and environmental factors, additional changes

in glycosylation are observed in diseases. Studying these interactions can for example lead to new antimicrobial strategies[79, 80].

Altered glycosylation patterns are associated with various diseases, including cancer, diabetes, and autoimmune disorders. Using glycan profiling in diagnostic tests for various conditions, including liver diseases and congenital disorders of glycosylation, constantly improves diagnostic accuracy and patient care. Mapping glycosylation changes in various diseases leads to the discovery of novel biomarkers, aids in detection and treatment[81].

Certain glycosylation abnormalities can be grouped in two categories called congenital disorders of glycosylation (CDG) I and II[23]. Type I CDGs are caused by malfunctions during the synthesis or transfer of the precursor glycan to its target protein and result in unoccupied glycosylation sites. Type II CDGs are the result of disruptions in the genes, proteins or enzymes involved in the trimming and/or building phase of the glycan already bound to its glycosylation site on the protein. In type II CDGs, the glycosylation sites are occupied by abnormal glycans[23, 82].

Prevalent diseases such as rheumatoid arthritis (RA), diabetes, cancers and other inflammatory diseases have been reported to be associated with changes in glycosylation[83-85]. The most observed changes in glycosylation with diseases are the levels of galactosylation, bisection and fucosylation, the antennarity/branching of *N*-glycans and some recent methods also reported changes in the type of terminal sialic acids linkages. Although not always seen as a disease, aging is also reported to be associated with similar glycosylation changes as inflammation and led to the phenomenon called inflammaging[56]. Changes in glycosylation have also been reported with the menopause transition[60].

In this thesis, the glycosylation changes of the plasma protein are investigated and put into perspective with the theoretical knowledge about the total human glycosylation. Acute phase proteins and immunoglobulins are the proteins impacted the most in the immune response to diseases and inflammation, it is natural that not only their levels but also their glycosylation changes strongly with disease. Immunoglobulin G and A are often found to be the main contributors to the global glycosylation changes, likely due to their high abundance (IgG) and exposure to pathogen due to their presence in many mucosal layers (IgA). While IgG and its glycosylation is already broadly investigated in clinical studies due to its relatively high abundance and its recognized marker of inflammation role, IgA receives less attention, also due to the higher complexity of its analysis. This prompted further investigation of IgA glycosylation in the disease of focus of this thesis (IBD) and in a study where IgA is known to be the pivotal point of the condition in IgA Nephropathy (IgAN) patients.

1.11. Diseases approached in this thesis

1.11.1. Inflammatory bowel diseases (IBD)

The two main diseases of IBD are Crohn's Disease (CD) and Ulcerative Colitis (UC). They are both chronic inflammation of the intestinal tract and are considered autoimmune diseases. IBD is not to be confused with IBS, which stands for irritable bowel syndrome, in which the patients suffer from abdominal pain and abnormal bowel movements. About one percent of the world population is affected by IBD and yet there is no definitive way to cure these diseases[86]. Medication and surgery have beneficial effects for the quality of life of the patients but relapses can occur in many cases[87-89]. The exact causes of IBD are still unknown but several risk factors have been identified[90].

The differential diagnosis of CD and UC is not an easy task as the symptoms are very similar. There is a need to segregate patients suffering from CD or UC as early as possible because the medication and eventual surgical interventions can differ. When IBD onset occurs in young patients, the final diagnosis is often confirmed years after the first medical visit.

One of the differences between the CD and UC is that UC is affecting more localized portions of the intestinal tract while CD can spread in multiple locations (**Figure 6**). Because of this, UC patients can more often undergo successful surgical treatment to remove the inflamed portion of the intestine while CD patients do not benefit as much from such interventions.

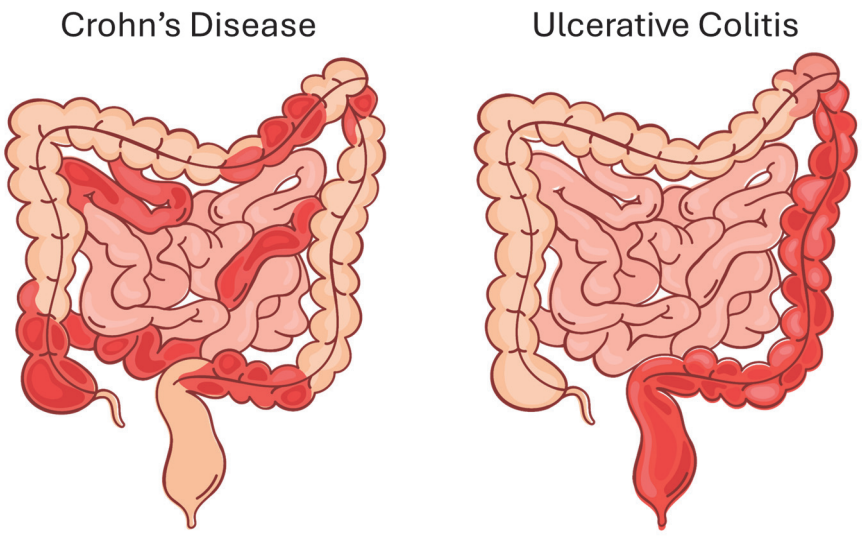

Figure 6: Schematic representation of Crohn's Disease and Ulcerative Colitis [91]**.** *In Crohn's Disease, the inflammation appears in a patchy pattern while in Ulcerative Colitis the inflammation tends to be localized in a single portion of the intestinal tract.*

1.11.2. Glycosylation changes with IBD

Glycosylation has early been identified to play a role in inflammatory bowel disease. Long before mass-spectrometric techniques, lectin based assays have revealed a high content of oligomannose in the colonic mucus UC patients and changes in sialylation, fucosylation, galactosylation and total carbohydrate content in the glycoproteins of both CD and UC patients[92-96].

Advances in derivatization and chromatographic techniques allowed new approaches to the analysis of glycans and helped to remove some of the bias that can be introduced by lectin-based assays. These new techniques also allow distinguishing the protein specific changes *i.e.* subclasses of IgG, and offer more powerful analysis tools to investigate micro- and macro-heterogeneity aspects and linkage specific information of glycoproteins.

Lower galactosylation of IgG is reported to be the strongest glycan marker of inflammation and has widely been associated with UC and CD[97-101]. IgG contributes for the major part of the total plasma protein glycosylation of diantennary glycans and the changes in IgG glycosylation are also visible in non-targeted total plasma glycome analysis[102].

A recent paper[103] on the total serum of IBD patients reports lower galactosylation of diantennary glycans in CD and UC, higher bisection, higher fucosylation of triantennary glycans in IBD and tetraantennary glycans in CD, and was able to associate glycosylation with clinical markers and treatment escalation relating to the findings of this thesis reported in **chapter 3**.

IgA levels, and the glycosylation of its *O*-glycans, mainly the decreased number of N-acetylgalactosamines per hinge glycopeptide, have been reported to be associated with CD with limited clinical diagnostic power[96, 104]. **Chapter 5** of this thesis builds on this and investigates further the changes of IgA glycosylation and reports novel associations in *N*- and *O*-glycosylation in IBD[105].

Several genome studies have found associations between the genes encoding glycosylation and glycosyltransferase enzymes with IBD[106, 107]. Among others, they report alterations in the genes regulating IgG glycosylation or other glycosylation pathways in patients with IBD. Altered *N*-glycosylation of proteins like lower branching and lower overall glycosylation has been associated to elevated T Cell signaling and increased immune response in UC patients[108]. In other proteins such as α1-acid glycoprotein, antitrypsin and haptoglobin, glycosylation changes have been reported and some have been proposed as markers of IBD[109, 110]. Increased branching and increased sialylation of transferrin has been reported in UC patients[111, 112].

In **chapter 3** of this thesis, novel information about the terminal sialic acids of the total plasma *N*-glycome linkage is reported and comes to further increase our knowledge and understanding of IBD mechanisms[3].

1.11.3. IgA Nephropathy

IgA Nephropathy, also known as Berger's disease, is a kidney damaging disease characterized by the deposition of the immunoglobulin A (IgA) antibody in the glomeruli in the kidney[113, 114]. Some patients can live for several years without complications due to the slow progression of the disease. However, once the condition reaches an advanced stage and kidney function deteriorates significantly, patients begin to experience pain and require intensive medical support, such as frequent dialysis sessions or a full kidney transplant.

The exact cause of the disease remains unknown, but it is known that during the immune response, the immune system produces antibodies recognizing abnormally glycosylated IgA. The antibodies bind to galactosyl-deficient IgA (gd-IgA) and this complex forms a deposit in the glomerular mesangium and causes damage and inflammation to the kidney which can progress to total renal failure[115].

Tests like protein in urine and blood in the urine can indicate the first signs of potential kidney malfunction. The main current biomarker to detect IgAN is the measure of Gd-IgA or autoantibodies in kidney tissue biopsies. There is currently no treatment that can prevent IgAN or repair the failing glycosylation process causing the abnormally glycosylated IgA. Like for IBD, there is no permanent cure for nephropathy although some medications exist to mitigate and slow down disease progression by either trying to reduce the production of Gd-IgA or with immunomodulatory treatments to reduce the formation of the immune complexes deposits. Patients can take some medications like angiotensin-converting enzyme to reduce blood pressure or corticosteroids to minimize kidney inflammation but none of these actually treat the disease.

As the disease can go unnoticed during early stages, the possibility to have an easily accessible biomarker becomes of interest for clinicians.

1.11.4. Glycosylation changes with IgA nephropathy

To this day, much less is known about the glycosylation changes in IgA Nephropathy than in other diseases such as RA, diabetes, cancers or even IBD. The primary glycosylation change in IgA Nephropathy is the under-galactosylation of *O*-glycans in the hinge region of IgA1, resulting in the formation of galactose-deficient IgA1(Gd-IgA1) and polymeric IgA complexes which influences the interactions with mesangial cells and inflammatory response[116]. The level of Gd-IgA1 is negatively correlated with the estimated glomerular filtration rate (eGFR) which is an indicator of disease severity[117]. Mice models with gene knockout of galactosyltransferase *b4GalT* have shown kidney lesions similar to human IgAN[118]. Many hypotheses have been made regarding the origin of the galactose deficient IgA and its potential implication in the cascade of immune response and activation of the complement system.

Unlike IgA1 that possesses nine potential sites of glycosylation in its hinge region, IgA2 is not glycosylated in the hinge region and is then believed to not play a major role in the pathology. On average, three to six of the potential *O*-glycosylation sites of IgA1 are occupied with short core-1 glycans (GalNAc-Gal) or Tn antigen (GalNAc) which can have an additional one or two sialic acids.

Several lectin-based assays using HAA or jacalin have identified Gd-IgA to associate with disease severity, however their selective affinity for certain types of terminal glycans can induce bias in the binding of certain glycoforms of IgA, thus not representing the complete picture of IgAN glycosylation changes[119-121]. In **chapter 4** of this thesis, our investigation approach based on capturing affinities for the peptide portion of IgA and analysis of digested glycopeptides by LC-MS remove this bias inherent to HAA and jacalin based assays.

Most of the effect of IgA glycosylation is believed to be due to the changes in the *O*-glycans, but nephropathy also impacts the *N*-glycosylation of IgA1, where elevated oligomannose and sialylated diantennary structures have been reported[122, 123]. There were no reports of changes of IgA2 glycosylation with IgAN, probably due to its tenfold lower abundance in serum and less explored role in inflammation, although it is reported to have a stronger proinflammatory effect than IgA1[124].

In **chapter 4,** glycosylation changes of IgA1 and IgA2 are reported in IgAN patients with a better prediction power for IgAN and glomerular function than the currently available eGFR ELISA techniques.

1.12. Methodology

The study of glycosylation in humans began in the mid-20th century when researchers first recognized that proteins and lipids often carry carbohydrate modifications that are often essential for the biological function[125, 126]. Early methods relied on labor-intensive techniques like paper chromatography and lectin agglutination to detect glycan structures[127]. The development of enzymatic tools, such as glycosidases, allowed for the first structural analyses of *N*- and *O*-linked glycans[128]. Initial studies focused on understanding congenital disorders of glycosylation (CDGs), highlighting the clinical importance of glycan modifications[129]. Mass spectrometry and HPLC technologies, introduced in the 1980s and 1990s, revolutionized glycan analysis by allowing high-resolution profiling[130-132]. Early glycomic studies revealed the diversity and complexity of human glycans, particularly in plasma glycoproteins like immunoglobulins[133]. These foundational works established glycosylation as a critical post-translational modification influencing immunity, development, and disease. The field has since expanded rapidly with advances in analytical techniques and bioinformatics[134-136].

The research presented in this thesis relies on two main analytical workflows. The first one is based on MALDI-TOF-MS for the analysis of plasma-released glycans[102], and the second relies on LC-ESI-MS for the targeted analysis of IgA glycopeptides[105, 137].

For plasma *N*-glycan analysis, a method developed within the research group was applied. This method enhances the robustness of sialic acid analysis in plasma-derived glycans using MALDI-TOF-MS[138]. This approach for the analysis of human plasma glycans released by PNGase F employs a simple and efficient chemical derivatization to stabilize sialic acids in a linkage-specific manner. It also allows for high-throughput analysis, supporting the acquisition of up to 384 samples per MS run, with excellent suitability for automation and large-scale studies[139].

The second major analytical workflow employed in this thesis focuses on the analysis of IgA glycopeptides. In this thesis, IgA antibodies are captured from plasma samples with camelid antibody domains immobilized on agarose beads and protein digestion is performed with TPCK-treated trypsin generating IgA glycopeptides. IgA glycoprotein purification and digestion is performed in 96-well filtration and microtitration plates, and the mass spectrometric analysis is executed by reverse-phase (RP)-LC-ESI-MS with optimized LC-MS conditions by adding low concentrations of trifluoroacetic acid (TFA) to the eluents for the chromatographic separation part, resulting in co-elution of glycopeptides sharing a specific peptide portion, and enabling robust, high-throughput data processing, as described in two chapters of this thesis [105, 137].

Both the optimized sample preparation and data acquisition strategies resulted in large datasets that exceeded the processing capabilities of standard instrument software. To manage this, two in-house developed software were employed for efficient processing of both MALDI-MS and LC-MS data [140, 141]. These tools allowed simultaneous data alignment, calibration, and analyte extraction directly from open-format (LC-)MS data files, supporting the high-throughput nature of the research presented in this thesis.

1.13. Scope of the thesis

This thesis explores the glycomic signatures of two immune-mediated diseases, inflammatory bowel disease and IgA nephropathy. For this, both protein-specific glycosylation and global glycosylation of total plasma and serum proteins are studied from patient cohorts.

Chapter 1 provides some biological and biomedical background on protein glycosylation as well as the diseases studied in this thesis.

Chapter 2, entitled “Human plasma protein *N*-glycosylation” conveys knowledge about the 25 most abundant glycosylated human plasma proteins in health and disease with a review article. The goal of this chapter is to put together the pieces of scattered knowledge of the most abundant plasma glycoproteins and to provide a global representation of human glycosylation in a single picture. To evaluate the pertinence of this theoretically built plasma *N*-glycosylation spectrum, it is compared with some averaged measurements of the total plasma *N*-glycome. When comparing total glycosylation profiles of healthy individuals and patients, this theoretical spectrum can help researchers make informed hypotheses about potential target proteins based on observations of the total plasma glycans.

Chapter 3 of the thesis titled “Plasma *N*-Glycan Signatures Are Associated With Features of Inflammatory Bowel Diseases” is focused on the analysis of the total

plasma *N*-glycosylation (TPNG) in two cohorts of patients with IBD. As the mechanisms of the diseases are still unknown, mapping the glycosylation changes in IBD can help with early detection and to predict patient outcomes. The large-scale robotized sample preparation platform coupled to a MALDI-TOF analyzer proves to be a robust platform to analyze more than 3500 samples and report a multitude of associations of the TPNG with CD and UC and to give new leads for further research on targeted glycoproteins and personalized medication.

In **chapter 4** of this thesis, a new large-scale sample preparation platform coupled with reverse-phase LC-MS detection is used to analyze plasma samples of patients suffering from IgA Nephropathy. In the context of this disease, deficient IgA glycosylation is already recognized and used as biomarker of disease severity, but the previous studies using lectin-based methods for capturing IgA introduce some bias due to the specific affinities of Jacalin and HAA for the glycosylated part of IgA. The newly developed workflow used here captures IgA with affinities for the peptide part of the protein, removing this bias of certain glycoforms, and allows to focus better on the newly reported glycosylation changes and lead to new findings in IgA Nephropathy.

Chapter 5 of this thesis reports the findings of the analysis of captured IgA in a subset of the IBD samples from the discovery cohort described in **chapter 3**, with the same LCMS method as developed in **chapter 4**. This study is the largest study of IgA in the context of IBD and provides new insights into glycosylation changes with the disease.

Chapter 6 of this thesis places the work in a broader perspective and provides some recommendation for further research.

1.14. Notes for reading the thesis

Due to the format of the supplementary information for each respective chapter and the substantial dimensions of the tables, the supplementary material is not suitable for printing in a readable manner. Consequently, the reader is invited to visit the journal websites of each article to access the supplementary material. To facilitate this process, direct links to the online versions of the articles are included at the end of each chapter.

1.15. References

(1) Varki, A. Biological roles of glycans. *Glycobiology* **2017**, *27* (1), 3-49

(2) Taniguchi, N.; Takahashi, M.; Kizuka, Y.; Kitazume, S.; Shuvaev, V. V.; Ookawara, T.; Furuta, A. Glycation vs. glycosylation: a tale of two different chemistries and biology in Alzheimer's disease. *Glycoconjugate J* **2016**, *33* (4), 487-497

(3) Clerc, F.; Reiding, K. R.; Jansen, B. C.; Kammeijer, G. S.; Bondt, A.; Wuhrer, M. Human plasma protein N-glycosylation. *Glycoconj J* **2016**, *33* (3), 309-343

(4) Varki, A.; Cummings, R. D.; Esko, J. D.; Stanley, P.; Hart, G. W.; Aebi, M.; Mohnen, D.; Kinoshita, T.; Packer, N. H.; Prestegard, J. H.; Schnaar, R. L.; Seeberger, P. H. *Essentials of Glycobiology 4th edition*; Cold Spring Harbor Laboratory Press, **2022**. DOI: 10.1101/9781621824213.

(5) Parekh, R. B.; Tse, A.; Dwek, R. A.; Williams, A.; Rademacher, T. W. Tissue-specific N-glycosylation, site-specific oligosaccharide patterns and lentil lectin recognition of rat Thy-1. *The EMBO journal* **1987**, *6* (5), 1233-1244

(6) Haeryfar, S. M.; Hoskin, D. W. Thy-1: more than a mouse pan-T cell marker. *The Journal of Immunology* **2004**, *173* (6), 3581-3588

(7) Harazono, A.; Kawasaki, N.; Kawanishi, T.; Hayakawa, T. Site-specific glycosylation analysis of human apolipoprotein B100 using LC/ESI MS/MS. *Glycobiology* **2005**, *15* (5), 447-462

(8) Varki, A. Biological roles of oligosaccharides: all of the theories are correct. *Glycobiology* **1993**, *3* (2), 97-130

(9) Reily, C.; Stewart, T. J.; Renfrow, M. B.; Novak, J. Glycosylation in health and disease. *Nature Reviews Nephrology* **2019**, *15* (6), 346-366

(10) Holst, S.; Bakar, N. A.; van Scherpenzeel, M.; Wuhrer, M.; Lefeber, D. J. Glycomics as an Innovative Approach for Personalized Medicine. In *Handbook of Biomarkers and Precision Medicine*, Chapman and Hall/CRC, **2019**; pp 394-404.

(11) Dalziel, M.; Crispin, M.; Scanlan, C. N.; Zitzmann, N.; Dwek, R. A. Emerging principles for the therapeutic exploitation of glycosylation. *Science* **2014**, *343* (6166),

(12) Krištić, J.; Lauc, G. Ubiquitous importance of protein glycosylation. In *High-Throughput Glycomics and Glycoproteomics*, Springer, **2017**; pp 1-12.

(13) Solá, R. J.; Griebenow, K. Glycosylation of therapeutic proteins. *BioDrugs* **2010**, *24* (1), 9-21

(14) Dammen-Brower, K.; Epler, P.; Zhu, S.; Bernstein, Z. J.; Stabach, P. R.; Braddock, D. T.; Spangler, J. B.; Yarema, K. J. Strategies for Glycoengineering Therapeutic Proteins. *Front Chem* **2022**, *10*, 863118

(15) Seeberger, P. H. Monosaccharide Diversity. In *Essentials of Glycobiology*, Varki, A., Cummings, R. D., Esko, J. D., Stanley, P., Hart, G. W., Aebi, M., Mohnen, D., Kinoshita, T., Packer, N. H., Prestegard, J. H., et al. Eds.; Cold Spring Harbor Laboratory Press, **2022**; pp 21-32.

(16) Varki, A. Loss of N-glycolylneuraminic acid in humans: mechanisms, consequences, and implications for hominid evolution. *American Journal of Physical Anthropology: The Official Publication of the American Association of Physical Anthropologists* **2001**, *116* (S33), 54-69

(17) Varki, A.; Cummings, R. D.; Aebi, M.; Packer, N. H.; Seeberger, P. H.; Esko, J. D.; Stanley, P.; Hart, G.; Darvill, A.; Kinoshita, T.; Prestegard, J. J.; Schnaar, R. L.; Freeze, H. H.; Marth, J. D.; Bertozzi, C. R.; Etzler, M. E.; Frank, M.; Vliegenthart, J. F.; Lütteke, T.; Perez, S.; Bolton, E.; Rudd, P.; Paulson, J.; Kanehisa, M.; Toukach, P.; Aoki-Kinoshita, K. F.; Dell, A.; Narimatsu, H.; York, W.; Taniguchi, N.; Kornfeld, S. Symbol Nomenclature for Graphical Representations of Glycans. *Glycobiology* **2015**, *25* (12), 1323-1324

(18) Reiding, K. R.; Blank, D.; Kuijper, D. M.; Deelder, A. M.; Wuhrer, M. High-Throughput Profiling of Protein N-Glycosylation by MALDI-TOF-MS Employing Linkage-Specific Sialic Acid Esterification. *Anal Chem* **2014**, *86* (12), 5784-5793

(19) Lebrilla, C. B.; Liu, J.; Widmalm, G.; Prestegard, J. H. Oligosaccharides and Polysaccharides. In *Essentials of Glycobiology*, Varki, A., Cummings, R. D., Esko, J. D., Stanley, P., Hart, G. W., Aebi, M., Mohnen, D., Kinoshita, T., Packer, N. H., Prestegard, J. H., et al. Eds.; Cold Spring Harbor Laboratory Press, **2022**; pp 33-42.

(20) Rini, J. M.; Moremen, K. W.; Davis, B. G.; Esko, J. D. Glycosyltransferases and Glycan-Processing Enzymes. In *Essentials of Glycobiology*, Varki, A., Cummings, R. D., Esko, J. D., Stanley, P., Hart, G. W., Aebi, M., Mohnen, D., Kinoshita, T., Packer, N. H., Prestegard, J. H., et al. Eds.; Cold Spring Harbor Laboratory Press, **2022**; pp 67-78.

(21) Colley, K. J.; Varki, A.; Haltiwanger, R. S.; Kinoshita, T. Cellular Organization of Glycosylation. In *Essentials of Glycobiology*, Varki, A., Cummings, R. D., Esko, J. D., Stanley, P., Hart, G. W., Aebi, M., Mohnen, D., Kinoshita, T., Packer, N. H., Prestegard, J. H., et al. Eds.; Cold Spring Harbor Laboratory Press, **2022**; pp 43-52.

(22) Freeze, H. H. Genetic defects in the human glycome. *Nat Rev Genet* **2006**, *7* (7), 537-551

(23) Lefeber, D. J.; Freeze, H. H.; Steet, R.; Kinoshita, T. Congenital Disorders of Glycosylation. In *Essentials of Glycobiology*, Varki, A., Cummings, R. D., Esko, J. D., Stanley, P., Hart, G. W., Aebi, M., Mohnen, D., Kinoshita, T., Packer, N. H., Prestegard, J. H., et al. Eds.; Cold Spring Harbor Laboratory Press, **2022**; pp 599-614.

(24) Lowenthal, M. S.; Davis, K. S.; Formolo, T.; Kilpatrick, L. E.; Phinney, K. W. Identification of novel N-glycosylation sites at noncanonical protein consensus motifs. *Journal of proteome research* **2016**, *15* (7), 2087-2101

(25) Blom, N.; Sicheritz-Pontén, T.; Gupta, R.; Gammeltoft, S.; Brunak, S. Prediction of post-translational glycosylation and phosphorylation of proteins from the amino acid sequence. *Proteomics* **2004**, *4* (6), 1633-1649

(26) Pugalenthi, G.; Nithya, V.; Chou, K.-C.; Archunan, G. Nglyc: a random forest method for prediction of N-glycosylation sites in eukaryotic protein sequence. *Protein and Peptide Letters* **2020**, *27* (3), 178-186

(27) Pakhrin, S. C.; Pokharel, S.; Aoki-Kinoshita, K. F.; Beck, M. R.; Dam, T. K.; Caragea, D.; Kc, D. B. LMNglyPred: prediction of human N-linked glycosylation sites using embeddings from a pre-trained protein language model. *Glycobiology* **2023**, *33* (5), 411-422

(28) Hou, X.; Wang, Y.; Bu, D.; Wang, Y.; Sun, S. EMNGly: predicting N-linked glycosylation sites using the language models for feature extraction. *Bioinformatics* **2023**, *39* (11), btad650

(29) Stanley, P.; Moremen, K. W.; Lewis, N. E.; Taniguchi, N.; Aebi, M. N-Glycans. In *Essentials of Glycobiology*, Varki, A., Cummings, R. D., Esko, J. D., Stanley, P., Hart, G. W., Aebi, M., Mohnen, D., Kinoshita, T., Packer, N. H., Prestegard, J. H., et al. Eds.; Cold Spring Harbor Laboratory Press, **2022**; pp 103-116.

(30) Freeze, H. H.; Boyce, M.; Zachara, N. E.; Hart, G. W.; Schnaar, R. L. Glycosylation Precursors. In *Essentials of Glycobiology*, Varki, A., Cummings, R. D., Esko, J. D., Stanley, P., Hart, G. W., Aebi, M., Mohnen, D., Kinoshita, T., Packer, N. H., Prestegard, J. H., et al. Eds.; Cold Spring Harbor Laboratory Press, **2022**; pp 53-66.

(31) Routier, F. H.; Doering, T. L.; Cummings, R. D.; Aebi, M. Fungi. In *Essentials of Glycobiology*, Varki, A., Cummings, R. D., Esko, J. D., Stanley, P., Hart, G. W., Aebi, M., Mohnen, D., Kinoshita, T., Packer, N. H., Prestegard, J. H., et al. Eds.; Cold Spring Harbor Laboratory Press, **2022**; pp 307-318.

(32) Ten Hagen, K. G.; Nakato, H.; Tiemeyer, M.; Esko, J. D. Arthropoda. In *Essentials of Glycobiology*, Varki, A., Cummings, R. D., Esko, J. D., Stanley, P., Hart, G. W., Aebi, M., Mohnen, D., Kinoshita, T., Packer, N. H., Prestegard, J. H., et al. Eds.; Cold Spring Harbor Laboratory Press, **2022**; pp 349-364.

(33) O'Neill, M. A.; Darvill, A. G.; Etzler, M. E.; Mohnen, D.; Perez, S.; Mortimer, J. C.; Pauly, M. Viridiplantae and Algae. In *Essentials of Glycobiology*, Varki, A., Cummings, R. D., Esko, J. D., Stanley, P., Hart, G. W., Aebi, M., Mohnen, D., Kinoshita, T., Packer, N. H., Prestegard, J. H., et al. Eds.; Cold Spring Harbor Laboratory Press, **2022**; pp 319-334.

(34) Brockhausen, I.; Wandall, H. H.; Hagen, K. G. T.; Stanley, P. O-GalNAc Glycans. In *Essentials of Glycobiology*, Varki, A., Cummings, R. D., Esko, J. D., Stanley, P., Hart, G. W., Aebi, M., Mohnen, D., Kinoshita, T., Packer, N. H., Prestegard, J. H., et al. Eds.; Cold Spring Harbor Laboratory Press, **2022**; pp 117-128.

(35) Stanley, P.; Wuhrer, M.; Lauc, G.; Stowell, S. R.; Cummings, R. D. Structures Common to Different Glycans. In *Essentials of Glycobiology*, 4th ed.; Varki, A., Cummings, R. D., Esko, J. D., Stanley, P., Hart, G. W., Aebi, M., Mohnen, D., Kinoshita, T., Packer, N. H., Prestegard, J. H., et al. Eds.; Cold Spring Harbor Laboratory Press, **2022**; pp 165-184.

(36) Karlsson, N. G.; Jin, C.; Rojas-Macias, M. A.; Adamczyk, B. Next Generation O-Linked Glycomics. *Trends in Glycoscience and Glycotechnology* **2017**, *29* (166), E35-E46

(37) Momcilovic, A.; de Haan, N.; Hipgrave Ederveen, A. L.; Bondt, A.; Koeleman, C. A. M.; Falck, D.; de Neef, L. A.; Mesker, W. E.; Tollenaar, R.; de Ru, A.; van Veelen, P.; Wuhrer, M.; Dotz, V. Simultaneous Immunoglobulin A and G Glycopeptide Profiling for High-Throughput Applications. *Anal Chem* **2020**, *92* (6), 4518-4526

(38) Wang, C.; Eufemi, M.; Turano, C.; Giartosio, A. Influence of the carbohydrate moiety on the stability of glycoproteins. *Biochemistry-Us* **1996**, *35* (23), 7299-7307

(39) Lu, F.; Ma, Y.; Zang, J.; Qing, M.; Ma, Z.; Chi, Y.; Chi, Y. High-temperature glycosylation modifies the molecular structure of ovalbumin to improve the freeze-thaw stability of its high internal phase emulsion. *International Journal of Biological Macromolecules* **2023**, *233*, 123560

(40) Walther, R.; Zelikin, A. N. Chemical (neo) glycosylation of biological drugs. *Advanced Drug Delivery Reviews* **2021**, *171*, 62-76

(41) Duman, J. G. Animal ice-binding (antifreeze) proteins and glycolipids: an overview with emphasis on physiological function. *Journal of Experimental Biology* **2015**, *218* (12), 1846-1855

(42) Caramelo, J. J.; Parodi, A. J. A sweet code for glycoprotein folding. *Febs Lett* **2015**, *589* (22), 3379-3387

(43) Guay, K. P.; Ke, H.; Canniff, N. P.; George, G. T.; Eyles, S. J.; Mariappan, M.; Contessa, J. N.; Gershenson, A.; Gierasch, L. M.; Hebert, D. N. ER chaperones use a protein folding and quality control glyco-code. *Molecular Cell* **2023**, *83* (24), 4524-4537. e4525

(44) Nagae, M.; Morita-Matsumoto, K.; Arai, S.; Wada, I.; Matsumoto, Y.; Saito, K.; Hashimoto, Y.; Yamaguchi, Y. Structural change of N-glycan exposes hydrophobic surface of human transferrin. *Glycobiology* **2014**,

(45) Ma, B.; Wang, R.; Chen, B.; Liu, W.; Zhou, S.; Li, X.; Gong, J.; Shang, S.; Li, Y.; Xu, D. Insights into the effect of protein glycosylation on carbohydrate substrate binding. *International Journal of Biological Macromolecules* **2023**, *235*, 123833

(46) Delorme, E.; Lorenzini, T.; Giffin, J.; Martin, F.; Jacobsen, F.; Boone, T.; Elliott, S. Role of glycosylation on the secretion and biological activity of erythropoietin. *Biochemistry-Us* **1992**, *31* (41), 9871-9876

(47) Chen, Y.; Hojo, S.; Matsumoto, N.; Yamamoto, K. Regulation of Mac-2BP secretion is mediated by its N-glycan binding to ERGIC-53. *Glycobiology* **2013**, *23* (7), 904-916

(48) Frappaolo, A.; Karimpour-Ghahnavieh, A.; Sechi, S.; Giansanti, M. G. The close relationship between the Golgi trafficking machinery and protein glycosylation. *Cells* **2020**, *9* (12), 2652

(49) Flintegaard, T. V.; Thygesen, P.; Rahbek-Nielsen, H.; Levery, S. B.; Kristensen, C.; Clausen, H.; Bolt, G. N-Glycosylation Increases the Circulatory Half-Life of Human Growth Hormone. *Endocrinology* **2010**, *151* (11), 5326-5336

(50) Chen, B.; Liu, W.; Li, Y.; Ma, B.; Shang, S.; Tan, Z. Impact of N-linked glycosylation on therapeutic proteins. *Molecules* **2022**, *27* (24), 8859

(51) Roth, J.; Zuber, C. Quality control of glycoprotein folding and ERAD: the role of N-glycan handling, EDEM1 and OS-9. *Histochemistry and cell biology* **2017**, *147* (2), 269-284

(52) Wang, Z.; Zhu, J.; Lu, H. Antibody glycosylation: impact on antibody drug characteristics and quality control. *Applied microbiology and biotechnology* **2020**, *104*, 1905-1914

(53) Taniguchi, N. Branched N-glycans and their implications for cell adhesion, signaling and clinical applications for cancer biomarkers and in therapeutics. *Biochemistry and Molecurar Biology Reports* **2011**, *44* (12), 772-781

(54) Lin, B.; Qing, X.; Liao, J.; Zhuo, K. Role of protein glycosylation in host-pathogen interaction. *Cells* **2020**, *9* (4), 1022

(55) Cummings, R. D.; Schnaar, R. L.; Esko, J. D.; Woods, R. J.; Drickamer, K.; Taylor, M. E. Principles of Glycan Recognition. In *Essentials of Glycobiology*, Varki, A., Cummings, R. D., Esko, J. D., Stanley, P., Hart, G. W., Aebi, M., Mohnen, D., Kinoshita, T., Packer, N. H., Prestegard, J. H., et al. Eds.; Cold Spring Harbor Laboratory Press, **2022**; pp 387-402.

(56) Dall'Olio, F.; Vanhooren, V.; Chen, C. C.; Slagboom, P. E.; Wuhrer, M.; Franceschi, C. N-glycomic biomarkers of biological aging and longevity: a link with inflammaging. *Ageing Res Rev* **2013**, *12* (2), 685-698

(57) Dall'Olio, F. Glycobiology of aging. *Biochemistry and Cell Biology of Ageing: Part I Biomedical Science* **2018**, 505-526

(58) Vanhooren, V.; Desmyter, L.; Liu, X. E.; Cardelli, M.; Franceschi, C.; Federico, A.; Libert, C.; Laroy, W.; Dewaele, S.; Contreras, R.; Chen, C. N-glycomic changes in serum proteins during human aging. *Rejuvenation research* **2007**, *10* (4), 521-531a

(59) Ruhaak, L. R.; Uh, H. W.; Beekman, M.; Koeleman, C. A.; Hokke, C. H.; Westendorp, R. G.; Wuhrer, M.; Houwing-Duistermaat, J. J.; Slagboom, P. E.; Deelder,

A. M. Decreased levels of bisecting GlcNAc glycoforms of IgG are associated with human longevity. *Plos One* **2010**, *5* (9), e12566

(60) Deris, H.; Kifer, D.; Cindric, A.; Petrovic, T.; Cvetko, A.; Trbojevic-Akmacic, I.; Kolcic, I.; Polasek, O.; Newson, L.; Spector, T.; Menni, C.; Lauc, G. Immunoglobulin G glycome composition in transition from premenopause to postmenopause. *iScience* **2022**, *25* (3), 103897

(61) Pučić, M.; Knežević, A.; Vidič, J.; Adamczyk, B.; Novokmet, M.; Polašek, O.; Gornik, O.; Šupraha-Goreta, S.; Wormald, M. R.; Redžić, I. High throughput isolation and glycosylation analysis of IgG–variability and heritability of the IgG glycome in three isolated human populations. *Molecular & Cellular Proteomics* **2011**, *10* (10),

(62) Langlois, M. R.; Delanghe, J. R. Biological and clinical significance of haptoglobin polymorphism in humans. *Clin Chem* **1996**, *42* (10), 1589-1600

(63) Zhang, S.; Jiang, K.; Sun, C.; Lu, H.; Liu, Y. Quantitative analysis of site-specific N-glycans on sera haptoglobin β chain in liver diseases. *Acta Bioch Bioph Sin* **2013**, *45* (12), 1021-1029

(64) Pompach, P.; Brnakova, Z.; Sanda, M.; Wu, J.; Edwards, N.; Goldman, R. Site-specific glycoforms of haptoglobin in liver cirrhosis and hepatocellular carcinoma. *Molecular & cellular proteomics : MCP* **2013**, *12* (5), 1281-1293

(65) Torano, A.; Tsuzukida, Y.; Liu, Y. S.; Putnam, F. W. Location and structural significance of the oligosaccharides in human Ig-A1 and IgA2 immunoglobulins. *Proc Natl Acad Sci U S A* **1977**, *74* (6), 2301-2305

(66) Rainio, J.; Ahola, S.; Kangastupa, P.; Kultti, J.; Tuomi, H.; Karhunen, P. J.; Helander, A.; Niemelä, O. Comparison of Ethyl Glucuronide and Carbohydrate-Deficient Transferrin in Different Body Fluids for Post-mortem Identification of Alcohol Use. *Alcohol and Alcoholism* **2014**, *49* (1), 55-59

(67) Gonzalez-Quintela, A.; Alende, R.; Gude, F.; Campos, J.; Rey, J.; Meijide, L. M.; Fernandez-Merino, C.; Vidal, C. Serum levels of immunoglobulins (IgG, IgA, IgM) in a general adult population and their relationship with alcohol consumption, smoking and common metabolic abnormalities. *Clinical and Experimental Immunology* **2008**, *151* (1), 42-50

(68) Knežević, A.; Gornik, O.; Polašek, O.; Pučić, M.; Redžić, I.; Novokmet, M.; Rudd, P. M.; Wright, A. F.; Campbell, H.; Rudan, I. Effects of aging, body mass index, plasma lipid profiles, and smoking on human plasma N-glycans. *Glycobiology* **2010**, *20* (8), 959-969

(69) Tsai, J. S.; Chen, S. C.; Huang, K. C.; Lue, B. H.; Lee, L. T.; Chiu, T. Y.; Chen, C. Y.; Guo, F. R.; Chuang, L. M. Plasma zinc alpha2-glycoprotein levels are elevated in smokers and correlated with metabolic syndrome. *Eur J Clin Invest* **2015**, *45* (5), 452-459

(70) Saldova, R.; Huffman, J. E.; Adamczyk, B.; Mužinić, A.; Kattla, J. J.; Pučić, M.; Novokmet, M.; Abrahams, J. L.; Hayward, C.; Rudan, I.; Wild, S. H.; Wright, A. F.; Polašek, O.; Lauc, G.; Campbell, H.; Wilson, J. F.; Rudd, P. M. Association of Medication with the Human Plasma N-Glycome. *Journal of proteome research* **2012**, *11* (3), 1821-1831

(71) Suzuki, T.; Cummings, R. D.; Aebi, M.; Parodi, A. Glycans in Glycoprotein Quality Control. In *Essentials of Glycobiology*, Varki, A., Cummings, R. D., Esko, J. D., Stanley, P., Hart, G. W., Aebi, M., Mohnen, D., Kinoshita, T., Packer, N. H., Prestegard, J. H., et al. Eds.; Cold Spring Harbor Laboratory Press, **2022**; pp 529-538.

(72) Lewis, A. L.; Szymanski, C. M.; Schnaar, R. L.; Aebi, M. Bacterial and Viral Infections. In *Essentials of Glycobiology*, Varki, A., Cummings, R. D., Esko, J. D., Stanley, P., Hart, G. W., Aebi, M., Mohnen, D., Kinoshita, T., Packer, N. H., Prestegard, J. H., et al. Eds.; Cold Spring Harbor Laboratory Press, **2022**; pp 555-568.

(73) Angulo, J.; Zimmer, J.; Imberty, A.; Prestegard, J. H. Structural Biology of Glycan Recognition. In *Essentials of Glycobiology*, Varki, A., Cummings, R. D., Esko, J. D., Stanley, P., Hart, G. W., Aebi, M., Mohnen, D., Kinoshita, T., Packer, N. H., Prestegard, J. H., et al. Eds.; Cold Spring Harbor Laboratory Press, **2022**; pp 403-418.

(74) Johannssen, T.; Lepenies, B. Glycan-based cell targeting to modulate immune responses. *Trends in Biotechnology* **2017**, *35* (4), 334-346

(75) Dube, D. H.; Bertozzi, C. R. Glycans in cancer and inflammation—potential for therapeutics and diagnostics. *Nature reviews Drug discovery* **2005**, *4* (6), 477-488

(76) Anderluh, M.; Berti, F.; Bzducha-Wróbel, A.; Chiodo, F.; Colombo, C.; Compostella, F.; Durlik, K.; Ferhati, X.; Holmdahl, R.; Jovanovic, D. Emerging glyco-based strategies to steer immune responses. *The FEBS journal* **2021**, *288* (16), 4746-4772

(77) Chang, D.; Zaia, J. Why glycosylation matters in building a better flu vaccine. *Molecular & Cellular Proteomics* **2019**, *18* (12), 2348-2358

(78) Palma, J. A.; Bunyatov, M. I.; Hulbert, S. W.; Jewett, M. C.; DeLisa, M. P. Bacterial glycoengineering: Cell-based and cell-free routes for producing biopharmaceuticals with customized glycosylation. *Current Opinion in Chemical Biology* **2024**, *81*, 102500

(79) Tortorella, A.; Leone, L.; Lombardi, A.; Pizzo, E.; Bosso, A.; Winter, R.; Petraccone, L.; Del Vecchio, P.; Oliva, R. The impact of N-glycosylation on the properties of the antimicrobial peptide LL-III. *Scientific Reports* **2023**, *13* (1), 3733

(80) Bellavita, R.; Braccia, S.; Galdiero, S.; Falanga, A. Glycosylation and lipidation strategies: Approaches for improving antimicrobial peptide efficacy. *Pharmaceuticals* **2023**, *16* (3), 439

(81) Sackstein, R.; Hoffmeister, K. M.; Stowell, S. R.; Kinoshita, T.; Varki, A.; Freeze, H. H. Glycans in Acquired Human Diseases. In *Essentials of Glycobiology*, Varki, A.,

Cummings, R. D., Esko, J. D., Stanley, P., Hart, G. W., Aebi, M., Mohnen, D., Kinoshita, T., Packer, N. H., Prestegard, J. H., et al. Eds.; Cold Spring Harbor Laboratory Press, **2022**; pp 615-630.

(82) Freeze, H. H. Congenital disorders of glycosylation: CDG-I, CDG-II, and beyond. *Current molecular medicine* **2007**, *7* (4), 389-396

(83) Dotz, V.; Wuhrer, M. N-glycome signatures in human plasma: associations with physiology and major diseases. *Febs Lett* **2019**, *593* (21), 2966-2976

(84) Pinho, S. S.; Alves, I.; Gaifem, J.; Rabinovich, G. A. Immune regulatory networks coordinated by glycans and glycan-binding proteins in autoimmunity and infection. *Cell Mol Immunol* **2023**, *20* (10), 1101-1113

(85) Pongracz, T.; Mayboroda, O. A.; Wuhrer, M. The Human Blood N-Glycome: Unraveling Disease Glycosylation Patterns. *JACS Au* **2024**, *4* (5), 1696-1708

(86) Dahlhamer, J. M.; Zammitti, E. P.; Ward, B. W.; Wheaton, A. G.; Croft, J. B. Prevalence of Inflammatory Bowel Disease Among Adults Aged >/=18 Years - United States, 2015. *MMWR Morb Mortal Wkly Rep* **2016**, *65* (42), 1166-1169

(87) Becker, J. M. Surgical therapy for ulcerative colitis and Crohn's disease. *Gastroenterology Clinics* **1999**, *28* (2), 371-390

(88) Bouguen, G.; Peyrin-Biroulet, L. Surgery for adult Crohn's disease: what is the actual risk? *Gut* **2011**, *60* (9), 1178-1181

(89) Gupta, N.; Cohen, S. A.; Bostrom, A. G.; Kirschner, B. S.; Baldassano, R. N.; Winter, H. S.; Ferry, G. D.; Smith, T.; Abramson, O.; Gold, B. D. Risk factors for initial surgery in pediatric patients with Crohn's disease. *Gastroenterology* **2006**, *130* (4), 1069-1077

(90) Ye, B. D.; McGovern, D. P. Genetic variation in IBD: progress, clues to pathogenesis and possible clinical utility. *Expert Rev Clin Immunol* **2016**, *12* (10), 1091-1107

(91) Intestines PNG Designed By FARAWAYKINGDOM from https//pngtree.com

(92) Teague, R.; Fraser, D.; Clamp, J. Changes in monosaccharide content of mucous glycoproteins in ulcerative colitis. *Br Med J* **1973**, *2* (5867), 645-646

(93) Rhodes, J.; Black, R.; Savage, A. Altered lectin binding by colonic epithelial glycoconjugates in ulcerative colitis and Crohn's disease. *Digestive diseases and sciences* **1988**, *33*, 1359-1363

(94) Clamp, J.; Fraser, G.; Read, A. Study of the carbohydrate content of mucus glycoproteins from normal and diseased colons. *Clinical Science (London, England: 1979)* **1981**, *61* (2), 229-234

(95) Jacobs, L. R.; Huber, P. W. Regional distribution and alterations of lectin binding to colorectal mucin in mucosal biopsies from controls and subjects with

inflammatory bowel diseases. *The Journal of clinical investigation* **1985**, *75* (1), 112-118

(96) Hodgson, H.; Jewell, D. Selective IgA deficiency and Crohn's disease: report of two cases. *Gut* **1977**, *18* (8), 644-646

(97) Trbojevic Akmacic, I.; Ventham, N. T.; Theodoratou, E.; Vuckovic, F.; Kennedy, N. A.; Krištic, J.; Nimmo, E. R.; Kalla, R.; Drummond, H.; Štambuk, J.; Dunlop, M. G.; Novokmet, M.; Aulchenko, Y.; Gornik, O.; Campbell, H.; Pucic Bakovic, M.; Satsangi, J.; Lauc, G.; Consortium, I.-B. Inflammatory Bowel Disease Associates with Proinflammatory Potential of the Immunoglobulin G Glycome. *Inflammatory Bowel Diseases* **2015**, *21* (6), 1237-1247

(98) Simurina, M.; de Haan, N.; Vuckovic, F.; Kennedy, N. A.; Stambuk, J.; Falck, D.; Trbojevic-Akmacic, I.; Clerc, F.; Razdorov, G.; Khon, A.; Latiano, A.; D'Inca, R.; Danese, S.; Targan, S.; Landers, C.; Dubinsky, M.; Inflammatory Bowel Disease Biomarkers, C.; McGovern, D. P. B.; Annese, V.; Wuhrer, M.; Lauc, G. Glycosylation of Immunoglobulin G Associates With Clinical Features of Inflammatory Bowel Diseases. *Gastroenterology* **2018**, *154* (5), 1320-1333 e1310

(99) Shinzaki, S.; Iijima, H.; Nakagawa, T.; Egawa, S.; Nakajima, S.; Ishii, S.; Irie, T.; Kakiuchi, Y.; Nishida, T.; Yasumaru, M.; Kanto, T.; Tsujii, M.; Tsuji, S.; Mizushima, T.; Yoshihara, H.; Kondo, A.; Miyoshi, E.; Hayashi, N. IgG oligosaccharide alterations are a novel diagnostic marker for disease activity and the clinical course of inflammatory bowel disease. *Am J Gastroenterol* **2008**, *103* (5), 1173-1181

(100) Miyoshi, E.; Shinzaki, S.; Fujii, H.; Iijima, H.; Kamada, Y.; Takehara, T. Role of aberrant IgG glycosylation in the pathogenesis of inflammatory bowel disease. *PROTEOMICS-Clinical Applications* **2016**, *10* (4), 384-390

(101) Campbell, B. J.; Yu, L.-G.; Rhodes, J. M. Altered glycosylation in inflammatory bowel disease: A possible role in cancer development. *Glycoconjugate J* **2001**, *18* (11), 851-858

(102) Clerc, F.; Novokmet, M.; Dotz, V.; Reiding, K. R.; de Haan, N.; Kammeijer, G. S. M.; Dalebout, H.; Bladergroen, M. R.; Vukovic, F.; Rapp, E.; Consortium, I.-B.; Targan, S. R.; Barron, G.; Manetti, N.; Latiano, A.; McGovern, D. P. B.; Annese, V.; Lauc, G.; Wuhrer, M. Plasma N-Glycan Signatures Are Associated With Features of Inflammatory Bowel Diseases. *Gastroenterology* **2018**, *155* (3), 829-843

(103) Shubhakar, A.; Jansen, B. C.; Adams, A. T.; Reiding, K. R.; Ventham, N. T.; Kalla, R.; Bergemalm, D.; Urbanowicz, P. A.; Gardner, R. A.; IBDBIOMConsortium; Wuhrer, M.; Halfvarson, J.; Satsangi, J.; Fernandes, D. L.; Spencer, D. I. R. Serum N-Glycomic Biomarkers Predict Treatment Escalation in Inflammatory Bowel Disease. *Journal of Crohn's & colitis* **2023**, *17* (6), 919-932

(104) Inoue, T.; Iijima, H.; Tajiri, M.; Shinzaki, S.; Shiraishi, E.; Hiyama, S.; Mukai, A.; Nakajima, S.; Iwatani, H.; Nishida, T.; Mizushima, T.; Yasui, T.; Isaka, Y.; Kanto, T.;

Tsujii, M.; Miyoshi, E.; Wada, Y.; Takehara, T. Deficiency of N-acetylgalactosamine in O-linked oligosaccharides of IgA is a novel biologic marker for Crohn's disease. *Inflamm Bowel Dis* **2012**, *18* (9), 1723-1734

(105) Dotz, V.; Visconti, A.; Lomax-Browne, H.; Clerc, F.; Ederveen, A. H.; Medjeral-Thomas, N.; Cook, H. T.; Pickering, M.; Wuhrer, M.; Falchi, M. O-and N-Glycosylation of Serum Immunoglobulin A is Associated with IgA Nephropathy and Glomerular Function. *Journal of the American Society of Nephrology* **2021**, *32* (10), 2455-2465

(106) Dias, A. M.; Pereira, M. S.; Padrao, N. A.; Alves, I.; Marcos-Pinto, R.; Lago, P.; Pinho, S. S. Glycans as critical regulators of gut immunity in homeostasis and disease. *Cellular Immunology* **2018**, *333*, 9-18

(107) Hanić, M.; Trbojević-Akmačić, I.; Lauc, G. Inflammatory bowel disease-glycomics perspective. *Biochimica et Biophysica Acta (BBA)-General Subjects* **2019**, *1863* (10), 1595-1601

(108) Dias, A. M.; Dourado, J.; Lago, P.; Cabral, J.; Marcos-Pinto, R.; Salgueiro, P.; Almeida, C. R.; Carvalho, S.; Fonseca, S.; Lima, M.; Vilanova, M.; Dinis-Ribeiro, M.; Reis, C. A.; Pinho, S. S. Dysregulation of T cell receptor N-glycosylation: a molecular mechanism involved in ulcerative colitis. *Human molecular genetics* **2014**, *23* (9), 2416-2427

(109) Vermeire, S.; Van Assche, G.; Rutgeerts, P. Laboratory markers in IBD: useful, magic, or unnecessary toys? *Gut* **2006**, *55* (3), 426-431

(110) Liverani, E.; Scaioli, E.; Digby, R. J.; Bellanova, M.; Belluzzi, A. How to predict clinical relapse in inflammatory bowel disease patients. *World journal of gastroenterology* **2016**, *22* (3), 1017-1033

(111) Gornik, O.; Lauc, G. Glycosylation of serum proteins in inflammatory diseases. *Disease markers* **2008**, *25* (4-5), 267-278

(112) Grzymisławski, M.; Derc, K.; Sobieska, M.; Wiktorowicz, K. Microheterogeneity of acute phase proteins in patients with ulcerative colitis. *World Journal of Gastroenterology: WJG* **2006**, *12* (32), 5191

(113) Lai, K. N.; Tang, S. C.; Schena, F. P.; Novak, J.; Tomino, Y.; Fogo, A. B.; Glassock, R. J. IgA nephropathy. *Nature Reviews Disease Primers* **2016**, *2* (1), 1-20

(114) Schena, F. P.; Nistor, I. Epidemiology of IgA Nephropathy: A Global Perspective. *Seminars in Nephrology* **2018**, *38* (5), 435-442

(115) Suzuki, H.; Kiryluk, K.; Novak, J.; Moldoveanu, Z.; Herr, A. B.; Renfrow, M. B.; Wyatt, R. J.; Scolari, F.; Mestecky, J.; Gharavi, A. G.; Julian, B. A. The Pathophysiology of IgA Nephropathy. *Journal of the American Society of Nephrology* **2011**, *22* (10), 1795-1803

(116) Oortwijn, B. D.; Roos, A.; Royle, L.; van Gijlswijk-Janssen, D. J.; Faber-Krol, M. C.; Eijgenraam, J.-W.; Dwek, R. A.; Daha, M. R.; Rudd, P. M.; van Kooten, C.

Differential glycosylation of polymeric and monomeric IgA: a possible role in glomerular inflammation in IgA nephropathy. *Journal of the American Society of Nephrology* **2006**, *17* (12), 3529-3539

(117) Medjeral-Thomas, N. R.; Lomax-Browne, H. J.; Beckwith, H.; Willicombe, M.; McLean, A. G.; Brookes, P.; Pusey, C. D.; Falchi, M.; Cook, H. T.; Pickering, M. C. Circulating complement factor H–related proteins 1 and 5 correlate with disease activity in IgA nephropathy. *Kidney international* **2017**, *92* (4), 942-952

(118) Nishie, T.; Miyaishi, O.; Azuma, H.; Kameyama, A.; Naruse, C.; Hashimoto, N.; Yokoyama, H.; Narimatsu, H.; Wada, T.; Asano, M. Development of immunoglobulin A nephropathy-like disease in β-1, 4-galactosyltransferase-I-deficient mice. *The American journal of pathology* **2007**, *170* (2), 447-456

(119) Tachibana, K.; Nakamura, S.; Wang, H.; Iwasaki, H.; Tachibana, K.; Maebara, K.; Cheng, L.; Hirabayashi, J.; Narimatsu, H. Elucidation of binding specificity of Jacalin toward O-glycosylated peptides: quantitative analysis by frontal affinity chromatography. *Glycobiology* **2006**, *16* (1), 46-53

(120) Moore, J. S.; Kulhavy, R.; Tomana, M.; Moldoveanu, Z.; Suzuki, H.; Brown, R.; Hall, S.; Kilian, M.; Poulsen, K.; Mestecky, J. Reactivities of N-acetylgalactosamine-specific lectins with human IgA1 proteins. *Molecular immunology* **2007**, *44* (10), 2598-2604

(121) Novak, J.; King, R. G.; Yother, J.; Renfrow, M. B.; Green, T. J. O-glycosylation of IgA1 and the pathogenesis of an autoimmune disease IgA nephropathy. *Glycobiology* **2024**, *34* (11),

(122) Linossier, M.-T.; Palle, S.; Berthoux, F. Different glycosylation profile of serum IgA1 in IgA nephropathy according to the glomerular basement membrane thickness: normal versus thin. *American journal of kidney diseases* **2003**, *41* (3), 558-564

(123) Amore, A.; Cirina, P.; Conti, G.; Brusa, P.; Peruzzi, L.; Coppo, R. Glycosylation of circulating IgA in patients with IgA nephropathy modulates proliferation and apoptosis of mesangial cells. *Journal of the American Society of Nephrology* **2001**, *12* (9), 1862-1871

(124) Steffen, U.; Koeleman, C. A.; Sokolova, M. V.; Bang, H.; Kleyer, A.; Rech, J.; Unterweger, H.; Schicht, M.; Garreis, F.; Hahn, J.; Andes, F. T.; Hartmann, F.; Hahn, M.; Mahajan, A.; Paulsen, F.; Hoffmann, M.; Lochnit, G.; Munoz, L. E.; Wuhrer, M.; Falck, D.; Herrmann, M.; Schett, G. IgA subclasses have different effector functions associated with distinct glycosylation profiles. *Nature communications* **2020**, *11* (1), 120

(125) Roberts, E. Effect of glycosylation on the enzymic oxidation and translocation of flavonoids. *Nature* **1960**, *185* (4712), 536-537

(126) Spiro, R. G. Studies on Fetuin, a Glycoprotein of Fetal Serum: I. ISOLATION, CHEMICAL COMPOSITION, AND PHYSIOCOCHEMICAL PROPERTIES. *J Biol Chem* **1960**, *235* (10), 2860-2869

(127) Allen, A. K.; Desai, N. N.; Neuberger, A.; Creeth, J. M. Properties of potato lectin and the nature of its glycoprotein linkages. *Biochem J* **1978**, *171* (3), 665-674

(128) Kornfeld, R.; Kornfeld, S. Assembly of asparagine-linked oligosaccharides. *Annual review of biochemistry* **1985**, *54* (1), 631-664

(129) Jaeken, J.; Matthijs, G. Congenital Disorders of Glycosylation. *Annual Review of Genomics and Human Genetics* **2001**, *2* (Volume 2, 2001), 129-151

(130) Dell, A. F.A.B.-Mass Spectrometry of Carbohydrates. In *Advances in Carbohydrate Chemistry and Biochemistry*, Tipson, R. S., Horton, D. Eds.; Vol. 45; Academic Press, **1987**; pp 19-72.

(131) Parekh, R. B.; Patel, T. P. Comparing the glycosylation patterns of recombinant glycoproteins. *Trends in Biotechnology* **1992**, *10*, 276-280

(132) Spellman, M. W. Carbohydrate characterization of recombinant glycoproteins of pharmaceutical interest. *Anal Chem* **1990**, *62* (17), 1714-1722

(133) Parekh, R. B.; Dwek, R. A.; Sutton, B. J.; Fernandes, D. L.; Leung, A.; Stanworth, D.; Rademacher, T. W.; Mizuochi, T.; Taniguchi, T.; Matsuta, K.; Takeuchi, F.; Nagano, Y.; Miyamoto, T.; Kobata, A. Association of rheumatoid arthritis and primary osteoarthritis with changes in the glycosylation pattern of total serum IgG. *Nature* **1985**, *316* (6027), 452-457

(134) Cao, W. Advancing mass spectrometry–based glycoproteomic software tools for comprehensive site-specific glycoproteome analysis. *Current Opinion in Chemical Biology* **2024**, *80*, 102442

(135) Gao, J.; Chen, H.; Yin, H.; Chen, X.; Yang, Z.; Wang, Y.; Wu, J.; Tian, Y.; Shao, H.; Wen, L.; Zhou, H. Decoding Protein Glycosylation by an Integrative Mass Spectrometry-Based De Novo Sequencing Strategy. *JACS Au* **2025**, *5* (2), 702-713

(136) Lu, J.; Guo, S.; Liu, Q.; Tursumamat, N.; Liu, S.; Wu, S.; Li, H.; Wei, J. Recent advances in analytical methods and bioinformatic tools for quantitative glycomics. *Anal Bioanal Chem* **2025**,

(137) Clerc, F.; Reiding, K. R.; de Haan, N.; Koeleman, C. A. M.; Hipgrave Ederveen, A. L.; Manetti, N.; Consortium, I.-B.; Dotz, V.; Annese, V.; Wuhrer, M. Immunoglobulin A Glycosylation Differs between Crohn's Disease and Ulcerative Colitis. *Journal of proteome research* **2023**, *22* (10), 3213-3224

(138) Reiding, K. R.; Blank, D.; Kuijper, D. M.; Deelder, A. M.; Wuhrer, M. High-throughput profiling of protein N-glycosylation by MALDI-TOF-MS employing linkage-specific sialic acid esterification. *Anal Chem* **2014**, *86* (12), 5784-5793

(139) Bladergroen, M. R.; Reiding, K. R.; Hipgrave Ederveen, A. L.; Vreeker, G. C.; Clerc, F.; Holst, S.; Bondt, A.; Wuhrer, M.; van der Burgt, Y. E. Automation of High-Throughput Mass Spectrometry-Based Plasma N-Glycome Analysis with Linkage-Specific Sialic Acid Esterification. *Journal of proteome research* **2015**, *14* (9), 4080-4086

(140) Jansen, B. C.; Reiding, K. R.; Bondt, A.; Hipgrave Ederveen, A. L.; Palmblad, M.; Falck, D.; Wuhrer, M. MassyTools: A High-Throughput Targeted Data Processing Tool for Relative Quantitation and Quality Control Developed for Glycomic and Glycoproteomic MALDI-MS. *Journal of proteome research* **2015**, *14* (12), 5088-5098

(141) Jansen, B. C.; Falck, D.; de Haan, N.; Hipgrave Ederveen, A. L.; Razdorov, G.; Lauc, G.; Wuhrer, M. LaCyTools: A Targeted Liquid Chromatography-Mass Spectrometry Data Processing Package for Relative Quantitation of Glycopeptides. *Journal of proteome research* **2016**, *15* (7), 2198-2210

Chapter 2

Human Plasma Protein *N*-Glycosylation

Human Plasma Protein *N*-Glycosylation

Florent Clerc[a], Karli R. Reiding[a], Bas C. Jansen[a], Guinevere S.M. Kammeijer[a], Albert Bondt[a,b], Manfred Wuhrer[a,c]

[a]*Center for Proteomics and Metabolomics, Leiden University Medical Center, Leiden, The Netherlands*

[b]*Department of Rheumatology, Leiden University Medical Center, Leiden, The Netherlands*

[c]*Division of BioAnalytical Chemistry, VU University Amsterdam, Amsterdam, The Netherlands*

Correspondence: Manfred Wuhrer, Center for Proteomics and Metabolomics, Leiden University Medical Center, P.O. Box 9600, 2300 RC Leiden, The Netherlands; m.wuhrer@lumc.nl; Tel: +31-71-52-68744

Published in Glycoconjugate Journal, 2016, 33 (3), 309-343

DOI: 10.1007/s10719-015-9626-2

Abstract

Glycosylation is the most abundant and complex protein modification, and can have a profound structural and functional effect on the conjugate. The oligosaccharide fraction is recognized to be involved in multiple biological processes, and to affect proteins physical properties, and has consequentially been labeled a critical quality attribute of biopharmaceuticals. Additionally, due to recent advances in analytical methods and analysis software, glycosylation is targeted in the search for disease biomarkers for early diagnosis and patient stratification. Biofluids such as saliva, serum or plasma are of great use in this regard, as they are easily accessible and can provide relevant glycosylation information. Thus, as the assessment of protein glycosylation is becoming a major element in clinical and biopharmaceutical research, this review aims to convey the current state of knowledge on the *N*-glycosylation of the major plasma glycoproteins alpha-1-acid glycoprotein, alpha-1-antitrypsin, alpha-1B-glycoprotein, alpha-2-HS-glycoprotein, alpha-2-macroglobulin, antithrombin-III, apolipoprotein B-100, apolipoprotein D, apolipoprotein F, beta-2-glycoprotein 1, ceruloplasmin, fibrinogen, immunoglobulin (Ig) A, IgG, IgM, haptoglobin, hemopexin, histidine-rich glycoprotein, kininogen-1, serotransferrin, vitronectin, and zinc-alpha-2-glycoprotein. In addition, the less abundant immunoglobulins D and E are included because of their major relevance in immunology and biopharmaceutical research. Where available, the glycosylation is described in a site-specific manner. In the discussion, we put the glycosylation of individual proteins into perspective and speculate how the individual proteins may contribute to a total plasma *N*-glycosylation profile determined at the released glycan level.

Keywords

N-glycosylation; plasma; glycoproteins; glycoproteomics; immunoglobulins;

Acknowledgments

This work was supported by the European Union Seventh Framework Programme projects HighGlycan (Grant No. 278535) and IBD-BIOM (Grant No. 305479) as well as by the Dutch Arthritis Foundation (RF 13-3-201) and a Zenith grant from The Netherlands Organization for Scientific Research (#93511033). We thank Rosina Plomp for her help with reviewing the IgE section.

Index

Introduction

Protein glycosylation is recognized to be involved in a multitude of biological processes such as receptor interaction, immune response, protein secretion and transport[1-6]. In addition, glycosylation affects protein properties such as solubility, stability and folding[7-10]. A given protein can have multiple sites of glycosylation, and its glycoforms can differ by site occupancy (macroheterogeneity) and occupying glycan structures (microheterogeneity)[11-13]. The biosynthetic pathways leading up to this variety of glycans depend on multiple parameters and can be influenced by many factors including genetic regulation, the availability of nucleotide sugars, the time spent in the endoplasmic reticulum and Golgi apparatus, as well as the accessibility of a particular glycosylation site[10, 14-17].

Protein glycosylation can differ between persons, but is remarkably stable per individual[18]. It is only when the homeostasis of a person changes, by lifestyle or pathological conditions, that the glycosylation will change notably[19]. Large studies comprising thousands of individuals have identified glycosylation to correlate with age, sex and lifestyle[14, 20, 21]. Examples of such changes are the increase in bisection and decrease of galactosylation and sialylation of IgG with age[19, 20, 22-24].

At the same time, specific studies based on smaller sample sets have revealed changes of glycosylation in various diseases, inflammatory states, congenital disorders of glycosylation (CDGs), but also throughout pregnancy where an increase in galactosylation and sialylation, as well as a decrease in bisection was reported[25-28]. In addition, specific glycoforms can be targeted by viruses or bacteria or serve as a pro- or anti-inflammatory signal[29-33]. All of this opens up the possibility to use glycans as an early biomarker for disease or to assist personalized medicine by patient stratification[34, 35].

Recent advances in chromatographic separation, mass spectrometry, robotization and automated data processing allow the rapid analysis of glycosylation, and facilitate the development of novel biomarkers[36-39]. While the glycosylation analysis of an easily obtainable biofluid like plasma can be of considerable interest to a clinical situation, the interpretation of data may be complicated when analyzing a complex protein mixture. For example, when analyzing total plasma *N*-glycosylation (TPNG) of a clinical cohort at the released glycan level, it is not directly apparent whether an observed change originates from a change in relative protein abundance, in the relative glycoforms of a specific protein, or whether it reflects a general regulatory effect influencing the glycosylation of many different glycoproteins. We expect that a better understanding of the glycosylation of individual proteins of human plasma will help to put total plasma *N*-glycomic changes into perspective.

As the previous review on plasma protein *N*-glycosylation originates from 2008[40], we here strive to convey the current state of knowledge on the subject, including a larger number of proteins. The proteins described in this review were selected based on their plasma levels, additionally including the immunoglobulin family due to its major clinical and biopharmaceutical interest. The 24 glycoproteins covered in this review account for approximately 30 mg/mL of the 70-75 mg/mL of the total plasma protein concentration, thus representing most of the human TPNG (albumin is present at levels of 40 mg/mL but is not glycosylated)[41-43].

Furthermore, we tried to limit our review to human plasma and serum but we also reported findings coming from other biological fluids when complementary information could be added. The *N*-glycosylation of the proteins is reported both on a general level and, where available, with site specific information about glycan composition, glycan structure and occupancy. The information is condensed in **Table 1** and a schematic representation of the relative protein contribution to each specific glycan composition is reported in **Figure 1**.

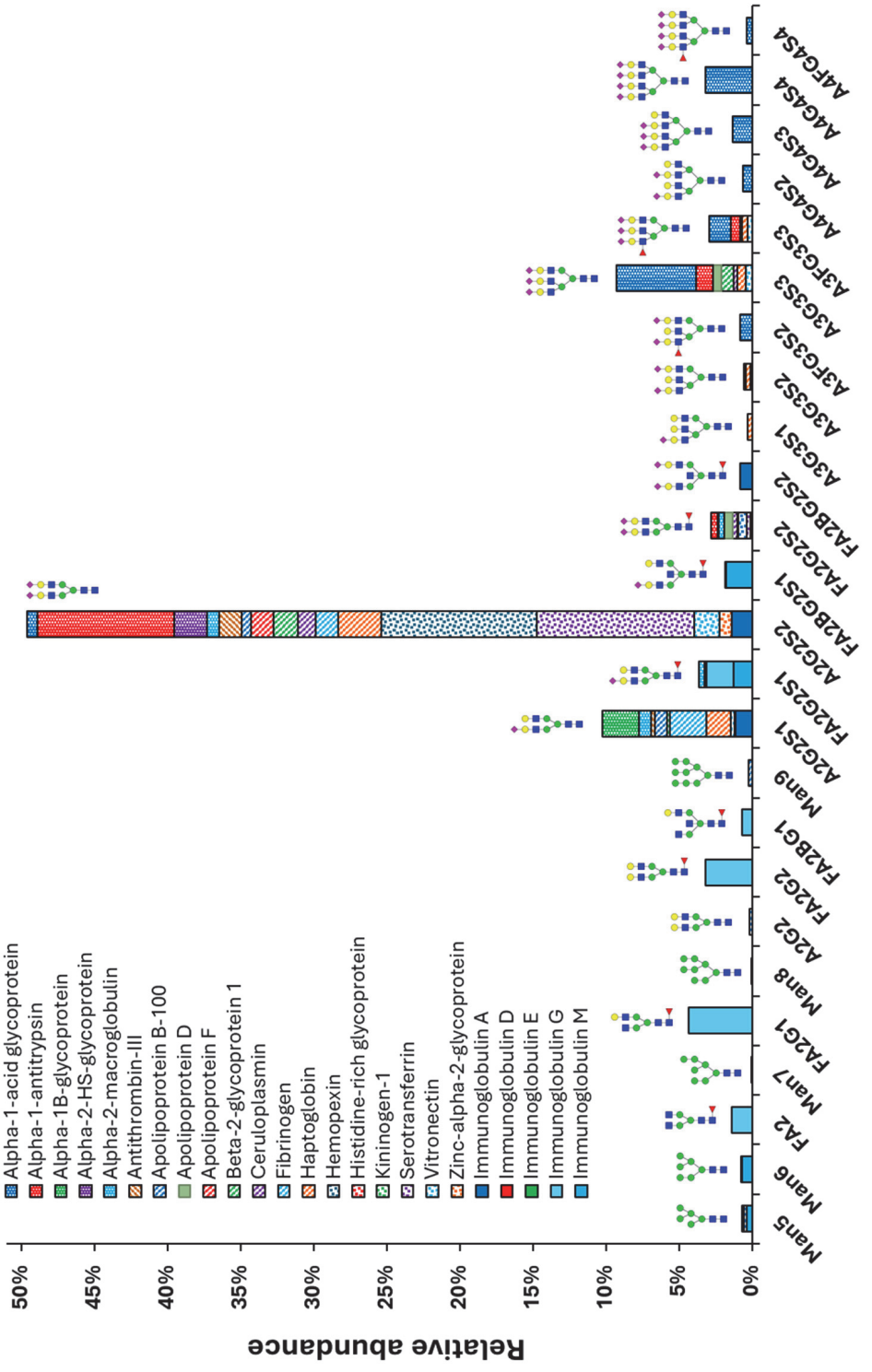
Relative abundance
50%
45%
40%
35%
30%
25%
20%
15%
10%
5%
0%
Alpha-1-acid glycoprotein
Alpha-1-antitrypsin
Alpha-1B-glycoprotein
Alpha-2-HS-glycoprotein
Alpha-2-macroglobulin
Antithrombin-III
Apolipoprotein B-100
Apolipoprotein D
Apolipoprotein F
Beta-2-glycoprotein 1
Ceruloplasmin
Fibrinogen
Haptoglobin
Hemopexin
Histidine-rich glycoprotein
Kininogen-1
Serotransferrin
Vitronectin
Zinc-alpha-2-glycoprotein
Immunoglobulin A
Immunoglobulin D
Immunoglobulin E
Immunoglobulin G
Immunoglobulin M
Man5
Man6
FA2
Man7
FA2G1
Man8
A2G2
FA2G2
FA2BG1
Man9
A2G2S1
FA2G2S1
A2G2S2
FA2BG2S1
FA2G2S2
FA2BG2S2
A3G3S1
A3G3S2
A3FG3S2
A3G3S3
A3FG3S3
A4G4S2
A4G4S3
A4G4S4
A4FG4S4

Figure 1. Schematic representation of the relative protein contribution to each specific glycan composition. *To obtain these numbers, the contribution of a glycan composition to the total glycan pool of a given protein was multiplied by the abundance of that protein as well as the number of glycosylation sites confirmed to be occupied. Protein concentrations were taken from large studies when available and a mean value was calculated from the reported ranges otherwise. The molecular mass used is as reported by SDS-PAGE for the glycoproteins or calculated from the phenotype distribution for haptoglobin. The general Oxford notation was used for naming the glycan structures. For details on the calculation see* ***Supplementary Table 1****.*

Table 1. Overview on plasma protein glycosylation. *(due to the very large size, the table 1 is available as electronic material online at https://pubmed.ncbi.nlm.nih.gov/26555091 and at the end of this chapter. Uniprot number, main role, concentrations, site occupancy and glycan composition of the abundant plasma glycoproteins as reported in the listed literature. The N-glycosylation of the proteins is reported both on a general level and, where available, with site specific information about glycan composition, glycan structure and site occupancy. Protein concentrations were taken from large studies when available and a mean value was calculated from the reported ranges otherwise. The general Oxford notation was used for naming the glycan structures, M for the unassigned high-mannose structures and Hy for hybrid structures. For details on the calculation see* ***Supplementary Table 1.***

Throughout the text, Oxford nomenclature has been used to annotate individual glycan structures or compositions with A giving the number of antennae, F for the fucose (location specific), B for bisecting *N*-acetylglucosamine, G for galactoses and S for sialic acids. The number directly after the letter indicates the quantity of the specific features and the number in parenthesis its linkage. UniProt numbering was used for sequence and site identification.

Alpha-1-acid glycoprotein (P02763; P19652)

Alpha-1-acid glycoprotein (AGP), also known as orosmucoid-1, is a 201 amino acid glycoprotein, which includes an 18 amino acid signal peptide. The molecular weight of the bare protein is 23.5 kDa, but the carbohydrate content leads to observed masses around 41-43 kDa[44]. Two isoforms are found in plasma (AGP1 and AGP2 encoded by *ORM1* and *ORM2* respectively), differing in 22 amino acids[44]. The protein is expressed by the liver and secreted in a monomeric form into the circulation, where it is observed in concentrations between 0.36 mg/mL and 1.46 mg/mL with a mean of 0.77 mg/mL, men having slightly higher levels than women[45, 46]. The concentration of AGP has been reported to increase with age in females but not in

males. Being an acute phase protein, its serum concentration rises in response to inflammatory stimuli, potentially increasing the concentration two- to four-fold[46].

The main functions of AGP are negative acute phase modulation of the complement system and transport of lipophilic compounds, both of these heavily modulated by the glycosylation of the protein[47, 48]. The immunomodulatory function is expected to be via interaction with selectins at a given site of injury (with sialyl-Lewis X as ligand), and inhibiting local complement deposition by charge and receptor competition[48]. As AGP may be used to transport lipophilic and acidic drugs to a site of injury, it is regarded as a good target for therapeutic development[47].

Glycosylation

AGP has five *N*-linked glycosylation sites, namely Asn33, Asn56, Asn72, Asn93 and Asn103. Overall, the glycosylation was determined to mainly consist of fully sialylated tri- and tetraantennary structures, with potential antennary fucosylation in the form of sialyl-Lewis X[44, 49]. Site specific glycosylation was determined by high-performance (HP)liquid chromatography (LC)-electrospray ionization (ESI)-mass spectrometry (MS) and matrix assisted laser desorption/ionization (MALDI)-time-of-flight (TOF)-MS of tryptic glycopeptides [50]. Asn33 mainly contains the triantennary structure A3G3S3 (60%) together with its antennary fucosylated variant A3FG3S3 (20%), as well as some non-complete sialylated glycoforms (A3G3S2, 12.5%). Asn56 contains similar structures (A3G3S3, 55%; A3FG3S3, 12.5%; A3G3S2, 12.5%) and a fraction of diantennary glycans (A2G2S2, 22.5%). Asn72 is occupied by a higher level of antennarity, having, next to its triantennary glycans (A3G3S3, 15%), a number of tetraantennary compositions (A4G4S4, 30%; A4G4S3, 15%; A4G4S2, 10%; A4FG4S3, 5%; A4FG4S4, 5%). A similar situation is seen in on Asn93 (A4G4S4, 22.5%; A4G4S3, 20%; A3G3S3, 17.5%; A4FG4S4, 7.5%; A4FG4S3, 7.5%; A3FG3S3, 7.5%; A4G4S2, 7.5%) and Asn103 (A4G4S4, 45%; A3G3S3, 20%; A4G4S2, 10%; A4G4S3, 7.5%; A3FG3S3, 5%)[49, 50] (**Table 1**).

The glycosylation of AGP changes considerably with varying conditions. For instance, during the early stages of an acute-phase immune response the levels of fucosylated glycans (sialyl-Lewis X) increase significantly[49, 51-53], which continues to increase throughout the acute phase immune response[54]. In rheumatoid arthritis both fucosylation and sialylation have shown to increase significantly[55].

Alpha-1-antitrypsin (P01009)

Alpha-1-antitrypsin (AAT), also known as alpha-1-protease inhibitor, alpha-1-antiproteinase or serpin A1, consists of 418 amino acids (including a 24 amino acid signal peptide) with an apparent mass of 51 kDa (including glycosylation). It is mainly

produced in the liver by hepatocytes, but is also synthesized in monocytes, intestinal epithelial cells, and in the cornea[56-60]. Due to its small size and polar properties, the glycoprotein can easily move into tissue fluids[56]. In healthy individuals, a plasma level of approximately 1.1 mg/mL is found, but the concentration can increase three- to four-fold during inflammation[61-64]. AAT occurs as three different amino acid sequences, of which the first is set as the standard sequence. Form 2 differs in the amino acid sequence 356-418 and form 3 lacks the amino acid sequence 307-418.

AAT inhibits a wide range of serine proteases, protecting tissues from enzymatic attacks[65]. Neutrophil elastase is its prime target, thereby preventing proteolytic destruction of elastase in the tissue of the lower respiratory tract (emphysema)[66]. It has been shown that AAT has anti-inflammatory properties and therefore it could potentially be used as a therapeutic agent for rheumatoid arthritis and type 1 diabetes[67, 68].

Glycosylation

Three *N*-glycosylation sites have been identified on AAT, located at Asn70, Asn107 and Asn271[56, 69, 70]. MALDI-TOF-MS analysis on released glycans revealed mainly di- and triantennary complex type species. Isoelectric focusing furthermore revealed eight different charge isoforms of AAT, of which isoform 4 (M4) and isoform 6 (M6) were the most abundant ones. Of M4, the most pronounced glycans were diantennary disialylated (A2G2S2) and triantennary trisialylated (A3G3S3) with a ratio of 2:1. Isoform M6 was mainly occupied with A2G2S2 structures[71].

LC-MS/MS analysis on tryptic glycopeptides treated with various specific exoglycosidases enabled a precise determination of the glycosylation in a site-specific manner[70]. Asn70 and Asn271 mainly contain diantennary disialylated (A2(2)G2(4)S2(6)) structures (91.3% and 99.3% respectively), while core fucosylation (F(6)A2(2)G2(4)S2(6)) is less abundant (8.6% and 0.7% respectively). Asn107 shows the highest variability of the sites, containing diantennary disialylated species A2(2)G2(4)S2(6), 52.5%, with possible core fucosylation F(6)A2(2)G2(4)S2(6), 1.5%), and 29.5% triantennary trisialylated species A3(2,4,2)G3(4)S3(6,3,6)) with possible antennary fucosylation (A3(2,4,2)F(3)G3(4)S3(6,3,6), 16.7% (**Table 1**). In addition, a small fraction of Asn107 is tetraantennary fully sialylated with potential antennary fucosylation. Interestingly, the diantennary structures contained mainly (α1,6-linked) core-fucosylation, while on triantennary structures the fucose was mainly detected as sialyl-Lewis X on the β1,4-linked *N*-acetylglucosamine of the α1,3-arm[70].

In a non-site-specific study, the glycosylation of AAT has been associated with physiological parameters such as BMI, cholesterol, glucose and insulin level. The same study showed that the changes in glycosylation could be found related to age

and sex[72]. Furthermore, additional AAT isoelectric isoforms were identified in CDG-I (CDG-Ia and CDG-Ic) *i.e.* non-, mono- and diglycosylation across the three sites. A clear pattern could be found for which sites were occupied, as only Asn70 was occupied in the monoglycosylated form, and Asn70 and Asn271 were occupied in the diglycosylated isoform[73].

Alpha-1B-glycoprotein (P04217)

Alpha-1B-glycoprotein (A1BG) is a 474 amino acid polypeptide with an apparent mass of 63 kDa (including glycosylation)[74]. The protein consists of five repetitive domains that show high homology with known immunoglobulin heavy and light chain variable domains, making the protein part of the immunoglobulin superfamily. A1BG is mainly produced in the liver, and is secreted to plasma to levels of approximately 0.22 mg/mL[74, 75]. The overall function of the protein is still unknown, but it has been found to bind cysteine-rich secretory protein 3 (CRISP3)[76], and has been associated with breast, liver, pancreas and bladder cancer, as well as with steroid-resistant nephrotic syndrome[77-81]. In addition, it has recently been proposed as an autoantigen in rheumatoid arthritis[82].

Glycosylation

In A1BG, the *N*-glycosylation consensus motif (Asn-X-Ser/Thr) has been found at four locations Asn44, Asn179, Asn363, and Asn371[74]. The occupancy of these sites has been verified by deglycosylated peptide LC-MS(/MS) and LC-Fourier transform ion cyclotron resonance (FTICR)-MS, but degrees of occupancy remain unknown[83, 84]. In addition, overall or site-specific glycosylation analysis also has not been performed for A1BG as of yet, although one source reports blood derived high-density lipoprotein (HDL)-associated A1BG Asn363 to be (at least) glycosylated with diantennary nonfucosylated monosialylated species[85]. Also, while not necessarily predictive for plasma glycoprotein glycosylation, in cerebrospinal fluid (CSF) Asn44 was shown to contain nonfucosylated di- (96%) and triantennary (4%) structures with at least one sialic acid[86]. Little is known about the changes in glycosylation of A1BG with disease.

Alpha-2-HS-glycoprotein (P02765)

Alpha-2-HS-glycoprotein (A2HSG), also known as fetuin-A, alpha-2-Z-globulin, ba-alpha-2-glycoprotein and alpha-2-Heremans-Schmid-glycoprotein, is a 367 amino acids (18 of signal peptide), 51-67 kDa glycoprotein[87-89]. It is built up from an A-chain (282 amino acids) and B-chain (27 amino acids) with a linker sequence (40 amino acids)[90, 91]. Originating from the liver, the protein is found at plasma levels of 0.3-0.6 mg/mL[91]. A2HSG acts at several sites and in a wide variety of (patho)physiological

processes in the human system. Prominent functions include the scavenging of phosphate and free calcium, thereby preventing calcification, as well as binding and protecting matrix metalloproteases. In addition, the protein is known to bind the insulin receptor[92-95].

Increased levels of A2HSG are associated with obesity and type 2 diabetes mellitus[96]. On the other hand, decreased levels of A2HSG are found to cause several negative growth effects[92]. Furthermore, the protein has shown to protect a fetus from the maternal immune system by inhibition of tumor necrosis factor[93, 97]

Glycosylation

The A-chain of A2HSG contains two *N*-glycosylation sites at Asn156 and Asn176, as well as two *O*-glycosylation sites at Thr256 and Thr270[88]. The B-chain contains one core 1 *O*-glycan on Ser346, and no *N*-glycans[89]. Exoglycosidase treatment has reported 6.2 sialic acids to be present per A2HSG molecule, of which 2.5 are α2,3-linked and 3.7 are α2,6-linked[98]. Sequentially, four galactoses in β1,4-linkage were released from *N*-acetylglucosamines, pointing towards two diantennary *N*-glycans in addition to the *O*-glycosylation[98]. LC-ESI-MS experiments have confirmed these findings, reporting around 96% A2G2S2 glycosylation to be present on A2HSG[99]. Furthermore, low levels of fucosylated glycans were observed, at least on Asn156[99, 100].

Differential abundance of Asn156 glycopeptides has been shown in pancreatic cancer and pancreatitis, with increased levels of fully sialylated triantennary glycans with or without fucose, and a decrease in the A2G2S2 structure in pancreatitis[101].

Alpha-2-macroglobulin (P01023)

Alpha-2-macroglobulin (alpha2M), also known as C3 or PZP-like alpha-2-macroglobulin domain-containing protein 5, is a 1474 amino acid (23 amino acid signal peptide) 720 kDa (glycosylated) glycoprotein consisting of four similar 180 kDa subunits (160 kDa without glycosylation) which are linked by disulfide bridges[102]. It is produced by the liver and present at plasma levels of approximately 1.2 mg/mL[103]. The main function of alpha2M is to bait and trap proteinases[102]. To do this, the protein contains a bait peptide sequence known to interact with many common plasma proteases such as trypsin, chymotrypsin, and various others in the complement system. Upon proteolysis, a conformation change in alpha2M traps the causative protease and the complex is subsequently cleared from the plasma[104-106].

Glycosylation

Eight *N*-glycosylation sites have been identified on each alpha2M subunit at Asn55, Asn70, Asn247, Asn396, Asn410, Asn869, Asn991 and Asn1424[83, 84, 100, 102, 107, 108]. The total pool of alpha2M-derived glycans was analyzed by LC-fluorescence with exoglycosidase digestion. This revealed a high abundance of diantennary structures, both non-fucosylated (55%) and core-fucosylated (30%), which are mainly mono- and disialylated (A2G2S2, A2G2S1, FA2G2S2, FA2G2S2)[109]. In addition, Man5-7 type structures was detected as well (8%) as species with a lower degree of galactosylation and sialylation. Low levels of triantennary structures have also been identified [109].

Interestingly, the high-mannose type glycans have been shown to specifically occur at Asn869 with a relative abundance of approximately 70%, the other 30% being FA1G1S1[109]. This high-mannose type glycosylation is likely the mean by which alpha2M interacts with mannose-binding lectin (MBL) to target proteases present on the surface of invading microorganisms[109]. The Asn869 occupancy ratio suggests that each alpha2M tetramer contains three oligomannose glycosylated Asn869 sites and one FA1G1S1, although this is speculative[109]. The other *N*-glycosylation sites mainly contain complex type glycans and glycoproteomic analysis suggests that the core-fucosylated species are present to at least some degree at specific sites Asn55 and Asn1424[100].

Changes in the glycosylation of alpha2M have been associated with autoimmune diseases and cancer. Site occupancy in particular has been linked with systemic lupus erythematosus, while a compositional change has been described in multiple sclerosis[110, 111].

Antithrombin-III (P01008)

Antithrombin-III (AT-III, generally referred to as antithrombin), encoded by the *SERPINC1* gene, is a single chain 464 amino acid (32 of signal peptide) protein of approximately 58 kDa, of which 17% are carbohydrates[112-114]. It is part of the serine protease inhibitor family. The concentration of antithrombin in blood was found to be 0.15 mg/mL[115]. The protein can be found in an α and β form which differ in the number of occupied glycosylation sites and of which α is 10-20 times more abundant [116]. Antithrombin participates in the regulation of blood coagulation by inactivating thrombin, factor IXa, Xa, XIa, XIIa, and other serine proteases [117]. Its function is enhanced by heparin and heparan sulfate [118-120]. Several thrombosis disorders are associated with antithrombin deficiency (ATD), both inherited and acquired. Type I ATD shows reduced concentrations of antithrombin, while type II ATD generally

shows normal concentrations with reduced heparin binding and thus lower functionality[121].

Glycosylation

The sequence of antithrombin shows four potential *N*-glycosylation sites: Asn128, Asn167, Asn187 and Asn224. The α form is fully glycosylated, while the β form is not glycosylated at Asn167[122, 123]. The β form binds heparin more efficiently and thus shows an enhanced anticoagulant effect. Several studies suggest that the Asn-X-Thr motif of Asn128, Asn187 and Asn224 are in general glycosylated more easily than the Asn-X-Ser motif of Asn167[124-126].

The glycans present on AT-III are mainly of the diantennary complex type without core fucose, bearing one (0-30%) or two (70-100%) α2,6-linked sialic acids, as it was established using chemical and enzymatic methods[127, 128]. Using MALDI and LC-ESI-MS these findings have been confirmed in a site-specific manner[116, 120, 129, 130]. β-AT was exclusively decorated with three diantennary fully sialylated structures (A2G2S2, 4.2%), with trace amounts of core fucose on one of the glycan (FA2G2S2, 1.3%). At Asn128 and Asn224 of α-AT, only the A2G2S1 and A2G2S2 structures were identified. At Asn167, occupied only in the α form of AT-III, A3G3S3 has additionally been detected, whereas Asn187 showed the most variability, bearing also a minor amount of fucose (FA2G2S2). Furthermore, at Asn187 some A3G3S2 has been observed. All glycoforms other than A2G2S2 are mentioned to be minor, although no relative or absolute quantification has been performed[116, 120, 129, 130].

A mutation associated with type II antithrombin deficiency (K241E), although not adjacent to a glycosylation consensus sequence, was found to result in decreased heparin binding due to the presence of core fucose[131].

Apolipoprotein B-100 (P04114)

Apolipoprotein (Apo) B-100 is a 550 kDa 4560 amino acid protein (4536 amino acids without the signal peptide, corresponding to a theoretical mass of 513 kDa without glycosylation) found in low density and very low density lipoproteins (LDL and VLDL)[132, 133]. A shorter isoform found in chylomicrons, named Apo B-48, is coded by the same gene, but contains only 48% of Apo B-100 sequence[134, 135]. Apo B-100 is exclusively synthetized by the liver, while Apo B-48 is synthetized in the small intestine[136]. Apo B-100 is found in plasma at concentrations of approximately 0.5 mg/mL (0.88 to 0.97mmol)[34, 61, 137, 138]. The protein has a major role in the assembly of VLDL and lipoproteins, and transports the majority of plasma cholesterol[139-141]. It can be covalently linked to Apo A to form the lipoprotein(a) particle. Apo A itself is a

low abundant plasma glycoprotein possessing one *N*-glycosylation site located at Asn263 (mainly occupied by diantennary mono- and disialylated *N*-glycans)[142, 143].

In coronary heart disease, the ratio of LDL-Apo A/B100 is used for estimating the risk of acute myocardial infarction[137]. Apo B-100 and Apo B-48 mutations caused by *APOB100* and *MTP* (microsomal triglyceride transfer protein) gene defects are associated with metabolic disorders like abetalipoproteinaemia, hypobetalipoproteinemia and hypercholesterolemia[144-146].

Glycosylation

Apo B-100 is highly glycosylated and contains 19 potential *N*-glycosylation sites located at Asn34, Asn185, Asn983, Asn1368, Asn1377, Asn1523, Asn2239, Asn2560, Asn2779, Asn2982, Asn3101, Asn3224, Asn3336, Asn3358, Asn3411, Asn3465, Asn3895, Asn4237 and Asn4431. Of these, 17 are reported occupied by diantennary complex type glycans, as well as by high mannose and hybrid type structures[11, 142]. LC-fluorescence with exoglycosidase digestion has revealed the major glycans to be A2G2S1(6) (29.2%), A2G2S2(6) (23.6%), A2G2 (7.2%), Man9 (8.6%) and Man5 (6.9%)[142]. In addition, low levels of the Man6-8 have been reported. Most of the sialic acids were α2,6-linked (91%)[142].

A site specific analysis of the glycosylation has been performed by LC-ESI-MS(/MS) on tryptic and chymotryptic glycopeptides[11]. It was shown that the high mannose type glycans were mainly present on sites Asn185, Asn1368, Asn1377, Asn3336 and Asn3358, while the complex type (mono- and disialylated diantennary) glycans were located at Asn983, Asn2239, Asn2779, Asn2982, Asn3101, Asn3224, Asn3465, Asn3895, Asn4237 and Asn4431. Ans3895 is exceptional in this regard, as triantennary compositions have been observed as well. The largest variation is present on sites Asn1523 and Asn3411, as these display oligomannose, hybrid and complex structures. Asn3411, the nearest *N*-glycosylation site to the receptor of the LDL-binding site shows degrees of fucosylation. Asn34 and Asn2560 are not reported to be glycosylated[11].

The role of the glycans structures in LDL and/or Apo B-100 has been examined in several studies but their exact function is still unknown, although its degree of sialylation might serve the atherogenic properties of LDLs[142, 147-149].

Apolipoprotein D (P05090)

Apolipoprotein D (Apo D), also referred to as thin line polypeptide, is a small glycoprotein of 189 amino acids (with a signal peptide of 20 amino acids), with a molecular weight varying between 19 and 32 kDa depending on its glycosylation[150, 151]. While it shares their name, it does in fact not resemble other apolipoproteins,

and shares more homology with the lipocalin protein family[152]. It was originally assimilated to the apolipoprotein family due to its early association with lipid transport. Apo D is mainly synthetized in fibroblasts and to a lesser extend in the liver and intestine, where the other apolipoproteins are usually produced[153]. Its plasma levels are approximately 0.1 mg/mL[154, 155]. The common form of Apo D in plasma is a monomer, although it can also exist as a heterodimer linked to apolipoprotein A-2 via a disulfide bridge.

Apo D can form complexes with lecithin cholesterol acyltransferase and is implicated in the transport and transformation of lipids[152, 156-158]. It has been reported to have a potential role in colorectal cancer[153]. In addition, the protein is present at high concentrations in the cyst fluid where its concentration can be 500 times higher, which can be associated with an increased risk of breast cancer[159 160, 161]. Apo D has a tendency to accumulate in CSF and peripheral nerves of patients with Alzheimer's disease and other neurodegenerative conditions[162, 163]. A positive correlation between age and Apo D levels has been reported in females, but not in men[164, 165].

Glycosylation

Two glycosylation sites have been reported and confirmed for Apo D, namely Asn65 and Asn98[83, 84, 166]. These are mainly occupied by complex type *N*-glycans ranging from diantennary to tetraantennary structures, with potential elongation of the antennae in the form of *N*-acetyllactosamine (LacNAc) repeats[166]. LC-MS with exoglycosidase digestion has revealed the most abundant glycoforms per site as well. Asn65 mainly contains nonfucosylated triantennary structures with full sialylation (A3G3S3), less abundant signals including di- and tetraantennary species with high degrees of sialylation (A2G2S2; A4G4S4). Contrarily, Asn98 predominantly contains fucosylated species, also ranging from di- to tetraantennary, here the main signal being diantennary (A2FG2S2)[86, 100, 166, 167]. Treatment with β-galactosidase failed to trim one antenna of its galactosylation, strongly suggesting the presence of the antennary fucosylation, known to prevent this digestion[166, 168]. Studies have shown the implication of Apo D in conditions like Alzheimer's disease but no information about the role of glycosylation has been reported yet.

Apolipoprotein F (Q13790)

Apolipoprotein F (Apo F), also called lipid transfer inhibitor protein (LTIP), is a glycoprotein with an apparent mass of 29 kDa. The polypeptide chain of 326 amino acids is processed, with the first 165 amino acids being the signal peptide and the propeptide, resulting in a theoretical mass of 17.4 kDa for the peptide backbone of the mature protein[169]. Apo F is expressed in the liver and is secreted in plasma to concentrations of 0.07 mg/mL in females and of 0.10 mg/mL in males[169-171]. The

protein regulates cholesterol transport, inhibits cholesteryl ester transfer protein (CETP), and is found in combination with lipoproteins of all subclasses (high density, low density and very low density lipoproteins (HDL, LDL, VLDL)) as well as with apolipoproteins A1 and A2[171, 172].

Glycosylation

Three potential *N*-glycosylation sites of Apo F are located at Asn118, Asn139 and Asn267, as well as one *O*-glycosylation site at Thr291[170, 173]. Asn118 and Asn139 are glycosylated with high-mannose structures, as proven by exoglycosidase treatment, but will not contribute to plasma glycosylation as they are part of the proprotein[173]. Asn267, on the other hand, is not sensitive to this treatment, suggesting that it would contain complex-type *N*-glycans[173]. The presence of sialic acids on the protein has been indicated by sialidase treatment with western blotting as readout[170]. However, as *O*-glycanase has also shown the presence of *O*-glycans on the protein, it is unclear whether the sialylation arises from the *N*- or *O*-glycosylation[170]. In CSF, the *O*-glycans on Thr291 are reported to be of core 1 or 8 type[174]. No disease-related information is available with regard to the glycosylation of Apo F.

Beta-2-glycoprotein 1 (P02749)

Beta-2-glycoprotein 1 (B2GPI) is also called apolipoprotein H, APC inhibitor, activated protein C-binding protein, and anticardiolipin cofactor. It is a 50 kDa (including around 19% carbohydrate content) 345 amino acid single polypeptide chain (with a signal peptide of 19 amino acid) belonging to the complement control protein (CCP) superfamily[175]. It consists of five similar CCP domains of approximately 60 amino acids[176]. B2GPI is mostly synthetized in hepatocytes and is found in blood at around 0.2 mg/mL[177]. The main function of B2GPI is the scavenging of negatively charged compounds such as DNA, sialylated glycoproteins, and (phospho)lipids, which may otherwise induce unwanted coagulation and platelet aggregation[178-180]. The precise binding properties of the protein depend on the conformation, *i.e.* open or closed, which is proposed to be dependent on the glycosylation[181-183].

The serum level of B2GPI increases with age, and is reduced during pregnancy and for patients suffering from stroke and myocardial infarctions[181, 184]. Additionally, it is the major antigen in antiphospholipid syndrome[181, 182].

Glycosylation

B2GPI possesses four theoretical *N*-glycosylation sites at Asn162, Asn183, Asn193 and Asn253, as well as an *O*-glycosylation site at Thr149[175, 181, 185, 186]. The *N*-glycosylation sites have been confirmed by crystallography (finding attached *N*-

acetylglucosamines and mannoses) as well as by deglycosylated Lys-C peptide reverse phase (RP)-LC-MS after lectin capture[83, 186]. Generally the glycosylation of B2GPI is of the di- and triantennary type containing high levels of sialylation, with minor amounts of fucosylation [182]. Site-specific information is available only for Asn162 and Asn193[182].

Glycopeptide LC-ESI-quadrupole (Q)-TOF-MS revealed the glycosylation of Asn162 to be 67% diantennary disialylated (A2G2S2) and 22% triantennary trisialylated (A3G3S3), minor species including the di- and triantennary species lacking one sialic acid (5% and 3% respectively)[182]. The Asn193 site showed the same compositions, but with a higher level of triantennary species (35%) and a corresponding lower percentage of diantennary species (49%). Minor species again include the incompletely sialylated variants (8% and 7% for the di- and triantennary species respectively)[182]. The findings were confirmed by MALDI-QTOF-MS, although a lower degree of sialylation was observed. This difference is likely due to the tendency of MALDI ionization to induce in-source and metastable decay of sialylated glycan species[182, 187]. For the two noncharacterized *N*-glycosylation sites (Asn183 and Asn253) di- and triantennary glycans are expected as well, given the 19% of the total protein weight being attributed to the carbohydrate content[186].

Patients suffering from antiphospholipid syndrome (APS) showed a decrease in the amount triantennary sialylated glycans, and thus a relative increase in diantennary fully sialylated ones. This effect was particularly pronounced for Asn162[182].

Ceruloplasmin (P00450)

Ceruloplasmin (CP), also called ferroxidase, is a 132 kDa (120 kDa without glycosylation) 1065 amino acid (19 of which are signal peptide) glycoprotein synthesized by the liver[188]. It consists of a single polypeptide chain, and belongs to the multicopper oxidase family[188]. Concentrations for CP range from 0.15 to 0.96 mg/mL with a mean of 0.36 mg/mL, while elevated levels have been reported upon inflammatory stimulation[34, 189, 190]. CP can bind six to seven atoms of copper, in this manner containing and transporting 95% of the copper found in plasma. The main function of the protein, however, is in iron metabolism. CP has ferroxidase activity oxidizing Fe^{2+} to Fe^{3+} without releasing radical oxygen species, while also facilitating iron transport across the cell membrane[188].

Glycosylation

Of the seven potential CP *N*-glycosylation sites Asn138, Asn227, Asn358, Asn397, Asn588, Asn762 and Asn926, four (Asn138, Asn358, Asn397, and Asn762) are confirmed to be glycosylated[83]. The remaining sites (Asn227, Asn588, and Asn926)

are all in a β-strand within a hydrophobic region, potentially preventing site occupation[188]. NMR spectroscopy has revealed the overall CP glycan species to be sialylated diantennary A2(2)G2(4)S2(6) and sialylated triantennary A2(2,2,4)G4(4)S3(6,6,3/6). Partial core fucosylation has been found for the diantennary species, while of the triantennary species the α2,3-linked sialic acid-containing arm can be α1,3-fucosylated to form sialyl-Lewis X[191].

For the confirmed *N*-glycosylation sites, tryptic glycopeptide LC-ESI-MS(/MS) was used to study the site-specific glycosylation on a compositional level, and relatively similar ratios of di- and triantennary glycan species were found across the sites[192]. Asn138 is mainly occupied by the diantennary structures A2G2S2 (49%) and FA2G2S2 (26%), followed by the triantennary structures A3G3S3 (12%) and A3FG3S3 (10%). Small amounts of difucosylated species have been detected as well (FA3FG3S3, 3%). Asn358 contains a higher abundance of diantennary species (A2G2S2 83%, and FA2G2S2 12%), the triantennary species A3G3S3 only accounting for 5%. For Asn397 the main glycan is A2G2S2 (73%), followed by A3G3S3 (17%), A3FG3S3 (6%) and FA2G2S2 (4%). Analysis of Asn762 showed the main glycan to be A2G2S2 as well (46%), with the additional compositions A3G3S3 (20%), FA2G2S2 (16%), A3FG3S3 (13%), FA3FG3S3 (2%), A4G4S4 (1%) and A4FG4S4 (1%)[192]. No information about the glycosylation of human ceruloplasmin in disease was found with the preparation of this review.

Fibrinogen (P02671; P02675; P02679)

Fibrinogen is a 340 kDa glycoprotein that is synthesized in the liver by hepatocytes, and plays a key role in blood clotting[193, 194]. The protein consists of two sets of three different polypeptide chains named the α-chain (610 amino acids), β-chain (461 amino acids), and γ-chain (411 amino acids), arranged in a $\alpha_2\beta_2\gamma_2$ hexamer linked by disulfide bonds[195-197]. In plasma, fibrinogen is typically found at concentrations of 2-6 mg/mL with a mean of 3mg/mL, with women having slightly higher levels, and it is also present in platelets, lymph nodes, and interstitial fluid[195, 197-200].

Fibrinogen is cleaved by thrombin into fibrin, one of the essential components of blood clots after injury[194, 195, 201]. Furthermore, it acts as a cofactor in platelet aggregation, assists rebuilding of epithelium, and can protect against infections in interferon γ (IFNγ)-mediated hemorrhage[195, 202, 203]. In addition, the protein can facilitate the immune response via the innate and T-cell pathways[204-207].

Glycosylation

The α-chain of fibrinogen is not *N*-glycosylated, even though it harbors two potential *N*-glycosylation sites at Asn453 and Asn686. The β- and γ-chain are *N*-glycosylated at

Asn394 and Asn78, respectively[195, 208, 209]. By MALDI-TOF-MS and HPLC with exoglycosidase digestion, the predominant glycan structures present on these chains were found to be A2G2S1 (53%) and A2G2S2 (33%). Sialic acids are mainly α2,6-linked, but a degree of α2-3-linkage has been reported as well depending on the source or analytical method[210, 211]. Bisecting *N*-acetylglucosamine and core fucosylation are found in minor quantities[211]. Comparisons between plasma and serum *N*-glycan profiles revealed that fibrinogen could contribute for 22% to the total intensity of the diantennary monosialylated structures (A2G2S1)[211].

Site-specific analysis showed diantennary glycans with zero, one or two sialic acids on Asn394 (β-chain) and Asn78 (γ-chain)[208]. The glycosylation sites have been confirmed in studies at the level of deglycosylated glycopeptides, showing occupancy of Asn394 of the β-chain and Asn78 of the γ-chain, and surprisingly on the α-chain Asn686 as well[83, 84, 107, 209]. The β-chain glycosylation site has furthermore been observed in a core-fucose targeted study[100]. In addition to *N*-glycosylation, all fibrinogen chains may carry *O*-glycans[208].

The general degree of sialylation may be influencing the solubility of fibrinogen, and thereby play a crucial role in blood clotting processes resulting in different fiber structures[212-216]. In the Asahi mutant of the γ-chain, Asn334 has been reported to contain an additional *N*-glycosylation site[217]. Patients exhibiting the Asahi variant of fibrinogen displayed abnormally long blood clothing time, suggesting that the effect induced by that extra glycosylation site disturbs the fibrin polymerization process[217, 218].

Haptoglobin (P00738)

Haptoglobin (Hp) is a 406 amino acid (18 of signal peptide) acute-phase glycoprotein with a peptide backbone of 45 kDa. It is synthesized in the liver by hepatocytes as a single polypeptide chain and is also found in skin[219, 220]. During its synthesis, Hp is cleaved into a light α chain and a heavy β chain that are connected via disulfide bonds. Two variants of the α chain originating from the sequence Val19-Gln160 and differing by the subsequence Glu38-Pro96 can exist, α^1 having this subsequence once while α^2 has it twice, resulting in α chains of 83 or 142 amino acids with a respective molecular mass of 9 kDa and 16 kDa. The 40 kDa β chain is made of 245 amino acids originating from the sequence Ile162-Asn406[221, 222]. The combination of different allelic variants of the α chain (α^1 and α^2) with β chain(s) creates the polymorphism observed in Hp. There are three major Hp phenotypes called Hp1-1, Hp2-1 and Hp2-2. They respectively have a configuration of $(\alpha^1\beta)_2$, $(\alpha^1\beta)_2+(\alpha^2\beta)_{n=0, 1, 2, \ldots}$ and $(\alpha^2\beta)_{n=3, 4, 5, \ldots}$ which are observed at different ratios among ethnicities[223-226]. Caucasians have around 13% of phenotype Hp1-1, 46% of Hp2-1 and 41% of Hp2-2. Hp is typically found at a plasma levels in the range of 0.6-2.3 mg/mL with a mean of 1.32 mg/mL[223].

Elevated Hp levels have been reported with inflammation and malignant diseases[224, 227, 228]. It should be taken into account that the concentration as well as the molecular mass including glycosylation may vary among phenotypes (86-900 kDa)[223]. The half-life of Hp is found to be on average four days.

The major function of Hp is to protect tissues from oxidative damage by capturing hemoglobin[222, 229]. It has been reported that Hp polymorphism has an effect on its physiological properties, for instance Hp1-1 binds hemoglobin stronger than Hp2-2[230]. Certain diseases seem to be dependent on the polymorphism, as individuals with the Hp1-1 phenotype seem to have a higher concentration of induced antibodies in their plasma after vaccination, infections or liver diseases compared to the other phenotypes[223, 226].

Glycosylation

Four *N*-glycosylation sites have been identified on the β-chain of Hp, located at Asn184, Asn207, Asn211 and Asn241[231-233]. Analysis with (nano-)RPLC-ESI-MS/MS and MALDI-MS/MS of Hp glycopeptides (trypsin and GluC) revealed that all sites are occupied by complex type *N*-glycans [13, Zhang, S., 2013, 14, Pompach, P., 2013]. The site occupancy for Asn184 was determined at 97.7%, Asn207 at 97.4%, Asn211 at 98.5% and Asn241 had a site occupancy of 95.8%. Treatment with α2,3-sialidase showed that the sialic acids were mainly α2,6-linked, while β1,4-galactosidase treatment revealed that only antenna fucosylation was present, which was in agreement with the obtained CID fragmentation spectra[232].

Two recent studies showed some discrepencies in the relative abundances for the identified sites. For example, Asn184 was found to contain mainly diantennary species with two sialic acids (A2G2S2, 88% and 46%), followed by diantennary monosialylated (A2G2S1, 7% and 38%) and triantennary disialylated (A3G3S2, 4% and 3%) glycans. A low percentage of fucosylation was identified (A3FG2S2, 1% and 3%; A3FG3S2, 0.3% and 1%)[231, 232].

A possible reason for this discrepancy is that the first study did not differentiate the two *N*-glycosylation sites (Asn207 and Asn211) on the same peptide backbone that showed 7 different combinations. The major combinations were 1) one diantennary fully sialylated (A2G2S2) and one triantennary disialylated (A3G3S2, 45%), 2) two diantennary disialylated glycans (A2G2S2, 30%), and one diantennary fully sialylated (A2G2S2) and 3) one triantennary disialylated and fucosylated (A3FG3S2, 12%). The combination of a diantennary monosialylated (A2G2S1) with a diantennary disialylated glycan (A2G2S2) accounted for 6%, the diantennary and triantennary fully sialylated species (A2G2S2 and A3G3S3) for 5%, and the remaining combinations accounted for approximately 1% in total [231]. The second study

reported the glycoforms for each site separately due to an additional GluC protease treatment. Asn207 seems to contain mainly A2G2S2 (47%) and A2G2S1 (39%), followed by A3G3S1 (7%) next to some minor tetraantennary and fucosylated species. Interestingly, glycosylation site Asn211 appears to have a higher degree of triantennary species, with A2G2S2 (40%), A3G3S3 (29%), A3FG3S3 (21%), and A3G3S2 (10%)[232].

The two studies report that Asn241 carries mainly diantennary glycans, A2G2S2 being the most abundant variant with 87% and 47% (values reported in the two separate studies), followed by A2G2S1 (4% and 26%), A3G3S1 (n.d. and 10%), A3G3S2 (6% and 8%), A3G3S3 (n.d. and 4%) and A2FG2S1 (<1% and 2%). Low levels of tetraantennary species have been detected as well, with and without fucosylation varying from mono- to tetrasialylated[231, 232].

Both studies evaluated the glycosylation of Hp in patients with liver cirrhosis (LCH) and hepatocellular carcinoma (HCC). No difference in site occupancy could be observed between healthy and disease, but the number of detected glycoforms was increased (healthy 34 glycoforms, LCH 56 glycoforms, HCC 62 glycoforms)[232]. Increased branching and fucosylation were reported, with species carrying up to five fucoses[231, 233]. Furthermore an increase in sialylation was noticeable for the glycopeptide containing *N*-glycosylation sites Asn207 and Asn211[231]. Those carbohydrate structures have been reported in another study along with some new ones but they were not quantified[13].

Furthermore, core-fucosylation was identified on the *N*-glycosylation site Asn184[234]. Diantennary disialylated structures contained core-fucosylation (FA2G2S2) instead of antennary fucosylation. Several reports reveal that fucosylation plays an important role in many diseases such as pancreatic cancer, LCH and HCC[235, 236]. Another recent study examined the galectin-1 binding ability of Hp in the sera of metastatic breast cancer patients, where the binding was twice as strong, possibly due to a difference in glycoforms[237, 238].

It is interesting to see that two studies from the same year report different glycosylation patterns for Hp[231, 232]. This might be caused by a different ethnicity of the sample donors, as one study has been performed in China and the other in the United States, two geographical regions that have been reported to have different phenotype distributions[223]. That difference has not yet been taken into account in glycomics studies.

Hemopexin (P02790)

Hemopexin (HPX), also known as beta-1B-glycoprotein, is a 462 amino acid (23 are part of the signal peptide) single polypeptide chain plasma glycoprotein with a

peptide backbone of 51 kDa and an apparent mass ranging from 57 to 80 kDa depending on its glycosylation[239-241]. The protein is mainly expressed by the liver and found in serum at levels of 0.8 mg/mL in adults while levels in newborns have been measured around 20% of that value[242, 243]. It is also expressed in the central nervous system, in the retina and in the peripheral nerves. The protein structure is controlled by six disulfide bridges next to its glycosylation[240]. HPX is an acute phase response glycoprotein, capable of binding heme with the highest known affinity of all plasma proteins. When a heme is captured, the complex can be recovered from plasma by the HPX receptor (such as found on the membrane of liver parenchymal cells) leading to internalization, catabolization of the heme and recycling of the proteins involved. After the process, HPX is free to return to the circulation. HPX is found to be expressed in large quantities in case of inflammation, a state in which heme is highly abundant in plasma. As heme would otherwise induce oxidative stress, the function of HPX can be described as antioxidant[240].

Glycosylation

HPX contains five confirmed *N*-glycosylation sites located at Asn64, Asn187, Asn240, Asn246 and Asn453[83, 84, 107, 244-247]. In general, plasma HPX *N*-glycosylation consists mainly of diantennary structures with high levels of galactosylation, while low levels of triantennary and fucosylated structures have also been reported[100, 233, 248-250]. The degree of sialylation of the protein remains to be fully investigated, but lectin capturing of α2,6-sialylated HPX glycopeptides followed by LC-MS(/MS) analysis has revealed the presence of fully sialylated antennae and only low levels of monosialylated diantennary glycans[101]. Combining the information, the main glycan composition on HPX is expected to be A2G2S2. Site-specific characterization has been achieved on a compositional level for *N*-glycosylation sites Asn64, Asn187 and Asn453, each of them showing similar ratios of glycoforms (85-94% diantennary nonfucosylated, 4-7% diantennary fucosylated, as well as low levels of triantennary structures)[86, 233]. Asn240 and Asn246 remain uncharacterized, likely due to their close proximity. The antennarity and the degree of fucosylation (core and antennary) have been reported to increase with LCH and HCC[251]. Notably, HPX also contains two *O*-glycosylation sites (Thr24 and Thr29) one of which is located on the *N*-terminal threonine (after removal of the signal peptide), and a potential minor *O*-glycosylation in the Ser30-Thr40 region[86, 244, 247].

Histidine-rich glycoprotein (P04196)

Histidine-rich glycoprotein (HRG), also called histidine-proline-rich glycoprotein (HPRG), has an apparent molecular mass of 72 kDa (peptide backbone of 60 kDa) and consists of 525 amino acid (507 without the signal peptide)[252, 253]. The protein occurs

in plasma in concentrations of 0.1-0.15 mg/mL, and is mainly produced by the liver parenchymal cells although some reports suggest synthesis in immune cells as well[254-257]. Levels in newborns are only approximately 20% of those in adults[258]. HRG is known to regulate immunity, coagulation and angiogenesis[259]. To achieve this, it interacts with many different ligands including heme, heparin, plasminogen, fibrinogen, thrombospondin and immunoglobulin G, as well as many cell surface receptors and divalent cations such as Zn^{2+} [257]. It is a negative acute phase protein, showing decreased plasma levels during inflammation, injury or pregnancy[260].

Glycosylation

HRG is expected to have a large degree of glycosylation, as 14% of the protein weight (around 10 kDa) has been attributed to the oligosaccharide portion[90]. Three *N*-glycosylation sites have been confirmed by glycoproteomic analysis, located at Asn63, Asn125 and Asn344[84, 107]. Another glycosylation site is theoretically present at Asn345, but the direct vicinity with the site Asn344 may sterically hinder its occupation and additionally complicates its analysis. Interestingly, a common polymorphisms can induce a new glycosylation site at Asn202 by replacing a proline by a serine at position 204, creating the motif Asn-X-Ser, and *N*-glycanase treatment revealed a mass difference of 2 kDa attributed to the new Asn202 carbohydrate compared to the unmodified form of HRG[261]. The sequence Asn87-Asp-Cys found in HRG has been reported to contain glycosylation (in bovine protein C) but no clear evidence of its presence has yet been made for human HRG[262, 263]. With regard to the classical sites, little is known, and to the best of our knowledge, neither site occupancy nor relative abundance of glycan structures have been studied. However, if a carbohydrate mass of 10 kDa needs to be distributed across three glycosylation sites, the average site would contain glycans of over 3300 Da (putting them into the tri- and tetraantennary range with high levels of galactosylation, sialylation and/or fucosylation). No reports about changes in glycosylation under disease conditions were found for HRG.

Kininogen-1 (P01042)

Kininogen-1, also called alpha-2-thiol proteinase inhibitor, Fitzgerald factor, high-molecular-weight kininogen (HMWK) or Williams-Fitzgerald-Flaujeac factor, has a single polypeptide chain of 644 amino acid (18 belonging to the signal peptide) and approximates 114 kDa apparent molecular mass (while its theoretical mass without glycosylation is 70 kDa)[264]. Kininogen can be cleaved into six different subchains called kininogen-1 heavy chain, T-kinin (Ile-Ser-bradykinin), bradykinin (kallidin I), lysyl-bradykinin (kallidin II), kininogen-1 light chain, and low molecular weight growth-promoting factor. In its intact form, the protein is a cysteine proteinase

inhibitor, implicated in blood coagulation and inflammatory response and it can bind calcium, while the individual subchains can have many other functions[265-268]. Kininogen is mainly synthetized in the liver to plasma concentrations of 55-100 µg/mL, where it is mostly found in complex with prekallikrein or factor XI to position the coagulation factors near factor XII[267, 269-272].

Glycosylation

Kininogen has four *N*-linked glycosylation sites at Asn48, Asn169, Asn205, Asn294 (all of which remain on the kininogen-1 heavy chain after cleavage) and eight *O*-linked glycans at sites Thr401, Thr533, Thr542, Thr546, Thr557, Thr571, Ser577 and Thr628[83, 84, 86, 107, 264]. While no overall or site-specific glycosylation analysis has been performed yet, core-fucosylation has been reported for sites Asn48, Asn205 and Asn294 on the basis of RP LC-MS^n after capturing with *L. culinaris* lectin[100]. In addition, two-dimensional gel electrophoresis, with staining for triantennary structures carrying sialyl-Lewis X has demonstrated the natural presence of this epitope on the protein, as well as its upregulation in patients with stomach cancer[273]. Kininogen is expected to be highly glycosylated by large *N*- and *O*-glycan structures, as the observed protein mass is more than 40 kDa higher than the mass calculated from the amino acid sequence. Kininogen glycosylation changes due to diseases have not yet been described.

Serotransferrin (P02787)

Serotransferrin (STF), also known as transferrin, β1 metal binding globulin or siderophilin, is a 698 amino acid protein (19 amino acids of which are signal peptide) with a molecular mass of approximately 77 kDa (without glycosylation)[8, 274]. The protein consists of two globular domains, the *N*-lobe and the C-lobe which divided into two subdomains each (N1, N2, C1 and C2). The two main domains are connected by a short linker peptide[274-276]. The *N*-lobe is 336 amino acids in size and spans from Val25 to Glu347, while the C-lobe is 343 amino acids long and ranges from Val361 to Lys683[274]. The lobes can interact to form a hydrophilic metal ion binding site[274]. STF is mostly produced by hepatocytes, although other tissues have also shown expression, albeit at significantly lower amounts[274]. The plasma concentration is highly stable from the age of 2 years on, with a range between 2 and 3 mg/mL[274, 277]. Levels may increase during pregnancy up to 5 mg/mL[278].

STF is an iron binding protein and it regulates iron levels in biological fluids. It can bind two Fe^{3+} ions and transport those throughout the body, avoiding the toxicity of free radical formation that may be caused by free Fe^{3+} ions[274]. Iron is essential for DNA replication as it is a co-factor of ribonucleotide reductase[279]. Several studies have shown that the number of transferrin receptors at the surface of cells was

closely correlated with their proliferation state and their iron status[280, 281]. In addition, STF has been associated with several diseases like atransferrinemia and cardiovascular diseases[274]. In inflammation and allergic reactions, the STF levels are found to be significantly reduced in plasma[274]. The protein has also shown potential as a therapeutic agent. For instance, oxidative damage caused by radiotherapy can be reduced by infusion with apo-transferrin[282]. The proprieties of STF and its receptor can be exploited to deliver drugs specifically into the brain and cancer cells[283]. Additionally, conjugates consisting of the protein and a drug have been shown to yield high specific cytotoxicity (e.g. Tf-ADR versus HeLa, HL-60 and H-MESO-1 cell lines)[283, 284].

Glycosylation

STF has two *N*-glycosylation sites located at Asn432 and Asn630 and a potential minor site at Asn491 (Asn-X-Cys)[8, 83, 278, 285, 286]. Around 6% of the total weight of the protein is due to the carbohydrate content[281]. Lectin mobility (ConA – Sepharose column) followed by sequential exoglycosidase treatments on two STF samples of healthy patients showed that, overall, the main glycans are A2G2S2 (96-97%), FA2G2S2 (2-3%) and A3G3S2 (1%)[287]. The glycosylation per site has been studied using nano-LC-ESI-MS combined with exoglycosidase treatment[285, 286]. The sites at Asn432 and Asn630 proved to be the main contributors to the total glycome, while the non-standard glycosylation site at Asn491 was glycosylated at a level of approximately 2%[285, 286].

The glycans present on Asn432 are A2G2S2 (93.5%), A3G3S2 (2.5%), A2G2S1 (2.4%) and A2FG2S2 (1.6%), while Asn630 contains A2G2S2 (85.9%), FA2G2S2 (6.9%), A2FG2S2 (2.8%), A2G2S1 (2.2%), A3G3S2 (1.0%), as well as some lower abundant species with increased fucosylation[285, 286]. The fucosylated antenna is most likely of sialyl-Lewis X type (at the α1,3-linked arm, β1,4-linked antenna) as it was shown by NMR spectroscopy of material purified from the amniotic fluid of pregnant women[288]. A single type of glycosylation was detected on the minor glycosylation site at Asn491, namely A2G2S2[285]. STF *N*-glycosylation has been investigated in other biologic fluids like CSF, where similar structures have been found along with some disease-related ones[8, 289].

The glycosylation of STF has shown to be different across fluids and phenotypes with the abundance of A2G2S2 being significantly reduced in human amniotic fluid (55%) or in the plasma of hepatoma patients (37-63%)[287, 288]. The percentage of triantennary structures is largely increased in amniotic fluid to 32%, while the abundance of triantennary structures in the serum of hepatoma patients ranges from 21 to 63%[287, 288]. Abnormal isoforms of serotransferrin, especially variation in the sialic acid content, are a very sensitive and reliable biomarkers of many CDGs,

and potentially for idiopathic normal pressure hydrocephalus (iNPH) patients[289, 290]. Isoelectric focusing (IEF) of serotransferrin is the first test used to rapidly reveal *N*-glycosylation related CDGs while apolipoprotein C-III is the protein of choice for the test of *O*-glycosylation related CDGs[291, 292]. Interestingly, carbohydrate deficient STF levels can also be used as indicator of heavy alcohol usage, even post mortem[8, 293].

Vitronectin (P04004)

Vitronectin (VN), also called S-protein, serum spreading factor, or V75, is a 459 amino acid 52.4 kDa member of the pexin family and of the adhesive glycoproteins group[294-297]. The apparent molecular mass of 75 kDa is due to post translational modifications including glycosylation. VN is mainly produced in the liver and it is found in plasma at concentration of 0.2-0.4 mg/mL, where it is mostly present in monomeric or dimeric form[34, 296]. VN is also found in other body fluids such as seminal plasma, urine, amniotic fluid, CSF, bronchoalveolar lavage fluid and in platelets[296].

VN is an adhesive glycoprotein, and shows a role in blood coagulation, extracellular matrix binding, regulation of cell adhesion and spreading, and innate immunity[294, 295]. It also protects the membrane from the damages caused by the terminal cytolytic complement pathway. Underexpression of the protein has been correlated with liver conditions like fibrosis, while elevated levels have been reported in inflammatory states[298-300]. VN is also found to be implicated in HCC where specific glycoforms have been identified[301].

Glycosylation

Three *N*-glycosylation sites have been identified in VN at Asn86, Asn169 and Asn242 by LC-MS(/MS)[83, 107]. Without site specificity, the major VN carbohydrate forms reported by LC-fluorescence are diantennary and triantennary complex type glycans, with a low percentage of hybrid structures[302]. Sialic acids are mainly found α2,6-linked, as determined by sialidase and acid treatments, and NMR. About 19% α2,3-linkage has been detected on the α1,6-arm of the diantennary structures and on the β1,6-linked *N*-acetyllactosamine of the α1,3-arm of triantennary structures. Core fucosylation of vitronectin accounts for 7.9%[302].

When looking at the glycosylation in a site-specific manner by trypsin digestion and LC-ESI-MS(/MS) analysis, Asn86 shows mainly A2G2S2 species (45%), as well as A3G3S3 (33%) and A3FG3S3 (20%)[301]. At Asn169, a higher variety of glycan structures are observed. Next to the fully sialylated diantennary structures (A2G2S2, 76%) and its monosialylated variant (6%), around 18% sialylated hybrid structures have been detected (ranging from 3 to 5 mannoses). Asn242 bears diantennary di- and monosialylated *N*-glycans (A2G2S2, 50%; A2G2S1, 20%), with possible core fucose

on the fully sialylated variant (FA2G2S2, 10%). In addition, triantennary fully sialylated structures have been detected with and without fucose (A3G3S3, 10%; FA3G3S3, 10%)[301].

Core fucosylation of VN has been reported at Asn242 in healthy individuals and on Asn86 in HCC patients[100]. Hybrid type and fucosylated glycans of VN have been reported to increase in patients suffering from HCC and other cancers, and thus shows potential as biomarker[301, 303]. A possible explanation for the increase of hybrid type glycans is that the alpha mannosidase in the Golgi apparatus is suppressed in HCC[17].

Zinc-alpha-2-glycoprotein (P25311)

Zinc-alpha-2-glycoprotein (ZAG, not to be confused with *ZAG* which is the short name of its *AZGP1* gene), also abbreviated Zn-alpha-2-glycoprotein or Zn-alpha-2-GP, is a 41 kDa glycoprotein (15% of the mass being carbohydrate) comprising a single 298 amino acid chain (20 amino acid signal peptide), with two intra-chain disulfide bridges[304-306]. The protein is produced by the liver and occurs in plasma at concentrations around 0.03-0.11 mg/mL with a mean at 0.05 mg/mL. As with many plasma glycoproteins, the functions of ZAG are diverse. The protein has been shown to interact with the beta-3-adrenoreceptor on adipocyte cells, inducing the depletion of fatty acids[307]. While its serum variant originates from hepatocytes, ZAG is expressed in many cell types including adipose tissue, buccal cells and prostate epithelial cells, and occurs in many body fluids like seminal fluid where its concentration is six time higher than in serum[307]. Functions of the on-site produced ZAG include fertilization, melanin production, regulation of the immune response, and many others. In addition, the serum concentration of ZAG shows a large increase in various types of cancer, making it a particularly good biomarker for female breast and male prostatic carcinomas[307].

Glycosylation

Four *N*-glycosylation sites have been detected on ZAG at Asn109, Asn112, Asn128 and Asn259[83, 84, 107, 246, 308, 309]. For three of the sites (Asn112, Asn128 and Asn259) proton nuclear magnetic resonance (^{1}H-NMR) spectroscopy has revealed the major *N*-glycan structure to be diantennary and disialylated A2(2)G2(4)S2(6)[305]. For Asn259 specifically, partial sialylation (90%) of the α1,6-linked antenna has been reported. The general presence of diantennary *N*-glycans, and the sialylation thereof, has been verified by proteomic experiments, but to date no extensive study has been made on its glycan microheterogeneity[174, 310]. Asn109 and Asn128 have for instance been suggested to carry in part core fucosylated *N*-glycans, but this has hitherto remained

unconfirmed[100]. No information about the effect of diseases on ZAG glycosylation was found in literature.

Immunoglobulins

Immunoglobulins (Igs) are a major component of the adaptive immune system[311]. There are five distinct classes in humans (IgA, IgD, IgE, IgG and IgM), which all share common components. Generally, immunoglobulins consist of two heavy chains and two light chains. These chains contain one variable part (H_L or V_L, respectively) and three or more constant domains on the heavy chain (C_Hn), or one on the light chain (C_L). Furthermore, immunoglobulins can be subdivided into a fragment antigen-binding (Fab) and a fragment crystallizable (Fc) portion. The Fab domain consists of the V_H and V_L domains and the adjacent *N*-terminal constant C_H1/C_L domain. The Fc domain is built up of the remainder of the heavy chains. Immunoglobulins thus contain two Fab domains per Fc domain. Each immunoglobulin has its own specific heavy chains (α, δ, ε, γ or μ) which are joined by one or more disulfide bridges. The light chain can occur in two variants (λ and κ) that are shared by all immunoglobulins. Some immunoglobulins additionally contain a flexible hinge region between the C_H1 and C_H2 domains (IgA, IgD and IgG). The remaining immunoglobulins (IgE and IgM) have a rigid Ig domain instead of a hinge region. Immunoglobulin *N*-linked glycosylation occurs mostly on the heavy chains, accounting for between 2% and 14% of the protein weight. However, the light chain can also contain *N*- and *O*-linked glycans [311].

Immunoglobulin A (P01876; P01877)

Immunoglobulin alpha (IgA) is an antibody that exists in two subclasses (IgA1 and IgA2), and in both mono- and dimeric form. Compared to IgA2, IgA1 contains a 13 amino acid extended hinge region, which is heavily *O*-glycosylated[312, 313]. Serum IgA consists mostly of the 160 kDa IgA monomer (mIgA), has a concentration of 2.62 mg/mL (of which approximately 90% is IgA1), and is produced by the bone marrow[313, 314]. Secretory IgA (sIgA) is observed at mucosal surfaces and produced locally, mainly occurring as a dimer of two mIgA units and a set of two connecting peptides, the J-chain and the secretory component[312, 314]. Secretory IgA is a key player in the immune defense at mucosal surfaces. Pathogenic microorganisms are prevented from attaching to the mucosal surface by sIgA surrounding the pathogen, which is then repelled by the mucosal surface due to the high abundance of hydrophilic amino acids and glycosylation[312]. The precise role of IgA in the circulation is not clear.

Glycosylation

IgA is *N*-glycosylated at Asn144 (IgA1) and Asn131 (IgA2) in the C_H2 domain as well as at Asn340 (IgA1) and Asn327 (IgA2) and in the tail piece domain[315]. IgA2 contains 2 additional *N*-glycosylation sites at Asn47 of the C_H1 domain and at Asn205 of the C_H2 domain[315]. While glycosylation studies have been performed for IgA1, the glycosylation of IgA2 remains to be characterized.

The main *N*-glycans present on IgA1 as detected by hydrophilic interaction liquid chromatography (HILIC)-HPLC with exoglycosidase digestion are diantennary disialylated (A2G2S2, 24%), diantennary monosialylated (A2G2S1, 20%) and fucosylated diantennary bisected disialylated (FA2BG2S2, 14%)[316]. The amount of nonsialylated glycans detected was marginal, being at levels for total IgA of 6% for the Fc region and 2% for the Fab region[316]. A site-specific study showed that the fucosylated glycans are mostly present on the Asn340 site[317]. Furthermore it was shown that the main glycoform on the IgA1 Asn144 containing glycopeptide was A2G2S1, while the Asn340 containing glycopeptide carried mainly the FA2G2S2[318].

The role of *N*-glycosylation of IgA in diseases is not well understood. The glycan might have an influence on the binding of IgA to the FcαR receptor, although this finding was not validated in a later study[316, 319]. Binding to the FcαR receptor can induce a pro- or anti-inflammatory response[320]. In addition, the presence or absence of sialic acids on the glycans may influence the clearance of IgA from the circulation by the asialoglycoprotein receptor[311].

Immunoglobulin D (P01880)

Immunoglobulin delta (IgD) has, compared to the other immunoglobulins, a rather long hinge region of 64 amino acids resulting in a total apparent mass of 175 kDa. The average concentration of IgD in plasma is 0.03 mg/mL, but it can range from <0.003 mg/mL to 0.4 mg/mL without any clear sex or age dependence[321-323]. Compared to the other immunoglobulins, it has a short half-life of 2.8 days[324]. IgD can be found in a secreted isoform (sIgD), as well as membrane bound on immature B cells[325]. The protein is involved in immunity and inflammation, by binding to respiratory bacteria, resulting in clearance[32].

Glycosylation

Three *N*-glycosylation sites have been identified on the heavy chain of IgD, located at Asn225, Asn316 and Asn367, as well as seven *O*-glycosylation sites at Ser109, Ser110, Thr113, Thr126, Thr127, Thr131 and Thr132[326-328]. HILIC-HPLC analysis with exoglycosidase digestion on released IgD *N*-glycans revealed a mixture of high mannose and complex type glycosylation. The total pool contained 35% core

fucosylation, <1% terminal *N*-acetylglucosamine, 33% bisection, 20% terminal galactosylation and 31.5% monosialylation and 21.5% disialylation (sialic acids being α2,6-linked). The most abundant glycoforms detected were Man8 (14.4%), Man9 (13.5%), FA2G2S2 (7.6%), FA2G2S1 (7.3%), FA2BG2S2 (6.5%) and A2G2S1 (6.1%). Interestingly, monoglucosylated Man8 and Man9 (Man8Glc, Man9Glc; 2.4%, 3.3%) were observed as well[329]. The high mannose glycans were preferably found at the Asn225 site, while the complex type glycans were abundant at Asn316 and Asn367[328]. The absence of glycans at Asn225 has been shown to completely inhibit the secretion of IgD[330].

Immunoglobulin E (P01854)

Immunoglobulin epsilon (IgE) is a 188 kDa antibody lacking a hinge region, but that instead contains an extra C domain in its heavy chain[331]. The protein exists as a membrane-bound receptor form and in a soluble form[332]. IgE has a serum concentration of around 0.3 μg/mL, making it the lowest abundant immunoglobulin[333]. No in-depth study has yet been performed to elucidate where IgE is synthesized[331]. The primary function of IgE is the induction of an anti-parasitic immune response by activation of mast cells and basophils through the FcεRI receptor[334]. This mechanism is also proposed to play a role in the formation of allergic responses[333, 335].

Glycosylation

Carbohydrates form 12% of the IgE molecular mass, making it the most glycosylated antibody in plasma[336]. The protein contains six *N*-glycosylation sites, located at Asn21, Asn49, Asn99, Asn146, Asn252 and Asn275[337]. An additional potential site at Asn264 was not found to be glycosylated[338]. HILIC-HPLC with exoglycosidase digestion of 2-aminobenzamide-labeled glycans showed the overall species to be mainly core-fucosylated diantennary with either one sialic acid (FA2G2S1) or two (FA2G2S2) (18% and 25% respectively)[329]. These glycans have, to lesser extent, been found in non-fucosylated form (A2G2S1, 11%; A2G2S2, 11%), and with bisecting *N*-acetylglucosamine (FA2BG2S1, 8.2%). In addition, 14.2% of the glycan pool proved to be high-mannose type (mainly Man5)[329].

By performing site-specific analysis by LC-MS/MS of tryptic glycopeptides, it was found that Asn21 mainly contains FA2G2S1 (30%), FA2BG2S1 (30%), FA2G2S2 (15%) and FA2BG2S2 (10%), while Asn49 is occupied by FA2G2S2 (30%), FA2G2S1 (18%), FA2BG2S2 (15%), and FA2BG2S1 (15%)[338]. Asn99 contains FA2G2S2 (40%), FA2G2S1 (20%) and bisected species in lower relative abundance (<10%). Asn146 is glycosylated by FA2G2S2 (50%), FA2BG2S2 (30%), and around 10% of FA2G2S1, while Asn252 is highly bisected, mainly containing FA2BG2S1 (35%) and FA2BG2S2 (25%),

as well as a lesser amount of the nonbisected species FA2G2S2 (15%) and FA2G2S1 (10%)[338]. Interestingly, the Asn275 site almost exclusively shows oligomannosidic structures, the main species being Man5 (50%), but higher numbers of mannoses are found as well (Man6, 15%; Man7, 10%; Man8, 10%; Man9, 5%)[336, 338].

In the same study, IgE from hyperimmune donors was seen to be similarly glycosylated as normal IgE, while IgE derived from monoclonal myelomas showed the loss of bisection and a drastic appearance of triantennary structures (up to 50% per site)[338]. There is evidence that IgE glycosylation is important in binding to the FcεRI receptor and can be implicated in the initiation of anaphylaxis[339, 340]. In contrast, other sources indicate that the glycans in the Fc region are only minor contributors to the binding of IgE to the FcεRI receptor[341].

Immunoglobulin G (P01857; P01859; P01860; P01861)

Immunoglobulin gamma (IgG) is a glycoprotein with a total molecular mass of approximately 150 kDa[311, 342]. The light chain consists of a domain covering the variable region (V_L) as well as a constant (C_L) domain. The heavy chain contains four domains with one domain which comprises the variable region (H_L) followed by three constant domains: C_H1, C_H2 and C_H3. Each light chain is paired with the H_L and C_H1 domain of the heavy chain to form a Fab portion, whilst C_H2 and C_H3 domains of the two heavy chains together form the Fc portion. Between the two Fab portions and the Fc portion a flexible hinge region is positioned, which makes it possible for the two Fab arms to move individually[311, 331]. The antibody is highly stable with a half-life of approximately 12 days[343, 344]. Based on the amino acid sequence of the constant regions of the heavy chains, IgGs can be divided into four subclasses namely, IgG1 (P01857), IgG2 (P01859), IgG3 (P01860) and IgG4 (P01861)[345, 346]. Notably, IgG3 has a larger hinge region (62 amino acids) compared to the other subclasses (12 amino acids).

During a secondary immune response IgG is secreted in high amounts by B cells[347]. In healthy individuals the concentration of IgG in serum is between 7 and 18 mg/mL[348]. The average subclass-specific concentrations in plasma are reported as 5.03 mg/mL for IgG1, 3.42 mg/mL for IgG2, 0.58 mg/mL for IgG3 and 0.38 mg/mL for IgG4[349]. IgG molecules are important for activating the complement system through the classical pathway (antibody-triggered) as well as binding to specific receptors on macrophages and neutrophils[331, 347]. The IgG subclasses differ in their ability to activate the complement system. The primary activators of the complement system are IgG1 and IgG3, whereas IgG2 can also activate it at a lower level. IgG4, on the other hand, is not capable of activating the complement system[331]. Furthermore, IgG molecules are the only antibodies that can pass from a mother to her child via the

placenta, and maternal IgG has been shown to gradually decrease throughout pregnancy[331, 350, 351].

The majority of therapeutic antibodies is derived from IgG1, where the glycosylation plays an important role for their function[35, 331, 351-354].

Glycosylation

Glycosylation can occur on both the Fc and Fab portions of the IgG molecules[355]. The Fc region has been extensively studied with a highly conserved *N*-glycosylation site in the C2H domain at Asn297. Notably, this site may have a different number for different IgG subclasses and variants[355].

Another possible *N*-glycosylation site may be found at Asn322 of IgG3 although no occupation has yet been described[355]. The Fab portion is known to be *N*-glycosylated in 15-25% of the cases[356].

The overall glycosylation of IgG has been the subject of many studies using a variety of different methods[24]. In a recent glycosylation MALDI-TOF-MS study on a released glycan level, the most abundant glycans were complex types, *i.e.* FA2G1 (31%), FA2G2 (23%), FA2G2S1(6) (13%), FA2 (10%) and FA2BG1 (5%)[357]. Only a small portion of the glycans were found to be high mannose (0.21%), of which Man8 (0.06%) was the most abundant, followed by Man9 (0.05%). Overall, 92% of the total IgG pool was core-fucosylated, 13% bisected, 18% monosialylated and 3% disialylated. 12% of the glycans contained α2,6-linked sialic acids, against 0.2% α2,3-sialylated species[357]. These findings are in agreement with previously reported sialylation values obtained by lectin interaction[358]. Next to the study of overall IgG glycosylation, differences between the Fab and Fc have also been studied by MALDI-TOF-MS after affinity capturing of the different regions[357]. The Fc region shows a similar profile as the total IgG profile, albeit with a lesser degree of sialylation. FA2G1 (32%) was again the most pronounced glycan, followed by FA2G2 (27%), FA2G2S1(6) (15%), FA2 (9%) and FA2BG1 (5%), while the amount of high mannose type species was found to be very low (0.1%). In contrast to Fc, the Fab region showed a significantly higher degree of sialylation, with 40% of the species being monosialylated, and 52% being disialylated. Also bisection and high mannose species were seen to be higher (45% and 4% respectively). Specific compositions included FA2BG2S1(6) as most abundant with 21%, followed by A2G2S2(6) (17%), FA2BG2S2(6) (16%), FA2G2S2(6) (16%) and FA2G2S1(6) (10%). For the high mannose types Man6 was the most abundant with 1.2% followed by Man8 (1.0%) and M5 (0.7%)[357].

Affinity capturing followed by LC-MS with CID and electron-transfer dissociation (ETD) fragmentation of tryptic IgG glycopeptides revealed that the various IgG subclasses are similarly glycosylated, but with some notable differences[359, 360]. IgG1

tends to show higher galactosylation than the other subclasses, whereas IgG2 shows the highest degree of core-fucosylation and IgG3 the least. IgG4 was found more difficult to study due to its relatively low abundance[359]. Another study examined the *O*-glycosylation of IgG3 in the hinge region, revealing that the threonine sites (T) in the three repeated peptide sequences (CPRCPEPKSCD**T**PPP) are partially occupied with core 1-type *O*-glycans[361].

A vast body of literature exists describing disease-associated changes of IgG glycosylation, as well as the regulation and immunological effects of such glycosylation changes. In the following, only a very concise view of this field will be given, and we would like to refer the interested reader to more specialized reviews[342, 362, 363].

IgG glycosylation has been strongly associated with age, with a negative correlation between age and galactosylation[19, 20, 364, 365]. IgG FA2 seems to have a strong pro-inflammatory effect through various mechanisms, e.g. the lectin pathway of the complement system[19, 365, 366]. Increased levels of FA2 glycans and/or lowered levels of FA2G2 glycans is found in many diseases, including rheumatoid arthritis, Crohn's disease, granulomatosis with polyangiitis, tuberculosis, HIV and myositis[366-370]. Several studies revealed that core-fucosylation is an important factor in the binding capacity of the Fc region to the Fc_{γ}RIIIa receptor[371, 372]. The lack of core-fucosylation suggests improvement in the binding extensively resulting in a higher degree of antibody-dependent cell mediated cytotoxicity (ADCC) receptor[371, 372]. The presence of sialic acids is able to reduce the binding capacity of the antibody to the Fc_{γ}RIIIa receptor, as a consequence the activity of ADCC is decreased and anti-inflammatory effects are enhanced, although this only appears to be the case for α2,6-linked sialylation[33, 355, 373, 374]. Interestingly, during pregnancy the glycosylation also appears to change, especially in the Fc region where the levels of galactosylation and sialylation increase[28, 375-377] . This might be to suppress the immune response of the mother against her child[375]. Alterations in glycosylation have also been reported to occur in a subclass specific level, for example in patient suffering from hepatocellular carcinoma, cirrhosis, or myositis[367].

Immunoglobulin M (P01871)

Immunoglobulin mu (IgM) is a 970 kDa (in pentameric form) antibody, consisting of five 190 kDa subunits (of 452 amino acids)[311, 331, 378]. The protein can be membrane-bound on the B1- and B2-cells where they are produced[379], or secreted into blood at plasma concentrations of 0.5-2.5 mg/mL[348]. In circulation, IgM exists either as a pentamer with coupling J-chain, or occasionally as hexamer lacking the J-chain[380]. No hinge region has been reported for the immunoglobulin, but it contains an extra C domain instead[331]. In total, pentameric IgM consists of 10 heavy chains, 10 light

chains and 1 J-chain, arranged in a mushroom-shaped molecule, leading up to being the largest antibody in human plasma by far[381].

IgM antibodies are an early and main activator of the classical complement pathway[331], but also play a role in homeostasis, inflammation, infection, atherosclerosis and autoimmunity[378]. The protein is additionally involved in apoptosis[378], as absence of IgM shows a three- to four-fold decrease in apoptotic cell uptake by macrophages[382]. Furthermore, IgM has been described in several studies regarding acute coronary syndromes and cardiovascular diseases, where an elevated urine excretion of IgM has been reported[383, 384]. The presence of glycans on non-antigen bound IgM may also assist the agglutination of virus particles present in serum via viral lectin hemagglutinins[311].

Glycosylation

IgM contains *N*-glycosylation sites at Asn46, Asn209, Asn272, Asn279 and Asn439, of which Asn439 is only 17% occupied[311, 385, 386]. HILIC-HPLC-MS has shown the overall *N*-glycosylation to be mainly diantennary with core fucosylation, either with- or without bisecting *N*-acetylglucosamine (FA2BG2S1, 26%; FA2G2S1, 19%), followed by the oligomannose compositions Man6 and Man5 (10% and 6%, respectively)[386]. By lectin capturing, the high-mannose compositions have been attributed to Asn297 and Asn439, leaving the complex type glycosylation to be found at Asn209 and Asn272[311, 387]. Interestingly, the partially occupied Asn439 shows larger high-mannose structures (Man6-8) than site Asn297 (Man5-6), suggesting that the former is difficult to access by both the dolichol precursor and the mannosidases required for trimming of the structure. Depending on the source, Asn46 can be occupied by either oligomannose or complex type *N*-glycans[311, 387].

Discussion

Here we present an overview of the *N*-glycosylation of 24 major plasma glycoproteins. It has been shown for many of these proteins that glycosylation changes are implicated in serious pathological states such as cancers, autoimmune diseases and CDG and that their glycosylation pattern could be used as biomarkers, prognostic tools or even as anchor points for targeted treatments[15, 35, 290, 388, 389]. These findings have resulted in an increasing interest in the glycosylation analysis of easily accessible biofluids such as plasma, and many correlations have been established between disease (states) and the abundance of specific glycosylation traits. Recent advances in sample preparation methods, separation techniques, mass spectrometry, and the development of robotized platforms are easing routine analysis of the total plasma *N*-glycome and allow the screening of large cohorts in reasonable times, thus enhancing the possibilities to search for putative biomarkers

and predictions tools[38, 210, 390-392]. This, however, requires that the observed differences in glycosylation can be interpreted in a biologically meaningful manner, and traced back to changes in the levels of glycosylated proteins, and to possible glycosylation changes of specific proteins.

The information contained in this review stems from many sources and methodologies. When exploring protein glycosylation to its full complexity, this comprises the occupancy per site and the relative abundances of glycoforms present per site, as well as information on linkages and isomer distribution. No single analysis method is capable of providing all this information in a comprehensive manner, let alone on a complex sample such as human plasma. Consequently, different levels of detail are available with respect to the glycosylation of the major glycoproteins that make up human plasma. Analysis methods encountered in this review are very diverse, including NMR, lectin capturing, LC-fluorescence, as well as several mass spectrometric methods[109, 390, 393]. NMR has proven definitive for providing structural features of a glycan, but is limited by sample throughput and amount of material needed, as well as by its inability to characterize multiple species present in a complex sample[390]. Mass spectrometric methods applied in bottom-up studies of glycopeptides generally only provide glycosylation information on a compositional level, but may in addition provide site-specific glycosylation information by revealing the amino acid sequence as well as glycan attachment site[359]. As such, high-throughput mass spectrometric screening methods have been used to identify and confirm many of the glycosylation sites in human plasma, although the use of deglycosylated peptides has prevented characterization of the glycans themselves[83, 84, 100]. A particularly successful combination of methodologies for in-depth study of glycosylation has proven to be LC-MS(/MS) with exoglycosidase digestion and/or lectin capturing, which has been used to study a fair number of the proteins covered in this review[211, 329].

Well-studied proteins covered in this review include alpha-1-acid glycoprotein, alpha-1-antitrypsin, haptoglobin, serotransferrin, vitronectin, and IgG, while others such as histidine-rich glycoprotein and kininogen-1 still remain to be studied at the most basic level (**Table 1**). Overall characterization reveals a high degree of galactosylation and sialylation across the plasma *N*-glycome, the most abundant species for most sites having full coverage of all their antennae. Next to receptor interaction and charge induction, the terminal sialic acids are known to play a large role in determining the half-life of proteins, and less than full sialylation would lead to hepatic clearance via the asialoglycoprotein receptor [394].

Specifically, the major detected glycan species are A2G2S2 and its monosialylated variant (**Figure 1, Table 1**), with β1,2-linked antennary *N*-acetylglucosamines, β1,4-linked galactoses, and α2,6-linked *N*-acetylneuraminic acids[191, 305]. These are found

on the majority of glycoproteins, and are particularly abundant on serotransferrin, fibrinogen, ceruloplasmin and alpha-2-macroglobulin. Potential fucosylation for these diantennary structures mostly occurs in α1,6-linkage on the core *N*-acetylglucosamine.

The more truncated *N*-glycosylation, *i.e.* lack of sialic acid termini and incomplete galactosylation, is reserved for immunoglobulin G, and to lesser extent apolipoprotein B-100[11, 357]. Interestingly, immunoglobulin G is the only major plasma protein we have found to contain core-fucosylation as well as incomplete galactosylation/sialylation, meaning that the total plasma *N*-glycome species FA2, FA2G1 and FA2G2 predominantly reflect the glycosylation of this protein[357]. Similarly, immunoglobulin M is the major carrier of the bisected species FA2BG2S1, with IgG and the lowly abundant immunoglobulin E contributing to the expression of this compositional glycan to a lesser extent[329, 357, 386].

The high mannose type glycosylation is also differentially distributed. Whereas the lower size oligomannose structures Man5 and Man6 are distributed across alpha-2-macroglobulin, apolipoprotein B-100 and immunoglobulin M, the larger structure Man9 mainly originating from apolipoprotein B-100[11, 109, 386]. In addition, the high mannose structures have been reported on the Fab portion of IgG[357].

Tri- and tetraantennary structures are found in lower abundance than the diantennary structures, and have some discerning features. Whereas diantennary glycans are mainly sialylated with an α2,6-linkage, for the triantennary species on average one in three sialic acids is α2,3-linked[70]. Furthermore, potential fucosylation is predominantly α1,3-antennary, and located at the α2,3-sialylated antenna to form sialyl Lewis X, which itself is favored on the β1,4-linked N-acetylglucosamine of the α1,3-branch[70]. These fucosylated and non-fucosylated triantennary glycans are commonly expressed in minor amounts for sites that also have diantennary glycosylation (examples including alpha-1-antitrypsin and ceruloplasmin), but represent the most abundant glycosylation type for alpha-1-acid glycoprotein. Among the proteins covered in this review alpha-1-acid glycoprotein also stands out by expressing tetraantennary *N*-glycan species (also with potential sialyl-Lewis X). Other candidates likely to contain the larger tri- and tetraantennary structures are kininogen-1 and histidine-rich glycoprotein (judged by the difference between apparent and calculated mass), but this has not been confirmed yet, possibly due to the technical difficulty associated with the analysis of these glycosylations.

When combining the contributions of the 24 major glycoproteins covered in this review to calculate a theoretical total plasma *N*-glycome, a remarkable congruence is observed with a TPNG profile registered for *N*-glycans released from human plasma (**Figure 1** and **Figure 2**).

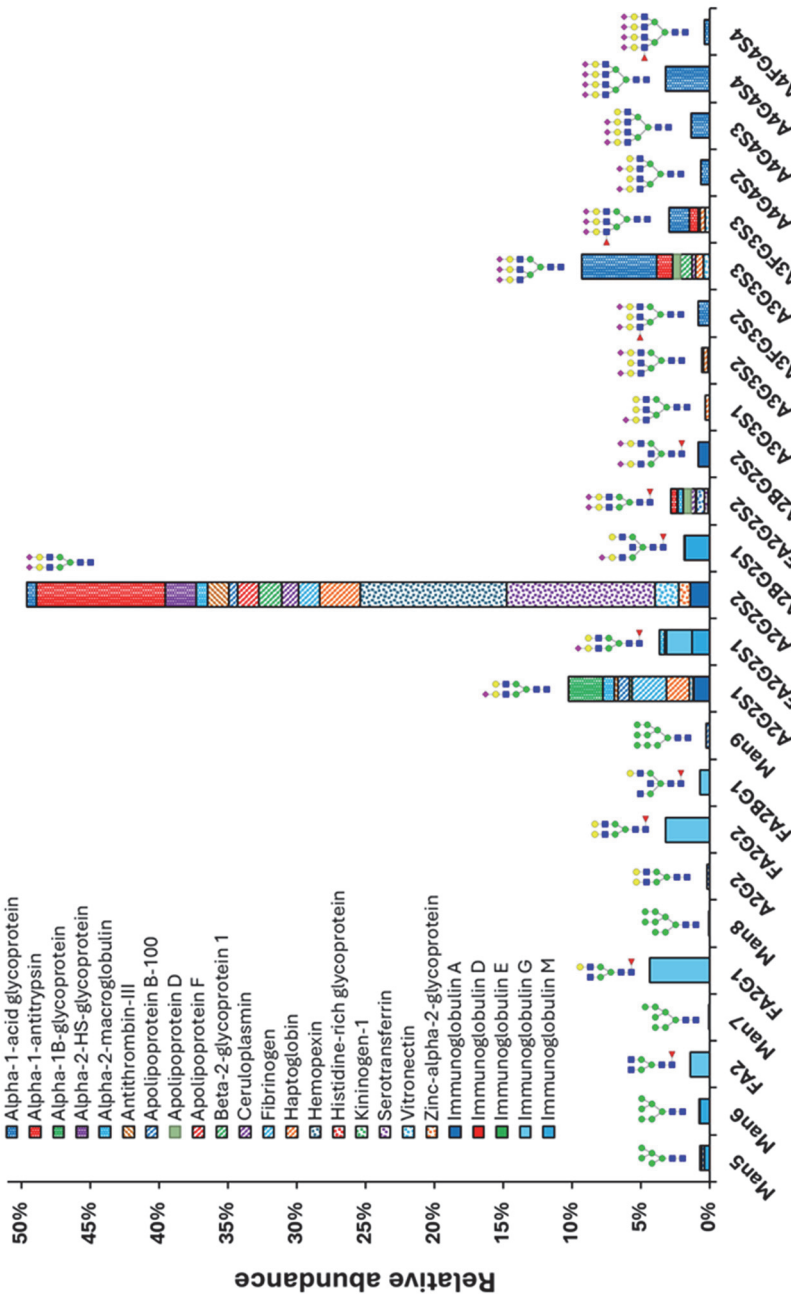

Figure 1. Schematic representation of the relative protein contribution to each specific glycan composition (cf. chapter introduction).

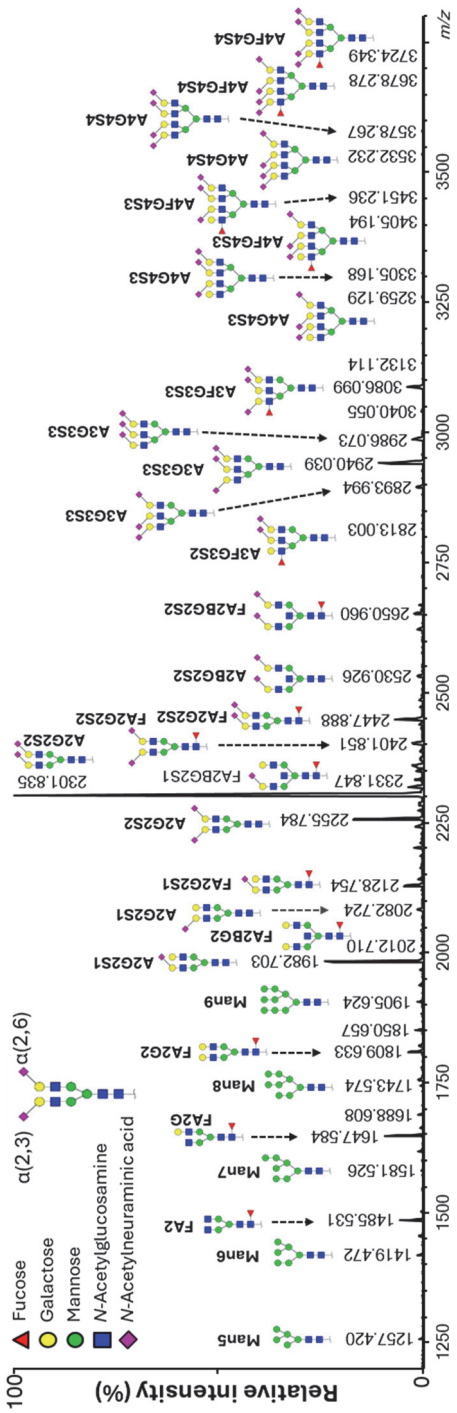

Figure 2. Typical reflectron positive mode MALDI-TOF-MS spectrum of the total *N*-glycosylation of pooled human plasma after enzymatic *N*-glycan release, ethyl esterification, and hydrophilic-interaction liquid chromatography (HILIC) enrichment[210]. *Glycan species are assigned as [M + Na]+ on basis of the reviewed plasma structures. Where multiple options are possible, the most abundant has been used for assignment. Sialic acid orientation is on basis of observed mass after ethyl esterification, while the other linkages are presumed on basis of literature. For fucosylation, diantennary structures are reported to mostly carry an α1,6-linked fucose on the reducing end N-acetylglucosamine, while tri- and tetraantennary structures are reported to mostly have α1,3-linked antennary fucosylation in the form of Lewis X (or sialyl-Lewis X when the antenna carries an α2,3-linked sialic acid). For the tri- and tetraantennary structures, antennae representation has been simplified for readability purposes.*

Truncated fucosylated diantennary structures, mono- and disialylated diantennaries, as well as tri- and tetraantennary structures and their relative fucosylation are roughly in the correct ratios when compared to MALDI-TOF-MS with sialic acid-linkage-specific stabilization. The differences between the theoretical and measured *N*-glycome could be due to variations in the sample types or origins used in each study, as we have seen that phenotypes could occur at different ratios among ethnicities, but also due to the approximations in the protein concentrations that are often values averaged from multiple papers, or even to the remaining low abundant glycoproteins not covered by this review, although they should only account for a few percent of the total plasma *N*-glycome.

In all, we expect the knowledge gathered in this review to facilitate the clinical interpretation of plasma-wide glycosylation analysis. This review underlines the necessity for further protein-specific glycosylation analysis to fill the still considerable gaps in our understanding.

Access to supplementary material:
https://link.springer.com/article/10.1007/s10719-015-9626-2

References

(1) Opdenakker, G.; Rudd, P. M.; Ponting, C. P.; Dwek, R. Concepts and principles of glycobiology. *The FASEB journal* **1993**, *7* (14), 1330-1337

(2) Rudd, P. M.; Elliott, T.; Cresswell, P.; Wilson, I. A.; Dwek, R. A. Glycosylation and the immune system. *Science* **2001**, *291* (5512), 2370-2376

(3) Taniguchi, N. Branched N-glycans and their implications for cell adhesion, signaling and clinical applications for cancer biomarkers and in therapeutics. *Biochemistry and Molecurar Biology Reports* **2011**, *44* (12), 772-781

(4) Sperandio, M.; Gleissner, C. A.; Ley, K. Glycosylation in immune cell trafficking. *Immunological Reviews* **2009**, *230* (1), 97-113

(5) Chen, Y.; Hojo, S.; Matsumoto, N.; Yamamoto, K. Regulation of Mac-2BP secretion is mediated by its N-glycan binding to ERGIC-53. *Glycobiology* **2013**, *23* (7), 904-916

(6) Varki, A.; Cummings, R. D.; Esko, J. D.; Stanley, P.; Hart, G. W.; Aebi, M.; Mohnen, D.; Kinoshita, T.; Packer, N. H.; Prestegard, J. H.; Schnaar, R. L.; Seeberger, P. H. *Essentials of Glycobiology 4th edition*; Cold Spring Harbor Laboratory Press, **2022**. DOI: 10.1101/9781621824213.

(7) Tams, J. W.; Vind, J.; Welinder, K. G. Adapting protein solubility by glycosylation.: N-Glycosylation mutants of Coprinus cinereus peroxidase in salt and organic solutions. *Biochimica et Biophysica Acta (BBA)-Protein Structure and Molecular Enzymology* **1999**, *1432* (2), 214-221

(8) Nagae, M.; Morita-Matsumoto, K.; Arai, S.; Wada, I.; Matsumoto, Y.; Saito, K.; Hashimoto, Y.; Yamaguchi, Y. Structural change of N-glycan exposes hydrophobic surface of human transferrin. *Glycobiology* **2014**,

(9) Varki, A. Biological roles of oligosaccharides: all of the theories are correct. *Glycobiology* **1993**, *3* (2), 97-130

(10) Molinari, M. N-glycan structure dictates extension of protein folding or onset of disposal. *Nat Chem Biol* **2007**, *3* (6), 313-320

(11) Harazono, A.; Kawasaki, N.; Kawanishi, T.; Hayakawa, T. Site-specific glycosylation analysis of human apolipoprotein B100 using LC/ESI MS/MS. *Glycobiology* **2005**, *15* (5), 447-462

(12) Hulsmeier, A. J.; Paesold-Burda, P.; Hennet, T. N-glycosylation site occupancy in serum glycoproteins using multiple reaction monitoring liquid chromatography-mass spectrometry. *Molecular & Cellular Proteomics* **2007**, *6* (12), 2132-2138

(13) Chandler, K. B.; Pompach, P.; Goldman, R.; Edwards, N. Exploring Site-Specific N-Glycosylation Microheterogeneity of Haptoglobin Using Glycopeptide CID Tandem Mass Spectra and Glycan Database Search. *Journal of proteome research* **2013**, *12* (8), 3652-3666

(14) Huffman, J. E.; Knezevic, A.; Vitart, V.; Kattla, J.; Adamczyk, B.; Novokmet, M.; Igl, W.; Pucic, M.; Zgaga, L.; Johannson, A.; Redzic, I.; Gornik, O.; Zemunik, T.; Polasek, O.; Kolcic, I.; Pehlic, M.; Koeleman, C. A.; Campbell, S.; Wild, S. H.; Hastie, N. D.; Campbell, H.; Gyllensten, U.; Wuhrer, M.; Wilson, J. F.; Hayward, C.; Rudan, I.; Rudd, P. M.; Wright, A. F.; Lauc, G. Polymorphisms in B3GAT1, SLC9A9 and MGAT5 are associated with variation within the human plasma N-glycome of 3533 European adults. *Human molecular genetics* **2011**, *20* (24), 5000-5011

(15) Ohtsubo, K.; Marth, J. D. Glycosylation in Cellular Mechanisms of Health and Disease. *Cell* **2006**, *126* (5), 855-867

(16) Thaysen-Andersen, M.; Packer, N. H. Site-specific glycoproteomics confirms that protein structure dictates formation of N-glycan type, core fucosylation and branching. *Glycobiology* **2012**, *22* (11), 1440-1452

(17) Wei, T.; Liu, Q.; He, F.; Zhu, W.; Hu, L.; Guo, L.; Zhang, J. The role of N-acetylglucosaminyltransferases V in the malignancy of human hepatocellular carcinoma. *Experimental and molecular pathology* **2012**, *93* (1), 8-17

(18) Gornik, O.; Wagner, J.; Pučić, M.; Knežević, A.; Redžić, I.; Lauc, G. Stability of N-glycan profiles in human plasma. *Glycobiology* **2009**, *19* (12), 1547-1553

(19) Dall'Olio, F.; Vanhooren, V.; Chen, C. C.; Slagboom, P. E.; Wuhrer, M.; Franceschi, C. N-glycomic biomarkers of biological aging and longevity: a link with inflammaging. *Ageing Res Rev* **2013**, *12* (2), 685-698

(20) Kristic, J.; Vuckovic, F.; Menni, C.; Klaric, L.; Keser, T.; Beceheli, I.; Pucic-Bakovic, M.; Novokmet, M.; Mangino, M.; Thaqi, K.; Rudan, P.; Novokmet, N.; Sarac, J.; Missoni, S.; Kolcic, I.; Polasek, O.; Rudan, I.; Campbell, H.; Hayward, C.; Aulchenko, Y.; Valdes, A.; Wilson, J. F.; Gornik, O.; Primorac, D.; Zoldos, V.; Spector, T.; Lauc, G. Glycans are a novel biomarker of chronological and biological ages. *The journals of gerontology. Series A, Biological sciences and medical sciences* **2014**, *69* (7), 779-789

(21) Lauc, G.; Huffman, J. E.; Pucic, M.; Zgaga, L.; Adamczyk, B.; Muzinic, A.; Novokmet, M.; Polasek, O.; Gornik, O.; Kristic, J.; Keser, T.; Vitart, V.; Scheijen, B.; Uh, H. W.; Molokhia, M.; Patrick, A. L.; McKeigue, P.; Kolcic, I.; Lukic, I. K.; Swann, O.; van Leeuwen, F. N.; Ruhaak, L. R.; Houwing-Duistermaat, J. J.; Slagboom, P. E.; Beekman, M.; de Craen, A. J.; Deelder, A. M.; Zeng, Q.; Wang, W.; Hastie, N. D.; Gyllensten, U.; Wilson, J. F.; Wuhrer, M.; Wright, A. F.; Rudd, P. M.; Hayward, C.; Aulchenko, Y.; Campbell, H.; Rudan, I. Loci associated with N-glycosylation of human immunoglobulin G show pleiotropy with autoimmune diseases and haematological cancers. *PLoS Genet* **2013**, *9* (1), e1003225

(22) Kobata, A. Glycobiology in the field of aging research--introduction to glycogerontology. *Biochimie* **2003**, *85* (1-2), 13-24

(23) Ruhaak, L. R.; Uh, H. W.; Beekman, M.; Hokke, C. H.; Westendorp, R. G.; Houwing-Duistermaat, J.; Wuhrer, M.; Deelder, A. M.; Slagboom, P. E. Plasma protein

N-glycan profiles are associated with calendar age, familial longevity and health. *Journal of proteome research* **2011**, *10* (4), 1667-1674

(24) Huhn, C.; Selman, M. H.; Ruhaak, L. R.; Deelder, A. M.; Wuhrer, M. IgG glycosylation analysis. *Proteomics* **2009**, *9* (4), 882-913

(25) Adamczyk, B.; Tharmalingam, T.; Rudd, P. M. Glycans as cancer biomarkers. *Biochim Biophys Acta* **2012**, *1820* (9), 1347-1353

(26) Freeze, H. H. Genetic defects in the human glycome. *Nat Rev Genet* **2006**, *7* (7), 537-551

(27) Jaeken, J.; Matthijs, G. Congenital disorders of glycosylation: a rapidly expanding disease family. *Annu. Rev. Genomics Hum. Genet.* **2007**, *8*, 261-278

(28) Bondt, A.; Selman, M. H.; Deelder, A. M.; Hazes, J. M.; Willemsen, S. P.; Wuhrer, M.; Dolhain, R. J. Association between galactosylation of immunoglobulin G and improvement of rheumatoid arthritis during pregnancy is independent of sialylation. *Journal of proteome research* **2013**, *12* (10), 4522-4531

(29) Weis, W.; Brown, J. H.; Cusack, S.; Paulson, J. C.; Skehel, J. J.; Wiley, D. C. Structure of the influenza virus haemagglutinin complexed with its receptor, sialic acid. *Nature* **1988**, *333* (6172), 426-431

(30) Shields, R. L.; Lai, J.; Keck, R.; O'Connell, L. Y.; Hong, K.; Meng, Y. G.; Weikert, S. H. A.; Presta, L. G. Lack of Fucose on Human IgG1 N-Linked Oligosaccharide Improves Binding to Human FcγRIII and Antibody-dependent Cellular Toxicity. *J Biol Chem* **2002**, *277* (30), 26733-26740

(31) Audfray, A.; Varrot, A.; Imberty, A. Bacteria love our sugars: Interaction between soluble lectins and human fucosylated glycans, structures, thermodynamics and design of competing glycocompounds. *Comptes Rendus Chimie* **2013**, *16* (5), 482-490

(32) Chen, K.; Xu, W.; Wilson, M.; He, B.; Miller, N. W.; Bengten, E.; Edholm, E. S.; Santini, P. A.; Rath, P.; Chiu, A.; Cattalini, M.; Litzman, J.; J, B. B.; Huang, B.; Meini, A.; Riesbeck, K.; Cunningham-Rundles, C.; Plebani, A.; Cerutti, A. Immunoglobulin D enhances immune surveillance by activating antimicrobial, proinflammatory and B cell-stimulating programs in basophils. *Nature immunology* **2009**, *10* (8), 889-898

(33) Nimmerjahn, F.; Ravetch, J. V. Anti-inflammatory actions of intravenous immunoglobulin. *Annual review of immunology* **2008**, *26*, 513-533

(34) Huttenhain, R.; Surinova, S.; Ossola, R.; Sun, Z.; Campbell, D.; Cerciello, F.; Schiess, R.; Bausch-Fluck, D.; Rosenberger, G.; Chen, J. C.; Rinner, O.; Kusebauch, U.; Hajduch, M.; Moritz, R. L.; Wollscheid, B.; Aebersold, R. N-Glycoprotein SRMAtlas A RESOURCE OF MASS SPECTROMETRIC ASSAYS FOR N-GLYCOSITES ENABLING CONSISTENT AND MULTIPLEXED PROTEIN QUANTIFICATION FOR CLINICAL APPLICATIONS. *Molecular & Cellular Proteomics* **2013**, *12* (4), 1005-1016

(35) Dalziel, M.; Crispin, M.; Scanlan, C. N.; Zitzmann, N.; Dwek, R. A. Emerging Principles for the Therapeutic Exploitation of Glycosylation. *Science* **2014**, *343* (6166), 1235681

(36) Larkin, A.; Imperiali, B. The expanding horizons of asparagine-linked glycosylation. *Biochemistry-Us* **2011**, *50* (21), 4411-4426

(37) Marino, K.; Bones, J.; Kattla, J. J.; Rudd, P. M. A systematic approach to protein glycosylation analysis: a path through the maze. *Nat Chem Biol* **2010**, *6* (10), 713-723

(38) Bladergroen, M. R.; Reiding, K. R.; Hipgrave Ederveen, A. L.; Vreeker, G. C.; Clerc, F.; Holst, S.; Bondt, A.; Wuhrer, M.; van der Burgt, Y. E. Automation of High-Throughput Mass Spectrometry-Based Plasma N-Glycome Analysis with Linkage-Specific Sialic Acid Esterification. *Journal of proteome research* **2015**, *14* (9), 4080-4086

(39) Stockmann, H.; Duke, R. M.; Millan Martin, S.; Rudd, P. M. Ultrahigh Throughput, Ultrafiltration-Based N-Glycomics Platform for Ultraperformance Liquid Chromatography (ULTRA(3)). *Anal Chem* **2015**, *87* (16), 8316-8322

(40) Klein, A. Human Total Serum N-Glycome. *Adv Clin Chem* **2008**, *46*, 51-85

(41) Van Slyke, D. D.; Hiller, A.; Phillips, R. A.; Hamilton, P. B.; Dole, V. P.; Archibald, R. M.; Eder, H. A. The estimation of plasma protein concentration from plasma specific gravity. *J Biol Chem* **1950**, *183*, 331-347

(42) Dill, D.; Costill, D. L. Calculation of percentage changes in volumes of blood, plasma, and red cells in dehydration. *Journal of applied physiology* **1974**, *37* (2), 247-248

(43) Peters Jr, T. *All about albumin: biochemistry, genetics, and medical applications*; Academic press, **1995**.

(44) Schmid, K.; Kaufmann, H.; Isemura, S.; Bauer, F.; Emura, J.; Motoyama, T.; Ishiguro, M.; Nanno, S. Structure of α1-acid glycoprotein. Complete amino acid sequence, multiple amino acid substitutions, and homology with the immunoglobulins. *Biochemistry-Us* **1973**, *12* (14), 2711-2724

(45) Kushner, I. The phenomenon of the acute phase response. *Annals of the New York Academy of Sciences* **1982**, *389* (1), 39-48

(46) Blain, P. G.; Mucklow, J. C.; Rawlins, M. D.; Roberts, D. F.; Routledge, P. A.; Shand, D. G. Determinants of plasma alpha 1-acid glycoprotein (AAG) concentrations in health. *British Journal of Clinical Pharmacology* **1985**, *20* (5), 500-502

(47) Fournier, T.; Medjoubi-N, N.; Porquet, D. Alpha-1-acid glycoprotein. *Biochimica et Biophysica Acta (BBA)-Protein Structure and Molecular Enzymology* **2000**, *1482* (1), 157-171

(48) Williams, J. P.; Weiser, M. R.; Pechet, T. T. V.; Kobzik, L.; Moore, F. D.; Hechtman, H. B. *α1-Acid glycoprotein reduces local and remote injuries after intestinal ischemia in the rat*; **1997**.

(49) Dage, J. L.; Ackermann, B. L.; Halsall, H. B. Site localization of sialyl Lewisx antigen on α1-acid glycoprotein by high performance liquid chromatography-electrospray mass spectrometry. *Glycobiology* **1998**, *8* (8), 755-760

(50) Imre, T.; Kremmer, T.; Heberger, K.; Molnár-Szöllősi, É.; Ludanyi, K.; Pocsfalvi, G.; Malorni, A.; Drahos, L.; Vekey, K. Mass spectrometric and linear discriminant analysis of N-glycans of human serum alpha-1-acid glycoprotein in cancer patients and healthy individuals. *Journal of proteomics* **2008**, *71* (2), 186-197

(51) Van Dijk, W.; Havenaar, E.; Brinkman-Van der Linden, E. α1-Acid glycoprotein (orosomucoid): pathophysiological changes in glycosylation in relation to its function. *Glycoconjugate J* **1995**, *12* (3), 227-233

(52) Brinkman-van der Linden, E. C.; van Ommen, E. C.; van Dijk, W. Glycosylation of alpha 1-acid glycoprotein in septic shock: changes in degree of branching and in expression of sialyl Lewis(x) groups. *Glycoconjugate J* **1996**, *13* (1), 27-31

(53) Havenaar, E. C.; Axford, J. S.; Brinkman-van der Linden, E. C.; Alavi, A.; Van Ommen, E. C.; van het Hof, B.; Spector, T.; Mackiewicz, A.; Van Dijk, W. Severe rheumatoid arthritis prohibits the pregnancy-induced decrease in alpha3-fucosylation of alpha1-acid glycoprotein. *Glycoconjugate J* **1998**, *15* (7), 723-729

(54) Wieruszeski, J. M.; Fournet, B.; Konan, D.; Biou, D.; Durand, G. 400-MHz 1H-NMR spectroscopy of fucosylated tetrasialyl oligosaccharides isolated from normal and cirrhotic α1-acid glycoprotein. *Febs Lett* **1988**, *238* (2), 390-394

(55) Ryden, I.; Pahlsson, P.; Lundblad, A.; Skogh, T. Fucosylation of alpha1-acid glycoprotein (orosomucoid) compared with traditional biochemical markers of inflammation in recent onset rheumatoid arthritis. *Clin Chim Acta* **2002**, *317* (1-2), 221-229

(56) Carrell, R. W.; Jeppsson, J. O.; Laurell, C. B.; Brennan, S. O.; Owen, M. C.; Vaughan, L.; Boswell, D. R. Structure and Variation of Human Alpha-1-Antitrypsin. *Nature* **1982**, *298* (5872), 329-334

(57) van Furth, R.; Kramps, J. A.; Diesselhof-den Dulk, M. M. Synthesis of alpha 1-anti-trypsin by human monocytes. *Clin Exp Immunol* **1983**, *51* (3), 551-557

(58) Perlmutter, D. H.; Kay, R. M.; Cole, F. S.; Rossing, T. H.; Van Thiel, D.; Colten, H. R. The cellular defect in alpha 1-proteinase inhibitor (alpha 1-PI) deficiency is expressed in human monocytes and in Xenopus oocytes injected with human liver mRNA. *Proceedings of the National Academy of Sciences* **1985**, *82* (20), 6918-6921

(59) Perlmutter, D. H.; Daniels, J. D.; Auerbach, H. S.; De Schryver-Kecskemeti, K.; Winter, H. S.; Alpers, D. H. The alpha 1-antitrypsin gene is expressed in a human intestinal epithelial cell line. *J Biol Chem* **1989**, *264* (16), 9485-9490

(60) Twining, S. S.; Fukuchi, T.; Yue, B. Y.; Wilson, P. M.; Boskovic, G. Corneal synthesis of alpha 1-proteinase inhibitor (alpha 1-antitrypsin). *Investigative ophthalmology & visual science* **1994**, *35* (2), 458-462

(61) Haab, B. B.; Geierstanger, B. H.; Michailidis, G.; Vitzthum, F.; Forrester, S.; Okon, R.; Saviranta, P.; Brinker, A.; Sorette, M.; Perlee, L.; Suresh, S.; Drwal, G.; Adkins, J. N.; Omenn, G. S. Immunoassay and antibody microarray analysis of the HUPO Plasma Proteome Project reference specimens: Systematic variation between sample types and calibration of mass spectrometry data. *Proteomics* **2005**, *5* (13), 3278-3291

(62) Kalsheker, N.; Morley, S.; Morgan, K. Gene regulation of the serine proteinase inhibitors alpha1-antitrypsin and alpha1-antichymotrypsin. *Biochem Soc Trans* **2002**, *30* (2), 93-98

(63) Perlmutter, D. H. Liver injury in alpha1-antitrypsin deficiency: an aggregated protein induces mitochondrial injury. *J Clin Invest* **2002**, *110* (11), 1579-1583

(64) Boskovic, G.; Twining, S. S. Retinol and retinaldehyde specifically increase alpha1-proteinase inhibitor in the human cornea. *Biochem J* **1997**, *322 (Pt 3)*, 751-756

(65) Beatty, K.; Bieth, J.; Travis, J. Kinetics of association of serine proteinases with native and oxidized alpha-1-proteinase inhibitor and alpha-1-antichymotrypsin. *J Biol Chem* **1980**, *255* (9), 3931-3934

(66) Carrell, R.; Travis, J. αAntitrypsin and the serpins: variation and countervariation. *Trends in Biochemical Sciences* **1985**, *10* (1), 20-24

(67) Bergin, D. A.; Hurley, K.; McElvaney, N. G.; Reeves, E. P. Alpha-1 antitrypsin: a potent anti-inflammatory and potential novel therapeutic agent. *Archivum immunologiae et therapiae experimentalis* **2012**, *60* (2), 81-97

(68) Grimstein, C.; Choi, Y.-K.; Wasserfall, C. H.; Satoh, M.; Atkinson, M. A.; Brantly, M. L.; Campbell-Thompson, M.; Song, S. Alpha-1 antitrypsin protein and gene therapies decrease autoimmunity and delay arthritis development in mouse model. *J Transl Med* **2011**, *9* (21), 1-13

(69) Mega, T.; Lujan, E.; Yoshida, A. Studies on the oligosaccharide chains of human alpha 1-protease inhibitor. I. Isolation of glycopeptides. *J Biol Chem* **1980**, *255* (9), 4053-4056

(70) Kolarich, D.; Weber, A.; Turecek, P. L.; Schwarz, H.-P.; Altmann, F. Comprehensive glyco-proteomic analysis of human α1-antitrypsin and its charge isoforms. *Proteomics* **2006**, *6* (11), 3369-3380

(71) Mills, K.; Mills, P. B.; Clayton, P. T.; Johnson, A. W.; Whitehouse, D. B.; Winchester, B. G. Identification of alpha(1)-antitrypsin variants in plasma with the use of proteomic technology. *Clin Chem* **2001**, *47* (11), 2012-2022

(72) Ruhaak, L. R.; Koeleman, C. A.; Uh, H.-W.; Stam, J. C.; van Heemst, D.; Maier, A. B.; Houwing-Duistermaat, J. J.; Hensbergen, P. J.; Slagboom, P. E.; Deelder, A. M. Targeted Biomarker Discovery by High Throughput Glycosylation Profiling of Human Plasma Alpha1-Antitrypsin and Immunoglobulin A. *Plos One* **2013**, *8* (9), e73082

(73) Mills, K.; Mills, P. B.; Clayton, P. T.; Mian, N.; Johnson, A. W.; Winchester, B. G. The underglycosylation of plasma alpha(1)-antitrypsin in congenital disorders of glycosylation type I is not random. *Glycobiology* **2003**, *13* (2), 73-85

(74) Ishioka, N.; Takahashi, N.; Putnam, F. W. Amino acid sequence of human plasma alpha 1B-glycoprotein: homology to the immunoglobulin supergene family. *Proc Natl Acad Sci U S A* **1986**, *83* (8), 2363-2367

(75) Mele, M.; Ferreira, P. G.; Reverter, F.; DeLuca, D. S.; Monlong, J.; Sammeth, M.; Young, T. R.; Goldmann, J. M.; Pervouchine, D. D.; Sullivan, T. J.; Johnson, R.; Segre, A. V.; Djebali, S.; Niarchou, A.; Consortium, G. T.; Wright, F. A.; Lappalainen, T.; Calvo, M.; Getz, G.; Dermitzakis, E. T.; Ardlie, K. G.; Guigo, R. Human genomics. The human transcriptome across tissues and individuals. *Science* **2015**, *348* (6235), 660-665

(76) Udby, L.; Sørensen, O. E.; Pass, J.; Johnsen, A. H.; Behrendt, N.; Borregaard, N.; Kjeldsen, L. Cysteine-rich secretory protein 3 is a ligand of alpha1B-glycoprotein in human plasma. *Biochemistry-Us* **2004**, *43* (40), 12877-12886

(77) Zeng, Z.; Hincapie, M.; Haab, B. B.; Hanash, S.; Pitteri, S. J.; Kluck, S.; Hogan, J. M.; Kennedy, J.; Hancock, W. S. The development of an integrated platform to identify breast cancer glycoproteome changes in human serum. *J Chromatogr A* **2010**, *1217* (19), 3307-3315

(78) Yoon, S. Y.; Kim, J. M.; Oh, J. H.; Jeon, Y. J.; Lee, D. S.; Kim, J. H.; Choi, J. Y.; Ahn, B. M.; Kim, S.; Yoo, H. S.; Kim, Y. S.; Kim, N. S. Gene expression profiling of human HBV- and/or HCV-associated hepatocellular carcinoma cells using expressed sequence tags. *Int J Oncol* **2006**, *29* (2), 315-327

(79) Tian, M.; Cui, Y. Z.; Song, G. H.; Zong, M. J.; Zhou, X. Y.; Chen, Y.; Han, J. X. Proteomic analysis identifies MMP-9, DJ-1 and A1BG as overexpressed proteins in pancreatic juice from pancreatic ductal adenocarcinoma patients. *BMC Cancer* **2008**, *8*, 241

(80) Kreunin, P.; Zhao, J.; Rosser, C.; Urquidi, V.; Lubman, D. M.; Goodison, S. Bladder cancer associated glycoprotein signatures revealed by urinary proteomic profiling. *Journal of proteome research* **2007**, *6* (7), 2631-2639

(81) Piyaphanee, N.; Ma, Q.; Kremen, O.; Czech, K.; Greis, K.; Mitsnefes, M.; Devarajan, P.; Bennett, M. R. Discovery and initial validation of alpha 1-B glycoprotein fragmentation as a differential urinary biomarker in pediatric steroid-

resistant nephrotic syndrome. *Proteomics. Clinical applications* **2011**, *5* (5-6), 334-342

(82) Biswas, S.; Sharma, S.; Saroha, A.; Bhakuni, D.; Malhotra, R.; Zahur, M.; Oellerich, M.; Das, H. R.; Asif, A. R. Identification of novel autoantigen in the synovial fluid of rheumatoid arthritis patients using an immunoproteomics approach. *Plos One* **2013**, *8* (2), e56246

(83) Bunkenborg, J.; Pilch, B. J.; Podtelejnikov, A. V.; Wisniewski, J. R. Screening for N-glycosylated proteins by liquid chromatography mass spectrometry. *Proteomics* **2004**, *4* (2), 454-465

(84) Liu, T.; Qian, W.-J.; Gritsenko, M. A.; Camp, D. G.; Monroe, M. E.; Moore, R. J.; Smith, R. D. Human Plasma N-Glycoproteome Analysis by Immunoaffinity Subtraction, Hydrazide Chemistry, and Mass Spectrometry. *Journal of proteome research* **2005**, *4* (6), 2070-2080

(85) Huang, J.; Lee, H.; Zivkovic, A. M.; Smilowitz, J. T.; Rivera, N.; German, J. B.; Lebrilla, C. B. Glycomic analysis of high density lipoprotein shows a highly sialylated particle. *Journal of proteome research* **2014**, *13* (2), 681-691

(86) Nilsson, J.; Rüetschi, U.; Halim, A.; Hesse, C.; Carlsohn, E.; Brinkmalm, G.; Larson, G. Enrichment of glycopeptides for glycan structure and attachment site identification. *Nature methods* **2009**, *6* (11), 809-811

(87) Brown, W. M.; Dziegielewska, K. M.; Saunders, N. R.; Christie, D. L.; Nawratil, P.; Muller-Esterl, W. The nucleotide and deduced amino acid structures of sheep and pig fetuin. Common structural features of the mammalian fetuin family. *Eur J Biochem* **1992**, *205* (1), 321-331

(88) Yoshioka, Y.; Gejyo, F.; Marti, T.; Rickli, E. E.; Burgi, W.; Offner, G. D.; Troxler, R. F.; Schmid, K. The complete amino acid sequence of the A-chain of human plasma alpha 2HS-glycoprotein. *J Biol Chem* **1986**, *261* (4), 1665-1676

(89) Gejyo, F.; Chang, J. L.; Burgi, W.; Schmid, K.; Offner, G. D.; Troxler, R. F.; Van Halbeek, H.; Dorland, L.; Gerwig, G. J.; Vliegenthart, J. F. Characterization of the B-chain of human plasma alpha 2HS-glycoprotein. The complete amino acid sequence and primary structure of its heteroglycan. *J Biol Chem* **1983**, *258* (8), 4966-4971

(90) Lebreton, J. P.; Joisel, F.; Raoult, J. P.; Lannuzel, B.; Rogez, J. P.; Humbert, G. Serum concentration of human alpha 2 HS glycoprotein during the inflammatory process: evidence that alpha 2 HS glycoprotein is a negative acute-phase reactant. *J Clin Invest* **1979**, *64* (4), 1118-1129

(91) Haglund, A. C.; Ek, B.; Ek, P. Phosphorylation of human plasma alpha2-Heremans-Schmid glycoprotein (human fetuin) in vivo. *Biochem J* **2001**, *357* (Pt 2), 437-445

(92) Brylka, L.; Jahnen-Dechent, W. The role of fetuin-A in physiological and pathological mineralization. *Calcified tissue international* **2013**, *93* (4), 355-364

(93) Jahnen-Dechent, W.; Heiss, A.; Schafer, C.; Ketteler, M. Fetuin-A regulation of calcified matrix metabolism. *Circ Res* **2011**, *108* (12), 1494-1509

(94) Ray, S.; Lukyanov, P.; Ochieng, J. Members of the cystatin superfamily interact with MMP-9 and protect it from autolytic degradation without affecting its gelatinolytic activities. *Biochim Biophys Acta* **2003**, *1652* (2), 91-102

(95) Mathews, S. T.; Chellam, N.; Srinivas, P. R.; Cintron, V. J.; Leon, M. A.; Goustin, A. S.; Grunberger, G. Alpha2-HSG, a specific inhibitor of insulin receptor autophosphorylation, interacts with the insulin receptor. *Molecular and cellular endocrinology* **2000**, *164* (1-2), 87-98

(96) Ix, J. H.; Sharma, K. Mechanisms linking obesity, chronic kidney disease, and fatty liver disease: the roles of fetuin-A, adiponectin, and AMPK. *Journal of the American Society of Nephrology : JASN* **2010**, *21* (3), 406-412

(97) Wang, H.; Zhang, M.; Soda, K.; Sama, A.; Tracey, K. J. Fetuin protects the fetus from TNF. *Lancet* **1997**, *350* (9081), 861-862

(98) Watzlawick, H.; Walsh, M. T.; Yoshioka, Y.; Schmid, K.; Brossmer, R. Structure of the N- and O-glycans of the A-chain of human plasma alpha 2HS-glycoprotein as deduced from the chemical compositions of the derivatives prepared by stepwise degradation with exoglycosidases. *Biochemistry-Us* **1992**, *31* (48), 12198-12203

(99) Wilson, N. L.; Schulz, B. L.; Karlsson, N. G.; Packer, N. H. Sequential analysis of N- and O-linked glycosylation of 2D-PAGE separated glycoproteins. *Journal of proteome research* **2002**, *1* (6), 521-529

(100) Jia, W.; Lu, Z.; Fu, Y.; Wang, H. P.; Wang, L. H.; Chi, H.; Yuan, Z. F.; Zheng, Z. B.; Song, L. N.; Han, H. H.; Liang, Y. M.; Wang, J. L.; Cai, Y.; Zhang, Y. K.; Deng, Y. L.; Ying, W. T.; He, S. M.; Qian, X. H. A Strategy for Precise and Large Scale Identification of Core Fucosylated Glycoproteins. *Molecular & Cellular Proteomics* **2009**, *8* (5), 913-923

(101) Kontro, H.; Joenvaara, S.; Haglund, C.; Renkonen, R. Comparison of sialylated N-glycopeptide levels in serum of pancreatic cancer patients, acute pancreatitis patients, and healthy controls. *Proteomics* **2014**, *14* (15), 1713-1723

(102) Sottrup-Jensen, L.; Stepanik, T. M.; Kristensen, T.; Wierzbicki, D. M.; Jones, C. M.; Lonblad, P. B.; Magnusson, S.; Petersen, T. E. Primary structure of human alpha 2-macroglobulin. V. The complete structure. *The Journal of biological chemistry* **1984**, *259* (13), 8318-8327

(103) Coan, M. H.; Roberts, R. C. A redetermination of the concentration of alpha 2-macroglobulin in human plasma. *Biological chemistry Hoppe-Seyler* **1989**, *370* (7), 673-676

(104) Gonias, S. L.; Pizzo, S. V. Conformation and protease binding activity of binary and ternary human alpha 2-macroglobulin-protease complexes. *J Biol Chem* **1983**, *258* (23), 14682-14685

(105) Thieme, R.; Kurz, S.; Kolb, M.; Debebe, T.; Holtze, S.; Morhart, M.; Huse, K.; Szafranski, K.; Platzer, M.; Hildebrandt, T. B.; Birkenmeier, G. Analysis of Alpha-2 Macroglobulin from the Long-Lived and Cancer-Resistant Naked Mole-Rat and Human Plasma. *Plos One* **2015**, *10* (6), e0130470

(106) Borth, W. Alpha 2-macroglobulin, a multifunctional binding protein with targeting characteristics. *Faseb J* **1992**, *6* (15), 3345-3353

(107) Chen, R.; Jiang, X.; Sun, D.; Han, G.; Wang, F.; Ye, M.; Wang, L.; Zou, H. Glycoproteomics Analysis of Human Liver Tissue by Combination of Multiple Enzyme Digestion and Hydrazide Chemistry. *Journal of proteome research* **2009**, *8* (2), 651-661

(108) Lin, Z.; Lo, A.; Simeone, D. M.; Ruffin, M. T.; Lubman, D. M. An N-glycosylation analysis of human alpha-2-macroglobulin using an integrated approach. *J Proteomics Bioinform* **2012**, *5*, 127

(109) Arnold, J. N.; Wallis, R.; Willis, A. C.; Harvey, D. J.; Royle, L.; Dwek, R. A.; Rudd, P. M.; Sim, R. B. Interaction of mannan binding lectin with alpha2 macroglobulin via exposed oligomannose glycans: a conserved feature of the thiol ester protein family? *The Journal of biological chemistry* **2006**, *281* (11), 6955-6963

(110) Panzironi, C.; Silvestrini, B.; Mo, M. Y.; Lahita, R.; Mruk, D.; Cheng, C. Y. An increase in the carbohydrate moiety of alpha 2-macroglobulin is associated with systemic lupus erythematosus (SLE). *Biochem Mol Biol Int* **1997**, *43* (6), 1305-1322

(111) Gunnarsson, M.; Stigbrand, T.; Jensen, P. E. Aberrant forms of alpha(2)-macroglobulin purified from patients with multiple sclerosis. *Clinica chimica acta; international journal of clinical chemistry* **2000**, *295* (1-2), 27-40

(112) Bock, S. C.; Wion, L. L.; Vehar, G. A.; Lawn, R. M. Cloning and expression of the cDNA for human antithrombin III. *Nucleic Acids Res* **1982**, *10* (24), 8113-8125

(113) Koide, T. Isolation and characterization of antithrombin III from human, porcine and rabbit plasma, and rat serum. *Journal of biochemistry* **1979**, *86* (6), 1841-1850

(114) Chandra, T.; Stackhouse, R.; Kidd, V. J.; Woo, S. L. Isolation and sequence characterization of a cDNA clone of human antithrombin III. *Proc Natl Acad Sci U S A* **1983**, *80* (7), 1845-1848

(115) Conard, J.; Brosstad, F.; Lie Larsen, M.; Samama, M.; Abildgaard, U. Molar antithrombin concentration in normal human plasma. *Haemostasis* **1983**, *13* (6), 363-368

(116) Demelbauer, U. M.; Plematl, A.; Kremser, L.; Allmaier, G.; Josic, D.; Rizzi, A. Characterization of glyco isoforms in plasma-derived human antithrombin by on-line

capillary zone electrophoresis-electrospray ionization-quadrupole ion trap-mass spectrometry of the intact glycoproteins. *Electrophoresis* **2004**, *25* (13), 2026-2032

(117) Maclean, P. S.; Tait, R. C. Hereditary and acquired antithrombin deficiency: epidemiology, pathogenesis and treatment options. *Drugs* **2007**, *67* (10), 1429-1440

(118) Rosenberg, R. D.; Damus, P. S. The purification and mechanism of action of human antithrombin-heparin cofactor. *J Biol Chem* **1973**, *248* (18), 6490-6505

(119) Rosenberg, J. S.; McKenna, P. W.; Rosenberg, R. D. Inhibition of human factor IXa by human antithrombin. *J Biol Chem* **1975**, *250* (23), 8883-8888

(120) Demelbauer, U. M.; Plematl, A.; Josic, D.; Allmaier, G.; Rizzi, A. On the variation of glycosylation in human plasma derived antithrombin. *J Chromatogr A* **2005**, *1080* (1), 15-21

(121) Patnaik, M. M.; Moll, S. Inherited antithrombin deficiency: a review. *Haemophilia : the official journal of the World Federation of Hemophilia* **2008**, *14* (6), 1229-1239

(122) Turk, B.; Brieditis, I.; Bock, S. C.; Olson, S. T.; Bjork, I. The oligosaccharide side chain on Asn-135 of alpha-antithrombin, absent in beta-antithrombin, decreases the heparin affinity of the inhibitor by affecting the heparin-induced conformational change. *Biochemistry-Us* **1997**, *36* (22), 6682-6691

(123) Peterson, C. B.; Blackburn, M. N. Isolation and characterization of an antithrombin III variant with reduced carbohydrate content and enhanced heparin binding. *J Biol Chem* **1985**, *260* (1), 610-615

(124) Kasturi, L.; Eshleman, J. R.; Wunner, W. H.; Shakin-Eshleman, S. H. The hydroxy amino acid in an Asn-X-Ser/Thr sequon can influence N-linked core glycosylation efficiency and the level of expression of a cell surface glycoprotein. *J Biol Chem* **1995**, *270* (24), 14756-14761

(125) Picard, V.; Ersdal-Badju, E.; Bock, S. C. Partial glycosylation of antithrombin III asparagine-135 is caused by the serine in the third position of its N-glycosylation consensus sequence and is responsible for production of the beta-antithrombin III isoform with enhanced heparin affinity. *Biochemistry-Us* **1995**, *34* (26), 8433-8440

(126) Pol-Fachin, L.; Franco Becker, C.; Almeida Guimarães, J.; Verli, H. Effects of glycosylation on heparin binding and antithrombin activation by heparin. *Proteins* **2011**, *79* (9), 2735-2745

(127) Franzén, L. E.; Svensson, S.; Larm, O. Structural studies on the carbohydrate portion of human antithrombin III. *J Biol Chem* **1980**, *255* (11), 5090-5093

(128) Mizuochi, T.; Fujii, J.; Kurachi, K.; Kobata, A. Structural studies of the carbohydrate moiety of human antithrombin III. *Archives of biochemistry and biophysics* **1980**, *203* (1), 458-465

(129) Demelbauer, U. M.; Zehl, M.; Plematl, A.; Allmaier, G.; Rizzi, A. Determination of glycopeptide structures by multistage mass spectrometry with low-energy collision-induced dissociation: comparison of electrospray ionization quadrupole ion trap and matrix-assisted laser desorption/ionization quadrupole ion trap reflectron time-of-flight approaches. *Rapid communications in mass spectrometry : RCM* **2004**, *18* (14), 1575-1582

(130) Plematl, A.; Demelbauer, U. M.; Josic, D.; Rizzi, A. Determination of the site-specific and isoform-specific glycosylation in human plasma-derived antithrombin by IEF and capillary HPLC-ESI-MS/MS. *Proteomics* **2005**, *5* (15), 4025-4033

(131) Martínez-Martínez, I.; Ordóñez, A.; Navarro-Fernández, J.; Pérez-Lara, A.; Gutiérrez-Gallego, R.; Giraldo, R.; Martínez, C.; Llop, E.; Vicente, V.; Corral, J. Antithrombin Murcia (K241E) causing antithrombin deficiency: a possible role for altered glycosylation. *Haematologica* **2010**, *95* (8), 1358-1365

(132) Johs, A.; Hammel, M.; Waldner, I.; May, R. P.; Laggner, P.; Prassl, R. Modular structure of solubilized human apolipoprotein B-100. Low resolution model revealed by small angle neutron scattering. *J Biol Chem* **2006**, *281* (28), 19732-19739

(133) Yang, C. Y.; Gu, Z. W.; Weng, S. A.; Kim, T. W.; Chen, S. H.; Pownall, H. J.; Sharp, P. M.; Liu, S. W.; Li, W. H.; Gotto, A. M.; Chan, L. Structure of Apolipoprotein B-100 of Human Low-Density Lipoproteins. *Arteriosclerosis* **1989**, *9* (1), 96-108

(134) Chen, S.-H.; Habib, G.; Yang, C.-Y.; Gu, Z.-W.; Lee, B. R.; Weng, S.-A.; Cai, S.; Deslypere, J.; Rosseneu, M. Apolipoprotein B-48 is the product of a messenger RNA with an organ-specific in-frame stop codon. *Science* **1987**, *238* (4825), 363-366

(135) Young, S. G.; Bertics, S. J.; Scott, T. M.; Dubois, B. W.; Curtiss, L. K.; Witztum, J. L. Parallel expression of the MB19 genetic polymorphism in apoprotein B-100 and apoprotein B-48. Evidence that both apoproteins are products of the same gene. *J Biol Chem* **1986**, *261* (7), 2995-2998

(136) Levy, E.; Marcel, Y.; Deckelbaum, R. J.; Milne, R.; Lepage, G.; Seidman, E.; Bendayan, M.; Roy, C. C. Intestinal apoB synthesis, lipids, and lipoproteins in chylomicron retention disease. *J Lipid Res* **1987**, *28* (11), 1263-1274

(137) McQueen, M. J.; Hawken, S.; Wang, X.; Ounpuu, S.; Sniderman, A.; Probstfield, J.; Steyn, K.; Sanderson, J. E.; Hasani, M.; Volkova, E.; Kazmi, K.; Yusuf, S. Lipids, lipoproteins, and apolipoproteins as risk markers of myocardial infarction in 52 countries (the INTERHEART study): a case-control study. *The Lancet* **2008**, *372* (9634), 224-233

(138) Cnop, M.; Havel, P.; Utzschneider, K.; Carr, D.; Sinha, M.; Boyko, E.; Retzlaff, B.; Knopp, R.; Brunzell, J.; Kahn, S. E. Relationship of adiponectin to body fat distribution, insulin sensitivity and plasma lipoproteins: evidence for independent roles of age and sex. *Diabetologia* **2003**, *46* (4), 459-469

(139) Olofsson, S. O.; Boren, J. Apolipoprotein B Secretory Regulation by Degradation. *Arterioscl Throm Vas* **2012**, *32* (6), 1334-1338

(140) Olofsson, S. O.; Bjursell, G.; Bostrom, K.; Carlsson, P.; Elovson, J.; Protter, A. A.; Reuben, M. A.; Bondjers, G. Apolipoprotein-B - Structure, Biosynthesis and Role in the Lipoprotein Assembly Process. *Atherosclerosis* **1987**, *68* (1-2), 1-17

(141) Vukmirica, J.; Nishimaki-Mogami, T.; Tran, K.; Shan, J.; McLeod, R. S.; Yuan, J.; Yao, Z. The N-linked oligosaccharides at the amino terminus of human apoB are important for the assembly and secretion of VLDL. *J Lipid Res* **2002**, *43* (9), 1496-1507

(142) Garner, B.; Harvey, D. J.; Royle, L.; Frischmann, M.; Nigon, F.; Chapman, M. J.; Rudd, P. M. Characterization of human apolipoprotein B100 oligosaccharides in LDL subfractions derived from normal and hyperlipidemic plasa: deficiency of alpha-N-acetylneuraminyllactosyl-ceramide in light and small dense LDL particles. *Glycobiology* **2001**, *11* (10), 791-802

(143) Garner, B.; Merry, A. H.; Royle, L.; Harvey, D. J.; Rudd, P. M.; Thillet, J. Structural Elucidation of the N-andO-Glycans of Human Apolipoprotein (a) ROLE OF O-GLYCANS IN CONFERRING PROTEASE RESISTANCE. *J Biol Chem* **2001**, *276* (25), 22200-22208

(144) Tarugi, P.; Lonardo, A.; Gabelli, C.; Sala, F.; Ballarini, G.; Cortella, I.; Previato, L.; Bertolini, S.; Cordera, R.; Calandra, S. Phenotypic expression of familial hypobetalipoproteinemia in three kindreds with mutations of apolipoprotein B gene. *J Lipid Res* **2001**, *42* (10), 1552-1561

(145) Collins, D. R.; Knott, T. J.; Pease, R. J.; Powell, L. M.; Wallis, S. C.; Robertson, S.; Pullinger, C. R.; Milne, R. W.; Marcel, Y. L.; Humphries, S. E. Truncated variants of apolipoprotein B cause hypobetalipoproteinaemia. *Nucleic Acids Res* **1988**, *16* (17), 8361-8375

(146) Raal, F. J.; Santos, R. D.; Blom, D. J.; Marais, A. D.; Charng, M.-J.; Cromwell, W. C.; Lachmann, R. H.; Gaudet, D.; Tan, J. L.; Chasan-Taber, S.; Tribble, D. L.; Flaim, J. D.; Crooke, S. T. Mipomersen, an apolipoprotein B synthesis inhibitor, for lowering of LDL cholesterol concentrations in patients with homozygous familial hypercholesterolaemia: a randomised, double-blind, placebo-controlled trial. *The Lancet 375* (9719), 998-1006

(147) Attie, A. D.; Weinstein, D. B.; Freeze, H. H.; Pittman, R. C.; Steinberg, D. Unaltered Catabolism of Desialylated Low-Density Lipoprotein in the Pig and in Cultured Rat Hepatocytes. *Biochem J* **1979**, *180* (3), 647-654

(148) Filipovic, I.; Schwarzmann, G.; Mraz, W.; Wiegandt, H.; Buddecke, E. Sialic-Acid Content of Low-Density Lipoproteins Controls Their Binding and Uptake by Cultured-Cells. *Eur J Biochem* **1979**, *93* (1), 51-55

(149) Fujioka, Y.; Taniguchi, T.; Ishikawa, Y.; Yokoyama, M. Significance of acidic sugar chains of apolipoprotein B-100 in cellular metabolism of low-density lipoproteins. *J Lab Clin Med* **2000**, *136* (5), 355-362

(150) Yang, C. Y.; Gu, Z. W.; Blancovaca, F.; Gaskell, S. J.; Yang, M. L.; Massey, J. B.; Gotto, A. M.; Pownall, H. J. Structure of Human Apolipoprotein-D - Locations of the Intermolecular and Intramolecular Disulfide Links. *Biochemistry-Us* **1994**, *33* (41), 12451-12455

(151) Blanco-Vaca, F.; Via, D. P.; Yang, C. Y.; Massey, J. B.; Pownall, H. J. Characterization of disulfide-linked heterodimers containing apolipoprotein D in human plasma lipoproteins. *J Lipid Res* **1992**, *33* (12), 1785-1796

(152) Drayna, D. T.; Mclean, J. W.; Wion, K. L.; Trent, J. M.; Drabkin, H. A.; Lawn, R. M. Human Apolipoprotein-D Gene - Gene Sequence, Chromosome Localization, and Homology to the Alpha-2u-Globulin Superfamily. *DNA-J Molec Cell Bio* **1987**, *6* (3), 199-204

(153) Bajo-Graneras, R.; Crespo-Sanjuan, J.; Garcia-Centeno, R. M.; Garrote-Adrados, J. A.; Gutierrez, G.; Garcia-Tejeiro, M.; Aguirre-Gervas, B.; Calvo-Nieves, M. D.; Bustamante, R.; Ganfornina, M. D.; Sanchez, D. Expression and potential role of apolipoprotein D on the death-survival balance of human colorectal cancer cells under oxidative stress conditions. *International journal of colorectal disease* **2013**, *28* (6), 751-766

(154) Curry, M. D.; Mcconathy, W. J.; Alaupovic, P. Quantitative-Determination of Human Apolipoprotein-D by Electroimmunoassay and Radial Immunodiffusion. *Biochim Biophys Acta* **1977**, *491* (1), 232-241

(155) Camato, R.; Marcel, Y. L.; Milne, R. W.; Lussiercacan, S.; Weech, P. K. Protein Polymorphism of a Human-Plasma Apolipoprotein-D Antigenic Epitope. *J Lipid Res* **1989**, *30* (6), 865-875

(156) Kostner, G. Studies on the cofactor requirements for lecithin: cholesterol acyltransferase. *Scand J Clin Lab Inv* **1974**, *33* (S137), 19-21

(157) Perdomo, G.; Henry Dong, H. Apolipoprotein D in lipid metabolism and its functional implication in atherosclerosis and aging. *Aging* **2009**, *1* (1), 17-27

(158) Rassart, E.; Bedirian, A.; Do Carmo, S.; Guinard, O.; Sirois, J.; Terrisse, L.; Milne, R. Apolipoprotein D. *Biochimica et Biophysica Acta (BBA) - Protein Structure and Molecular Enzymology* **2000**, *1482* (1–2), 185-198

(159) Balbin, M.; Freije, J. M. P.; Fueyo, A.; Sanchez, L. M.; Lopezotin, C. Apolipoprotein-D Is the Major Protein-Component in Cyst Fluid from Women with Human Breast Gross Cystic-Disease. *Biochem J* **1990**, *271* (3), 803-807

(160) Kesner, L.; Yu, W.; BRADLOW, H. Cyst fluid proteases. *Annals of the New York Academy of Sciences* **1990**, *586* (1), 198-203

(161) Kesner, L.; Yu, W.; Bradlow, H. L.; Breed, C. W.; Fleisher, M. Proteases in cyst fluid from human gross cyst breast disease. *Cancer research* **1988**, *48* (22), 6379-6383

(162) Boyles, J. K.; Notterpek, L. M.; Anderson, L. J. Accumulation of apolipoproteins in the regenerating and remyelinating mammalian peripheral nerve. Identification of apolipoprotein D, apolipoprotein A-IV, apolipoprotein E, and apolipoprotein A-I. *J Biol Chem* **1990**, *265* (29), 17805-17815

(163) Belloir, B.; Kovari, E.; Surini-Demiri, M.; Savioz, A. Altered apolipoprotein D expression in the brain of patients with Alzheimer disease. *Journal of neuroscience research* **2001**, *64* (1), 61-69

(164) Navarro, A.; del Valle, E.; Juarez, A.; Martinez, E.; Ordonez, C.; Astudillo, A.; Tolivia, J. Apolipoprotein D synthesis progressively increases in frontal cortex during human lifespan. *Age* **2010**, *32* (1), 85-96

(165) Ordonez, C.; Navarro, A.; Perez, C.; Martinez, E.; del Valle, E.; Tolivia, J. Gender differences in apolipoprotein D expression during aging and in Alzheimer disease. *Neurobiol Aging* **2012**, *33* (2), 433 e411-420

(166) Schindler, P. A.; Settineri, C. A.; Collet, X.; Fielding, C. J.; Burlingame, A. L. Site-specific detection and structural characterization of the glycosylation of human plasma proteins lecithin:cholesterol acyltransferase and apolipoprotein D using HPLC/electrospray mass spectrometry and sequential glycosidase digestion. *Protein Science* **1995**, *4* (4), 791-803

(167) Zeng, C. H.; Spielman, A. I.; Vowels, B. R.; Leyden, J. J.; Biemann, K.; Preti, G. A human axillary odorant is carried by apolipoprotein D. *P Natl Acad Sci USA* **1996**, *93* (13), 6626-6630

(168) Kobata, A. Use of endo-and exoglycosidases for structural studies of glycoconjugates. *Anal Biochem* **1979**, *100* (1), 1-14

(169) Day, J. R.; Albers, J. J.; Gilbert, T. L.; Whitmore, T. E.; McConathy, W. J.; Wolfbauer, G. Purification and Molecular-Cloning of Human Apolipoprotein F. *Biochem Bioph Res Co* **1994**, *203* (2), 1146-1151

(170) Morton, R. E.; Gnizak, H. M.; Greene, D. J.; Cho, K. H.; Paromov, V. M. Lipid transfer inhibitor protein (apolipoprotein F) concentration in normolipidemic and hyperlipidemic subjects. *J Lipid Res* **2008**, *49* (1), 127-135

(171) Wang, X.; Driscoll, D. M.; Morton, R. E. Molecular cloning and expression of lipid transfer inhibitor protein reveals its identity with apolipoprotein F. *J Biol Chem* **1999**, *274* (3), 1814-1820

(172) Morton, R. E.; Greene, D. J. Regulation of lipid transfer between lipoproteins by an endogenous plasma protein: selective inhibition among lipoprotein classes. *J Lipid Res* **1994**, *35* (5), 836-847

(173) Lagor, W. R.; Brown, R. J.; Toh, S. A.; Millar, J. S.; Fuki, I. V.; de la Llera-Moya, M.; Yuen, T.; Rothblat, G.; Billheimer, J. T.; Rader, D. J. Overexpression of

Apolipoprotein F Reduces HDL Cholesterol Levels In Vivo. *Arterioscl Throm Vas* **2009**, *29* (1), 40-U115

(174) Halim, A.; Nilsson, J.; Ruetschi, U.; Hesse, C.; Larson, G. Human urinary glycoproteomics; attachment site specific analysis of N- and O-linked glycosylations by CID and ECD. *Molecular & cellular proteomics : MCP* **2012**, *11* (4), M111 013649

(175) Lozier, J.; Takahashi, N.; Putnam, F. W. Complete amino acid sequence of human plasma beta 2-glycoprotein I. *P Natl Acad Sci USA* **1984**, *81* (12), 3640-3644

(176) Reid, K. B.; Day, A. J. Structure-function relationships of the complement components. *Immunology today* **1989**, *10* (6), 177-180

(177) Polz, E.; Kostner, G. M. The binding of beta 2-glycoprotein-I to human serum lipoproteins: distribution among density fractions. *Febs Lett* **1979**, *102* (1), 183-186

(178) Kroll, J.; Larsen, J. K.; Loft, H.; Ezban, M.; Wallevik, K.; Faber, M. DNA-binding proteins in Yoshida ascites tumor fluid. *Biochim Biophys Acta* **1976**, *434* (2), 490-501

(179) Kochl, S.; Fresser, F.; Lobentanz, E.; Baier, G.; Utermann, G. Novel interaction of apolipoprotein(a) with beta-2 glycoprotein I mediated by the kringle IV domain. *Blood* **1997**, *90* (4), 1482-1489

(180) Kuwana, M.; Matsuura, E.; Kobayashi, K.; Okazaki, Y.; Kaburaki, J.; Ikeda, Y.; Kawakami, Y. Binding of beta 2-glycoprotein I to anionic phospholipids facilitates processing and presentation of a cryptic epitope that activates pathogenic autoreactive T cells. *Blood* **2005**, *105* (4), 1552-1557

(181) De Groot, P. G. β2-Glycoprotein I: evolution, structure and function. *Journal of Thrombosis and Haemostasis* **2011**, *9* (7), 1275-1284

(182) Kondo, A.; Miyamoto, T.; Yonekawa, O.; Giessing, A. M.; Østerlund, E. C.; Jensen, O. N. Glycopeptide profiling of beta-2-glycoprotein I by mass spectrometry reveals attenuated sialylation in patients with antiphospholipid syndrome. *Journal of proteomics* **2009**, *73* (1), 123-133

(183) Hammel, M.; Kriechbaum, M.; Gries, A.; Kostner, G. M.; Laggner, P.; Prassl, R. Solution structure of human and bovine beta(2)-glycoprotein I revealed by small-angle X-ray scattering. *J Mol Biol* **2002**, *321* (1), 85-97

(184) de Laat, B.; de Groot, P. G.; Derksen, R. H.; Urbanus, R. T.; Mertens, K.; Rosendaal, F. R.; Doggen, C. J. Association between beta2-glycoprotein I plasma levels and the risk of myocardial infarction in older men. *Blood* **2009**, *114* (17), 3656-3661

(185) Bouma, B.; de Groot, P. G.; van den Elsen, J. M. H.; Ravelli, R. B. G.; Schouten, A.; Simmelink, M. J. A.; Derksen, R. H. W. M.; Kroon, J.; Gros, P. *Adhesion mechanism of human β2-glycoprotein I to phospholipids based on its crystal structure*; **1999**. DOI: 10.1093/emboj/18.19.5166.

(186) Kristensen, T.; Schousboe, I.; Boel, E.; Mulvihill, E. M.; Hansen, R. R.; Møller, K. B.; Møller, N. P. H.; Sottrup-Jensen, L. Molecular cloning and mammalian expression of human β 2-glycoprotein I cDNA. *Febs Lett* **1991**, *289* (2), 183-186

(187) Powell, A. K.; Harvey, D. J. Stabilization of sialic acids in N-linked oligosaccharides and gangliosides for analysis by positive ion matrix-assisted laser desorption/ionization mass spectrometry. *Rapid communications in mass spectrometry : RCM* **1996**, *10* (9), 1027-1032

(188) Takahashi, N.; Ortel, T. L.; Putnam, F. W. Single-chain structure of human ceruloplasmin: the complete amino acid sequence of the whole molecule. *Proc Natl Acad Sci U S A* **1984**, *81* (2), 390-394

(189) Twomey, P. J.; Viljoen, A.; House, I. M.; Reynolds, T. M.; Wierzbicki, A. S. Relationship between serum copper, ceruloplasmin, and non–ceruloplasmin-bound copper in routine clinical practice. *Clin Chem* **2005**, *51* (8), 1558-1559

(190) Mackiewicz, A.; Ganapathi, M.; Schultz, D.; Kushner, I. Monokines regulate glycosylation of acute-phase proteins. *The Journal of experimental medicine* **1987**, *166* (1), 253-258

(191) Endo, M.; Suzuki, K.; Schmid, K.; Fournet, B.; Karamanos, Y.; Montreuil, J.; Dorland, L.; van Halbeek, H.; Vliegenthart, J. F. The structures and microheterogeneity of the carbohydrate chains of human plasma ceruloplasmin. A study employing 500-MHz 1H-NMR spectroscopy. *J Biol Chem* **1982**, *257* (15), 8755-8760

(192) Harazono, A.; Kawasaki, N.; Itoh, S.; Hashii, N.; Ishii-Watabe, A.; Kawanishi, T.; Hayakawa, T. Site-specific N-glycosylation analysis of human plasma ceruloplasmin using liquid chromatography with electrospray ionization tandem mass spectrometry. *Anal Biochem* **2006**, *348* (2), 259-268

(193) Herrick, S.; Blanc-Brude, O.; Gray, A.; Laurent, G. Fibrinogen. *The international journal of biochemistry & cell biology* **1999**, *31* (7), 741-746

(194) Doolittle, R. F. Fibrinogen and fibrin. *Annual review of biochemistry* **1984**, *53* (1), 195-229

(195) Weisel, J. W. Fibrinogen and Fibrin. In *Advances in Protein Chemistry*, David, A. D. P., John, M. S. Eds.; Vol. Volume 70; Academic Press, **2005**; pp 247-299.

(196) Kollman, J. M.; Pandi, L.; Sawaya, M. R.; Riley, M.; Doolittle, R. F. Crystal structure of human fibrinogen. *Biochemistry-Us* **2009**, *48* (18), 3877-3886

(197) Fuss, C.; Palmaz, J. C.; Sprague, E. A. Fibrinogen: structure, function, and surface interactions. *Journal of vascular and interventional radiology : JVIR* **2001**, *12* (6), 677-682

(198) Pieters, M.; de Maat, M. P. M.; Jerling, J. C.; Hoekstra, T.; Kruger, A. Fibrinogen concentration and its role in CVD risk in black South Africans – effect of urbanisation. *Thrombosis and Haemostasis* **2011**, *106* (9), 448-456

(199) Carling, M. S.; Jeppsson, A.; Wessberg, P.; Henriksson, A.; Baghaei, F.; Brisby, H. Preoperative Fibrinogen Plasma Concentration Is Associated With Perioperative Bleeding and Transfusion Requirements in Scoliosis Surgery. *Spine* **2011**, *36* (7), 549-555 510.1097/BRS.1090b1013e3181d1952dc

(200) Lang, T.; Johanning, K.; Metzler, H.; Piepenbrock, S.; Solomon, C.; Rahe-Meyer, N.; Tanaka, K. A. The effects of fibrinogen levels on thromboelastometric variables in the presence of thrombocytopenia. *Anesthesia and analgesia* **2009**, *108* (3), 751-758

(201) Henschen, A.; Mcdonagh, J. Fibrinogen, fibrin and factor XIII. *New Comprehensive Biochemistry* **1986**, *13*, 171-241

(202) Zaidi, T.; McIntire, L.; Farrell, D.; Thiagarajan, P. Adhesion of platelets to surface-bound fibrinogen under flow. *Blood* **1996**, *88* (8), 2967-2972

(203) Clark, R. A.; Lanigan, J. M.; DellaPelle, P.; Manseau, E.; Dvorak, H. F.; Colvin, R. B. Fibronectin and fibrin provide a provisional matrix for epidermal cell migration during wound reepithelialization. *J Invest Dermatol* **1982**, *79* (5), 264-269

(204) Hogg, D. H.; Blombäck, B. The mechanism of the fibrinogen-thrombin reaction. *Thrombosis Research* **1978**, *12* (6), 953-964

(205) Johnson, L. L.; Berggren, K. N.; Szaba, F. M.; Chen, W.; Smiley, S. T. Fibrin-mediated protection against infection-stimulated immunopathology. *The Journal of experimental medicine* **2003**, *197* (6), 801-806

(206) Flick, M. J.; Du, X.; Degen, J. L. Fibrin (ogen)-αMβ2 interactions regulate leukocyte function and innate immunity in vivo. *Experimental Biology and Medicine* **2004**, *229* (11), 1105-1110

(207) Kaptoge, S.; White, I.; Thompson, S.; Wood, A.; Lewington, S.; Lowe, G.; Danesh, J. Associations of plasma fibrinogen levels with established cardiovascular disease risk factors, inflammatory markers, and other characteristics: individual participant meta-analysis of 154,211 adults in 31 prospective studies: the fibrinogen studies collaboration. *American journal of epidemiology* **2007**, *166* (8), 867-879

(208) Zauner, G.; Hoffmann, M.; Rapp, E.; Koeleman, C. A.; Dragan, I.; Deelder, A. M.; Wuhrer, M.; Hensbergen, P. J. Glycoproteomic analysis of human fibrinogen reveals novel regions of O-glycosylation. *Journal of proteome research* **2012**, *11* (12), 5804-5814

(209) Lewandrowski, U.; Moebius, J.; Walter, U.; Sickmann, A. Elucidation of N-Glycosylation Sites on Human Platelet Proteins : A Glycoproteomic Approach. *Molecular & Cellular Proteomics* **2006**, *5* (2), 226-233

(210) Reiding, K. R.; Blank, D.; Kuijper, D. M.; Deelder, A. M.; Wuhrer, M. High-throughput profiling of protein N-glycosylation by MALDI-TOF-MS employing linkage-specific sialic acid esterification. *Anal Chem* **2014**, *86* (12), 5784-5793

(211) Adamczyk, B.; Struwe, W. B.; Ercan, A.; Nigrovic, P. A.; Rudd, P. M. Characterization of Fibrinogen Glycosylation and Its Importance for Serum/Plasma N-Glycome Analysis. *Journal of proteome research* **2012**, *12* (1), 444-454

(212) Martinez, J.; Keane, P. M.; Gilman, P. B.; Palascak, J. E. The Abnormal Carbohydrate-Composition of the Dysfibrinogenemia Associated with Liver-Disease. *Annals of the New York Academy of Sciences* **1983**, *408* (Jun), 388-396

(213) Dang, C. V.; Shin, C. K.; Bell, W. R.; Nagaswami, C.; Weisel, J. W. Fibrinogen Sialic-Acid Residues Are Low Affinity Calcium-Binding Sites That Influence Fibrin Assembly. *J Biol Chem* **1989**, *264* (25), 15104-15108

(214) Langer, B. G.; Weisel, J. W.; Dinauer, P. A.; Nagaswami, C.; Bell, W. R. Deglycosylation of Fibrinogen Accelerates Polymerization and Increases Lateral Aggregation of Fibrin Fibers. *J Biol Chem* **1988**, *263* (29), 15056-15063

(215) Woodhead, J. L.; Nagaswami, C.; Matsuda, M.; Arocha-Pinango, C. L.; Weisel, J. W. The ultrastructure of fibrinogen Caracas II molecules, fibers, and clots. *J Biol Chem* **1996**, *271* (9), 4946-4953

(216) Sugo, T.; Nakamikawa, C.; Takano, H.; Mimuro, J.; Yamaguchi, S.; Mosesson, M. W.; Meh, D. A.; DiOrio, J. P.; Takahashi, N.; Takahashi, H.; Nagai, K.; Matsuda, M. Fibrinogen Niigata with impaired fibrin assembly: an inherited dysfibrinogen with a Bbeta Asn-160 to Ser substitution associated with extra glycosylation at Bbeta Asn-158. *Blood* **1999**, *94* (11), 3806-3813

(217) Yamazumi, K.; Shimura, K.; Terukina, S.; Takahashi, N.; Matsuda, M. A gamma methionine-310 to threonine substitution and consequent N-glycosylation at gamma asparagine-308 identified in a congenital dysfibrinogenemia associated with posttraumatic bleeding, fibrinogen Asahi. *J Clin Invest* **1989**, *83* (5), 1590-1597

(218) Sugo, T.; Sekine, O.; Nakamikawa, C.; Endo, H.; Arocha-Pinango, C. L.; Matsuda, M. Mode of perturbation of Asahi fibrin assembly by the extra oligosaccharides. *Ann N Y Acad Sci* **2001**, *936*, 223-225

(219) Li, P.; Gao, X. H.; Chen, H. D.; Zhang, Y.; Wang, Y.; Wang, H.; Wang, Y.; Xie, Y. Localization of haptoglobin in normal human skin and some skin diseases. *International journal of dermatology* **2005**, *44* (4), 280-284

(220) Smeets, M. B.; Fontijn, J.; Kavelaars, A.; Pasterkamp, G.; De Kleijn, D. P. V. The acute phase protein haptoglobin is locally expressed in arthritic and oncological tissues. *International Journal of Experimental Pathology* **2003**, *84* (2), 69-74

(221) Raugei, G.; Bensi, G.; Colantuoni, V.; Romano, V.; Santoro, C.; Costanzo, F.; Cortese, R. Sequence of human haptoglobin cDNA: evidence that the alpha and beta subunits are coded by the same mRNA. *Nucleic Acids Res* **1983**, *11* (17), 5811-5819

(222) Dobryszycka, W. Biological functions of haptoglobin - New pieces to an old puzzle. *Eur J Clin Chem Clin* **1997**, *35* (9), 647-654

(223) Langlois, M. R.; Delanghe, J. R. Biological and clinical significance of haptoglobin polymorphism in humans. *Clin Chem* **1996**, *42* (10), 1589-1600

(224) Galicia, G.; Ceuppens, J. L. *Haptoglobin Function and Regulation in Autoimmune Diseases*; INTECH Open Access Publisher, **2011**.

(225) Van Vlierberghe, H.; Langlois, M.; Delanghe, J. Haptoglobin polymorphisms and iron homeostasis in health and in disease. *Clin Chim Acta* **2004**, *345* (1-2), 35-42

(226) Carter, K.; Worwood, M. Haptoglobin: a review of the major allele frequencies worldwide and their association with diseases. *International journal of laboratory hematology* **2007**, *29* (2), 92-110

(227) Moretti, J.; Borel, J.; Dobryszycka, W.; Jayle, M.-F. Détermination de la demi-vie de l'haptoglobine plasmatique humaine. *Biochim Biophys Acta* **1963**, *69*, 205-211

(228) Bharti, A.; Ma, P. C.; Maulik, G.; Singh, R.; Khan, E.; Skarin, A. T.; Salgia, R. Haptoglobin alpha-subunit and hepatocyte growth factor can potentially serve as serum tumor biomarkers in small cell lung cancer. *Anticancer Res* **2004**, *24* (2C), 1031-1038

(229) Lim, Y. K.; Jenner, A.; Ali, A. B.; Wang, Y.; Hsu, S. I.; Chong, S. M.; Baumman, H.; Halliwell, B.; Lim, S. K. Haptoglobin reduces renal oxidative DNA and tissue damage during phenylhydrazine-induced hemolysis. *Kidney international* **2000**, *58* (3), 1033-1044

(230) Tseng, C. F.; Lin, C. C.; Huang, H. Y.; Liu, H. C.; Mao, S. J. T. Antioxidant role of human haptoglobin. *Proteomics* **2004**, *4* (8), 2221-2228

(231) Zhang, S.; Jiang, K.; Sun, C.; Lu, H.; Liu, Y. Quantitative analysis of site-specific N-glycans on sera haptoglobin β chain in liver diseases. *Acta Bioch Bioph Sin* **2013**, *45* (12), 1021-1029

(232) Pompach, P.; Brnakova, Z.; Sanda, M.; Wu, J.; Edwards, N.; Goldman, R. Site-specific glycoforms of haptoglobin in liver cirrhosis and hepatocellular carcinoma. *Molecular & cellular proteomics : MCP* **2013**, *12* (5), 1281-1293

(233) Pompach, P.; Ashline, D. J.; Brnakova, Z.; Benicky, J.; Sanda, M.; Goldman, R. Protein and site specificity of fucosylation in liver-secreted glycoproteins. *Journal of proteome research* **2014**, *13* (12), 5561-5569

(234) Wang, D.; Hincapie, M.; Rejtar, T.; Karger, B. L. Ultrasensitive Characterization of Site-Specific Glycosylation of Affinity-Purified Haptoglobin from Lung Cancer

Patient Plasma Using 10 µm i.d. Porous Layer Open Tubular Liquid Chromatography–Linear Ion Trap Collision-Induced Dissociation/Electron Transfer Dissociation Mass Spectrometry. *Anal Chem* **2011**, *83* (6), 2029-2037

(235) Nakano, M.; Nakagawa, T.; Ito, T.; Kitada, T.; Hijioka, T.; Kasahara, A.; Tajiri, M.; Wada, Y.; Taniguchi, N.; Miyoshi, E. Site-specific analysis of N-glycans on haptoglobin in sera of patients with pancreatic cancer: A novel approach for the development of tumor markers. *International Journal of Cancer* **2008**, *122* (10), 2301-2309

(236) Zhu, J.; Lin, Z.; Wu, J.; Yin, H.; Dai, J.; Feng, Z.; Marrero, J.; Lubman, D. M. Analysis of serum haptoglobin fucosylation in hepatocellular carcinoma and liver cirrhosis of different etiologies. *Journal of proteome research* **2014**, *13* (6), 2986-2997

(237) Carlsson, M. C.; Cederfur, C.; Schaar, V.; Balog, C.; Lepur, A.; Touret, F.; Salomonsson, E.; Deelder, A. M.; Fernö, M.; Olsson, H. Galectin-1-binding glycoforms of haptoglobin with altered intracellular trafficking, and increase in metastatic breast cancer patients. *Plos One* **2011**, *6* (10), e26560

(238) Carlsson, M. C.; Balog, C. I.; Kilsgard, O.; Hellmark, T.; Bakoush, O.; Segelmark, M.; Ferno, M.; Olsson, H.; Malmstrom, J.; Wuhrer, M.; Leffler, H. Different fractions of human serum glycoproteins bind galectin-1 or galectin-8, and their ratio may provide a refined biomarker for pathophysiological conditions in cancer and inflammatory disease. *Biochim Biophys Acta* **2012**, *1820* (9), 1366-1372

(239) Delanghe, J. R.; Langlois, M. R. Hemopexin: a review of biological aspects and the role in laboratory medicine. *Clin Chim Acta* **2001**, *312* (1-2), 13-23

(240) Tolosano, E.; Altruda, F. Hemopexin: structure, function, and regulation. *DNA Cell Biol* **2002**, *21* (4), 297-306

(241) Takahashi, N.; Takahashi, Y.; Putnam, F. W. Complete amino acid sequence of human hemopexin, the heme-binding protein of serum. *Proc Natl Acad Sci U S A* **1985**, *82* (1), 73-77

(242) Weeke, B.; Krasilnikoff, P. A. The Concentration Of 21 Serum Proteins In Normal Children And Adults. *Acta Med Scand* **1972**, *192* (1-6), 149-155

(243) Kanakoudi, F.; Drossou, V.; Tzimouli, V.; Diamanti, E.; Konstantinidis, T.; Germenis, A.; Kremenopoulos, G. Serum concentrations of 10 acute-phase proteins in healthy term and preterm infants from birth to age 6 months. *Clin Chem* **1995**, *41* (4), 605-608

(244) Takahashi, N.; Takahashi, Y.; Putnam, F. W. Structure of human hemopexin: O-glycosyl and N-glycosyl sites and unusual clustering of tryptophan residues. *P Natl Acad Sci USA* **1984**, *81* (7), 2021-2025

(245) Kristiansen, T. Z.; Bunkenborg, J.; Gronborg, M.; Molina, H.; Thuluvath, P. J.; Argani, P.; Goggins, M. G.; Maitra, A.; Pandey, A. A proteomic analysis of human bile. *Molecular & Cellular Proteomics* **2004**, *3* (7), 715-728

(246) Ramachandran, P.; Boontheung, P.; Xie, Y.; Sondej, M.; Wong, D. T.; Loo, J. A. Identification of N-linked glycoproteins in human saliva by glycoprotein capture and mass spectrometry. *Journal of proteome research* **2006**, *5* (6), 1493-1503

(247) Frantikova, V.; Borvak, J.; Kluh, I.; Moravek, L. Amino acid sequence of the N-terminal region of human hemopexin. *Febs Lett* **1984**, *178* (2), 213-216

(248) Lee, J. H.; Cho, C. H.; Kim, S. H.; Kang, J. G.; Yoo, J. S.; Chang, C. L.; Ko, J. H.; Kim, Y. S. Semi-quantitative measurement of a specific glycoform using a DNA-tagged antibody and lectin affinity chromatography for glyco-biomarker development. *Molecular & cellular proteomics : MCP* **2015**, *14* (3), 782-795

(249) Yin, H.; Lin, Z.; Nie, S.; Wu, J.; Tan, Z.; Zhu, J.; Dai, J.; Feng, Z.; Marrero, J.; Lubman, D. M. Mass-Selected Site-Specific Core-Fucosylation of Ceruloplasmin in Alcohol-Related Hepatocellular Carcinoma. *Journal of proteome research* **2014**, *13* (6), 2887-2896

(250) Benicky, J.; Sanda, M.; Pompach, P.; Wu, J.; Goldman, R. Quantification of fucosylated hemopexin and complement factor H in plasma of patients with liver disease. *Anal Chem* **2014**, *86* (21), 10716-10723

(251) Debruyne, E. N.; Vanderschaeghe, D.; Van Vlierberghe, H.; Vanhecke, A.; Callewaert, N.; Delanghe, J. R. Diagnostic value of the hemopexin N-glycan profile in hepatocellular carcinoma patients. *Clin Chem* **2010**, *56* (5), 823-831

(252) Poon, I. K.; Patel, K. K.; Davis, D. S.; Parish, C. R.; Hulett, M. D. Histidine-rich glycoprotein: the Swiss Army knife of mammalian plasma. *Blood* **2011**, *117* (7), 2093-2101

(253) Kassaar, O.; McMahon, S. A.; Thompson, R.; Botting, C. H.; Naismith, J. H.; Stewart, A. J. Crystal structure of histidine-rich glycoprotein N2 domain reveals redox activity at an interdomain disulfide bridge: implications for angiogenic regulation. *Blood* **2014**, *123* (12), 1948-1955

(254) Borza, D. B.; Tatum, F. M.; Morgan, W. T. Domain structure and conformation of histidine-proline-rich glycoprotein. *Biochemistry-Us* **1996**, *35* (6), 1925-1934

(255) Saito, H.; Goodnough, L. T.; Boyle, J. M.; Heimburger, N. Reduced histidine-rich glycoprotein levels in plasma of patients with advanced liver cirrhosis. Possible implications for enhanced fibrinolysis. *Am J Med* **1982**, *73* (2), 179-182

(256) Drasin, T.; Sahud, M. Blood-type and age affect human plasma levels of histidine-rich glycoprotein in a large population. *Thrombosis Research* **1996**, *84* (3), 179-188

(257) Leung, L. L.; Harpel, P. C.; Nachman, R. L.; Rabellino, E. M. Histidine-rich glycoprotein is present in human platelets and is released following thrombin stimulation. *Blood* **1983**, *62* (5), 1016-1021

(258) Corrigan Jr, J. J.; Jeter, M. A.; Bruck, D.; Feinberg, W. M. Histidine-rich glycoprotein levels in children: The effect of age. *Thrombosis Research* **1990**, *59* (3), 681-686

(259) Jones, A. L.; Hulett, M. D.; Parish, C. R. Histidine-rich glycoprotein: A novel adaptor protein in plasma that modulates the immune, vascular and coagulation systems. *Immunol Cell Biol* **2005**, *83* (2), 106-118

(260) Saigo, K.; Yoshida, A.; Ryo, R.; Yamaguchi, N.; Leung, L. L. Histidine-rich glycoprotein as a negative acute phase reactant. *American journal of hematology* **1990**, *34* (2), 149-150

(261) Hennis, B. C.; van Boheemen, P. A.; Wakabayashi, S.; Koide, T.; Hoffmann, J. J.; Kievit, P.; Dooijewaard, G.; Jansen, J. G.; Kluft, C. Identification and genetic analysis of a common molecular variant of histidine-rich glycoprotein with a difference of 2kD in apparent molecular weight. *Thromb Haemost* **1995**, *74* (6), 1491-1496

(262) Koide, T.; Foster, D.; Yoshitake, S.; Davie, E. W. Amino acid sequence of human histidine-rich glycoprotein derived from the nucleotide sequence of its cDNA. *Biochemistry-Us* **1986**, *25* (8), 2220-2225

(263) Stenflo, J.; Fernlund, P. Amino acid sequence of the heavy chain of bovine protein C. *J Biol Chem* **1982**, *257* (20), 12180-12190

(264) Lottspeich, F.; Kellermann, J.; Henschen, A.; Foertsch, B.; MüLler-Esterl, W. The amino acid sequence of the light chain of human high-molecular-mass kiniogen. *Eur J Biochem* **1985**, *152* (2), 307-314

(265) Griffin, J. H.; Cochrane, C. G. Mechanisms for the involvement of high molecular weight kininogen in surface-dependent reactions of Hageman factor. *Proceedings of the National Academy of Sciences* **1976**, *73* (8), 2554-2558

(266) Kaplan, A. P.; Silverberg, M. The coagulation-kinin pathway of human plasma. *Blood* **1987**, *70* (1), 1-15

(267) Margolius, H. S. Kallikreins and Kinins: Some Unanswered Questions About System Characteristics and Roles in Human Disease. *Hypertension* **1995**, *26* (2), 221-229

(268) Weisel, J. W.; Nagaswami, C.; Woodhead, J. L.; DeLa Cadena, R. A.; Page, J. D.; Colman, R. W. The shape of high molecular weight kininogen. Organization into structural domains, changes with activation, and interactions with prekallikrein, as determined by electron microscopy. *J Biol Chem* **1994**, *269* (13), 10100-10106

(269) Thompson, R. E.; Mandle Jr, R.; Kaplan, A. P. Association of factor XI and high molecular weight kininogen in human plasma. *J Clin Invest* **1977**, *60* (6), 1376

(270) Mandle, R. J.; Colman, R. W.; Kaplan, A. P. Identification of prekallikrein and high-molecular-weight kininogen as a complex in human plasma. *Proceedings of the National Academy of Sciences* **1976**, *73* (11), 4179-4183

(271) Reddigari, S.; Kaplan, A. P. Quantification of human high molecular weight kininogen by immunoblotting with a monoclonal anti-light chain antibody. *Journal of immunological methods* **1989**, *119* (1), 19-25

(272) Adam, A.; Albert, A.; Calay, G.; Closset, J.; Damas, J.; Franchimont, P. Human kininogens of low and high molecular mass: quantification by radioimmunoassay and determination of reference values. *Clin Chem* **1985**, *31* (3), 423-426

(273) Bones, J.; Byrne, J. C.; O'Donoghue, N.; McManus, C.; Scaife, C.; Boissin, H.; Nastase, A.; Rudd, P. M. Glycomic and glycoproteomic analysis of serum from patients with stomach cancer reveals potential markers arising from host defense response mechanisms. *Journal of proteome research* **2011**, *10* (3), 1246-1265

(274) Gomme, P. T.; McCann, K. B.; Bertolini, J. Transferrin: structure, function and potential therapeutic actions. *Drug Discov Today* **2005**, *10* (4), 267-273

(275) Bailey, S.; Evans, R. W.; Garratt, R. C.; Gorinsky, B.; Hasnain, S.; Horsburgh, C.; Jhoti, H.; Lindley, P. F.; Mydin, A. Molecular structure of serum transferrin at 3.3-.ANG. resolution. *Biochemistry-Us* **1988**, *27* (15), 5804-5812

(276) Kurokawa, H.; Mikami, B.; Hirose, M. Crystal Structure of Diferric Hen Ovotransferrin at 2.4 Å Resolution. *Journal of Molecular Biology* **1995**, *254* (2), 196-207

(277) Vahlquist, A.; Rask, L.; Peterson, P. A.; Berg, T. The concentrations of retinol-binding protein, prealbumin, and transferrin in the sera of newly delivered mothers and children of various ages. *Scandinavian journal of clinical and laboratory investigation* **1975**, *35* (6), 569-575

(278) Leger, D.; Campion, B.; Decottignies, J. P.; Montreuil, J.; Spik, G. Physiological significance of the marked increased branching of the glycans of human serotransferrin during pregnancy. *Biochem J* **1989**, *257* (1), 231-238

(279) Chitambar, C. R.; Matthaeus, W. G.; Antholine, W. E.; Graff, K.; O'Brien, W. J. Inhibition of leukemic HL60 cell growth by transferrin-gallium: effects on ribonucleotide reductase and demonstration of drug synergy with hydroxyurea. *Blood* **1988**, *72* (6), 1930-1936

(280) Trowbridge, I. S.; Shackelford, D. A. Structure and Function of Transferrin Receptors and Their Relationship to Cell-Growth. *Biochem Soc Symp* **1986**, (51), 117-129

(281) Thorstensen, K.; Romslo, I. The Role of Transferrin in the Mechanism of Cellular Iron Uptake. *Biochem J* **1990**, *271* (1), 1-10

(282) Koterov, A. N.; Pushkareva, N. B.; Nikol'skii, A. V. [The radiation-modifying capacity of xenogenic apotransferrin for the number of endogenous colony forming units in the spleen of irradiated mice]. *Radiatsionnaia biologiia, radioecologiia / Rossiiskaia akademiia nauk* **2003**, *43* (6), 647-653

(283) Daniels, T. R.; Delgado, T.; Helguera, G.; Penichet, M. L. The transferrin receptor part II: Targeted delivery of therapeutic agents into cancer cells. *Clinical Immunology* **2006**, *121* (2), 159-176

(284) Daniels, T. R.; Delgado, T.; Rodriguez, J. A.; Helguera, G.; Penichet, M. L. The transferrin receptor part I: Biology and targeting with cytotoxic antibodies for the treatment of cancer. *Clin Immunol* **2006**, *121* (2), 144-158

(285) Satomi, Y.; Shimonishi, Y.; Takao, T. N-glycosylation at Asn(491) in the Asn-Xaa-Cys motif of human transferrin. *Febs Lett* **2004**, *576* (1-2), 51-56

(286) Satomi, Y.; Shimonishi, Y.; Hase, T.; Takao, T. Site-specific carbohydrate profiling of human transferrin by nano-flow liquid chromatography/electrospray ionization mass spectrometry. *Rapid communications in mass spectrometry : RCM* **2004**, *18* (24), 2983-2988

(287) Yamashita, K.; Koide, N.; Endo, T.; Iwaki, Y.; Kobata, A. Altered Glycosylation of Serum Transferrin of Patients with Hepatocellular-Carcinoma. *J Biol Chem* **1989**, *264* (5), 2415-2423

(288) van Rooijen, J. J. M.; Jeschke, U.; Kamerling, J. P.; Vliegenthart, J. F. G. Expression of N-linked sialyl Lex determinants and O-glycans in the carbohydrate moiety of human amniotic fluid transferrin during pregnancy. *Glycobiology* **1998**, *8* (11), 1053-1064

(289) Futakawa, S.; Nara, K.; Miyajima, M.; Kuno, A.; Ito, H.; Kaji, H.; Shirotani, K.; Honda, T.; Tohyama, Y.; Hoshi, K.; Hanzawa, Y.; Kitazume, S.; Imamaki, R.; Furukawa, K.; Tasaki, K.; Arai, H.; Yuasa, T.; Abe, M.; Arai, H.; Narimatsu, H.; Hashimoto, Y. A unique N-glycan on human transferrin in CSF: a possible biomarker for iNPH. *Neurobiology of Aging* **2012**, *33* (8), 1807-1815

(290) Grünewald, S.; Matthijs, G.; Jaeken, J. Congenital disorders of glycosylation: a review. *Pediatr Res* **2002**, *52* (5), 618-624

(291) Jaeken, J. Congenital disorders of glycosylation. *Ann Ny Acad Sci* **2010**, *1214*, 190-198

(292) Lefeber, D. J.; Morava, E.; Jaeken, J. How to find and diagnose a CDG due to defective N-glycosylation. *Journal of inherited metabolic disease* **2011**, *34* (4), 849-852

(293) Rainio, J.; Ahola, S.; Kangastupa, P.; Kultti, J.; Tuomi, H.; Karhunen, P. J.; Helander, A.; Niemelä, O. Comparison of Ethyl Glucuronide and Carbohydrate-

Deficient Transferrin in Different Body Fluids for Post-mortem Identification of Alcohol Use. *Alcohol and Alcoholism* **2014**, *49* (1), 55-59

(294) Preissner, K. T. Structure and Biological Role of Vitronectin. *Annual Review of Cell Biology* **1991**, *7* (1), 275-310

(295) Preissner, K. T.; Reuning, U. Vitronectin in Vascular Context: Facets of a Multitalented Matricellular Protein. *Semin Thromb Hemost* **2011**, *37* (04), 408-424

(296) Preissner, K. T.; Seiffert, D. Role of Vitronectin and Its Receptors in Haemostasis and Vascular Remodeling. *Thrombosis Research* **1998**, *89* (1), 1-21

(297) Schvartz, I.; Seger, D.; Shaltiel, S. Vitronectin. *The international journal of biochemistry & cell biology* **1999**, *31* (5), 539-544

(298) Montaldo, C.; Mattei, S.; Baiocchini, A.; Rotiroti, N.; Nonno, F. D.; Pucillo, L. P.; Cozzolino, A. M.; Battistelli, C.; Amicone, L.; Ippolito, G.; van Noort, V.; Conigliaro, A.; Alonzi, T.; Tripodi, M.; Mancone, C. Spike-in SILAC proteomic approach reveals the vitronectin as an early molecular signature of liver fibrosis in hepatitis C infections with hepatic iron overload. *Proteomics* **2014**, *14* (9), 1107-1115

(299) Seiffert, D.; Geisterfer, M.; Gauldie, J.; Young, E.; Podor, T. J. IL-6 stimulates vitronectin gene expression in vivo. *The Journal of Immunology* **1995**, *155* (6), 3180-3185

(300) Chauhan, A. K.; Moore, T. L. Presence of plasma complement regulatory proteins clusterin (Apo J) and vitronectin (S40) on circulating immune complexes (CIC). *Clinical & Experimental Immunology* **2006**, *145* (3), 398-406

(301) Hwang, H.; Lee, J. Y.; Lee, H. K.; Park, G. W.; Jeong, H. K.; Moon, M. H.; Kim, J. Y.; Yoo, J. S. In-depth analysis of site-specific N-glycosylation in vitronectin from human plasma by tandem mass spectrometry with immunoprecipitation. *Anal Bioanal Chem* **2014**, *406* (30), 7999-8011

(302) Ogawa, H.; Yoneda, A.; Seno, N.; Hayashi, M.; Ishizuka, I.; Hase, S.; Matsumoto, I. Structures of the N-Linked Oligosaccharides on Human Plasma Vitronectin. *Eur J Biochem* **1995**, *230* (3), 994-1000

(303) Lee, H.-J.; Cha, H.-J.; Lim, J.-S.; Lee, S. H.; Song, S. Y.; Kim, H.; Hancock, W. S.; Yoo, J. S.; Paik, Y.-K. Abundance-Ratio-Based Semiquantitative Analysis of Site-Specific N-Linked Glycopeptides Present in the Plasma of Hepatocellular Carcinoma Patients. *Journal of proteome research* **2014**, *13* (5), 2328-2338

(304) Tsai, J. S.; Chen, S. C.; Huang, K. C.; Lue, B. H.; Lee, L. T.; Chiu, T. Y.; Chen, C. Y.; Guo, F. R.; Chuang, L. M. Plasma zinc alpha2-glycoprotein levels are elevated in smokers and correlated with metabolic syndrome. *Eur J Clin Invest* **2015**, *45* (5), 452-459

(305) Araki, T.; Gejyo, F.; Takagaki, K.; Haupt, H.; Schwick, H. G.; Burgi, W.; Marti, T.; Schaller, J.; Rickli, E.; Brossmer, R.; et al. Complete amino acid sequence of human

plasma Zn-alpha 2-glycoprotein and its homology to histocompatibility antigens. *P Natl Acad Sci USA* **1988**, *85* (3), 679-683

(306) Burgi, W.; Schmid, K. Preparation and properties of Zn-alpha 2-glycoprotein of normal human plasma. *J Biol Chem* **1961**, *236*, 1066-1074

(307) Hassan, M. I.; Waheed, A.; Yadav, S.; Singh, T. P.; Ahmad, F. Zinc alpha 2-glycoprotein: a multidisciplinary protein. *Mol Cancer Res* **2008**, *6* (6), 892-906

(308) Delker, S. L.; West, A. P., Jr.; McDermott, L.; Kennedy, M. W.; Bjorkman, P. J. Crystallographic studies of ligand binding by Zn-alpha2-glycoprotein. *J Struct Biol* **2004**, *148* (2), 205-213

(309) Hassan, M. I.; Bilgrami, S.; Kumar, V.; Singh, N.; Yadav, S.; Kaur, P.; Singh, T. P. Crystal structure of the novel complex formed between zinc alpha2-glycoprotein (ZAG) and prolactin-inducible protein (PIP) from human seminal plasma. *Journal of molecular biology* **2008**, *384* (3), 663-672

(310) Sanchez, L. M.; Chirino, A. J.; Bjorkman, P. Crystal structure of human ZAG, a fat-depleting factor related to MHC molecules. *Science* **1999**, *283* (5409), 1914-1919

(311) Arnold, J. N.; Wormald, M. R.; Sim, R. B.; Rudd, P. M.; Dwek, R. A. The impact of glycosylation on the biological function and structure of human immunoglobulins. *Annual review of immunology* **2007**, *25*, 21-50

(312) van Egmond, M.; Damen, C. A.; van Spriel, A. B.; Vidarsson, G.; van Garderen, E.; van de Winkel, J. G. IgA and the IgA Fc receptor. *Trends in immunology* **2001**, *22* (4), 205-211

(313) Woof, J. M.; Kerr, M. A. The function of immunoglobulin A in immunity. *The Journal of pathology* **2006**, *208* (2), 270-282

(314) Kutteh, W.; Prince, S.; Mestecky, J. Tissue origins of human polymeric and monomeric IgA. *The Journal of Immunology* **1982**, *128* (2), 990-995

(315) Torano, A.; Tsuzukida, Y.; Liu, Y. S.; Putnam, F. W. Location and structural significance of the oligosaccharides in human Ig-A1 and IgA2 immunoglobulins. *Proc Natl Acad Sci U S A* **1977**, *74* (6), 2301-2305

(316) Mattu, T. S.; Pleass, R. J.; Willis, A. C.; Kilian, M.; Wormald, M. R.; Lellouch, A. C.; Rudd, P. M.; Woof, J. M.; Dwek, R. A. The Glycosylation and Structure of Human Serum IgA1, Fab, and Fc Regions and the Role of N-Glycosylation on Fcα Receptor Interactions. *J Biol Chem* **1998**, *273* (4), 2260-2272

(317) Tanaka, A.; Iwase, H.; Hiki, Y.; Kokubo, T.; Ishii-Karakasa, I.; Toma, K.; Kobayashi, Y.; Hotta, K. Evidence for a site-specific fucosylation of N-linked oligosaccharide of immunoglobulin A1 from normal human serum. *Glycoconj J* **1998**, *15* (10), 995-1000

(318) Klapoetke, S. C.; Zhang, J.; Becht, S. Glycosylation characterization of Human IgA1 with differential deglycosylation by UPLC-ESI TOF MS. *J Pharm Biomed Anal* **2011**, *56* (3), 513-520

(319) Gomes, M. M.; Wall, S. B.; Takahashi, K.; Novak, J.; Renfrow, M. B.; Herr, A. B. Analysis of IgA1 N-glycosylation and its contribution to FcαRI binding. *Biochemistry-Us* **2008**, *47* (43), 11285-11299

(320) Monteiro, R. C.; Van De Winkel, J. G. IgA Fc receptors. *Annual review of immunology* **2003**, *21*, 177-204

(321) Rowe, D. S.; Anderson, S. G.; Tackett, L. A research standard for human serum immunoglobulin D. *Bulletin of the World Health Organization* **1970**, *43* (4), 607-609

(322) Rowe, D. S.; Fahey, J. L. A New Class of Human Immunoglobulins. Ii. Normal Serum Igd. *J Exp Med* **1965**, *121*, 185-199

(323) Zegers, B. J.; Stoop, J. W.; Reerink-Brongers, E. E.; Sander, P. C.; Aalberse, R. C.; Ballieux, R. E. Serum immunoglobulins in healthy children and adults. Levels of the five classes, expressed in international units per millilitre. *Clin Chim Acta* **1975**, *65* (3), 319-329

(324) Rogentine, G. N.; Rowe, D. S.; Bradley, J.; Waldmann, T. A.; Fahey, J. L. Metabolism of human immunoglobulin D (IgD). *J Clin Invest* **1966**, *45* (9), 1467-1478

(325) Van Boxel, J. A.; Paul, W. E.; Terry, W. D.; Green, I. Communications. IgD-bearing human lymphocytes. *Journal of immunology* **1972**, *109* (3), 648-651

(326) Takayasu, T.; Suzuki, S.; Kametani, F.; Takahashi, N.; Shinoda, T.; Okuyama, T.; Munekata, E. Amino acid sequence of galactosamine-containing glycopeptides in the hinge region of a human immunoglobulin D. *Biochem Biophys Res Commun* **1982**, *105* (3), 1066-1071

(327) Takahashi, N.; Tetaert, D.; Debuire, B.; Lin, L. C.; Putnam, F. W. Complete amino acid sequence of the delta heavy chain of human immunoglobulin D. *Proc Natl Acad Sci U S A* **1982**, *79* (9), 2850-2854

(328) Mellis, S. J.; Baenziger, J. U. Structures of the O-glycosidically linked oligosaccharides of human IgD. *J Biol Chem* **1983**, *258* (19), 11557-11563

(329) Arnold, J. N.; Radcliffe, C. M.; Wormald, M. R.; Royle, L.; Harvey, D. J.; Crispin, M.; Dwek, R. A.; Sim, R. B.; Rudd, P. M. The Glycosylation of Human Serum IgD and IgE and the Accessibility of Identified Oligomannose Structures for Interaction with Mannan-Binding Lectin. *The Journal of Immunology* **2004**, *173* (11), 6831-6840

(330) Gala, F. A.; Morrison, S. L. The Role of Constant Region Carbohydrate in the Assembly and Secretion of Human IgD and IgA1. *J Biol Chem* **2002**, *277* (32), 29005-29011

(331) Murphy, K. M. *Janeway's immunobiology*; Garland Science, **2011**.

(332) Waxdal, M. J.; Konigsberg, W. H.; Henley, W. L.; Edelman, G. M. The covalent structure of a human G-immunoglobulin. II. Isolation and characterization of the cyanogen bromide fragments. *Biochemistry-Us* **1968**, *7* (5), 1959-1966

(333) Johansson, S. G. Raised levels of a new immunoglobulin class (IgND) in asthma. *Lancet* **1967**, *2* (7523), 951-953

(334) Gounni, A. S.; Lamkhioued, B.; Ochiai, K.; Tanaka, Y.; Delaporte, E.; Capron, A.; Kinet, J. P.; Capron, M. High-affinity IgE receptor on eosinophils is involved in defence against parasites. *Nature* **1994**, *367* (6459), 183-186

(335) Gould, H. J.; Sutton, B. J. IgE in allergy and asthma today. *Nat Rev Immunol* **2008**, *8* (3), 205-217

(336) Dorrington, K. J.; Bennich, H. H. Structure-Function Relationships in Human Immunoglobulin E. *Immunological Reviews* **1978**, *41* (1), 3-25

(337) Flanagan, J. G.; Rabbitts, T. H. The sequence of a human immunoglobulin epsilon heavy chain constant region gene, and evidence for three non-allelic genes. *EMBO J* **1982**, *1* (5), 655-660

(338) Plomp, R.; Hensbergen, P. J.; Rombouts, Y.; Zauner, G.; Dragan, I.; Koeleman, C. A.; Deelder, A. M.; Wuhrer, M. Site-specific N-glycosylation analysis of human immunoglobulin e. *Journal of proteome research* **2014**, *13* (2), 536-546

(339) Björklund, J. E. M.; Karlsson, T.; Magnusson, C. G. M. N-glycosylation influences epitope expression and receptor binding structures in human IgE. *Molecular Immunology* **1999**, *36* (3), 213-221

(340) Shade, K.-T. C.; Platzer, B.; Washburn, N.; Mani, V.; Bartsch, Y. C.; Conroy, M.; Pagan, J. D.; Bosques, C.; Mempel, T. R.; Fiebiger, E.; Anthony, R. M. A single glycan on IgE is indispensable for initiation of anaphylaxis. *The Journal of Experimental Medicine* **2015**, *212* (4), 457-467

(341) Woof, J. M.; Burton, D. R. Human antibody-Fc receptor interactions illuminated by crystal structures. *Nat Rev Immunol* **2004**, *4* (2), 89-99

(342) Zauner, G.; Selman, M. H.; Bondt, A.; Rombouts, Y.; Blank, D.; Deelder, A. M.; Wuhrer, M. Glycoproteomic analysis of antibodies. *Molecular & cellular proteomics : MCP* **2013**, *12* (4), 856-865

(343) Spiegelberg, H. L.; Fishkin, B. G. The catabolism of human γG immunoglobulins of different heavy chain subclasses. III. The catabolism of heavy chain disease proteins and of Fc fragments of myeloma proteins. *Clinical and Experimental Immunology* **1972**, *10* (4), 599-607

(344) Spiegelberg, H. L.; Fishkin, B. G.; Grey, H. M. Catabolism of human gammaG-immunoglobulins of different heavy chain subclasses. I. Catabolism of gammaG-myeloma proteins in man. *J Clin Invest* **1968**, *47* (10), 2323-2330

(345) Jefferis, R. Glycosylation as a strategy to improve antibody-based therapeutics. *Nat Rev Drug Discov* **2009**, *8* (3), 226-234

(346) Balbin, M.; Grubb, A.; de Lange, G. G.; Grubb, R. DNA sequences specific for Caucasian G3m(b) and (g) allotypes: allotyping at the genomic level. *Immunogenetics* **1994**, *39* (3), 187-193

(347) Alberts, B.; Johnson, A.; Lewis, J.; Raff, M.; Roberts, K.; Walter, P. *Molecular Biology of the Cell (4th edition)*; Garland Science, **2003**.

(348) Gonzalez-Quintela, A.; Alende, R.; Gude, F.; Campos, J.; Rey, J.; Meijide, L. M.; Fernandez-Merino, C.; Vidal, C. Serum levels of immunoglobulins (IgG, IgA, IgM) in a general adult population and their relationship with alcohol consumption, smoking and common metabolic abnormalities. *Clinical and Experimental Immunology* **2008**, *151* (1), 42-50

(349) Schauer, U.; Stemberg, F.; Rieger, C. H.; Borte, M.; Schubert, S.; Riedel, F.; Herz, U.; Renz, H.; Wick, M.; Carr-Smith, H. D.; Bradwell, A. R.; Herzog, W. IgG subclass concentrations in certified reference material 470 and reference values for children and adults determined with the binding site reagents. *Clin Chem* **2003**, *49* (11), 1924-1929

(350) Larsson, A.; Palm, M.; Hansson, L.-O.; Basu, S.; Axelsson, O. V. E. Reference values for α1-acid glycoprotein, α1-antitrypsin, albumin, haptoglobin, C-reactive protein, IgA, IgG and IgM during pregnancy. *Acta Obstetricia et Gynecologica Scandinavica* **2008**, *87* (10), 1084-1088

(351) Simister, N. E. Placental transport of immunoglobulin G. *Vaccine* **2003**, *21* (24), 3365-3369

(352) Chames, P.; Van Regenmortel, M.; Weiss, E.; Baty, D. Therapeutic antibodies: successes, limitations and hopes for the future. *British Journal of Pharmacology* **2009**, *157* (2), 220-233

(353) Reusch, D.; Haberger, M.; Selman, M. H.; Bulau, P.; Deelder, A. M.; Wuhrer, M.; Engler, N. High-throughput work flow for IgG Fc-glycosylation analysis of biotechnological samples. *Anal Biochem* **2013**, *432* (2), 82-89

(354) Reusch, D.; Tejada, M. L. Fc glycans of therapeutic antibodies as critical quality attributes (CQAs). *Glycobiology* **2015**,

(355) Maverakis, E.; Kim, K.; Shimoda, M.; Gershwin, M. E.; Patel, F.; Wilken, R.; Raychaudhuri, S.; Ruhaak, L. R.; Lebrilla, C. B. Glycans in the immune system and The Altered Glycan Theory of Autoimmunity: A critical review. *Journal of Autoimmunity* **2015**, *57* (0), 1-13

(356) Stadlmann, J.; Pabst, M.; Altmann, F. Analytical and Functional Aspects of Antibody Sialylation. *Journal of Clinical Immunology* **2010**, *30* (Suppl 1), 15-19

(357) Bondt, A.; Rombouts, Y.; Selman, M. H.; Hensbergen, P. J.; Reiding, K. R.; Hazes, J. M.; Dolhain, R. J.; Wuhrer, M. Immunoglobulin G (IgG) Fab glycosylation analysis using a new mass spectrometric high-throughput profiling method reveals pregnancy-associated changes. *Molecular & cellular proteomics : MCP* **2014**, *13* (11), 3029-3039

(358) Dalziel, M.; McFarlane, I.; Axford, J. S. Lectin analysis of human immunoglobulin G N-glycan sialylation. *Glycoconj J* **1999**, *16* (12), 801-807

(359) Wuhrer, M.; Stam, J. C.; van de Geijn, F. E.; Koeleman, C. A.; Verrips, C. T.; Dolhain, R. J.; Hokke, C. H.; Deelder, A. M. Glycosylation profiling of immunoglobulin G (IgG) subclasses from human serum. *Proteomics* **2007**, *7* (22), 4070-4081

(360) Yuan, W.; Sanda, M.; Wu, J.; Koomen, J.; Goldman, R. Quantitative analysis of immunoglobulin subclasses and subclass specific glycosylation by LC–MS–MRM in liver disease. *Journal of proteomics* **2015**, *116*, 24-33

(361) Plomp, R.; Dekkers, G.; Rombouts, Y.; Visser, R.; Koeleman, C. A.; Kammeijer, G. S.; Jansen, B. C.; Rispens, T.; Hensbergen, P. J.; Vidarsson, G.; Wuhrer, M. Hinge-Region O-Glycosylation of Human Immunoglobulin G3 (IgG3). *Molecular & cellular proteomics : MCP* **2015**, *14* (5), 1373-1384

(362) Schwab, I.; Nimmerjahn, F. Role of sialylation in the anti-inflammatory activity of intravenous immunoglobulin - F(ab')(2) versus Fc sialylation. *Clin Exp Immunol* **2014**, *178 Suppl 1*, 97-99

(363) Bohm, S.; Kao, D.; Nimmerjahn, F. Sweet and sour: the role of glycosylation for the anti-inflammatory activity of immunoglobulin G. *Current topics in microbiology and immunology* **2014**, *382*, 393-417

(364) Selman, M. H.; McDonnell, L. A.; Palmblad, M.; Ruhaak, L. R.; Deelder, A. M.; Wuhrer, M. Immunoglobulin G glycopeptide profiling by matrix-assisted laser desorption ionization Fourier transform ion cyclotron resonance mass spectrometry. *Anal Chem* **2010**, *82* (3), 1073-1081

(365) Parekh, R.; Isenberg, D.; Ansell, B.; Roitt, I.; Dwek, R.; Rademacher, T. Galactosylation Of Igg Associated Oligosaccharides: Reduction In Patients With Adult And Juvenile Onset Rheumatoid Arthritis And Relation To Disease Activity. *The Lancet* **1988**, *331* (8592), 966-969

(366) Parekh, R.; Isenberg, D.; Rook, G.; Roitt, I.; Dwek, R.; Rademacher, T. A comparative analysis of disease-associated changes in the galactosylation of serum IgG. *Journal of Autoimmunity* **1989**, *2* (2), 101-114

(367) Perdivara, I.; Peddada, S. D.; Miller, F. W.; Tomer, K. B.; Deterding, L. J. Mass Spectrometric Determination of IgG Subclass-Specific Glycosylation Profiles in Siblings Discordant for Myositis Syndromes. *Journal of proteome research* **2011**, *10* (7), 2969-2978

(368) Moore, J. S.; Wu, X.; Kulhavy, R.; Tomana, M.; Novak, J.; Moldoveanu, Z.; Brown, R.; Goepfert, P. A.; Mestecky, J. Increased levels of galactose-deficient IgG in sera of HIV-1-infected individuals. *AIDS* **2005**, *19* (4), 381-389

(369) Wuhrer, M.; Stavenhagen, K.; Koeleman, C. A.; Selman, M. H.; Harper, L.; Jacobs, B. C.; Savage, C. O.; Jefferis, R.; Deelder, A. M.; Morgan, M. Skewed Fc glycosylation profiles of anti-proteinase 3 immunoglobulin G1 autoantibodies from granulomatosis with polyangiitis patients show low levels of bisection, galactosylation, and sialylation. *Journal of proteome research* **2015**, *14* (4), 1657-1665

(370) Parekh, R. B.; Dwek, R. A.; Sutton, B. J.; Fernandes, D. L.; Leung, A.; Stanworth, D.; Rademacher, T. W.; Mizuochi, T.; Taniguchi, T.; Matsuta, K.; et al. Association of rheumatoid arthritis and primary osteoarthritis with changes in the glycosylation pattern of total serum IgG. *Nature* **1985**, *316* (6027), 452-457

(371) Ferrara, C.; Grau, S.; Jager, C.; Sondermann, P.; Brunker, P.; Waldhauer, I.; Hennig, M.; Ruf, A.; Rufer, A. C.; Stihle, M.; Umana, P.; Benz, J. Unique carbohydrate-carbohydrate interactions are required for high affinity binding between FcgammaRIII and antibodies lacking core fucose. *Proc Natl Acad Sci U S A* **2011**, *108* (31), 12669-12674

(372) Okazaki, A.; Shoji-Hosaka, E.; Nakamura, K.; Wakitani, M.; Uchida, K.; Kakita, S.; Tsumoto, K.; Kumagai, I.; Shitara, K. Fucose depletion from human IgG1 oligosaccharide enhances binding enthalpy and association rate between IgG1 and FcgammaRIIIa. *J Mol Biol* **2004**, *336* (5), 1239-1249

(373) Raju, T. S. Terminal sugars of Fc glycans influence antibody effector functions of IgGs. *Curr Opin Immunol* **2008**, *20* (4), 471-478

(374) Anthony, R. M.; Nimmerjahn, F.; Ashline, D. J.; Reinhold, V. N.; Paulson, J. C.; Ravetch, J. V. Recapitulation of IVIG anti-inflammatory activity with a recombinant IgG Fc. *Science* **2008**, *320* (5874), 373-376

(375) Kibe, T.; Fujimoto, S.; Ishida, C.; Togari, H.; Wada, Y.; Okada, S.; Nakagawa, H.; Tsukamoto, Y.; Takahashi, N. Glycosylation and Placental Transport of Immunoglobulin G. *Journal of Clinical Biochemistry and Nutrition* **1996**, *21* (1), 57-63

(376) van de Geijn, F. E.; Wuhrer, M.; Selman, M. H.; Willemsen, S. P.; de Man, Y. A.; Deelder, A. M.; Hazes, J. M.; Dolhain, R. J. Immunoglobulin G galactosylation and sialylation are associated with pregnancy-induced improvement of rheumatoid arthritis and the postpartum flare: results from a large prospective cohort study. *Arthritis research & therapy* **2009**, *11* (6), R193

(377) Selman, M. H.; Derks, R. J.; Bondt, A.; Palmblad, M.; Schoenmaker, B.; Koeleman, C. A.; van de Geijn, F. E.; Dolhain, R. J.; Deelder, A. M.; Wuhrer, M. Fc specific IgG glycosylation profiling by robust nano-reverse phase HPLC-MS using a sheath-flow ESI sprayer interface. *Journal of proteomics* **2012**, *75* (4), 1318-1329

(378) Ehrenstein, M. R.; Notley, C. A. The importance of natural IgM: scavenger, protector and regulator. *Nat Rev Immunol* **2010**, *10* (11), 778-786

(379) Thurnheer, M. C.; Zuercher, A. W.; Cebra, J. J.; Bos, N. A. B1 Cells Contribute to Serum IgM, But Not to Intestinal IgA, Production in Gnotobiotic Ig Allotype Chimeric Mice. *The Journal of Immunology* **2003**, *170* (9), 4564-4571

(380) Randall, T. D.; Brewer, J. W.; Corley, R. B. Direct evidence that J chain regulates the polymeric structure of IgM in antibody-secreting B cells. *J Biol Chem* **1992**, *267* (25), 18002-18007

(381) Czajkowsky, D. M.; Shao, Z. The human IgM pentamer is a mushroom-shaped molecule with a flexural bias. *Proceedings of the National Academy of Sciences* **2009**, *106* (35), 14960-14965

(382) Quartier, P.; Potter, P. K.; Ehrenstein, M. R.; Walport, M. J.; Botto, M. Predominant role of IgM-dependent activation of the classical pathway in the clearance of dying cells by murine bone marrow-derived macrophages in vitro. *European Journal of Immunology* **2005**, *35* (1), 252-260

(383) Tofik, R.; Ekelund, U.; Torffvit, O.; Sward, P.; Rippe, B.; Bakoush, O. Increased urinary IgM excretion in patients with chest pain due to coronary artery disease. *BMC Cardiovascular Disorders* **2013**, *13* (1), 72

(384) Caidahl, K.; Hartford, M.; Karlsson, T.; Herlitz, J.; Pettersson, K.; de Faire, U.; Frostegård, J. IgM-phosphorylcholine autoantibodies and outcome in acute coronary syndromes. *International Journal of Cardiology* **2013**, *167* (2), 464-469

(385) Putnam, F. W.; Florent, G.; Paul, C.; Shinoda, T.; Shimizu, A. Complete amino acid sequence of the Mu heavy chain of a human IgM immunoglobulin. *Science* **1973**, *182* (4109), 287-291

(386) Arnold, J. N.; Wormald, M. R.; Suter, D. M.; Radcliffe, C. M.; Harvey, D. J.; Dwek, R. A.; Rudd, P. M.; Sim, R. B. Human Serum Igm Glycosylation: Identification Of Glycoforms That Can Bind To Mannan-Binding Lectin. *J Biol Chem* **2005**, *280* (32), 29080-29087

(387) Pabst, M.; Kuster, S. K.; Wahl, F.; Krismer, J.; Dittrich, P. S.; Zenobi, R. A microarray-MALDI-MS approach for site-specific protein N-glycosylation analysis, as demonstrated for human serum IgM. *Molecular & Cellular Proteomics* **2015**,

(388) Arnold, J. N.; Saldova, R.; Hamid, U. M. A.; Rudd, P. M. Evaluation of the serum n-linked glycome for the diagnosis of cancer and chronic inflammation. *Proteomics* **2008**, *8* (16), 3284-3293

(389) Jaeken, J.; Hennet, T.; Freeze, H.; Matthijs, G. On the nomenclature of congenital disorders of glycosylation (CDG). *Journal of inherited metabolic disease* **2008**, *31* (6), 669-672

(390) Schubert, M.; Walczak, M. J.; Aebi, M.; Wider, G. Posttranslational Modifications of Intact Proteins Detected by NMR Spectroscopy: Application to Glycosylation. *Angewandte Chemie* **2015**, *127* (24), 7202-7206

(391) Shubhakar, A.; Reiding, K. R.; Gardner, R. A.; Spencer, D. I.; Fernandes, D. L.; Wuhrer, M. High-Throughput Analysis and Automation for Glycomics Studies. *Chromatographia* **2015**, *78* (5-6), 321-333

(392) Stockmann, H.; O'Flaherty, R.; Adamczyk, B.; Saldova, R.; Rudd, P. M. Automated, high-throughput serum glycoprofiling platform. *Integrative biology : quantitative biosciences from nano to macro* **2015**,

(393) Huffman, J. E.; Pučić-Baković, M.; Klarić, L.; Hennig, R.; Selman, M. H.; Vučković, F.; Novokmet, M.; Krištić, J.; Borowiak, M.; Muth, T. Comparative performance of four methods for high-throughput glycosylation analysis of immunoglobulin G in genetic and epidemiological research. *Molecular & Cellular Proteomics* **2014**, *13* (6), 1598-1610

(394) Morell, A. G.; Gregoriadis, G.; Scheinberg, I. H.; Hickman, J.; Ashwell, G. The role of sialic acid in determining the survival of glycoproteins in the circulation. *J Biol Chem* **1971**, *246* (5), 1461-1467

Table 1. Overview of plasma protein glycosylation

Glycoprotein	Uniprot number	Function	Plasma concentration range (mg/mL)	Avg. plasma concentration (mg/mL)	*N*-glycosylation sites	Site occupancy (%)	Glycan species	Changes under disease or inflammation	Changes with age	Glycosylation references (numbered)
Alpha-1-acid glycoprotein	P02763; P19652	Negative acute phase, transport of lipophilic compounds	0.36-1.46	0.77	Overall		A3G3S3 (33.5%); A4G4S4 (19.5%); A3FG3S3 (9%); A4G4S3 (8.2%); A3G3S2 (5%); A2G2S2 (4.5%); A4G4S2 (4%); A4FG4S4 (2.5%)	Conc↑, F↑, S↑	Conc↑ for females	[44, 49-55]
					Asn33		A3G3S3 (60%); A3FG3S3 (20%); A3G3S2 (12.5%)			
					Asn56		A3G3S3 (55%); A2G2S2 (22.5%); A3FG3S3 (12.5%); A3G3S2 (12.5);			
					Asn72		A4G4S4 (30%); A4G4S3 (15%); A3G3S3 (15%); A4G4S2 (10%); A4FG4S3 (5%); A4FG4S4 (5%)			
					Asn93		A4G4S4 (22.5%); A4G4S3 (20%); A3G3S3 (17.5%); A4FG4S4 (7.5%); A4FG3S3 (7.5%); A3FG3S3 (7.5%); A4G4S2 (7.5%)			
					Asn103		A4G4S4 (45%); A3G3S3 (20%); A4G4S2 (10%); A4G4S3 (7.5%); A3FG3S3 (5%)			

Glycoprotein	Uniprot number	Function	Plasma concentration range (mg/mL)	Avg. plasma concentration (mg/mL)	*N*-glycosylation sites	Site occupancy (%)	Glycan species	Changes under disease or inflammation	Changes with age	Glycosylation references (numbered)
Alpha-1-antitrypsin	P01009	Serine protease inhibitor	1.1	1.1	Overall Asn70 Asn107 Asn271		A2G2S2 (81%); A3G3S3 (9.8%); A3FG3S3 (5.6%); FA2G2S2 (3.6%) A2G2S2 (91.3%); FA2G2S2 (8.6%) A2G2S2 (52.5%); A3G3S3 (29.5%); A3FG3S3 (16.7%); FA2G2S2 (1.5%) A2G2S2 (99.3%); FA2G2S2 (0.7%)	Conc↑, complex	Glycosylation↓ except A2G1 and A3FG2S2↑	[56, 69-73]
Alpha-1B-glycoprotein	P04217	Uncertain, likely inflammation	0.22	0.22	Overall Asn44 Asn179 Asn363 Asn371		A2G2S1 (100%) A2G2S1 (100%)			[74, 83-86]
Alpha-2-HS-glycoprotein	P02765	Phosphate and calcium scavenger, metalloprotease protection	0.3-0.6	0.45	Overall Asn156 Asn176		A2G2S2 (96%); FA2G2S2 (4%)	Conc↑, (F)A3G3S3↑, A2G2S2↓ Glycosylation ↑↓		[88, 89, 98-101]
Alpha-2-macrogobulin	P01023	Protease scavenger	1-2	1.2	Overall		A2G2S2 (35%); A2G2S1 (35%); FA2G2S2 (15%); FA2G2S1 (15%); M5-7 (8%)	General ↑, Man↑, G↑		[83, 84, 100, 102, 107-111]

Glycoprotein	Uniprot number	Function	Plasma concentration range (mg/mL)	Avg. plasma concentration (mg/mL)	*N*-glycosylation sites	Site occupancy (%)	Glycan species	Changes under disease or inflammation	Changes with age	Glycosylation references (numbered)
					Asn55		A2G2S2; FA2G2S2			
					Asn70		A2G2S2			
					Asn247		A2G2S2			
					Asn396		A2G2S2			
					Asn410		A2G2S2			
					Asn869		Man5-7			
					Asn991		A2G2S2			
					Asn1424		A2G2S2; FA2G2S2			
Antithrombin-III	P01008	Serine protease inhibitor, coagulation	0.15	0.15	Overall		A2G2S2 (85%); A2G2S1 (15%)	Conc↓ (thrombosis), FA↑		[116, 120, 122-131]
					Asn128		A2G2S2; A2G2S1			
					Asn167		A2G2S2; A2G2S1; A3G3S3			
					Asn187		A2G2S2; A2G2S1; FA2G2S2; A3G3S3			
					Asn224		A2G2S2; A2G2S1; A3G3S2			
Apolipoprotein B-100	P04114	Cholesterol transport (LDL)	0.5	0.5	Overall		A2G2S1 (29.2%); A2G2S2 (23.6%); Man9 (8.6%); A2G2 (7.2%); Man5 (6.9%)			[11, 142, 147-149]
					Asn34	0%	---			
					Asn185		Man5-9			
					Asn983		A2G2S1; A2G2S2			
					Asn1368		Man5-9			

Glycoprotein	Uniprot number	Function	Plasma concentration range (mg/mL)	Avg. plasma concentration (mg/mL)	*N*-glycosylation sites	Site occupancy (%)	Glycan species	Changes under disease or inflammation	Changes with age	Glycosylation references (numbered)
					Asn1377		Man5-9			
					Asn1523		Man5-9; Hy; A1G1S1; A2G2S1; A2G2S2			
					Asn2239		A2G2S1; A2G2S2			
					Asn2560	0%	---			
					Asn2779		A2G2S1; A2G2S2			
					Asn2982		A2G2S1; A2G2S2			
					Asn3101		A2G2S1; A2G2S2			
					Asn3224		A2G2S1; A2G2S2			
					Asn3336		Man5-9			
					Asn3358		Man5-9			
					Asn3411		Man5-9; Hy; A1G1S1; A2G2S1; A2G2S2			
					Asn3465		A2G2S1; A2G2S2			
					Asn3895		A2G2S2; A3G3S3			
					Asn4237		A2G2S1; A2G2S2			
					Asn4431		A2G2S1; A2G2S2			
Apolipoprotein D	P05090	Cholesterol transport (HDL)	0.1	0.1	Overall		A2FG2S2; A3G3S3	Conc↑	Conc↑(Females)	[83, 84, 86, 100, 166-168]
					Asn65		A2G2S2; A3G3S2; A3G3S3; A4G4S4			
					Asn98		A2G2FS1; A2G2S2; A2FG2S2; A3FG3S2; A3FG3S3; A4FG4S3			

Glycoprotein	Uniprot number	Function	Plasma concentration range (mg/mL)	Avg. plasma concentration (mg/mL)	*N*-glycosylation sites	Site occupancy (%)	Glycan species	Changes under disease or inflammation	Changes with age	Glycosylation references (numbered)
Apolipoprotein F	Q13790	Cholesterol transport (VLDL)	0.073-0.096 (F-M)	0.0845	Overall					[170, 173, 174]
		Proprotein			Asn118		Man5-9			
		Proprotein			Asn139		Man5-9			
					Asn267					
Beta-2-glycoprotein 1	P02749	Scavenger of negatively charged compounds	0.2	0.2	Overall		A2G2S2 (58%); A3G3S3 (28.5%); A2G2S1 (6.5%); A3G3S2 (5%)	Conc↓, A3S↓, A2G2S2↑	Conc↑	[83, 175, 181, 182, 185-187]
					Asn162		A2G2S2 (67%); A3G3S3 (22%); A2G2S1 (5%); A3G3S2 (3%)	A3↓, A2↑		
					Asn183		A2; A3			
					Asn193		A2G2S2 (49%); A3G3S3 (35%); A2G2S1 (8%); A3G3S2 (7%)	A3↓, A2↑		
					Asn253		A2; A3			
Ceruloplasmin	P00450	Copper dependent iron oxidation (Fe2+ to Fe3+)	0.15-0.96	0.355	Overall		A2G2S2 (62.75%); FA2G2S2 (14.5%); A3G3S3 (13.5%); A3G3FS3 (7.25%)	Conc↑		[83, 188, 191, 192]
					Asn138		A2G2S2 (49%); FA2G2S2 (26%); A3G3S3 (12%); A3FG3S3 (10%); FA3FG3S3 (3%)			
					Asn227	0%	---			

Glycoprotein	Uniprot number	Function	Plasma concentration range (mg/mL)	Avg. plasma concentration (mg/mL)	*N*-glycosylation sites	Site occupancy (%)	Glycan species	Changes under disease or inflammation	Changes with age	Glycosylation references (numbered)
					Asn358		A2G2S2 (83%); FA2G2S2 (12%); A3G3S3 (5%)			
					Asn397		A2G2S2 (73%); A3G3S3 (17%); A3FG3S3 (6%); FA2G2S2 (4%)			
					Asn588		---			
					Asn762		A2G2S2 (46%); A3G3S3 (20%); FA2G2S2 (16%); A3FG3S3 (13%); FA3FG3S3 (2%); A4G4S4 (1%); A4FG4S4 (1%)			
					Asn926	0%	---			
Fibrinogen		Coagulation (platelet aggregation)	2.0-4.5	3	Overall		A2G2S1(6) (53%); A2G2S2(6) (33%)			[83, 84, 100, 107, 195, 208-218]
Fibrinogen alpha chain	P02671				Asn453	0%	---			
					Asn686	0%	---			
Fibrinogen beta-chain	P02675				Asn394		A2G2S1(6); A2G2S2(6)			
Fibrinogen gamma-chain	P02679				Asn78		A2G2S1(6); A2G2S2(6)			
					Asn334		A2G2S1(6); A2G2S2(6)	Glycosylation↑ in mutants		
Haptoglobin	P00738	Scavenger of hemoglobin,	0.8-2.5	1.32	Overall		A2G2S2 (45%); A2G2S1 (26%); A3G3S3 (9%);	Conc↑, glycosylation		[13, 223, 231-238]

Glycoprotein	Uniprot number	Function	Plasma concentration range (mg/mL)	Avg. plasma concentration (mg/mL)	*N*-glycosylation sites	Site occupancy (%)	Glycan species	Changes under disease or inflammation	Changes with age	Glycosylation references (numbered)
		acute phase response					A3FG3S3 (6%); A3G3S2 (5%); A3G3S1 (5%); A2FG2S1 (2%); A2FG2S2 (1%); A2G2S2 (46%); A2G2S1 (38%); A3G3S3 (4%); A3G3S2 (3%); A3G3S1 (2%); A2FG2S2 (3%); A2FG2S1 (3%); A3FG3S3 (1%)	complex, branching↑, F↑		
					Asn184	97.7%	A2G2S2 (47%); A2G2S1 (39%); A3G3S1 (7%); A4G4S1 (2%); A3FG3S1 (2%); A4G4S2 (1%); A2FG2S1 (1%); A2FG2S2 (1%)	S↑		
					Asn207	97.4%	A2G2S2 (40%); A3G3S3 (29%), A3FG3S3 (21%); A3G3S2 (10%)	S↑		
					Asn211	98.5%	A2G2S2 (47%); A2G2S1 (26%); A3G3S1 (10%); A3G3S2 (8%); A3G3S3 (4%); A2FG2S1 (2%); A2FG2S2 (1%); A3FG3S2 (1%); A4G4S1 (1%);			
					Asn241	95.8%				

Glycoprotein	Uniprot number	Function	Plasma concentration range (mg/mL)	Avg. plasma concentration (mg/mL)	*N*-glycosylation sites	Site occupancy (%)	Glycan species	Changes under disease or inflammation	Changes with age	Glycosylation references (numbered)
Hemopexin	P02790	Acute phase heme scavenger	0.4-1.5	0.8	Overall		A2G2S2 (90%); FA2G2S2 (5%)	Conc↑, Antennarity↑, F↑	Conc↑	[83, 84, 86, 100, 101, 107, 233, 244-251]
					Asn64		A2G2S2(6) (90%); FA2G2S2 (5%)			
					Asn187		A2G2S2(6) (90%); FA2G2S2 (5%)			
					Asn240					
					Asn246					
					Asn453		A2G2S2(6) (90%); FA2G2S2 (5%)			
Histdine-rich glycoprotein	P04196	Negative acute phase immunity, coagulation and angiogenesis regulator	0.1-0.15	0.125	Overall		A3-A4?	Conc↓	Conc↑	[84, 90, 107, 261-263]
					Asn63					
					Asn125					
					Asn344					
					Asn345					
Kininogen-1	P01042	Coagulation	0.055-0.090	0.0725	Overall		A3-A4?, Fc	Sialyl-Lewis X↑		[83, 84, 86, 100, 107, 264, 273]
					Asn48		Fc			
					Asn169					
					Asn205		Fc			
					Asn294		Fc			

Glycoprotein	Uniprot number	Function	Plasma concentration range (mg/mL)	Avg. plasma concentration (mg/mL)	*N*-glycosylation sites	Site occupancy (%)	Glycan species	Changes under disease or inflammation	Changes with age	Glycosylation references (numbered)
Serotransferrin	P02787	Iron transport	2-3	2.5	Overall		A2G2S2 (96.5%); FA2G2S2 (2.5%); A3G3S2 (1%)	Conc↑↓ (pregnancy↑, inflammation↓), A3↑(hepatoma), glycosylation changed (CDGs, alcohol↓)	Conc↑ (stable from 2yo)	[8, 83, 278, 281, 285-293]
		Minor Asn-X-Cys site			Asn432		A2G2S2 (93.5%); A3G3S2 (2.5%); A2G2S1 (2.4%); A2FG2S2 (1.6%)			
					Asn491	2%	A2G2S2 (100%)			
					Asn630		A2G2S2 (85.9%); FA2G2S2 (6.9%); A2FG2S2 (2.8%); A2G2S1 (2.2%); A3G3S2 (1.0%); FA3G3S2 (0.9%); FA2FG2S2 (0.3%)			
Vitronectin	P04004	Cell adhesion, coagulation	0.2-0.4	0.3	Overall		A2G2S2 (57%); A3G3S3 (14.3%); A3FG3S3 (10%); A2G2S1 (8.7%); Hy (6%); FA2G2S2 (3.3%)	Conc↑↓ (inflammation↑, liver fibrosis↓), hybrid↑(HCC), F↑ (HCC)		[17, 83, 100, 107, 301-303]
					Asn86		A2G2S2 (45%); A3G3S3 (33%); A3FG3S3 (20%)			
					Asn169		A2G2S2 (76%); Hy (18%); A2G2S1 (6%)			
					Asn242		A2G2S2 (50%); A2G2S1 (20%); FA2G2S2 (10%);			

Glycoprotein	Uniprot number	Function	Plasma concentration range (mg/mL)	Avg. plasma concentration (mg/mL)	*N*-glycosylation sites	Site occupancy (%)	Glycan species	Changes under disease or inflammation	Changes with age	Glycosylation references (numbered)
							A3G3S3 (10%); A3FG3S3 (10%)			
Zinc-alpha-2-glycoprotein	P25311	Fat metabolism	0.05	0.05	Overall		A2G2S2 (97%); A2G2S1 (3%)	Conc↑ (cancer)		[83, 84, 100, 107, 174, 246, 305, 308-310]
					Asn109					
					Asn112		A2G2S2 (100%)			
					Asn128		A2G2S2 (100%)			
					Asn259		A2G2S2 (90%); A2G2S1 (10%)			
Immunoglobulin A 1	P01876	Immunity (mucosal; FcaRI)	2.62	2.62	Overall		A2G2S2 (24%); A2G2S1 (20%); FA2BG2S2 (14%)			[311, 315-320]
				0.9	Asn144		A2G2S1 (50%); A2G2S2 (27%); A2BG2S1 (10%)			
					Asn340		FA2G2S2 (46%); FA2BG2S2 (40%); FA2G2S1 (13%)			
Immunoglobulin A 2	P01877			0.1	Asn47					
					Asn92					
					Asn131					
					Asn205					
					Asn327					
Immunoglobulin D	P01880	Immunity	0.03; <0.003-0.4	0.035	Overall		Man8 (14.4%); Man9 (13.5%); FA2G2S2 (7.6%);			[326-330]

Glycoprotein	Uniprot number	Function	Plasma concentration range (mg/mL)	Avg. plasma concentration (mg/mL)	*N*-glycosylation sites	Site occupancy (%)	Glycan species	Changes under disease or inflammation	Changes with age	Glycosylation references (numbered)
							FA2G2S1 (7.3%); FA2BG2S2 (6.5%); A2G2S1 (6.1%)			
					Asn225		Man8; Man9			
					Asn316		FA2G2S2; FA2G2S1; FA2BG2S2; A2G2S1			
					Asn367		FA2G2S2; FA2G2S1; FA2BG2S2; A2G2S1			
Immunoglobulin E	P01854	Immunity (parasitic infection; allergy)	0.0003	0.0003	Overall		FA2G2S2 (25%); FA2G2S1 (14.5%); FA2BG2S2 (13.5%); FA2BG2S1 (13.5%); Man5 (8.5%)	B↓, A3↓		[329, 336-341]
					Asn21		FA2G2S1 (30%); FA2BG2S1 (30%); FA2G2S2 (15%); FA2BG2S2 (10%)			
					Asn49		FA2G2S2 (30%); FA2G2S1 (18%); FA2BG2S2 (15%); FA2BG2S1 (15%)			
					Asn99		FA2G2S2 (40%); FA2G2S1 (20%)			
					Asn146		FA2G2S2 (50%); FA2BG2S2 (30%); FA2G2S1 (10%)			
					Asn252		FA2BG2S1 (35%); FA2BG2S2 (25%); FA2G2S2 (15%); FA2G2S1 (10%)			
					Asn264	0	---			
					Asn275		Man5 (50%); Man6 (15%); Man7 (10%);			

Glycoprotein	Uniprot number	Function	Plasma concentration range (mg/mL)	Avg. plasma concentration (mg/mL)	*N*-glycosylation sites	Site occupancy (%)	Glycan species	Changes under disease or inflammation	Changes with age	Glycosylation references (numbered)
							Man8 (10%); Man9 (5%)			
Immunoglobulin G		Immunity (primary; secondary; complement system)	7-18	11.8	Overall		FA2G1 (31%); FA2G2 (23%); FA2G2S1 (13%); FA2 (10%); FA2BG1 (5%)	Conc↓(pregnancy), FA2↑, FA2G2↓(RA, CD…), G↑+S↑(pregnancy), G↓	G↓	[19, 20, 24, 28, 33, 342, 355-377]
Immunoglobulin G1	P01857		5.03	5.03	Asn180					
Immunoglobulin G2	P01859		3.42	3.42	Asn176					
Immunoglobulin G3	P01860		0.58	0.58	Asn227					
			0.58	0.58	Asn322					
Immunoglobulin G4	P01861		0.38	0.38	Asn177					
Immunoglobulin M	P01871	Immunity (complement system)	0.5-2.0	1.47	Overall		FA2BG2S1 (26%); FA2G2S1 (19%); Man6 (10%); Man5 (6%)			[311, 385-387]
					Asn46		FA2BG2S1; FA2G2S1			
					Asn209		FA2BG2S1; FA2G2S1			
					Asn272		FA2BG2S1; FA2G2S1			
					Asn279		Man5; Man6			
					Asn439	17	Man6; Man7; Man8			

Chapter 3

Plasma *N*-Glycan Signatures Are Associated with Features of Inflammatory Bowel Diseases

Plasma *N*-Glycan Signatures Are Associated with Features of Inflammatory Bowel Diseases

Florent Clerc [a#], Mislav Novokmet [b#], Viktoria Dotz [a], Karli R. Reiding [a], Noortje de Haan [a], Guinevere S.M. Kammeijer [a], Hans Dalebout [a], Marco R. Bladergroen [a], Frano Vukovic [b], Erdmann Rapp [c/d], IBD-BIOM consortium, Stephan R. Targan [e], Gildardo Barron [e], Natalia Manetti [f], Anna Latiano [g], Dermot P.B. McGovern [e], Vito Annese [f/g], Gordan Lauc [b], Manfred Wuhrer [a*].

[a] *Center for Proteomics and Metabolomics, Leiden University Medical Center (LUMC), 2300 RC Leiden, The Netherlands*

[b] *Genos Ltd, Glycobiology Laboratory, 10000 Zagreb, Croatia*

[c] *Max Planck Institute for Dynamics of Complex Technical Systems, Sandtorstrasse 1, 39106 Magdeburg, Germany*

[d] *glyXera GmbH, Leipziger Strasse 44, 39120 Magdeburg, Germany.*

[e] *F. Widjaja Foundation Inflammatory Bowel and Immunobiology Research Institute, Cedars-Sinai Medical Center, Los Angeles, California, USA.*

[f] *Unit of Gastroenterology SOD2 (Strutture Organizzative Dipartimentali), Azienda Ospedaliero Universitaria (AOU) Careggi, Florence, Italy.*

[g] *Unit of Gastroenterology, IRCCS-CSS (Istituto di Ricovero e Cura a Carattere Scientifico–Casa Sollievo della Sofferenza) Hospital, San Giovanni Rotondo, Italy.*

[#] *these authors contributed equally*

*Corresponding Author

e-mail: m.wuhrer@lumc.nl, Phone: +31 71 52 68744.

Published in Gastroenterology, 2018, 155 (3), 829-843.

DOI: 10.1053/j.gastro.2018.05.030

Abbreviations: MALDI-TOF-MS = matrix-assisted laser desorption/ionization time-of-flight mass spectrometry, SA = sialic acid, TPNG = total plasma *N*-glycome.

Abstract

Background & aims

Biomarkers are needed for early detection of Crohn's disease (CD) and ulcerative colitis (UC) or to predict patient outcomes. Glycosylation is a common and complex posttranslational modification of proteins that affects their structure and activity. We compared plasma *N*-glycosylation profiles between patients with CD or UC and healthy individuals (controls).

Methods

We analyzed the total plasma *N*-glycomes of 2635 patients with inflammatory bowel diseases and 996 controls by mass spectrometry with a linkage-specific sialic acid derivatization technique. Plasma samples were acquired from 2 hospitals in Italy (discovery cohort, 1989 patients with inflammatory bowel disease [IBD] and 570 controls) and 1 medical center in the United States (validation cohort, 646 cases of IBD and 426 controls). Sixty-three glycoforms met our criteria for relative quantification and were extracted from the raw data with the software MassyTools. Common features shared by the glycan compositions were combined in 78 derived traits, including the number of antennae of complex-type glycans and levels of fucosylation, bisection, galactosylation, and sialylation. Associations of plasma *N*-glycomes with age, sex, CD, UC, and IBD-related parameters such as disease location, surgery and medication, level of C-reactive protein, and sedimentation rate were tested by linear and logistic regression.

Results

Plasma samples from patients with IBD had a higher abundance of large-size glycans compared with controls, a decreased relative abundance of hybrid and high-mannose structures, lower fucosylation, lower galactosylation, and higher sialylation (α2,3- and α2,6-linked). We could discriminate plasma from patients with CD from that of patients with UC based on higher bisection, lower galactosylation, and higher sialylation (α2,3-linked). Glycosylation patterns were associated with disease location and progression, the need for a more potent medication, and surgery. These results were replicated in a large independent cohort.

Conclusions

We performed high-throughput analysis to compare total plasma *N*-glycomes of individuals with vs without IBD and to identify patterns associated with disease features and the need for treatment. These profiles might be used in diagnosis and for predicting patients' responses to treatment.

Keywords: Crohn's Disease; ulcerative colitis; glycosylation; mass spectrometry

Background and context

The etiology of inflammatory bowel diseases is poorly understood and improved non-invasive diagnostic and prognostic tools are needed. Protein-linked carbohydrates (glycans) represent promising biomarker and therapeutic candidates.

New findings

This study found replicated associations of disease status and different clinical parameters with multiple glycosylation features of plasma proteins, including structures known to be crucial in immunological processes.

Limitations

Several dozens of different glycoproteins mainly derived from liver or immune cells contribute to the plasma glycan profile. Further studies assessing the glycosylation of specific proteins are needed to elucidate the mechanisms behind these glycosylation changes.

Impact

Multiple novel potential targets for diagnostic and prognostic approaches in inflammatory bowel disease management have been presented here.

Introduction

Inflammatory bowel diseases (IBDs), which include Crohn's disease (CD) and ulcerative colitis (UC), are chronic relapsing inflammatory conditions of the digestive tract. Approximately 1% of the population in developed countries is affected, and the prevalence in developing countries is rising rapidly[1]. Genetic variation, environmental risk factors, and a dysregulation of the mucosal immune system are associated with an increased risk of IBD, although the exact etiology of the disease remains unknown[2-4]. The diagnosis of IBD is not always straightforward, lacks a

criterion standard test, and usually relies on a combination of medical history, laboratory investigations, and diagnostic procedures[3, 4]. Established markers such as C-reactive protein (CRP), erythrocyte sedimentation rate, or fecal calprotectin have neither the sensitivity nor specificity to reliably distinguish inflammation from functional symptoms and can reflect various autoimmune diseases, cancer, inflammation, or infections[5, 6]. Endoscopic investigations are the most reliable way to confirm the presence of IBD, differentiate CD from UC, and evaluate the efficacy of therapy at the mucosal level, but they are invasive and carry risks linked to the procedure and sedation of the patients[7]. Recent data suggest that serologic markers, such as anti-Saccharomyces cerevisiae antibodies (ASCA) or anti-neutrophilic cytoplasmic antibodies (ANCA), may be promising, but their use is controversial, and they have not been widely adopted in the management of IBD[8]. Consequently, there is an urgent need for noninvasive prognostic tests that will allow clinicians to predict the natural course of disease and target expensive therapies to those most likely to benefit[9, 10].

Glycosylation is recognized to be a complex and highly abundant posttranslational modification of proteins that can significantly affect the structural and functional properties of the conjugate[11, 12]. The modification is involved in the regulation of biological processes ranging from protein secretion and transport to receptor interaction and modulation of the immune response[12, 13]. Protein glycoforms found in healthy individuals are quite stable over time but can dramatically change because of a pathologic condition, especially upon inflammation[14, 15]. Furthermore, protein glycosylation is involved in the pathophysiology of major diseases such as cancer, diabetes, and rheumatoid arthritis[13, 16], and has previously been associated with IBD[17-20]. A particular glycosylation phenotype, that is, the linkage of sialic acids (SAs), which can be of α2,3- or α2,6-type, is reported to affect various biological processes, for example, protein-receptor interactions and the immune response in tumor cells[21, 22]. Sialyl-Lewis X structures are formed exclusively with α2,3-linked SA, and we envision that the evaluation of SA linkages in the context of IBD can provide insights into disease mechanisms and help the development of targeted treatment strategies[15, 22-24].

To this end, we evaluated the total plasma *N*-glycome (TPNG) of 2635 IBD patients and 996 healthy control individuals (HCs) distributed over 2 independent cohorts. The glycans were released from the plasma proteins, and their SAs were derivatized with our recently developed linkage-specific derivatization method and analyzed using high-throughput matrix-assisted laser desorption/ionization time-of-flight mass spectrometry (MALDI-TOF-MS)[25, 26].

Materials and methods

Clinical samples

Plasma samples were acquired from 3 repositories in Italy and the United States. The Italian sample set was combined from the University Hospital Careggi (Florence, Italy) and IRCCS-CSS Hospital S. Giovanni (Rotondo, Italy)[27]. The American sample set was collected at the Pediatric and Adult IBD Centers at Cedars-Sinai Medical Center (Los Angeles, CA). Informed written consent was obtained from the participants, and ethical approval was provided by the Ethics Review Board of the University Hospital Careggi and Casa Sollievo della Sofferenza. Hospital (Italy) and by the Cedars-Sinai Institutional Review Board (United States), respectively. The patients were categorized according to the Montreal classification of IBD[28]. Because of its larger number of patient samples, the Italian sample set (1989 IBD patients and 570 HCs) was chosen as the discovery cohort and the American cohort (646 IBD patients and 426 HCs) for replication. The demographics of the individuals retained for statistical analysis are presented in **Table 1.**

Table 1: Demographics of the individuals included for cross-sectional statistical analysis

Italian cohort (discovery)				
Sample numbers	HC	CD	UC	All
Total (males)	570 (355)	905 (524)	1084 (648)	2559 (1527)
Age, mean ± SD				
Males	50.5 ± 17.4	37.1 ± 14.0	43.4 ± 15.5	42.9 ± 16.2
Females	55.4 ± 18.2	38.5 ± 15.1	39.9 ± 15.5	42.6 ± 17.2
All	52.3 ± 17.9	37.7 ± 14.5	42.0 ± 15.6	42.8 ± 16.7
American cohort (replication)				
Sample numbers	HC	CD	UC	All
Total (males)	426 (180)	389 (220)	257 (124)	1072 (524)
Age, mean ± SD				
Males	46.3 ± 14.8	36.4 ± 14.5	42.3 ± 17.0	41.2 ± 15.8
Females	44.5 ± 13.7	39.9 ± 15.7	41.4 ± 15.1	42.3 ± 14.8
All	45.2 ± 14.2	37.9 ± 15.1	41.8 ± 16.0	41.8 ± 15.3

Patient information				
	Italian		**American**	
Disease group (counts)	CD	UC	CD	UC
Disease Location (CD)				
Ileum+UpperGI (L1+L4)	306+19		81+8	
Colon+UpperGI (L2+L4)	158+6		55+3	
Ileum+Colon+UpperGI (L3+L4)	333+22		197+35	
Upper GI (L4)	60		46	
Disease Location (UC)				
Rectum (E1)		124		7
Sigmoid + Left colon (E2)		507		64
Entire colon (E3)		447		183
Disease behaviour (CD)				
Inflammatory (B1)	519		139	
Stenosing (B2)	249		109	
Fistulizing (B3)	128		136	
Perianal disease modifier				
Yes	187	27	133	
No	667	982	216	
Surgery				
No	557	939	146	120
Before sample collection	250	39	119	85
After sample collection	33	7	44	14
Medication				
Mesalazine	186	329		
Steroids	242	371	all	all
Azathioprine/6-mercaptopurine	198	220	69	87
Anti-TNFα	186	89	310	148
Inflammation markers				
CRP levels			125	74
Sedimentation rate			140	77

Mass spectrometric glycomics and data analysis

The Italian plasma samples were prepared as previously described[26] and analyzed by MALDI-TOF-MS at the Max Planck Institute for Dynamics of Complex Technical Systems in Magdeburg, Germany. The American samples were prepared and measured on a robotized platform at the Leiden University Medical Center in Leiden, The Netherlands[25]. For this, the samples were randomly distributed in equal proportions of cases and controls on 96-well plates. The glycans were enzymatically released from the plasma proteins using peptide-*N*-glycosidase F, and the SAs were

derivatized by linkage-specific esterification. The derivatized glycans were then purified by hydrophilic interaction liquid chromatography solid-phase extraction and were analyzed by MALDI-TOF-MS in reflectron-positive mode on Bruker ultrafleXtreme instruments (Bruker Daltonics, Bremen, Germany)[25, 26]. A detailed description of the material and methods can be found in the **Supplementary Material**.

Data processing

In total, 63 glycoforms passed our quality criteria for relative quantification and were extracted from the raw data with the software MassyTools[29] (**Supplementary Table 1**). Common features shared by the glycan compositions were combined in 78 derived traits, including the number of antennae of complex-type glycans (CA), and the levels of fucosylation (F), bisection (B), galactosylation (G), and sialylation (S) (**Supplementary Table 2**)[30]. The relative glycan intensities and calculated derived traits were corrected for batch effects. Data points deviating more than 5 standard deviations (SDs) from their respective means were considered outliers and were excluded from further analysis.

Statistical analysis

The associations of the TPNG with age-, sex-, CD-, UC-, and IBD-related parameters such as disease location, surgery, medication, CRP levels, and sedimentation rate were tested by linear and logistic regression (for continuous and binary outcome variables, respectively) on standardized data (subtraction of the mean and division by the SD) using R, version 3.3.2 (R Foundation for Statistical Computing, Vienna, Austria) and RStudio, version 1.0.136 (RStudio, Boston, MA) (see Supplementary Material). Age, sex, and their interaction were included as covariates in the models for the disease-related tests. The odds ratios (ORs) were calculated with their 95% confidence intervals (CIs) assuming a Student‘s t distribution and are referring to an increase of 1 SD in the tested traits. A meta-analysis of the associations with IBD found in the discovery and replication cohort was performed using a fixed effects model.

For the receiver operating characteristic analysis, 1 derived glycan trait was first selected from each of the derived trait classes (complex-type glycans, fucosylation, bisection, galactosylation, sialylation, E/L) based on having the strongest effect sizes in the meta-analysis and tested for significance in their prediction of diagnosis. Those found not to be significant were removed step-by-step from the equation until all remaining traits were deemed significant, thus achieving maximal prediction performance with a minimal set of traits. The model was trained on a random selection of 75% of the samples from the discovery cohort, and prediction was

validated on all available cases in the replication cohort. An internal prediction validation was also performed on the remaining cases of the discovery cohort (25%) to control for overfitting. The power of the prediction (area under the curve) was calculated on 10 repetitions of the random sampling in both cohorts.

In CD, we tested for association of the TPNG with localization of disease by comparing patients with ileal (L1) or colonic disease (L2) and associations with the disease severity by comparing concise CD (L1 or L2) to extended CD (ileocolon + upper gastrointestinal tract, L3 + L4), that is, L1 vs L2 vs L3 + L4 (see Supplementary Material). With respect to disease behavior in CD, we compared inflammatory (B1), stenosing (B2), and internal fistulizing behavior (B3) (B1 vs B2 vs B3), and furthermore compared patients with and without perianal disease. In UC, we compared distal disease (E1 + E2) and extensive disease (E3), that is, E1 + E2 vs E3, as indicated in **Table 1**. We also compared the TPNG profiles of colonic CD (L2) vs UC patients.

According to the clinical practices of the medical centers, patients were treated with mesalazine (mesalamine), steroids, azathioprine/6-mercaptopurine or anti–tumor necrosis factor (TNF)-α in the discovery (Italian) cohort, whereas all patients of the replication (US) cohort had been exposed to corticosteroid treatment accompanied by either azathioprine or anti– TNFα[31]. In the Italian cohort, patients were stratified into 4 groups according to the most potent drug class used at the time of sample collection. Patients exposed to both thiopurines and anti–TNF-α agents were classified as being exposed to anti–TNF-α agents for both cohorts. The TPNG profiles respective to each resulting drug class were compared with each other. Because the medication strategies differed between cohorts, we could not directly test for replication, but we looked for similarities instead.

Furthermore, we compared selected glycan traits of a small group of the replication cohort in paired samples (same individuals before and after surgery) using a Wilcoxon signed-rank test. Because cross-sectional surgery data were available in a larger patient group (Table 1), we tested for associations of the TPNG with the status of sample collection before (reference category) and after surgery in cross-sectional manner. We also tested the association of TPNG profiles with surgery by comparing patients requiring surgery with those who did not undergo surgery throughout the study period, thus testing for associations of the TPNG with the need of surgical intervention (see Supplementary Material).

Multiple testing correction was performed based on a false discovery rate of 5% (see **Supplementary Material**).

Results

The TPNG was analyzed by MALDI-TOF-MS for a total of 2635 IBD patients and 996 HCs from 2 independent cohorts. Sixty-three of the detected glycan compositions passed our quality criteria for relative quantification and were grouped into 78 derived traits based on their number of antennae, their bisection, galactosylation, fucosylation, and (linkage-specific) sialylation (Figure 1**, Supplementary Table 1, Supplementary Table 2**). Our primary objective was to find associations of the TPNG with UC or CD, compared with HCs, and CD vs UC. Additional secondary analyses were performed to evaluate the associations between the TPNG in patients and IBD-specific parameters, such as disease location, medication, and surgery. For the logistic models, we expressed the effect sizes as ORs, representing the odds of belonging to a group (eg, CD vs HC) in relation to an increase of 1 SD in the tested traits (eg, A2FS0G).

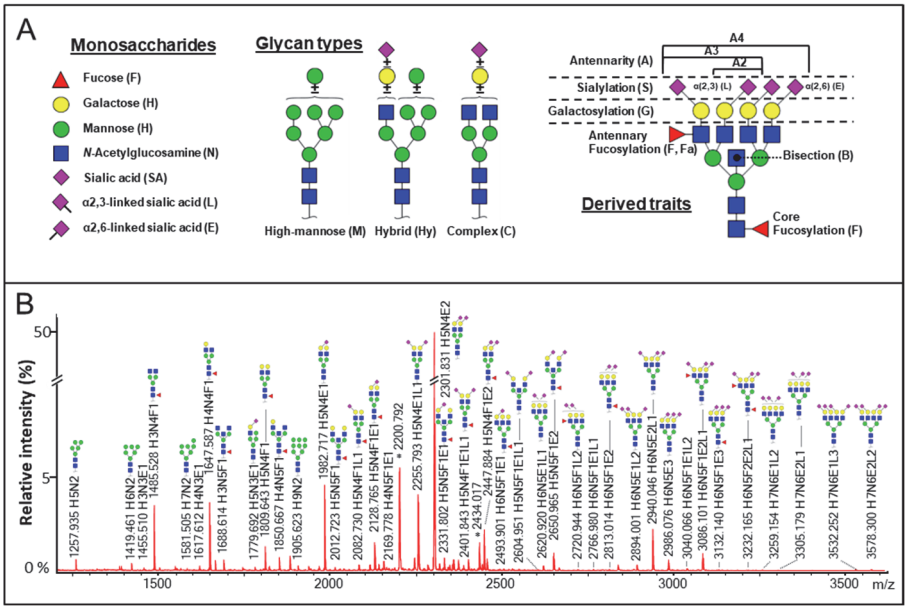

Figure 1. Glycan features and averaged spectrum of CD patients. *A) Schematic representation of glycan types and derived traits based on the common structural features of different individual glycans. B) Averaged MALDI-TOF-MS spectrum of CD patients from two 96-well plates of the discovery cohort (see Supporting information for details on the averaging of spectra). Major glycan peaks are assigned to compositions and structural schemes. The peaks marked with an asterisk (*) are satellites of the main peak.*

TPNG is associated with inflammatory bowel disease

The associations of the TPNG with IBD were tested by logistic regression on standardized data with age, sex, and their interaction as covariates in the model. In total, 45, 43, and 23 meta-analyzed associations were found in the 2 cohorts when comparing CD patients vs HCs, UC patients vs HCs, and UC vs CD patients, respectively (**Table 2, Supplementary Table 3**).

Table 2: Meta-analyzed associations of plasma *N*-glycans with CD and UC. *Red and blue labels indicate positive and negative replicated associations, respectively, with the second-called category being the reference. See Supplementary* ***Table 3*** *for the complete list of tests performed.*

Derived traits	Description of the derived traits	meta *p*-values			meta odds ratio (95% CI)		
		CD / Controls	UC / Controls	UC / CD	CD / Controls	UC / Controls	UC / CD
Glycan type							
CA2	Diantennary (A2) within complex-type	6.26E-28	5.60E-09	5.29E-16	0.53 (0.47-0.59)	0.75 (0.68-0.82)	1.34 (1.25-1.43)
CA3	Triantennary (A3) within complex-type	7.40E-28	2.06E-09	6.25E-15	1.88 (1.68-2.11)	1.35 (1.23-1.49)	0.76 (0.71-0.81)
CA4	Tetraantennary (A4) within complex-type	8.50E-08	2.43E-06	2.57E-01	1.32 (1.19-1.46)	1.27 (1.15-1.40)	1.04 (0.97-1.12)
TC	Complex-type within total	1.06E-28	8.14E-14	6.88E-08	1.83 (1.65-2.04)	1.45 (1.32-1.60)	0.82 (0.77-0.88)
TM	High-mannose (M) within total	3.63E-21	9.50E-12	4.85E-03	0.61 (0.55-0.67)	0.71 (0.65-0.78)	1.10 (1.03-1.18)
THy	Total hybrid within total	3.42E-32	2.51E-12	9.25E-25	0.52 (0.47-0.58)	0.71 (0.64-0.78)	1.48 (1.37-1.60)
TA2FS0	Total asialo fucosylated A2	1.25E-20	3.07E-07	1.00E-12	0.61 (0.55-0.67)	0.78 (0.71-0.86)	1.29 (1.20-1.38)
Fucosylation (F)							
CF	of complex-type	2.29E-13	1.70E-09	3.04E-06	0.68 (0.62-0.76)	0.74 (0.67-0.82)	1.18 (1.10-1.26)
CFa	Antennary F within complex-type	2.81E-01	4.24E-05	1.59E-07	1.05 (0.96-1.16)	0.82 (0.75-0.90)	0.83 (0.78-0.89)
A2Fa	Antennary F of A2	7.37E-23	5.85E-12	9.44E-05	0.59 (0.53-0.65)	0.70 (0.64-0.78)	1.15 (1.07-1.23)
A3Fa	Antennary F of A3	4.92E-04	4.69E-02	1.94E-17	1.19 (1.08-1.31)	0.91 (0.82-1.00)	0.73 (0.68-0.79)
A2F	of A2	2.97E-19	5.52E-10	1.42E-11	0.62 (0.56-0.69)	0.73 (0.67-0.81)	1.27 (1.19-1.36)
A3F	of A3	2.51E-05	2.02E-02	2.05E-25	1.24 (1.12-1.37)	0.89 (0.81-0.98)	0.68 (0.63-0.73)
A2SF	of A2 sialylated	1.30E-14	2.16E-10	2.24E-07	0.67 (0.61-0.74)	0.73 (0.66-0.80)	1.20 (1.12-1.29)
A2L0F	of A2 without α2,3 sialic acid (SA)	1.38E-17	2.78E-08	3.36E-12	0.64 (0.57-0.71)	0.76 (0.69-0.84)	1.28 (1.20-1.38)
A2LF	of A2 with α2,3 SA	1.79E-20	4.11E-29	5.73E-01	0.59 (0.52-0.66)	0.51 (0.45-0.57)	0.98 (0.91-1.05)
A3LF	of A3 with α2,3 SA	4.58E-04	3.90E-03	2.77E-25	1.19 (1.08-1.32)	0.87 (0.78-0.95)	0.68 (0.63-0.73)
A2EF	of A2 with α2,6 SA	1.85E-11	2.88E-08	2.34E-06	0.71 (0.64-0.79)	0.76 (0.69-0.84)	1.18 (1.10-1.27)
A3EF	of A3 with α2,6 SA	6.00E-06	3.80E-02	2.42E-26	1.26 (1.14-1.39)	0.90 (0.82-0.99)	0.67 (0.62-0.72)
Bisection (B)							
A2FB	of fucosylated A2	9.48E-13	2.16E-03	6.87E-06	1.49 (1.33-1.66)	1.17 (1.06-1.30)	0.85 (0.79-0.91)
A2FSB	of fucosylated sialylated A2	1.03E-14	1.15E-07	1.56E-02	1.51 (1.36-1.67)	1.31 (1.19-1.45)	0.92 (0.85-0.98)
A2F0S0B	of afucosylated nonsialylated A2	1.39E-10	4.60E-02	3.70E-20	1.41 (1.27-1.57)	0.90 (0.82-1.00)	0.71 (0.66-0.77)
Galactosylation (G)							
A2F0G	of afucosylated A2	1.26E-13	3.40E-05	5.55E-06	1.48 (1.33-1.64)	1.22 (1.11-1.34)	0.85 (0.79-0.91)
A2S0G	of asialo A2	1.12E-47	1.39E-13	2.11E-32	0.39 (0.35-0.45)	0.65 (0.58-0.73)	1.58 (1.47-1.70)

Derived traits	Description of the derived traits	meta *p*-values			meta odds ratio (95% CI)		
		CD / Controls	UC / Controls	UC / CD	CD / Controls	UC / Controls	UC / CD
A2FS0G	of fucosylated asialo A2	6.28E-51	1.34E-14	1.82E-36	0.37 (0.33-0.43)	0.64 (0.57-0.72)	1.63 (1.51-1.76)
A2F0SG	of afucosylated sialylated A2	2.03E-10	2.77E-07	5.49E-03	1.38 (1.25-1.53)	1.28 (1.17-1.41)	0.91 (0.85-0.97)
A2F0S0G	of afucosylated asialo A2	1.86E-10	1.15E-04	4.27E-04	0.72 (0.65-0.80)	0.82 (0.75-0.91)	1.14 (1.06-1.22)
Sialylation (S)							
CS	of complex	1.66E-22	3.89E-08	1.84E-12	1.70 (1.53-1.89)	1.31 (1.19-1.44)	0.78 (0.72-0.83)
A2S	of A2	1.12E-21	1.30E-08	1.27E-11	1.68 (1.51-1.87)	1.32 (1.20-1.45)	0.78 (0.73-0.84)
A2FS	of A2 fucosylated	1.47E-15	8.65E-03	1.38E-13	1.51 (1.37-1.67)	1.13 (1.03-1.24)	0.77 (0.72-0.82)
A2GS	per galactose in A2	8.27E-37	4.28E-12	9.34E-23	2.10 (1.87-2.35)	1.42 (1.28-1.56)	0.69 (0.64-0.74)
A3GS	per galactose in triantennary A3	2.06E-38	3.13E-20	5.75E-10	2.15 (1.92-2.41)	1.60 (1.45-1.77)	0.80 (0.75-0.86)
A2FGS	per galactose in fucosylated A2	2.24E-46	4.40E-09	7.40E-40	2.38 (2.12-2.68)	1.36 (1.22-1.50)	0.60 (0.55-0.65)
A3FGS	per galactose in fucosylated A3	1.59E-41	1.01E-15	5.94E-31	2.21 (1.97-2.48)	1.51 (1.37-1.67)	0.65 (0.60-0.70)
A3F0GS	per galactose in afucosylated A3	2.73E-15	1.39E-13	8.56E-01	1.51 (1.36-1.67)	1.45 (1.31-1.60)	0.99 (0.93-1.06)
A4F0GS	per galactose in afucosylated A4	1.12E-08	2.24E-12	9.32E-05	1.34 (1.21-1.48)	1.43 (1.30-1.59)	1.15 (1.07-1.23)
α2,3-linked sialylation (L)							
A2L	α2,3-linked (L) in A2	2.60E-13	5.88E-09	5.14E-03	1.46 (1.32-1.62)	1.34 (1.21-1.47)	0.91 (0.85-0.97)
A2F0L	L in afucosylated A2	1.89E-14	2.72E-16	5.73E-01	1.50 (1.36-1.67)	1.55 (1.40-1.72)	1.02 (0.95-1.09)
A2GL	L per galactose in A2	1.47E-12	2.24E-08	2.04E-02	1.44 (1.30-1.59)	1.32 (1.20-1.45)	0.92 (0.86-0.99)
A3GL	L per galactose in A3	4.95E-28	1.25E-24	3.87E-01	1.88 (1.68-2.10)	1.75 (1.57-1.95)	0.97 (0.91-1.04)
A2FGL	L per galactose in fucosylated A2	2.26E-15	3.33E-02	7.17E-24	1.53 (1.38-1.70)	1.11 (1.01-1.22)	0.69 (0.64-0.74)
A3FGL	L per galactose in fucosylated A3	2.38E-40	1.74E-22	1.12E-17	2.25 (1.99-2.53)	1.67 (1.51-1.85)	0.73 (0.68-0.78)
A2F0GL	L per galactose in afucosylated A2	3.51E-14	4.71E-16	5.36E-01	1.50 (1.35-1.66)	1.54 (1.39-1.71)	1.02 (0.95-1.09)
A3F0GL	L per galactose in afucosylated A3	6.98E-07	9.92E-17	3.18E-08	1.29 (1.17-1.42)	1.56 (1.41-1.74)	1.22 (1.14-1.31)
A4F0GL	L per galactose in afucosylated A4	1.27E-12	4.77E-14	6.02E-02	1.45 (1.31-1.61)	1.48 (1.34-1.64)	1.07 (1.00-1.14)
α2,6-linked sialylation (E)							
A2E	α2,6-linked (E) in A2	2.58E-17	2.57E-06	6.25E-10	1.56 (1.41-1.73)	1.25 (1.14-1.38)	0.80 (0.75-0.86)
A2FE	E in fucosylated A2	6.78E-12	1.98E-02	6.74E-09	1.42 (1.28-1.56)	1.12 (1.02-1.23)	0.82 (0.76-0.87)
A2GE	E per galactose in A2	7.00E-27	1.52E-07	5.89E-18	1.80 (1.61-2.00)	1.29 (1.18-1.43)	0.73 (0.68-0.78)
A2FGE	E per galactose in fucosylated A2	6.31E-35	3.72E-07	6.92E-25	1.99 (1.78-2.22)	1.29 (1.17-1.42)	0.68 (0.64-0.73)
A3FGE	E per galactose in fucosylated A3	1.47E-19	1.18E-04	1.74E-24	1.60 (1.45-1.78)	1.21 (1.10-1.33)	0.69 (0.64-0.74)
A3F0GE	E per galactose in afucosylated A3	8.01E-01	3.23E-07	5.02E-12	0.99 (0.90-1.09)	0.77 (0.70-0.85)	0.78 (0.73-0.84)
A4F0GE	E per galactose in afucosylated A4	2.14E-09	1.83E-06	6.21E-02	0.74 (0.67-0.82)	0.79 (0.72-0.87)	1.07 (1.00-1.14)

The TPNG-derived traits with the largest effect sizes between patients and HCs were found to be the lower levels of galactosylation in CD (metaOR [95% CI]$_{A2FS0G\ CD/HC}$, 0.37 [0.33–0.43]), the lower levels of fucosylation of diantennary species in UC (metaOR$_{A2LF\ UC/HC}$, [95% CI], 0.51 [0.45–0.57]), the higher levels of sialylation of diantennary fucosylated glycans in CD (metaOR$_{A2FGS\ CD/HC}$ [95% CI], 2.38 [2.12–2.68]), and specifically the α2,3-sialylation of fucosylated triantennary species in CD (metaOR$_{A3FGL\ CD/HC}$ [95% CI], 2.25 [1.99–2.53]). When comparing UC vs CD, the strongest associations were observed in the sialylation of diantennary fucosylated glycans (metaOR$_{A2FGS\ UC/CD}$ [95% CI], 0.60 [0.55–0.65]) and in fucosylation of triantennary glycans with α2,6-sialylation (metaOR$_{A3EF\ UC/CD}$ [95% CI] , 0.67 [0.62–0.72]), next to a higher level of galactosylation in UC (metaOR$_{A2FS0G\ UC/CD}$ [95% CI], 1.63 [1.51–1.76]) (Table 2).

Compared with HC, both CD and UC patients showed lower levels of diantennary glycans (CA2), higher levels of triantennary and tetra-antennary glycans (CA3 and CA4, respectively) and of complex glycans in general (TC), and lower levels of hybrid (THy) and high-mannose structures (TM). Compared with HCs, IBD patients had lower levels of diantennary fucosylated nonsialylated glycans (TA2FS0) that are mainly representative of IgG glycans[32] (Table 2**, Supplementary Table 3**).

IBD patients showed lower levels of fucosylation than HCs, especially for diantennary (sialylated) species (A2(S)F) with either α2,3- or α2,6-linked SAs (A2LF, A2EF) (Figure 2**,** Table 2). The fucosylation of triantennary glycans with α2,3- or α2,6-linked SAs (A3F, A3LF, A3EF) was lower in CD compared with UC patients.

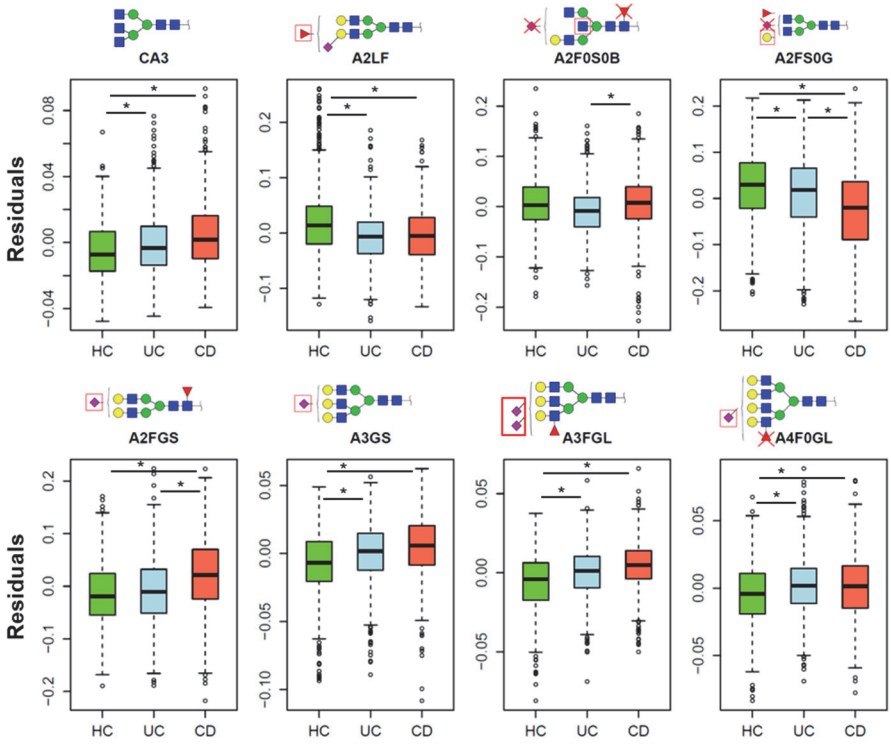

Figure 2: Main replicated associations between plasma *N*-glycan traits and IBD. *The 25th, 50th and 75th percentiles and whiskers at 1st quartile – 1.5 × IQR (Q1 – 1.5 × IQR) and Q3 + 1.5 × IQR based on the residuals after correction for age, sex, and age × sex are shown for data from the discovery cohort. P values, ORs and the 95% CIs are reported in Supplementary Table 3. Statistically significant and replicated associations are marked with an asterisk. IQR, interquartile range; Q, quartile.*

CD and UC patients displayed a higher bisection of diantennary fucosylated and sialylated glycans (A2FSB) compared with HCs, and CD patients had a higher bisection of nonfucosylated nonsialylated diantennary glycans (A2F0S0B) compared with UC patients (Table 2, Figure 2).

In IBD, the galactosylation of diantennary fucosylated glycans (A2FG) was lower than in HCs, whereas the galactosylation of nonfucosylated structures (A2F0G) was higher than in HCs. The galactosylation of diantennary structures without SA gradually decreased from HCs to UC patients to CD patients (A2(F)S0G and A2F0S0G), but in sialylated glycans (A2F0SG) it was higher in IBD patients compared with HCs (Table 2, Figure 2).

General sialylation was significantly increased in UC, and even more in CD, patients compared with HCs. CD and UC patients had higher relative levels of both α2,3- and α2,6-linked SA compared with HCs in all traits except for the α2,6-sialylation of tetra-antennary structures (A4F0GE), which was lower in IBD than HC. The strongest association distinguishing UC from CD was found in the sialylation per galactose in diantennary fucosylated glycans (A2FGS) (Table 2**,** Figure 2**)**

To explore the effect of known confounders of the TPNG[30, 33] also in IBD, we tested its associations with age and sex, stratified by disease group. Several traits of galactosylation, bisection, fucosylation, and sialylation showed associations with age (**Supplementary Table 4).** Some traits followed a nonlinear trend with age, for example A2FS0G in CD and UC patients but not in HCs (**Supplementary Figure 1**). We found previously unreported associations of SA linkage with sex. For instance, males had significantly higher fucosylation of diantennary glycans with α2,3-linked SA (A2LF) than the females in all 3 groups (**Supplementary Table 4**). For those patients in whom CRP levels and sedimentation rate were assessed (Table 1), we tested for associations with the TPNG. Multiple traits of sialylation, in particular α2,6-linked, as well as the fucosylation of triantennary glycans, were positively associated with both inflammation markers in CD, whereas IgG galactosylation showed a negative association. In UC patients, we observed similar associations, with additional negative associations with bisection (**Supplementary Table 4**).

Based on the associations found by logistic regression, we assessed receiver operating characteristic curves for the 3 groups. We found a good, fair, and poor discrimination for CD patients vs HCs, UC patients vs HCs, and UC vs CD patients, respectively, and this was replicated in the US cohort (**Figure 3**).

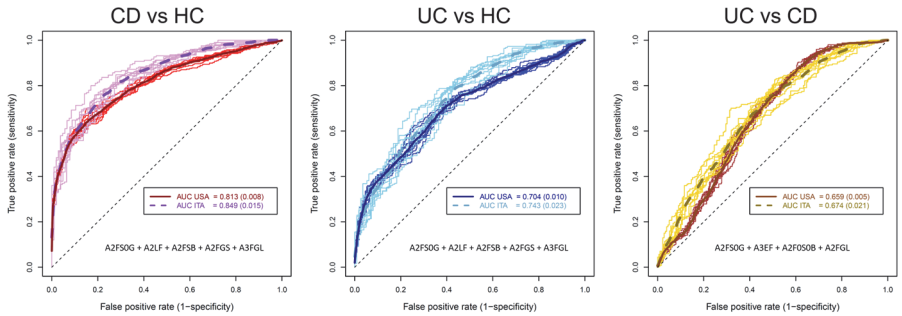

Figure 3: Receiver operating characteristic curves illustrating the power of selected glycan traits to predict CD and UC. *The means (and SDs) of 10 predictions are reported for the respective AUC for the 2 cohorts (Italy, discovery and United States, replication). In addition to the glycan traits listed in the respective panels, the interaction age × sex × glycan was included in the model. AUC, area under the curve*.

TPNG is associated with treatment

In CD patients, the need for increased drug potency was associated with elevated bisection (A2FSB) and sialylation (A2FGS, A2FGE, A3F(0)GE), as well as elevated fucosylation of triantennary structures with α2,3- and α2,6-linked SAs (A3F, A3LF, A3EF), whereas galactosylation (A2FSG, A2FS0G) was negatively associated with the need for more potent drugs (Figure 4**, Supplementary Table 5**). In UC patients of the discovery cohort, drug potency need was associated with higher antennarity, longer mannose branches (MM) and higher high-mannose–to–hybrid structures ratio (MHy), lower fucosylation (patients treated with mesalazine having higher levels than those taking other drugs), elevated bisection (especially anti–TNF-α users), lower galactosylation of diantennary glycans, and elevated sialylation (A2FGL, A3GL, A3FGL, A4F0GL), except for α2,3-linked sialylation in diantennary and afucosylated triantennary structures (A2L, A2F0L, A2GL, A2F0GL, A3F0GL) (Figure 4, **Supplementary Table 5**). In UC, only the associations with galactosylation of diantennary glycans were replicated.

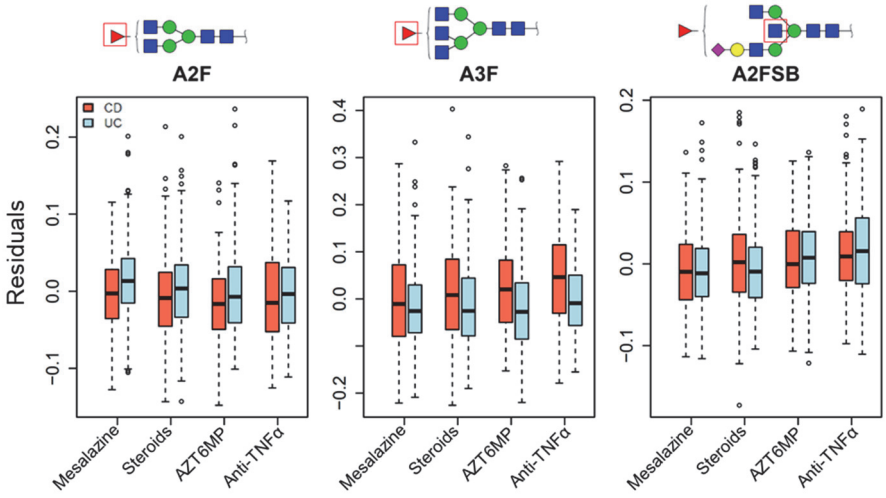

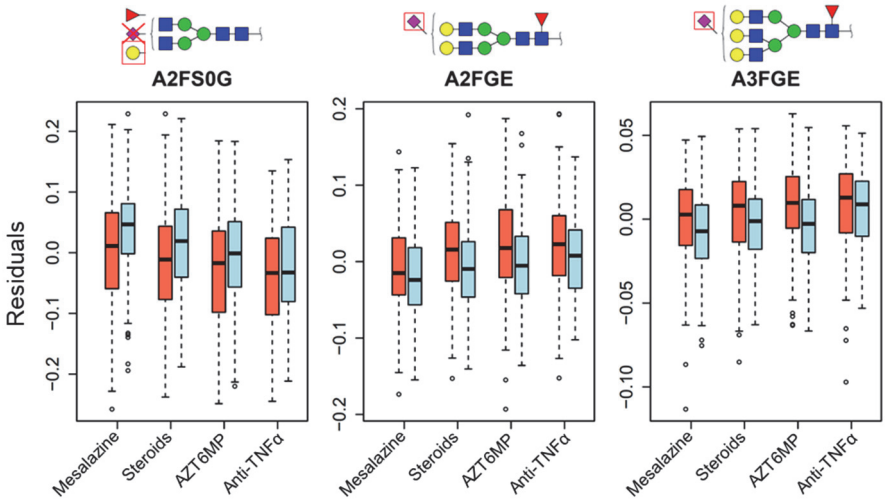

Figure 4: Main associations between plasma *N*-glycan traits and medication. *CD is colored red and UC is colored blue. The 25th, 50th, and 75th percentiles and whiskers at Q1 – 1.5 × IQR and Q3 + 1.5 × IQR based on the residuals after correction for age, sex, and the interaction thereof are shown for data from the discovery cohort. P values, ORs, and their 95% CIs are reported in Supplementary Table 5. IQR, interquartile range; Q, quartile* ***Supplementary Table 5****. IQR, interquartile range; Q, quartile.*

In the paired analysis of the TPNG from 9 UC patients of the replication cohort before and after surgery, we observed an increase in A2EF and IgG galactosylation and a decrease in A3FGL (**Figure 5**, and **Supplementary Table 6**). For CD patients (n = 19) we did not find any significant differences (**Supplementary Table 6**). Moreover, we performed a cross-sectional logistic regression analysis of the TPNG from patients whose plasma samples were collected before vs after surgery and did not find any replicated associations (**Supplementary Table 7**).

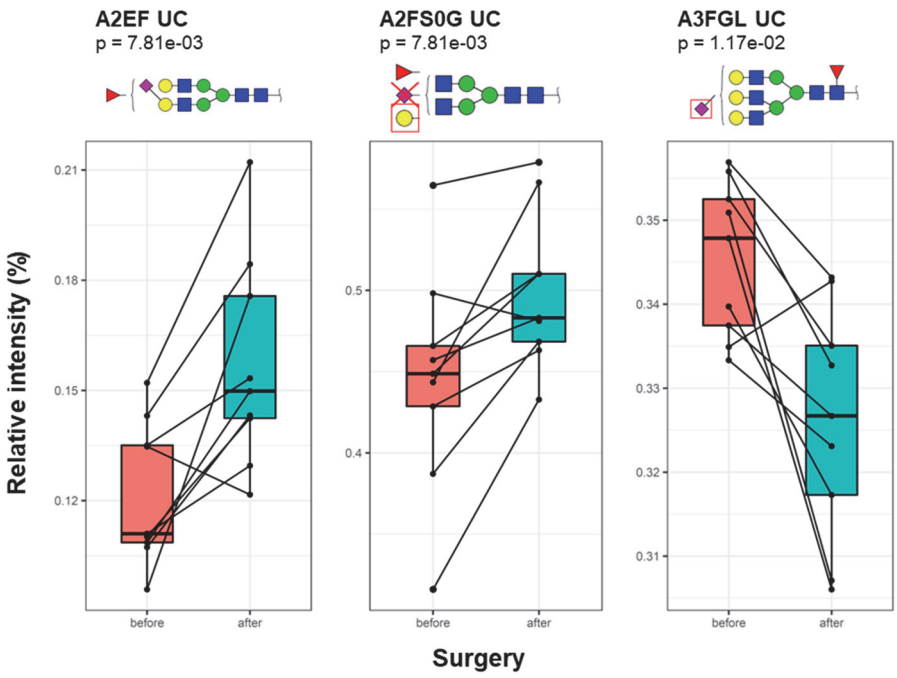

Figure 5: Postoperative *N*-glycosylation changes in UC patients. *P-values and relative intensities with 25th, 50th and 75th percentiles are shown with individual values for the 9 UC patients before and after surgery for the glycan traits significant after correction with false discovery rate of 10% (see **Supplementary Table 6** for the full list of tests performed, including CD data).*

Disease location and disease behavior

In both cohorts, UC patients in whom the colitis extended to the entire colon (E3) were found to have lower levels of galactosylation of the fucosylated and nonfucosylated diantennary nonsialylated glycans (A2(F)S0G) than distal colitis patients (E1 + E2) (**Supplementary Table 8**). Several fucosylation traits were higher in colonic CD than in ileal CD of the discovery cohort (L2 vs L1), but these associations were not replicated (**Supplementary Table 9).** Furthermore, no replicable associations of the TPNG were found with disease behavior, nor with the presence of perianal disease (**Supplementary Tables 10** and **11**). In the discovery cohort, the colonic CD subgroup (L2) vs UC showed similar associations as total CD vs UC, but those associations were not replicated (**Supplementary Table 12**).

Discussion

In this study we evaluated the differences in TPNG between 2635 IBD patients and 996 HCs by MALDI-TOF-MS. Glycosylation was found to differ between patients and HCs in all main glycosylation features, that is, complexity, fucosylation, bisection, galactosylation, and sialylation with discrimination of functionally distinct α2,3- and α2,6-linkage types. Novel associations of SA linkages with age and sex were found for both HCs and IBD patients. The availability of 2 distinct cohorts allowed the replication of the main findings and ensured the validity of the results.

One of the strongest and most robust associations with both CD and UC in our data appeared to be IgG galactosylation (A2FS0G)[32]. It was not only an important predictor for IBD in our receiver operating characteristic analyses but was also associated with the extent of disease and the need for surgery and more potent drugs. Moreover, it increased in UC patients after surgery. This is consistent with our recent findings on isolated IgG[20], and seems to mostly reflect the grade of inflammation, as is also evidenced by its strong negative association with CRP and sedimentation rate in our data and is in line with literature for IBD and other inflammatory conditions[34, 35]. In contrast, the galactosylation of afucosylated, sialylated diantennary glycans (A2F0(S)G) was higher in IBD. In healthy individuals, these glycans are mainly derived from hemopexin, serotransferrin, α1-antitrypsin, haptoglobin, fibrinogen, IgA, α1B-glycoprotein, and other acute-phase proteins from the liver[32]. Some of these proteins (e.g., α1-antitrypsin and haptoglobin) have been proposed as markers for IBD[36, 37]. At the same time, the per-galactose sialylation of related glycan traits (A2(F)GS) was also increased, contrary to IgG Fc sialylation, which was reported to decrease in CD, measured in the same cohort[20].

Although non-bisected A2FS-glycans are mostly attributable to a mixture of glycoproteins released by the liver, bisected A2FS-glycans are mostly derived from IgA, IgM, and the fragment antigen-binding portion of IgG.[32, 38]. Thus, the observed increase in diantennary sialylation might reflect acute-phase protein glycosylation and abundance changes, whereas the increased bisection of diantennary structures (A2FSB) in IBD may be attributed to increased bisection and/or levels of IgA or IgM[32, 39-41]. We reported on decreased IgG Fc bisection in UC in the same cohort as is analyzed here[20]. IgG bisection has been reported to enhance antibody-dependent cytotoxicity in vitro[42]. However, the role of bisection in IgA and IgM has not yet been established. Moreover, it needs to be taken into account that the applied analytical approach does not allow us to distinguish a bisecting GlcNAc from a nongalactosylated third antenna, because these result in exactly the same mass. Therefore, assignment is based on knowledge of the glycan biosynthetic pathways and literature on plasma protein glycosylation[12, 13, 32, 41].

Contrary to our results, no changes in fucosylation were found in the TPNG of UC patients in a previous study[43]. We found a decreased fucosylation of diantennary structures in IBD vs HCs, in colonic (L2) vs ileal (L1) or ileocolonic (L3) CD patients, and in UC with extensive (E3) compared with distal disease (E1 + E2). This likely reflects an increase of the mostly afucosylated liver-derived diantennary glycans compared with the mostly fucosylated IgG glycans (TA2FS0)[32, 34]. An increase of afucosylated IgG glycans as reported for UC[20], known to enhance antibody-dependent cellular cytotoxicity[44] may likewise contribute. Accordingly, we found a lower A2E fucosylation in UC before surgery compared with after surgery. Future studies are warranted to elucidate possible functional differences of IgG fucosylation between UC and CD. The fact that we found fewer or no replicated associations with disease location or disease behavior in CD may partly be due to the relatively small group sizes of the subcategories, which limited the power of our analyses.

The general relative increase of higher branched structures (CA3 and CA4) in IBD patients compared with HCs goes along with a general decrease of smaller structures (CA2 including IgG-derived TA2FS0; TM and THy). A decrease in TM could also be attributed to lower (relative) levels of proteins rich in high-mannose glycans (eg, α-2-macroglobulin, apolipoprotein B-100, and IgD, IgE, and IgM)[32, 43, 45, 46]. This is in line with our finding of a decreased A2F0S0G in IBD, which could possibly be linked to decreased levels of apolipoprotein B-100 in CD[45]. Higher branching, next to increased sialylation, has previously been reported for IBD, other autoimmune diseases, and acute inflammation[17, 43, 47, 48]. Similar *N*-glycome associations with disease and disease activity were found in a longitudinal study on rheumatoid arthritis, in which the serum *N*-glycome was measured with the same method as used here[49]. This was linked to an increase in the levels of acute phase proteins containing large, highly sialylated glycans, such as α1-acid glycoprotein and α1-antitrypsin[50, 51].

Plasma glycoproteins can contain SAs in 2 major linkage variants, that is, linked in the α2,3- or α2,6-position to an antenna galactose[13]. Because our novel method enabled us to discriminate between SA linkages, we were able to show some divergent, linkage-specific trends in our data. Although α2,3-sialylation was higher in IBD in various glycan traits, including both fucosylated and afucosylated structures, the α2,6-sialylation of afucosylated highly branched glycans (A3-4F0GE) was lower compared with HCs. These traits were strongly associated with inflammation markers in our data. Moreover, the expression of the enzyme generating α2,6-SAs was shown to be induced by inflammatory cytokines and to inhibit adhesion of B cells to endothelial cells[52]. Thus, although both α2,6- and α2,3-sialylation seem to increase during inflammation, our data suggest that in both CD and UC, the increased sialylation of highly branched structures is mainly driven by α2,3-sialyltransferases and, to a lesser extent, by α2,6-sialyltransferase. This may have consequences on the

immunologic pathways, because the ligands of SA-containing glycoproteins are mostly specific to the SA linkage type in humans. For instance, Siglecs on immune and epithelial cells recognize afucosylated α2,6-SA epitopes, whereas selectins specifically bind ligands carrying sialyl-Lewis X structures containing α2,3-SA and antennary fucose[21]. Correspondingly, the ORs of the α2,3-sialylation of fucosylated triantennary glycans (A3FGL) were considerably larger than those of the α2,6-sialylated variant (A3FGE). A3FGL decreased after surgery in UC patients only, which is in line with our meta-analysis finding of a lower A3FGL in HCs and indicates improvement in UC patients after surgical intervention. In a study of the serum glycome in rheumatoid arthritis, this trait did not differ between HCs and patients[49], which might point at a possible disease-specificity of A3FGL in IBD. The lack of significance in postoperative glycan changes in CD despite a higher sample size (n = 19 in CD vs n = 9 in UC) could be related to the fact that relapses occur more frequently in CD, whereas in UC surgery is able to cure the disease[37].

We observed a strongly reduced fucosylation of diantennary α2,3-sialylated (A2LF) glycans in IBD patients compared with HCs, which may be largely interpreted as an increase of nonfucosylated α2,3-sialylated diantennary structures (A2GL). These glycans are most likely liver derived, because immunoglobulins are known to mostly carry α2,6-linked SA and a core fucose[53, 54]. Moreover, as expected, the fucosylation of triantennary glycans (A3F) was strongly associated with inflammatory markers and, accordingly, was lower in UC compared with CD patients. This was furthermore true for both α2,6- and, α2,3-sialylated structures (A3EF, A3LF) and antennary fucosylation (A3Fa). The latter is most likely reflecting an overall increase of fucosylation of 2,3-sialylated antennae, resulting in increased sialyl-Lewis X structures on acute phase proteins known to occur during inflammation[55]. However, it was surprising that our findings of the various triantennary fucosylation traits were contradictory between the 2 cohorts when comparing UC and CD patients with HCs, which might be due to the different medication strategies between the cohorts, as further described in the following section.

We observed a decrease of IgG-related galactosylation (A2FS0G) with increasing drug potency in IBD. We assume that patients receiving more potent medication, such as anti–TNF-α, are likely to have a more severe disease[31, 56, 57] and, consequently, TPNG profiles, reflecting a stronger inflammation than, for example, mesalazine users. However, several other glycan traits showed rather unexpected association behavior, such as the fucosylation of triantennary glycans (A3F), which was higher in CD anti–TNF-α users compared with mesalazine-treated patients, whereas in Italian UC patients this was the case only for antennary fucosylation (A3Fa) (Supplementary Table 5). Surprisingly, A3Fa was lower in the Italian UC patients when compared with HCs (Supplementary Table 3). α2,3-sialylation in

diantennary, mainly afucosylated, structures was negatively associated with drug potency in Italian UC patients (eg, A2(F0)GL in anti-TNF vs mesalazine), whereas the fucosylated variant, A2FGL, showed a positive association (*i.e.*, increased in azathioprine/6-mercaptopurine compared with mesalazine). Moreover, this very same trait was distinguishing UC from CD in our meta-analysis and was not associated with inflammatory markers. When we compared UC patients with HCs, α2,3-sialylation in diantennary glycans including A2F0GL was positively associated with disease (Table 2). Thus, there seem to be underlying effects of interactions between CD or UC, medication, and various glycan traits, in particular, α2,3-sialylation and antennary fucosylation. This should be explored in more detail in future studies, preferably by taking into account disease scores.

Conclusion

To our knowledge, this study is the largest analysis of the TPNG in IBD patients to date and includes novel SA linkage-specific information. Here, we report on multiple associations of the TPNG with CD and UC in a case-control study, which were, in large part, replicated in an independent cohort. Glycan complexity, fucosylation, bisection, galactosylation, and sialylation were proven to differ in IBD patients compared with HCs. The novel information about SA linkages revealed yet unreported associations with age, sex, and IBD. Our high-throughput method allowed us to find differences within the groups of CD and UC patients regarding response to surgery and medication and disease localization. Established markers of inflammation, such as low galactosylation attributed to IgG and a higher sialylation and abundance of large structures typical of certain acute-phase proteins, were apparent in the TPNGs of CD and UC patients. Based on our data and knowledge of plasma protein glycosylation, we proposed protein scaffolds that might be affected in IBD. These specific proteins, for instance, IgA, haptoglobin, or α1-acid-glycoprotein, might be promising targets for future (glyco)proteomic investigations to gain insights into disease pathophysiology and to develop therapeutic targets. Future investigations, preferably in a longitudinal manner, are warranted to further elucidate the impact of the different treatments on the TPNG of IBD patients.

Overall, this study expands the knowledge about protein glycosylation and contributes to the further characterization of IBD by reporting multiple new associations and potential targets for further investigation.

Supplementary material

The supplementary material is available online at https://doi.org/10.1053/j.gastro.2018.05.030

https://www.gastrojournal.org/article/S0016-5085(18)34563-3/fulltext?referrer=https%3A%2F%2Fpubmed.ncbi.nlm.nih.gov%2F

Acknowledgments

This work was supported by the IBD-BIOM project (FP7 HEALTH Grant No. 305479). Research at the IBD Center at Cedars-Sinai was supported by the NIH grants U01DK062413, P01DK046763, R01HS021747 and U01AI067068. Mislav Novokmet, Gordan Lauc and Erdmann Rapp acknowledge support by the HTP-GlycoMet project (FP7 People, Marie Curie Actions, grant No. 324400).

Conflict of interest

Dermot P.B. McGovern has consulted for Janssen, Cidara, Q Biologics, and Pfizer. The other authors declare that they have no conflict of interests.

Author Contributions

Florent Clerc and Mislav Novokmet; acquisition of data; statistical analysis, interpretation of the data, drafting of the manuscript. Viktoria Dotz and Karli R. Reiding; critical revision of the manuscript for important intellectual content and interpretation of the data; editing. Noortje de Haan, Guinevere S.M. Kammeijer, Hans Dalebout, Marco R. Bladergroen, Frano Vukovic and Erdmann Rapp; technical support. Stephan R. Targan, Gildardo Barron, Natalia Manetti, Anna Latiano, Dermot P.B. McGovern, Vito Annese; study design and patient recruitment. Gordan Lauc and Manfred Wuhrer; study supervision. All authors had access to the study data and approved the final manuscript.

References

(1) Dahlhamer, J. M.; Zammitti, E. P.; Ward, B. W.; Wheaton, A. G.; Croft, J. B. Prevalence of Inflammatory Bowel Disease Among Adults Aged >/=18 Years - United States, 2015. *MMWR Morb Mortal Wkly Rep* **2016**, *65* (42), 1166-1169

(2) Ye, B. D.; McGovern, D. P. Genetic variation in IBD: progress, clues to pathogenesis and possible clinical utility. *Expert Rev Clin Immunol* **2016**, *12* (10), 1091-1107

(3) Magro, F.; Gionchetti, P.; Eliakim, R.; Ardizzone, S.; Armuzzi, A.; Barreiro-de Acosta, M.; Burisch, J.; Gecse, K. B.; Hart, A. L.; Hindryckx, P.; Langner, C.; Limdi, J. K.; Pellino, G.; Zagorowicz, E.; Raine, T.; Harbord, M.; Rieder, F.; European, C. s.; Colitis, O. Third European Evidence-based Consensus on Diagnosis and Management of Ulcerative Colitis. Part 1: Definitions, Diagnosis, Extra-intestinal Manifestations, Pregnancy, Cancer Surveillance, Surgery, and Ileo-anal Pouch Disorders. *Journal of Crohn's & colitis* **2017**, *11* (6), 649-670

(4) Gomollon, F.; Dignass, A.; Annese, V.; Tilg, H.; Van Assche, G.; Lindsay, J. O.; Peyrin-Biroulet, L.; Cullen, G. J.; Daperno, M.; Kucharzik, T.; Rieder, F.; Almer, S.; Armuzzi, A.; Harbord, M.; Langhorst, J.; Sans, M.; Chowers, Y.; Fiorino, G.; Juillerat, P.; Mantzaris, G. J.; Rizzello, F.; Vavricka, S.; Gionchetti, P.; Ecco. 3rd European Evidence-based Consensus on the Diagnosis and Management of Crohn's Disease 2016: Part 1: Diagnosis and Medical Management. *Journal of Crohn's & colitis* **2017**, *11* (1), 3-25

(5) Menees, S. B.; Powell, C.; Kurlander, J.; Goel, A.; Chey, W. D. A meta-analysis of the utility of C-reactive protein, erythrocyte sedimentation rate, fecal calprotectin, and fecal lactoferrin to exclude inflammatory bowel disease in adults with IBS. *Am J Gastroenterol* **2015**, *110* (3), 444-454

(6) Mosli, M. H.; Zou, G.; Garg, S. K.; Feagan, S. G.; MacDonald, J. K.; Chande, N.; Sandborn, W. J.; Feagan, B. G. C-Reactive Protein, Fecal Calprotectin, and Stool Lactoferrin for Detection of Endoscopic Activity in Symptomatic Inflammatory Bowel Disease Patients: A Systematic Review and Meta-Analysis. *Am J Gastroenterol* **2015**, *110* (6), 802-819; quiz 820

(7) Annese, V.; Daperno, M.; Rutter, M. D.; Amiot, A.; Bossuyt, P.; East, J.; Ferrante, M.; Gotz, M.; Katsanos, K. H.; Kiesslich, R.; Ordas, I.; Repici, A.; Rosa, B.; Sebastian, S.; Kucharzik, T.; Eliakim, R.; European, C. s.; Colitis, O. European evidence based consensus for endoscopy in inflammatory bowel disease. *Journal of Crohn's & colitis* **2013**, *7* (12), 982-1018

(8) Bonneau, J.; Dumestre-Perard, C.; Rinaudo-Gaujous, M.; Genin, C.; Sparrow, M.; Roblin, X.; Paul, S. Systematic review: new serological markers (anti-glycan, anti-GP2, anti-GM-CSF Ab) in the prediction of IBD patient outcomes. *Autoimmunity reviews* **2015**, *14* (3), 231-245

(9) Bennike, T.; Birkelund, S.; Stensballe, A.; Andersen, V. Biomarkers in inflammatory bowel diseases: current status and proteomics identification strategies. *World journal of gastroenterology* **2014**, *20* (12), 3231-3244

(10) Soubieres, A. A.; Poullis, A. Emerging Biomarkers for the Diagnosis and Monitoring of Inflammatory Bowel Diseases. *Inflamm Bowel Dis* **2016**, *22* (8), 2016-2022

(11) Hart, G. W.; Copeland, R. J. Glycomics hits the big time. *Cell* **2010**, *143* (5), 672-676

(12) Moremen, K. W.; Tiemeyer, M.; Nairn, A. V. Vertebrate protein glycosylation: diversity, synthesis and function. *Nature reviews Molecular cell biology* **2012**, *13* (7), 448-462

(13) Varki, A. Biological roles of glycans. *Glycobiology* **2017**, *27* (1), 3-49

(14) Gornik, O.; Wagner, J.; Pučić, M.; Knežević, A.; Redžić, I.; Lauc, G. Stability of N-glycan profiles in human plasma. *Glycobiology* **2009**, *19* (12), 1547-1553

(15) Hennig, R.; Cajic, S.; Borowiak, M.; Hoffmann, M.; Kottler, R.; Reichl, U.; Rapp, E. Towards personalized diagnostics via longitudinal study of the human plasma N-glycome. *Biochimica et Biophysica Acta (BBA) - General Subjects* **2016**, *1860* (8), 1728-1738

(16) Arnold, J. N.; Saldova, R.; Hamid, U. M. A.; Rudd, P. M. Evaluation of the serum n-linked glycome for the diagnosis of cancer and chronic inflammation. *Proteomics* **2008**, *8* (16), 3284-3293

(17) Gornik, O.; Lauc, G. Glycosylation of serum proteins in inflammatory diseases. *Disease markers* **2008**, *25* (4-5), 267-278

(18) Theodoratou, E.; Campbell, H.; Ventham, N. T.; Kolarich, D.; Pucic-Bakovic, M.; Zoldos, V.; Fernandes, D.; Pemberton, I. K.; Rudan, I.; Kennedy, N. A.; Wuhrer, M.; Nimmo, E.; Annese, V.; McGovern, D. P.; Satsangi, J.; Lauc, G. The role of glycosylation in IBD. *Nature reviews. Gastroenterology & hepatology* **2014**, *11* (10), 588-600

(19) Shinzaki, S.; Iijima, H.; Nakagawa, T.; Egawa, S.; Nakajima, S.; Ishii, S.; Irie, T.; Kakiuchi, Y.; Nishida, T.; Yasumaru, M.; Kanto, T.; Tsujii, M.; Tsuji, S.; Mizushima, T.; Yoshihara, H.; Kondo, A.; Miyoshi, E.; Hayashi, N. IgG oligosaccharide alterations are a novel diagnostic marker for disease activity and the clinical course of inflammatory bowel disease. *Am J Gastroenterol* **2008**, *103* (5), 1173-1181

(20) Simurina, M.; de Haan, N.; Vuckovic, F.; Kennedy, N. A.; Stambuk, J.; Falck, D.; Trbojevic-Akmacic, I.; Clerc, F.; Razdorov, G.; Khon, A.; Latiano, A.; D'Inca, R.; Danese, S.; Targan, S.; Landers, C.; Dubinsky, M.; McGovern, D. P. B.; Annese, V.; Wuhrer, M.; Lauc, G. Glycosylation of Immunoglobulin G Associates With Clinical Features of Inflammatory Bowel Diseases. *Gastroenterology* **2018**,

(21) Varki, A.; Gagneux, P. Multifarious roles of sialic acids in immunity. *Annals of the New York Academy of Sciences* **2012**, *1253* (1), 16-36

(22) Schultz, M. J.; Swindall, A. F.; Bellis, S. L. Regulation of the metastatic cell phenotype by sialylated glycans. *Cancer Metastasis Rev* **2012**, *31* (3-4), 501-518

(23) Dalziel, M.; Crispin, M.; Scanlan, C. N.; Zitzmann, N.; Dwek, R. A. Emerging Principles for the Therapeutic Exploitation of Glycosylation. *Science* **2014**, *343* (6166), 1235681

(24) McCarthy, C.; Saldova, R.; Wormald, M. R.; Rudd, P. M.; McElvaney, N. G.; Reeves, E. P. The role and importance of glycosylation of acute phase proteins with focus on alpha-1 antitrypsin in acute and chronic inflammatory conditions. *Journal of proteome research* **2014**, *13* (7), 3131-3143

(25) Bladergroen, M. R.; Reiding, K. R.; Hipgrave Ederveen, A. L.; Vreeker, G. C.; Clerc, F.; Holst, S.; Bondt, A.; Wuhrer, M.; van der Burgt, Y. E. Automation of High-Throughput Mass Spectrometry-Based Plasma N-Glycome Analysis with Linkage-Specific Sialic Acid Esterification. *Journal of proteome research* **2015**, *14* (9), 4080-4086

(26) Reiding, K. R.; Blank, D.; Kuijper, D. M.; Deelder, A. M.; Wuhrer, M. High-throughput profiling of protein N-glycosylation by MALDI-TOF-MS employing linkage-specific sialic acid esterification. *Anal Chem* **2014**, *86* (12), 5784-5793

(27) Latiano, A.; Palmieri, O.; Latiano, T.; Corritore, G.; Bossa, F.; Martino, G.; Biscaglia, G.; Scimeca, D.; Valvano, M. R.; Pastore, M.; Marseglia, A.; D'Incà, R.; Andriulli, A.; Annese, V. Investigation of Multiple Susceptibility Loci for Inflammatory Bowel Disease in an Italian Cohort of Patients. *Plos One* **2011**, *6* (7), e22688

(28) Satsangi, J.; Silverberg, M. S.; Vermeire, S.; Colombel, J. F. The Montreal classification of inflammatory bowel disease: controversies, consensus, and implications. *Gut* **2006**, *55* (6), 749-753

(29) Jansen, B. C.; Reiding, K. R.; Bondt, A.; Hipgrave Ederveen, A. L.; Palmblad, M.; Falck, D.; Wuhrer, M. MassyTools: A High-Throughput Targeted Data Processing Tool for Relative Quantitation and Quality Control Developed for Glycomic and Glycoproteomic MALDI-MS. *Journal of proteome research* **2015**, *14* (12), 5088-5098

(30) Reiding, K. R.; Ruhaak, L. R.; Uh, H. W.; El Bouhaddani, S.; van den Akker, E. B.; Plomp, R.; McDonnell, L. A.; Houwing-Duistermaat, J. J.; Slagboom, P. E.; Beekman, M.; Wuhrer, M. Human Plasma N-glycosylation as Analyzed by Matrix-Assisted Laser Desorption/Ionization-Fourier Transform Ion Cyclotron Resonance-MS Associates with Markers of Inflammation and Metabolic Health. *Molecular & cellular proteomics : MCP* **2017**, *16* (2), 228-242

(31) Pithadia, A. B.; Jain, S. Treatment of inflammatory bowel disease (IBD). *Pharmacological Reports* **2011**, *63* (3), 629-642

(32) Clerc, F.; Reiding, K. R.; Jansen, B. C.; Kammeijer, G. S.; Bondt, A.; Wuhrer, M. Human plasma protein N-glycosylation. *Glycoconj J* **2016**, *33* (3), 309-343

(33) Knežević, A.; Gornik, O.; Polašek, O.; Pučić, M.; Redžić, I.; Novokmet, M.; Rudd, P. M.; Wright, A. F.; Campbell, H.; Rudan, I. Effects of aging, body mass index, plasma lipid profiles, and smoking on human plasma N-glycans. *Glycobiology* **2010**, *20* (8), 959-969

(34) Trbojevic Akmacic, I.; Ventham, N. T.; Theodoratou, E.; Vuckovic, F.; Kennedy, N. A.; Krištic, J.; Nimmo, E. R.; Kalla, R.; Drummond, H.; Štambuk, J.; Dunlop, M. G.; Novokmet, M.; Aulchenko, Y.; Gornik, O.; Campbell, H.; Pucic Bakovic, M.; Satsangi, J.; Lauc, G.; Consortium, I.-B. Inflammatory Bowel Disease Associates with Proinflammatory Potential of the Immunoglobulin G Glycome. *Inflammatory Bowel Diseases* **2015**, *21* (6), 1237-1247

(35) Ercan, A.; Cui, J.; Chatterton, D. E.; Deane, K. D.; Hazen, M. M.; Brintnell, W.; O'Donnell, C. I.; Derber, L. A.; Weinblatt, M. E.; Shadick, N. A.; Bell, D. A.; Cairns, E.; Solomon, D. H.; Holers, V. M.; Rudd, P. M.; Lee, D. M. Aberrant IgG galactosylation precedes disease onset, correlates with disease activity, and is prevalent in autoantibodies in rheumatoid arthritis. *Arthritis Rheum* **2010**, *62* (8), 2239-2248

(36) Vermeire, S.; Van Assche, G.; Rutgeerts, P. Laboratory markers in IBD: useful, magic, or unnecessary toys? *Gut* **2006**, *55* (3), 426-431

(37) Liverani, E.; Scaioli, E.; Digby, R. J.; Bellanova, M.; Belluzzi, A. How to predict clinical relapse in inflammatory bowel disease patients. *World journal of gastroenterology* **2016**, *22* (3), 1017-1033

(38) Bondt, A.; Wuhrer, M.; Kuijper, T. M.; Hazes, J. M.; Dolhain, R. J. Fab glycosylation of immunoglobulin G does not associate with improvement of rheumatoid arthritis during pregnancy. *Arthritis research & therapy* **2016**, *18* (1), 274

(39) Bondt, A.; Nicolardi, S.; Jansen, B. C.; Stavenhagen, K.; Blank, D.; Kammeijer, G. S.; Kozak, R. P.; Fernandes, D. L.; Hensbergen, P. J.; Hazes, J. M.; van der Burgt, Y. E.; Dolhain, R. J.; Wuhrer, M. Longitudinal monitoring of immunoglobulin A glycosylation during pregnancy by simultaneous MALDI-FTICR-MS analysis of N- and O-glycopeptides. *Sci Rep* **2016**, *6*, 27955

(40) Klapoetke, S. C.; Zhang, J.; Becht, S. Glycosylation characterization of Human IgA1 with differential deglycosylation by UPLC-ESI TOF MS. *J Pharm Biomed Anal* **2011**, *56* (3), 513-520

(41) Stumpo, K. A.; Reinhold, V. N. The N-Glycome of Human Plasma. *Journal of proteome research* **2010**, *9* (9), 4823-4830

(42) Shinkawa, T.; Nakamura, K.; Yamane, N.; Shoji-Hosaka, E.; Kanda, Y.; Sakurada, M.; Uchida, K.; Anazawa, H.; Satoh, M.; Yamasaki, M.; Hanai, N.; Shitara, K. The absence of fucose but not the presence of galactose or bisecting N-acetylglucosamine of human IgG1 complex-type oligosaccharides shows the critical

role of enhancing antibody-dependent cellular cytotoxicity. *J. Biol. Chem.* **2003**, *278* (5), 3466-3473

(43) Miyahara, K.; Nouso, K.; Saito, S.; Hiraoka, S.; Harada, K.; Takahashi, S.; Morimoto, Y.; Kobayashi, S.; Ikeda, F.; Miyake, Y.; Shiraha, H.; Takaki, A.; Okada, H.; Amano, M.; Hirose, K.; Nishimura, S.-I.; Yamamoto, K. Serum Glycan Markers for Evaluation of Disease Activity and Prediction of Clinical Course in Patients with Ulcerative Colitis. *Plos One* **2013**, *8* (10), e74861

(44) Biermann, M. H.; Griffante, G.; Podolska, M. J.; Boeltz, S.; Sturmer, J.; Munoz, L. E.; Bilyy, R.; Herrmann, M. Sweet but dangerous - the role of immunoglobulin G glycosylation in autoimmunity and inflammation. *Lupus* **2016**, *25* (8), 934-942

(45) Levy, E.; Rizwan, Y.; Thibault, L.; Lepage, G.; Brunet, S.; Bouthillier, L.; Seidman, E. Altered lipid profile, lipoprotein composition, and oxidant and antioxidant status in pediatric Crohn disease. *The American journal of clinical nutrition* **2000**, *71* (3), 807-815

(46) Levo, Y.; Shalit, M.; Wollner, S.; Fich, A. Serum IgE levels in patients with inflammatory bowel disease. *Annals of allergy* **1986**, *56* (1), 85-87

(47) Connelly, M. A.; Gruppen, E. G.; Otvos, J. D.; Dullaart, R. P. F. Inflammatory glycoproteins in cardiometabolic disorders, autoimmune diseases and cancer. *Clin Chim Acta* **2016**, *459*, 177-186

(48) Ceciliani, F.; Pocacqua, V. The acute phase protein alpha1-acid glycoprotein: a model for altered glycosylation during diseases. *Curr Protein Pept Sci* **2007**, *8* (1), 91-108

(49) Reiding, K. R.; Vreeker, G. C. M.; Bondt, A.; Bladergroen, M. R.; Hazes, J. M. W.; van der Burgt, Y. E. M.; Wuhrer, M.; Dolhain, R. Serum Protein N-Glycosylation Changes with Rheumatoid Arthritis Disease Activity during and after Pregnancy. *Frontiers in medicine* **2017**, *4*, 241

(50) Dage, J. L.; Ackermann, B. L.; Halsall, H. B. Site localization of sialyl Lewisx antigen on α1-acid glycoprotein by high performance liquid chromatography-electrospray mass spectrometry. *Glycobiology* **1998**, *8* (8), 755-760

(51) Ruhaak, L. R.; Koeleman, C. A.; Uh, H.-W.; Stam, J. C.; van Heemst, D.; Maier, A. B.; Houwing-Duistermaat, J. J.; Hensbergen, P. J.; Slagboom, P. E.; Deelder, A. M. Targeted Biomarker Discovery by High Throughput Glycosylation Profiling of Human Plasma Alpha1-Antitrypsin and Immunoglobulin A. *Plos One* **2013**, *8* (9), e73082

(52) Abe, Y.; Smith, C. W.; Katkin, J. P.; Thurmon, L. M.; Xu, X.; Mendoza, L. H.; Ballantyne, C. M. Endothelial alpha 2,6-linked sialic acid inhibits VCAM-1-dependent adhesion under flow conditions. *Journal of immunology (Baltimore, Md. : 1950)* **1999**, *163* (5), 2867-2876

(53) Arnold, J. N.; Wormald, M. R.; Suter, D. M.; Radcliffe, C. M.; Harvey, D. J.; Dwek, R. A.; Rudd, P. M.; Sim, R. B. Human Serum Igm Glycosylation: Identification Of Glycoforms That Can Bind To Mannan-Binding Lectin. *J Biol Chem* **2005**, *280* (32), 29080-29087

(54) Saldova, R.; Stockmann, H.; O'Flaherty, R.; Lefeber, D. J.; Jaeken, J.; Rudd, P. M. N-Glycosylation of Serum IgG and Total Glycoproteins in MAN1B1 Deficiency. *Journal of proteome research* **2015**, *14* (10), 4402-4412

(55) Sarrats, A.; Saldova, R.; Pla, E.; Fort, E.; Harvey, D. J.; Struwe, W. B.; de Llorens, R.; Rudd, P. M.; Peracaula, R. Glycosylation of liver acute-phase proteins in pancreatic cancer and chronic pancreatitis. *Proteomics. Clinical applications* **2010**, *4* (4), 432-448

(56) Danese, S.; Colombel, J. F.; Peyrin-Biroulet, L.; Rutgeerts, P.; Reinisch, W. Review article: the role of anti-TNF in the management of ulcerative colitis – past, present and future. *Alimentary pharmacology & therapeutics* **2013**, *37* (9), 855-866

(57) Arnott, I. D. R.; Watts, D.; Satsangi, J. Azathioprine and anti-TNFα therapies in Crohn's disease: a review of pharmacology, clinical efficacy and safety. *Pharmacological Research* **2003**, *47* (1), 1-10

Chapter 4

O- and *N*-Glycosylation of Serum Immunoglobulin A Is Associated with IgA Nephropathy and Glomerular Function

O- and *N*-Glycosylation of Serum Immunoglobulin A Is Associated with IgA Nephropathy and Glomerular Function

Viktoria Dotz[#1], Alessia Visconti[#2], Hannah J. Lomax-Browne[#3], Florent Clerc[#1], Agnes L. Hipgrave Ederveen[1], Nicholas R. Medjeral-Thomas[3], H. Terence Cook[3], Matthew C. Pickering[3], Manfred Wuhrer[$1], Mario Falchi[$*2]

[1]*Center for Proteomics and Metabolomics, Leiden University Medical Center (LUMC), Postbus 9600, 2300 RC Leiden, The Netherlands*

[2]*Department of Twin Research & Genetic Epidemiology, King's College London, London, United Kingdom*

[3]*Centre for Inflammatory Disease, Department of Immunology and Inflammation, Imperial College London, London, United Kingdom*

#These authors contributed equally

$These authors contributed equally

*Corresponding Author

Published in Journal of the American Society of Nephrology, 2021, 32 (10), 2455-2465

DOI: 10.1681/ASN.2020081208

Significance statement

IgA nephropathy (IgAN) is the most common primary glomerular disease worldwide, with galactose-deficient IgA (gd-IgA) considered to play a key role in its pathogenesis. Although this association is widely reported, it is unclear how IgA glycosylation changes with the disease. A novel mass spectrometry–based approach provided a more complete picture of IgA glycosylation changes in IgAN and of the relationship between IgA glycosylation and kidney function. Multiple structural features of both *O*- and *N*-linked glycans were associated with the presence and severity of IgAN and kidney function. Our high-resolution data suggests that IgA *O*- and *N*-glycopeptides are promising targets for future studies on the pathophysiology of IgAN and as potential noninvasive biomarkers for disease prediction.

Abstract

Background

IgA nephropathy (IgAN) is the most common primary glomerular disease worldwide and is a leading cause of renal failure. The disease mechanisms are not completely understood, but a higher abundance of galactose-deficient IgA is recognized to play a crucial role in IgAN pathogenesis. Although both types of human IgA (IgA1 and IgA2) have several *N*-glycans as post-translational modification, only IgA1 features extensive hinge-region *O*-glycosylation. IgA1 galactose deficiency on the *O*-glycans is commonly detected by a lectin-based method. To date, limited detail is known about IgA *O*- and *N*-glycosylation in IgAN.

Methods

To gain insights into the complex *O*- and *N*-glycosylation of serum IgA1 and IgA2 in IgAN, we used liquid chromatography-mass spectrometry (LC-MS) for the analysis of tryptic glycopeptides of serum IgA from 83 patients with IgAN and 244 age- and sex-matched healthy controls.

Results

Multiple structural features of *N*-glycosylation of IgA1 and IgA2 were associated with IgAN and glomerular function in our cross-sectional study. These features included differences in galactosylation, sialylation, bisection, fucosylation, and *N*-glycan complexity. Moreover, IgA1 *O*-glycan sialylation was associated with both the disease and glomerular function. Finally, glycopeptides were a better predictor of

IgAN and glomerular function than galactose-deficient IgA1 levels measured by lectin-based ELISA.

Conclusions

Our high-resolution data suggest that IgA *O*- and *N*-glycopeptides are promising targets for future investigations on the pathophysiology of IgAN and as potential noninvasive biomarkers for disease prediction and deteriorating kidney function.

Keywords: IgA nephropathy, glycosylation, immunoglobulin, mass spectrometry, posttranslational modification

Introduction

IgA nephropathy (IgAN), or Berger disease, is the most common Glomerulonephritis (GN) worldwide[1]. The disease course is complex, varying from a mild form to a progressive disease leading to renal failure in up to 40% of patients within 20 years[1, 2]. Clinical presentation also differs greatly with sex, ethnicity, and age[1]. IgAN is diagnosed by the presence of IgA dominant or codominant mesangial deposits on renal biopsy[3]. Improved noninvasive biomarkers of disease severity and progression to CKD are needed to appropriately stratify patient treatment and develop novel, effective therapies.

IgAN pathogenesis is generally considered to follow the "four-hit hypothesis."[4] In this hypothesis, the pathogenesis is initiated by increased levels of circulating galactose-deficient IgA1 (gd-IgA; hit 1). gd-IgA is then recognized by antiglycan autoantibodies (hit 2), leading to the formation of immune complexes (hit 3) that may deposit in the kidney (hit 4) and cause glomerular inflammation, complement activation, and kidney injury[4].

IgA1, unlike IgA2, has a unique hinge region located between conserved regions 1 and 2 of the heavy chain[5]. The hinge region has nine potential sites for *O*-glycosylation, of which three to six are reported to be consistently glycosylated[6-8]. *O*-glycans located in the hinge region of IgA1 are typically core 1 glycans with the structure galactose *β*1–3*N*-acetylgalactosamine (GalNAc), which may be extended with up to two sialic acid residues[6] (**Figure 1**). The IgA1 hinge region of patients with IgAN is characterised by an increased presence of aberrantly glycosylated *O*-glycans, which terminate with GalNAc or sialylated GalNAc rather than galactose[9-13]. The levels of degalactosylated IgA (gd-IgA) are elevated in patients with progressive IgAN compared with stable patients, and a negative correlation between gd-IgA level and eGFR has been found[12].

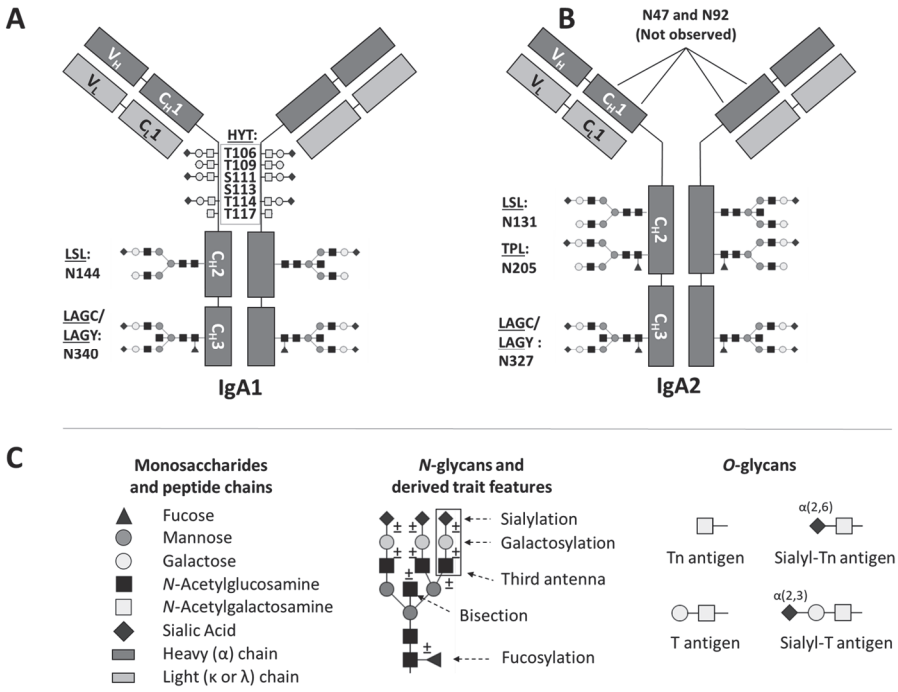

Figure 1: Schematic representation of IgA1 and IgA2 with examples for O- and N-glycan structures. *Schematic representation of IgA1 and IgA2 with examples for O- and N-glycan structures. (A) Each IgA1 heavy chain contains two N-glycosylation sites (i.e., at N144 and N340), which are occupied by complex-type N-glycans, next to six O-glycosylation sites (i.e., at T106, T109, S111, S113, T114, and T117). All six O-glycosylation sites in the hinge region of IgA1 are present on a single tryptic peptide (HYT)6-8. (B) With our MS-based approach, we observed three different N-glycosylation sites on IgA2 (i.e., at N131, N205, and N327), which were occupied with complex-type N-glycans. Glycopeptides indicating glycosylation on the two other potential N-glycosylation sites were not detected in our study. (C) Symbols and example structures of O- and N-glycans. In this work, we refer to the first three letters of the tryptic peptide sequence of the detected glycopeptides: HYT for the multiply O-glycosylated hinge-region peptide; LSL for the glycopeptide with the N-glycosylation site N144 or N131 on IgA1 or IgA2, respectively; TPL for the glycopeptide with the IgA2 N-glycosylation site N205; and LAG for the glycopeptide with the N-glycosylation site N340/N327 on IgA1/IgA2, which was detected with either a terminal tyrosine (LAGY) or as the truncated form (LAGC). Glycosylation site numbering was according to UniProtKB.*

Measurement of gd-IgA in blood samples is typically achieved by ELISA incorporating the use of a lectin, *Helix aspersa* agglutinin (HAA), which recognizes terminal GalNAc

residues on *O*-glycans. Another lectin, Jacalin, is often used to isolate IgA from samples for further analysis. Although lectin-based approaches are useful tools in this aspect, variability in their specificities and interferences, especially by the copresence of sialic acids, limits their robustness[14-16].

Although aberrant *O*-glycosylation of gd-IgA in IgAN has been widely reported, not much is known about the role of *N*-glycans. Both IgA1 and IgA2 are *N*-glycosylated. IgA1 contains two *N*-linked glycosylation sites on each heavy chain (Asn263/Asn459), and IgA2 contains an additional two or three *N*-glycans (**Figure 1**). The *N*-glycans on IgA are reported to be mainly complex-type, digalactosylated diantennary structures[6-8]. Elevated levels of sialylation[17] and mannosylation[18] of serum IgA1 *N*-glycans from patients with IgAN have been identified. Moreover, mice with a gene knockout (*β4GalT*) leading to agalactosylated *N*-glycans developed IgAN-like glomerular lesions upon IgA deposition[19].

Despite the involvement of IgA glycosylation in the pathogenesis of IgAN, it is still largely unclear how IgA glycosylation changes with the disease. The molecular nature of IgA *O*- and *N*-glycosylation in IgAN has hitherto been incompletely explored. Here, we used our new mass spectrometry (MS)–based approach for IgA *O*- and *N*-glycosylation analysis in a sizable patient-control cohort to obtain a more complete picture on the IgA glycosylation changes in IgAN at an unprecedented level of detail and resolution and to further investigate the relationship of IgA glycosylation and kidney function.

Methods

Study populations

Samples from patients with IgAN were collected as part of the Causes and Predictors of Outcome in IgA Nephropathy Study, a retrospective cohort study ethically approved by the U.K. National Research Ethics Service Committee. All individuals provided informed written consent (14/LO/0155). Here, we investigated 83 unrelated patients from the United Kingdom with serum samples available and complete clinical follow-up at the time of recruitment (Supplemental Table 1). eGFR, estimated by the Chronic Kidney Disease Epidemiology Collaboration equation, and corrected for body surface area, was used as a biomarker of renal function[12].

The control samples were randomly ascertained among healthy British twins from the TwinsUK adult twin registry[20] and age- and sex-matched with the patients with IgAN (**Supplemental Figure 1**). The sample included 244 individuals (49 monozygotic and 64 dizygotic twin pairs and 18 singletons) (**Supplemental Table 1**). St. Thomas'

Hospital Research Ethics Committee approved this study, and all twins provided informed written consent.

Measurement of serum IgA and gd-IgA levels

Serum IgA levels were measured using ELISA as previously described[21]. The capture antibody was the F(ab')2 fragment goat anti-human IgA (Jackson Immuno-Research, West Grove, PA), and the detection antibody was the F(ab')2 fragment biotinylated goat anti-human IgA1 (invitrogen, CA, USA).

Serum gd-IgA1 levels were measured using a lectin-based ELISA as previously described[21]. The capture antibody was a polyclonal rabbit antihuman IgA (Dako, Glostrup, Denmark). The detection involved HAA-biotin (Sigma, Darmstadt, Germany), followed by polystreptavidin horseradish peroxidase (Pierce, Waltham, MA).

The intraclass correlation coefficient for the IgA assay was 0.74 (95% confidence interval, 0.63 to 0.83), and that for the gd-IgA1 assay was 0.89 (95% confidence interval, 0.73 to 0.95).

IgA glycopeptide analysis by MS

A detailed description of the material and methods can be found in Supplemental Material. Briefly, serum samples from patients and controls together with 22 pooled plasma standards were pipetted onto 96-well plates in a randomized manner. IgA was captured from 10 μl of serum using CaptureSelectTM IgA affinity beads (ThermoFisher). (Glyco-)peptides were generated by reduction, alkylation, and digestion of the protein with trypsin. Tryptic digests were separated by reversed-phase nanoliquid chromatography (nano-LC) on a C18 column (75 μm × 100 mm, particle size 1.7 μm) and analyzed by MS using an Impact HD quadrupole time-of-flight MS system (Bruker Daltonics, Bremen, Germany) equipped with a nanoBooster, as described previously[22] and in the Supplemental Material.

Raw LC-MS data were converted to mzXML using MSConvert. LaCyTools[23] (version 1.0.1) was used to align the LC runs, to calibrate (Supplemental Table 2) the mass spectra, and to extract glycopeptide signal intensities. For the extraction step, a previously reported list of potential IgA glycopeptide analytes was used[24-26], in addition to manual identification of glycoforms in the averaged spectra of 20 samples of both healthy individuals and patients.

Quality control was performed on the basis of signal to noise, exact mass deviation, and isotopic pattern as described previously[23] and in the Supplemental Material. Sixty-nine glycopeptides were retained and quantified. Their absolute signal

intensities were normalized to the intensity sum of all glycopeptide species sharing the same tryptic peptide sequence, resulting in relative intensities. In this manuscript, IgA1 and IgA2 glycopeptide names are composed of the letter codes of the first three amino acids of the peptide sequence: HYT, LSL, TPL, and LAG, the last detected in two variants (*i.e.*, as LAGC and LAGY) (**Figure 1**). The peptide name is followed by the glycan composition indicating the number of hexoses (H), *N*-acetylhexosamines (N), fucoses (F), and sialic acids (S) (**Supplemental Table 2**).

Structurally similar glycopeptides were summarized into 52 derived traits calculated from the relative intensities, as illustrated in **Supplemental Table 3**. For example, the derived trait TPL_A2FB, bisection of fucosylated diantennary glycans, was calculated as the sum of all bisected diantennary structures within the TPL glycopeptide cluster divided by the sum of the abundances of all structures within the TPL cluster, *i.e.*, A2FB = (H4N5F1S0 + H5N5F1S0 + H4N5F1S1 + H5N5F1S1 + H5N5F1S2)/(H4N5F1S0 + H5N5F1S0 + H5N4F1S1 + H4N5F1S1 + H5N5F1S1 + H5N4F1S2 + H5N5F1S2). Because each measured glycopeptide structure carries different types of monosaccharides, derived traits can give a more composite and robust measure of the different glycosylation features (*i.e.*, for *N*-glycans[27], complexity/branching [diantennary versus triantennary], bisection, and fucosylation and for both *O*- and *N*-glycans, galactosylation and sialylation).

Statistical analyses

The relative intensities of the detected glycopeptides and the derived trait values were corrected for batch effects (plate, plate row, and column) in R (version 3.3.3) using the function ComBat from the R package sva (release 3.2) on log-transformed data. Outliers, defined as measurements deviating more than three SDs from the mean of each trait, were removed. To ensure the normality of their distribution, the relative intensities of the detected glycopeptides as well as of the derived traits were quantile normalized.

gd-IgA level and IgAN status (patients versus control) were tested for association with glycopeptides and derived traits using a linear mixed model using the function lmer from the R package lmerTest (version 3.1), including age, sex, and their interaction term as fixed effects and family structure as a random effect to correct for the nonindependence of the twin observations. To avoid potential spurious associations due to differences in glycan composition between patients and controls, association with gd-IgA levels was assessed using healthy individuals only. eGFR (assessed in patients with IgAN only) was tested for association using a linear regression model (function lm, from the stats R package, version 3.6.1). Age, sex, and their interaction term were included as covariates.

We considered an association significant when its *P* value passed a Bonferroni-derived threshold of $0.05/N_{eff}$, where N_{eff} is the effective number of independent tests taking into account the strong correlation among glycan relative intensities. N_{eff} was calculated using the approach proposed by Li and Ji[28] and multiplied by the number of phenotypes analyzed in this study. N_{eff} was 23(×3) for measured glycopeptides and 16(×3) for derived traits.

Power calculation was performed using the pwr R package (version 1.3) and asking for the power to detect, in a sample of 83 patients and 244 controls, a Cohen conventional medium effect size[29] of 0.5 of an SD at α-levels of $0.05/(23 \times 3)=7.3 \times 10^{-4}$ and $0.05/(16 \times 3)=1.0 \times 10^{-3}$ for measured and derived traits, respectively.

We further evaluated, for both IgAN and glomerular function, the predictive power of a model including only the gd-IgA serum levels and a model including either the glycopeptides or derived traits significantly associated with IgAN/glomerular function. In this second model, because of the high correlation among traits, if two traits had a Pearson correlation larger than 0.9, only the most significantly associated was used. Predictive powers were evaluated using the McFadden adjusted pseudo-R^2 [30] (evaluated *via* the function PseudoR2, from the DescTools R package, version 0.99.39) for the binary trait IgAN and adjusted R^2 for the continuous trait eGFR (evaluated *via* the lm function). The adjusted values allow for penalizing for the number of predictors in the model (k=1 when only gd-IgA levels are used and k>1 when the glycopeptides or derived traits are used).

Results

Glycosylation features are associated with the level of gd-IgA in healthy individuals

As a first comparison of the traditional lectin-based method and our MS-based approach for measuring IgA glycosylation, we assessed the cross-sectional associations between gd-IgA values and MS-detected glycosylation traits. Using data from 236 healthy individuals, we found associations between gd-IgA, 26 of 30 detected *O*-glycopeptides (HYT cluster), and all seven derived *O*-glycan traits (**Supplemental Table 4**). The strongest associations were observed with decreased sialylation (HYT_nS, HYT_nS > nG, HYT_SperG) and galactosylation (HYT_GalperGalNAc and HYT_nGal), along with a relative increase of GalNAcylation (HYT_nGalNAc > nG and HYT_nGalNAc) (**Figure 2**), which showed a similar trend in patients with IgAN (Supplemental Figure 2). *N*-glycosylation traits from the LAGC

cluster were also associated with gd-IgA, although to a lesser extent than *O*-glycosylation (**Supplemental Table 4**).

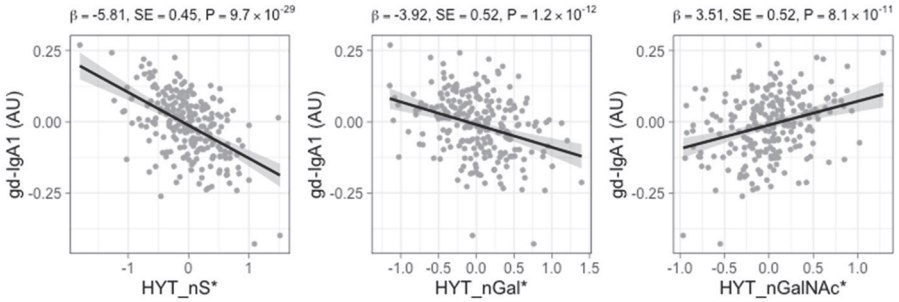

Figure 2 : Main associations between derived glycosylation traits and gd-IgA1 levels detected by HAA lectin in 236 healthy individuals. *Quantile-normalized age- and sex-corrected values are plotted, and each scatterplot reports effect size (β), SE, and P value (P) of the linear regression analysis. Derived traits HYT_nS, HYT_nGal, and HYT_nGalNAc correspond to average numbers of sialic acids, galactoses, and N-acetylgalactosamines, respectively. Monosaccharide symbols are depicted, in black and white, according with the nomenclature of the Consortium for Functional Glycomics and were generated using GlycoWorkbench55. AU, arbitrary units; * indicates derived traits.*

Moreover, we compared the associations between gd-IgA and glycopeptides with and without correction for IgA1 titer in a subset of 156 healthy individuals for whom IgA1 titer was available. IgA1 titer correction had negligible effects on the associations (**Supplemental Table 5**).

O- and *N*-Glycosylation of IgA Is associated with IgA Nephropathy

We used a patient-control study design, including 83 patients with IgAN and 244 healthy controls, to investigate cross-sectional associations between IgAN and IgA *O*- and *N*-glycosylation features detected by MS. This sample has ≥70% power to detect a difference of 0.5 of an SD between groups at Bonferroni-derived *P* values of $0.05/(23 \times 3)=7.3 \times 10^{-4}$ and $0.05/(16 \times 3)=1.0 \times 10^{-3}$ for measured and derived traits, respectively.

We found that galactosylation of the *N*-glycopeptides in the TPL and LSL clusters, next to sialylation in TPL and sialylation of the HYT *O*-glycopeptides, was lower in patients with IgAN compared with controls, whereas bisection and sialylation in LSL;

diantennary glycans in LAGCa, TPL, and LAGCb; and fucosylation in LAGCb were higher in patients (**Figure 3**, **Supplemental Table 6**).

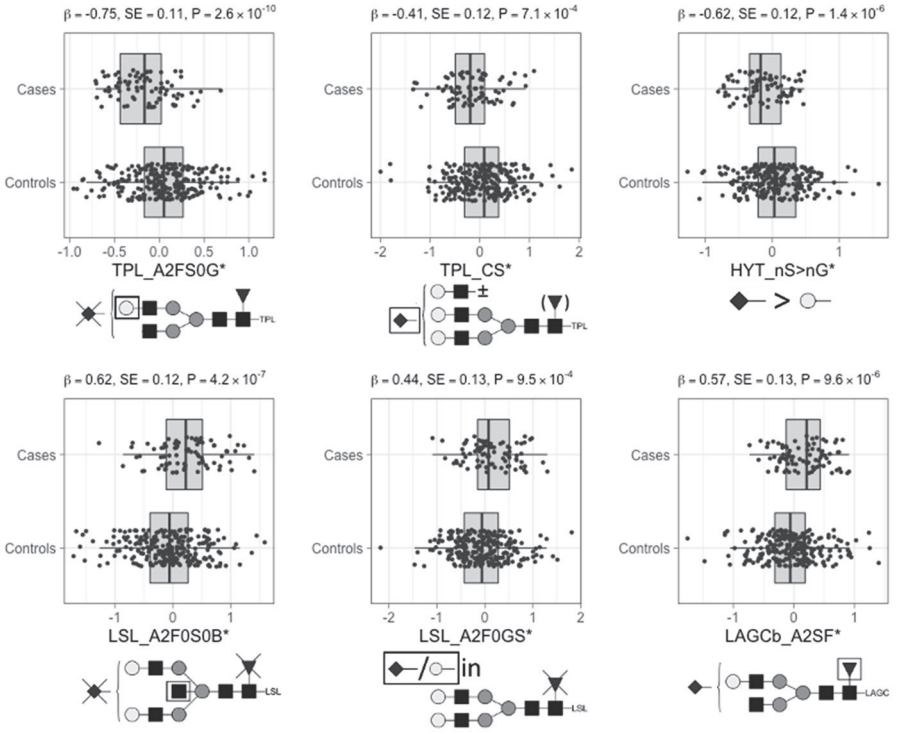

Figure 3: Main associations between derived glycosylation traits in serum IgA from healthy controls and individuals with IgAN (n=327). *Quantile-normalized age- and sex-corrected values are plotted, and each box plot reports effect size (β), SE, and P value (P) of the regression analysis. Glycopeptide-derived trait nomenclature refers to the first three letters of the tryptic amino acid sequence followed by the glycosylation features as calculated from detected glycopeptides (Supplemental Table 3). Glycosylation traits: A2FS0G, galactosylation of nonsialylated fucosylated diantennary glycans; CS, sialylation within complex glycans; nS > nG, relative intensity sum of structures in which the number of sialic acids exceeds the number of galactoses; A2F0S0B, bisection of nonfucosylated nonsialylated diantennary; A2F0GS, sialic acid per galactose in nonfucosylated diantennary; and A2SF, fucosylation of sialylated diantennary. Monosaccharide symbols are depicted, in black and white, according with the nomenclature of the Consortium for Functional Glycomics and were generated using GlycoWorkbench.[55]* indicates derived traits.*

O- and *N*-Glycosylation of IgA is associated with renal function

Using data from patients with IgAN, we sought association between glycan traits and eGFR, a marker of renal function. *N*-glycosylation features from all detected IgA glycopeptide clusters were associated with eGFR: bisection of LAGY, LSL, LAGC, and TPL was lower, whereas galactosylation and sialylation of TPL and LSL were higher in patients with higher eGFR (**Figure 4**, **Supplemental Table 7**). Regarding *O*-glycosylation, only sialylation showed significant, positive associations with eGFR (HYT_nS, HYT_SperG, and HYT_nS > nG), reflected in low levels of mono- or disialylated glycopeptides (*e.g.*, HYT_H4N4F0S1) and high levels of multisialylated ones (*e.g.*, HYT_H4N4F0S4) (**Figure 4**, **Supplemental Table 7**).

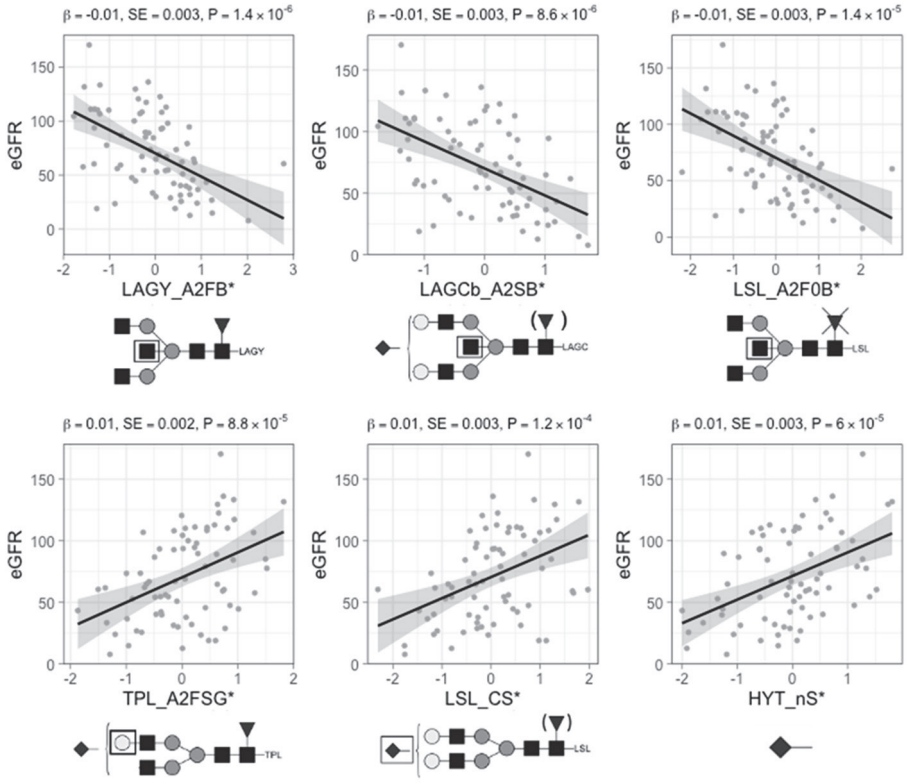

Figure 4: Main associations between IgA glycosylation traits and eGFR in 75 patients with IgAN. *Quantile-normalized age- and sex-corrected values are plotted, and each scatterplot reports effect size (β), SE, and P value (P) for the linear regression analysis. Glycopeptide-derived trait nomenclature refers to the first three*

*letters of the tryptic amino acid sequence followed by the glycosylation features as calculated from detected glycopeptides (Supplemental Table 3). Glycosylation traits: A2FB, bisection of fucosylated diantennary glycans; A2SB, bisection of sialylated diantennary; A2F0B, bisection of nonfucosylated diantennary; A2FSG, galactosylation of sialylated fucosylated diantennary; CS, sialylation within complex glycans; and nS, average number of sialic acids. Glycan structures are reported below each panel. Monosaccharide symbols are depicted, in black and white, according to the nomenclature of the Consortium for Functional Glycomics and were generated using GlycoWorkbench[55]. * Indicates derived traits.*

Glycopeptides and derived traits are better predictors of IgAN status and renal function than gd-IgA levels

Using McFadden adjusted pseudo-R^2 [30], we found that glycopeptides and derived traits that were associated with IgAN from our analyses were better predictors of the disease than gd-IgA levels, with pseudo-R^2 values of 0.14, 0.12 and 0.02 for glycopeptides, derived traits, and gd-IgA levels, respectively. Analogously, glycopeptides and derived traits associated with eGFR showed pseudo-R^2 values of 0.23 and 0.22, respectively, versus 0.07 of gd-IgA levels. These results suggest that MS glycosylation data may not only give insights into the pathophysiology of IgAN but can also provide leads for noninvasive biomarkers for disease and deteriorating kidney function.

A summary of the major associations with gd-IgA, IgAN, and glomerular function is visualized in **Figure 5** for derived traits and **Supplemental Figure 3** for measured glycopeptides.

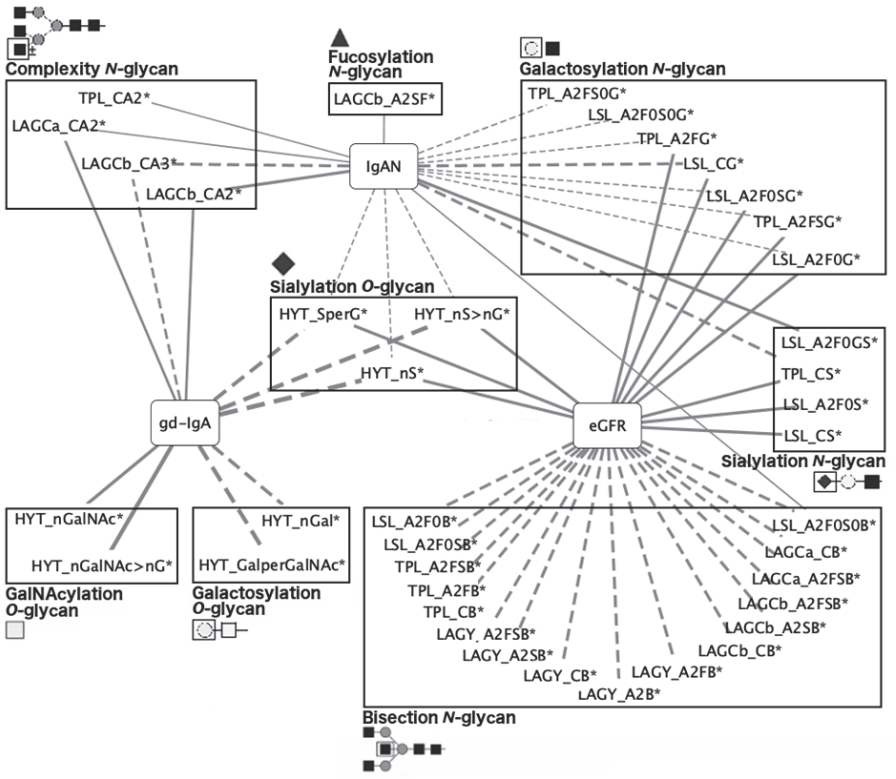

Figure 5: Summary of the associations of derived IgA glycan traits with gd-IgA levels, IgAN, and glomerular function. *Line thickness represents effect size (the thicker the line, the stronger the effect's absolute value). Solid lines indicate positive associations; dotted lines indicate negative associations. Derived traits are grouped by glycosylation features along with their structural representations. Monosaccharide symbols are depicted, in black and white, according to the nomenclature of the Consortium for Functional Glycomics and were generated using GlycoWorkbench[55]. * Indicates derived traits. Complete summary statistics are reported in* ***Supplemental Tables 4, 6, and*** *7.*

Discussion

This study is the first detailed report on site-specific *O*- and *N*-glycosylation signatures of serum IgA1 and IgA2 in IgAN. We analyzed a reasonably large cohort of 83 patients and 244 age- and sex-matched controls. Our high-resolution MS-based method features the relative quantitation of, in total, 69 *O*- and *N*-glycopeptide species, further summarized in 52 derived traits. Our data revealed disease

associations with *O*-glycan sialylation and with all main *N*-glycosylation features, which include complexity, bisection, galactosylation, fucosylation, and sialylation.

Altered glycosylation of IgA1 *O*-glycans in IgAN is widely reported. Our MS data reflect relative shifts of different glycosylation features due to total area normalization within a glycopeptide cluster. This is different to terminal GalNAc abundance detected by the lectin-based gd-IgA assay. Nevertheless, our MS data on relative *O*-glycan galactosylation and on the relative abundance of GalNAc on *O*-glycopeptides can be related to the traditional lectin-based detection of truncated *O*-glycans with terminal GalNAc (GalNAcα1-Ser/Thr; Tn antigen). Both gd-IgA and IgA titers represent absolute concentrations but become more comparable with our relative quantitation of MS data when gd-IgA is adjusted for IgA titers. Accordingly, we found a strong positive association of HAA lectin binding with the glycosylation trait HYT_nGalNAc > nG, which reflects the presence of terminal GalNAc, and consequently, a negative association with hinge-region galactosylation (HYT_GalperGalNAc, HYT_nGal) that is supposed to cap the HAA binding motif. Similarly, sialylation (HYT_nS > nG) was also inversely associated with the gd-IgA level. This can partly be explained by the fact that terminal α2,3-linked sialic acids can only be present when a galactose has been attached to the core GalNAc. This could also be explained by virtue of the lectin-based assay simply detecting gd-IgA as exposed GalNAc. In 2017, the first GWAS for aberrant *O*-glycosylation of IgA1 identified variants in the *C1GALT1* and *C1GALT1C1* genes that had large effects on gd-IgA1 levels[31]. These genes encode, respectively, the enzyme core 1 β1–3-galactosyltransferase (C1GalT1) and COSMC, its molecular chaperone—molecular partners that are essential for the galactosylation of IgA1 *O*-glycans[32]. Decreased expression and activity of C1GalT1 have been demonstrated in the B cells of patients with IgAN[33-35]. Further studies have also demonstrated that genetic variation at *CIGALT1* influences gd-IgA levels[36, 37]. A recent study has also shown that decreased expression of Golgi matrix protein GM130, which is involved in glycosyltransferase tethering, is associated with reduced C1GalT1 protein level and increased galactose deficiency of IgA1[38]. It is therefore likely that downregulated expression of *CIGALT1* in patients with IgAN leads to reduced levels of galactosylation and subsequent reduced levels of sialylation and increased levels of exposed GalNAc, as detected in the lectin ELISA and reflected in our results.

The relative abundance of sialic acids was the only derived *O*-glycosylation trait that associated with IgAN and renal decline in patients with IgAN. Our data suggest that decreased sialylation may also lead to increased presentation of terminal GalNAc, as lower sialylation significantly correlates with higher gd-IgA levels. It is unclear from our study if decreased sialylation is an alteration of IgA glycosylation in itself or a product of reduced galactosylation. Data on *O*-linked sialylation in IgAN are

conflicting. In agreement with our findings two small-scale MS-based studies without quantitation reported decreased numbers of galactose, GalNAc, and especially, sialic acid residues in both glomerular and serum IgA1 in pooled samples from patients with IgAN as compared with control serum pools[39, 40]. Conversely, increased expression of *ST6GALNAC2*, a gene encoding an enzyme that mediates sialylation of *O*-glycans, has been reported to be positively correlated with IgAN[41]. Interestingly, increased expression of another enzyme, ST6Gal1, correlates with gd-IgA levels[42]. Further studies are required to disentangle the relationship between sialylation and IgAN.

Regarding serum IgA *N*-glycosylation in IgAN, only a few small studies exist, and the possible implication of *N*-glycosylation in pathogenesis or renal decline is unknown. Here, we present the first detailed report on associations between serum IgA *N*-glycan galactosylation, sialylation, bisection, and fucosylation with IgAN and related clinical parameters. Previously, lower IgA1 Fc-region galactosylation and lower IgA2 sialylation in patients with IgAN were detected by lectin-based assays[43]. Intriguingly, our findings of decreased *N*-linked sialylation and galactosylation and increased bisection in IgAN and with worsening renal function are similar to the *N*-glycosylation differences reported for human salivary versus plasma IgA[25]. With this in mind, it is possible that our findings might partly reflect a disease-related increase of IgA molecular species connected to mucosal immune response, which has previously been suggested for IgAN[44].

It is also feasible that our results could reflect a causal relationship of IgA *N*-glycosylation and IgAN pathogenesis via increased formation of polymeric IgA. In comparison with monomeric, polymeric IgA is increased in patients with IgAN, and it has been implicated in higher immune complex formation and glomerular deposition[45]. Strikingly, mice with impaired terminal *N*-glycan galactosylation due to a knockout of the *β*4-galactosyltransferase I gene were shown to develop human IgAN-like glomerular lesions, with an increased serum IgA, especially the polymeric form[19]. Our finding of decreased sialylation in IgAN and with worsening renal function might also reflect a higher abundance of polymeric IgA, which was reported to exhibit a lower degree of sialylation compared with its monomeric form and thereby, enhance binding to mannose-binding lectin as well as to mesangial cells[46-48]. Similarly, a higher abundance of fucose and terminal GlcNAc (*e.g.*, bisecting GlcNAc or ungalactosylated antenna GlcNAc) might also be involved in enhanced binding to mannose-binding lectin and subsequent complement activation via the lectin pathway[48]. Desialylation and to a lesser extent, additional degalactosylation have been shown to enhance the binding of polymeric IgA1 to human mesangial cells, as compared with untreated IgA1 *in vitro*[49]. Of note, it is unclear to which extent this effect was attributed to *O*- or *N*-glycosylation or a combination thereof.

Notably, the *ST6GAL1* gene, coding for an enzyme responsible for the terminal sialylation of *N*-glycans on different proteins including IgA, was associated with IgAN in Han Chinese[50].

Large-scale *O*-glycomic studies, other than the one reported here and a site-specific *O*- and *N*-glycosylation associations study with rheumatoid arthritis[24], are hitherto lacking due to the technologically challenging nature of these studies. Although a few reports do exist that associate *N*-glycosylation of IgG with kidney disease or glomerular function[51-53], none are available for IgAN, hampering our ability to compare IgAN glycosylation signatures displayed by different molecules. Analogously, linking phenotypic associations of the total plasma *N*-glycome with those found here for IgA glycosylation is complicated as many different glycoproteins contribute to the total plasma *N*-glycome, with mostly overlapping structures[54]. An analysis of total serum glycans in kidney disease showed eGFR to be associated with higher absolute levels of biantennary digalactosylated disialylated glycans with and without bisection[53], yet information on the glycoproteins and glycosylation sites contributing to this signature is lacking. In comparison, our novel approach for specific IgA glycosylation analysis presented here provides these extra layers of information by covering all main glycosylation features present on 69 measured glycopeptides of IgA[54].

We have made a first attempt to elucidate the complex *O*- and *N*-glycosylation of human serum IgA in relation to IgAN in a comprehensive fashion with direct detection using high-resolution MS. Because of the small sample size, we could not build and validate a predictive model for IgAN pathogenesis and renal decline. However, we have shown that directly measured glycopeptide-level IgA glycosylations are better predictors of both IgAN status and renal function than gd-IgA levels alone. Our results widen the current view on the potential role of IgA glycosylation in IgAN pathogenesis and in renal decline and open new opportunities for investigations on glycopeptides as potential biomarkers for disease onset and progression. We envisage that these results, together with the increasing interest in the use of glycomics in clinical settings, will encourage increased inclusion of IgA glycomics in studies, which will promote the development of targeted analysis panels and of absolute quantification approaches, currently hindered by the lack of stable isotope-labeled glycopeptide standards.

In summary, we provide the first evidence of a possible role for IgA *N*-glycosylation in IgAN pathogenesis, which should be taken forward in mechanistic studies and could result in novel therapeutic and preventive approaches in the future.

Disclosures

H.T. Cook reports consultancy agreements with Alexion Pharmaceuticals, Apellis Pharmaceuticals, and Novartis and honoraria from Alexion Pharmaceuticals. V. Dotz is employed by Janssen Vaccines (a Johnson & Johnson company). M. C. Pickering reports consultancy agreements with Achillion Pharmaceuticals as a scientific advisor, Alexion Pharmaceuticals for scientific advisory board attendance, the ChemoCentryx Sciviaentific Advisory Board (meeting on May 7th, 2016) as an invited speaker, Gyroscope for scientific board membership, and Ra Pharma for scientific advisory board attendance; research funding from Achillion for the C3 Glomerulopathy Natural History Study, Alexion for preclinical studies in animal models, Laboratoires Français de Fractionnement et des Biotechnologies for preclinical studies in animal models, and Ra Pharma for complement C9 in lupus nephritis; honoraria from Gyroscope as advisory board fees; and scientific advisor or membership with Gyroscope Pharma via the advisory board. M. Falchi reports research funding from Sanofi for the identification of multi-disease drug targets through systems-immunology dissection of immune ageing. All remaining authors have nothing to disclose.

Funding

This work was supported by funding from Medical Research Council grant MR/K01353X/2. M. C. Pickering is a Wellcome Trust Senior Fellow in Clinical Science under grant 212252/Z/18/Z.

V.D., A.V., H.J.L.-B., and F.C. contributed equally to this work. M.W. and M.F. contributed equally to this work.

Published online ahead of print. Publication date available at www.jasn.org.

Present address: Dr. Viktoria Dotz, BioTherapeutics Analytical Development, Janssen Biologics BV, Einsteinweg 101, 2333 CB Leiden, The Netherlands

Acknowledgments

TwinsUK is funded by the Wellcome Trust, the Medical Research Council, the European Union, the Chronic Disease Research Foundation, the National Institute for Health Research–funded BioResource, the Clinical Research Facility, and the Biomedical Research Centre based at Guy's and St. Thomas' National Health Service (NHS) Foundation Trust in partnership with King's College London. We acknowledge support from the National Institute for Health Research Biomedical Research Centre based at Imperial College Healthcare National Health Service Trust and Imperial

College London and from the National Institute for Health Research Clinical Research Network.

The views expressed are those of the authors and are not necessarily those of the National Health Service, the National Institute for Health Research, or the Department of Health.

M. Falchi and M. Wuhrer designed the study; H. T. Cook, H. J. Lomax-Browne, N. R. Medjeral-Thomas, and M. C. Pickering collected the samples and clinical data in the Causes and Predictors of Outcome in IgA Nephropathy Study; H. J. Lomax-Browne measured serum IgA and gd-IgA levels; A. L. Hipgrave Ederveen optimized the LC-MS method; F. Clerc and A. L. Hipgrave Ederveen performed IgA glycopeptide analysis by MS; F. Clerc processed the raw data and calculated the derived traits; A. Visconti carried out the statistical analyses; V. Dotz, M. Falchi, F. Clerc, H. J. Lomax-Browne, A. Visconti, and M. Wuhrer interpreted the results; F. Clerc generated the figures for the glycopeptides and derived traits; A. Visconti generated the figures for the association study results; M. Falchi and A. Visconti generated the figures summarizing the association results; V. Dotz, M. Falchi, F. Clerc, H. J. Lomax-Browne, and A. Visconti drafted the manuscript; and all authors approved the final version of the manuscript. Glycoworkbench[55] was used to generate the monosaccharides symbols.

Data Sharing Statement

Data on study participants are available to *bona fide* researchers under managed access due to governance and ethical constraints. The raw data of patients with IgAN should be requested via contact with the corresponding author. Twins' raw data should be requested via the TwinsUK website (http://twinsuk.ac.uk/resources-for-researchers/access-our-data/), and requests are reviewed by the TwinsUK Resource Executive Committee regularly.

Supplemental Material

This article contains the following supplemental material online at http://jasn.asnjournals.org/lookup/suppl/doi:10.1681/ASN.2020081208/-/DCSupplemental

https://journals.lww.com/jasn/fulltext/2021/10000/o__and_n_glycosylation_of_serum_immunoglobulin_a.15.aspx

Supplemental Material. IgA glycopeptide analysis by mass spectrometry.

Supplemental Figure 1. Age distribution and sex proportion for the study sample.

Supplemental Figure 2. Selected associations between derived *O*-glycosylation traits and gd-IgA1 levels detected by HAA lectin in 83 patients with IgAN.

Supplemental Figure 3. Summary of the associations of measured IgA glycopeptides with gd-IgA levels, IgAN, and glomerular function.

Supplemental Table 1. Phenotypic details of the study sample.

Supplemental Table 2. Analytical characteristics of the detected glycopeptides per glycosylation site.

Supplemental Table 3. Derived IgA glycosylation traits calculated from detected glycopeptides with their technical (n = 22) versus biologic variation (83 patients with IgAN and 244 healthy controls).

Supplemental Table 4. Associations of IgA glycosylation with gd-IgA in healthy controls.

Supplemental Table 5. Associations of IgA glycosylation with gd-IgA with IgA1 titer correction in a subset of healthy controls.

Supplemental Table 6. Patient-control association study of IgA glycosylation.

Supplemental Table 7. Associations of IgA glycosylation with eGFR in patients with IgAN.

References

(1) Schena, F. P.; Nistor, I. Epidemiology of IgA Nephropathy: A Global Perspective. *Seminars in Nephrology* **2018**, *38* (5), 435-442

(2) Berthoux, F. C.; Mohey, H.; Afiani, A. Natural History of Primary IgA Nephropathy. *Seminars in Nephrology* **2008**, *28* (1), 4-9

(3) Jennette, J. C. The Immunohistology of IgA Nephropathy. *American Journal of Kidney Diseases* **1988**, *12* (5), 348-352

(4) Suzuki, H.; Kiryluk, K.; Novak, J.; Moldoveanu, Z.; Herr, A. B.; Renfrow, M. B.; Wyatt, R. J.; Scolari, F.; Mestecky, J.; Gharavi, A. G.; Julian, B. A. The pathophysiology of IgA nephropathy. *Journal of the American Society of Nephrology : JASN* **2011**, *22* (10), 1795-1803

(5) Kerr, M. A. The structure and function of human IgA. *Biochem J* **1990**, *271* (2), 285-296

(6) Mattu, T. S.; Pleass, R. J.; Willis, A. C.; Kilian, M.; Wormald, M. R.; Lellouch, A. C.; Rudd, P. M.; Woof, J. M.; Dwek, R. A. The Glycosylation and Structure of Human Serum IgA1, Fab, and Fc Regions and the Role of N-Glycosylation on Fcα Receptor Interactions. *J Biol Chem* **1998**, *273* (4), 2260-2272

(7) Tarelli, E.; Smith, A. C.; Hendry, B. M.; Challacombe, S. J.; Pouria, S. Human serum IgA1 is substituted with up to six O-glycans as shown by matrix assisted laser desorption ionisation time-of-flight mass spectrometry. *Carbohydrate Research* **2004**, *339* (13), 2329-2335

(8) Woof, J. M.; Russell, M. W. Structure and function relationships in IgA. *Mucosal Immunology* **2011**, *4* (6), 590-597

(9) Mestecky, J.; Tomana, M.; Crowley-Nowick, P. A.; Moldoveanu, Z.; Julian, B. A.; Jackson, S. Defective Galactosylation and Clearance of IgA1 Molecules as a Possible Etiopathogenic Factor in IgA Nephropathy1. In *IgA Nephropathy: The 25th Year: International Symposium, Nancy, August/September 1992*, Béné, M. C., Faure, G., Kessler, M. Eds.; Vol. 104; S.Karger AG, **1993**; p 0.

(10) Moldoveanu, Z.; Wyatt, R. J.; Lee, J. Y.; Tomana, M.; Julian, B. A.; Mestecky, J.; Huang, W. Q.; Anreddy, S. R.; Hall, S.; Hastings, M. C.; Lau, K. K.; Cook, W. J.; Novak, J. Patients with IgA nephropathy have increased serum galactose-deficient IgA1 levels. *Kidney international* **2007**, *71* (11), 1148-1154

(11) Sun, Q.; Zhang, Z.; Zhang, H.; Liu, X. Aberrant IgA1 glycosylation in IgA nephropathy: a systematic review. *Plos One* **2016**, *11* (11), e0166700

(12) Medjeral-Thomas, N. R.; Lomax-Browne, H. J.; Beckwith, H.; Willicombe, M.; McLean, A. G.; Brookes, P.; Pusey, C. D.; Falchi, M.; Cook, H. T.; Pickering, M. C.

Circulating complement factor H–related proteins 1 and 5 correlate with disease activity in IgA nephropathy. *Kidney international* **2017**, *92* (4), 942-952

(13) Hastings, M. C.; Moldoveanu, Z.; Julian, B. A.; Novak, J.; Sanders, J. T.; McGlothan, K. R.; Gharavi, A. G.; Wyatt, R. J. Galactose-deficient IgA1 in African Americans with IgA nephropathy: serum levels and heritability. *Clinical journal of the American Society of Nephrology: CJASN* **2010**, *5* (11), 2069

(14) Tachibana, K.; Nakamura, S.; Wang, H.; Iwasaki, H.; Tachibana, K.; Maebara, K.; Cheng, L.; Hirabayashi, J.; Narimatsu, H. Elucidation of binding specificity of Jacalin toward O-glycosylated peptides: quantitative analysis by frontal affinity chromatography. *Glycobiology* **2006**, *16* (1), 46-53

(15) Moore, J. S.; Kulhavy, R.; Tomana, M.; Moldoveanu, Z.; Suzuki, H.; Brown, R.; Hall, S.; Kilian, M.; Poulsen, K.; Mestecky, J. Reactivities of N-acetylgalactosamine-specific lectins with human IgA1 proteins. *Molecular immunology* **2007**, *44* (10), 2598-2604

(16) Yasutake, J.; Suzuki, Y.; Suzuki, H.; Hiura, N.; Yanagawa, H.; Makita, Y.; Kaneko, E.; Tomino, Y. Novel lectin-independent approach to detect galactose-deficient IgA1 in IgA nephropathy. *Nephrology Dialysis Transplantation* **2015**, *30* (8), 1315-1321

(17) Linossier, M.-T.; Palle, S.; Berthoux, F. Different glycosylation profile of serum IgA1 in IgA nephropathy according to the glomerular basement membrane thickness: normal versus thin. *American journal of kidney diseases* **2003**, *41* (3), 558-564

(18) Amore, A.; Cirina, P.; Conti, G.; Brusa, P.; Peruzzi, L.; Coppo, R. Glycosylation of circulating IgA in patients with IgA nephropathy modulates proliferation and apoptosis of mesangial cells. *Journal of the American Society of Nephrology* **2001**, *12* (9), 1862-1871

(19) Nishie, T.; Miyaishi, O.; Azuma, H.; Kameyama, A.; Naruse, C.; Hashimoto, N.; Yokoyama, H.; Narimatsu, H.; Wada, T.; Asano, M. Development of immunoglobulin A nephropathy-like disease in β-1, 4-galactosyltransferase-I-deficient mice. *The American journal of pathology* **2007**, *170* (2), 447-456

(20) Andrew, T.; Hart, D. J.; Snieder, H.; De Lange, M.; Spector, T. D.; MacGregor, A. J. Are twins and singletons comparable? A study of disease-related and lifestyle characteristics in adult women. *Twin Research and Human Genetics* **2001**, *4* (6), 464-477

(21) Lomax-Browne, H. J.; Visconti, A.; Pusey, C. D.; Cook, H. T.; Spector, T. D.; Pickering, M. C.; Falchi, M. IgA1 glycosylation is heritable in healthy twins. *Journal of the American Society of Nephrology: JASN* **2017**, *28* (1), 64

(22) Falck, D.; Jansen, B. C.; de Haan, N.; Wuhrer, M. High-Throughput Analysis of IgG Fc Glycopeptides by LC-MS. In *High-Throughput Glycomics and Glycoproteomics: Methods and Protocols*, Lauc, G., Wuhrer, M. Eds.; Springer New York, **2017**; pp 31-47.

(23) Jansen, B. C.; Falck, D.; de Haan, N.; Hipgrave Ederveen, A. L.; Razdorov, G.; Lauc, G.; Wuhrer, M. LaCyTools: A Targeted Liquid Chromatography-Mass Spectrometry Data Processing Package for Relative Quantitation of Glycopeptides. *Journal of proteome research* **2016**, *15* (7), 2198-2210

(24) Bondt, A.; Nicolardi, S.; Jansen, B. C.; Kuijper, T. M.; Hazes, J. M.; Van Der Burgt, Y. E.; Wuhrer, M.; Dolhain, R. J. IgA N-and O-glycosylation profiling reveals no association with the pregnancy-related improvement in rheumatoid arthritis. *Arthritis research & therapy* **2017**, *19* (1), 1-8

(25) Plomp, R.; de Haan, N.; Bondt, A.; Murli, J.; Dotz, V.; Wuhrer, M. Comparative Glycomics of Immunoglobulin A and G From Saliva and Plasma Reveals Biomarker Potential. *Front Immunol* **2018**, *9*, 2436

(26) Bondt, A.; Nicolardi, S.; Jansen, B. C.; Stavenhagen, K.; Blank, D.; Kammeijer, G. S.; Kozak, R. P.; Fernandes, D. L.; Hensbergen, P. J.; Hazes, J. M.; van der Burgt, Y. E.; Dolhain, R. J.; Wuhrer, M. Longitudinal monitoring of immunoglobulin A glycosylation during pregnancy by simultaneous MALDI-FTICR-MS analysis of N- and O-glycopeptides. *Sci Rep* **2016**, *6*, 27955

(27) Gudelj, I.; Lauc, G.; Pezer, M. Immunoglobulin G glycosylation in aging and diseases. *Cellular Immunology* **2018**, *333*, 65-79

(28) Li, J.; Ji, L. Adjusting multiple testing in multilocus analyses using the eigenvalues of a correlation matrix. *Heredity* **2005**, *95* (3), 221-227

(29) Cohen, J. *Statistical power analysis for the behavioral sciences*; Academic press, **2013**.

(30) McFadden, D. Conditional logit analysis of qualitative choice behavior. **1973**,

(31) Kiryluk, K.; Li, Y.; Moldoveanu, Z.; Suzuki, H.; Reily, C.; Hou, P.; Xie, J.; Mladkova, N.; Prakash, S.; Fischman, C. GWAS for serum galactose-deficient IgA1 implicates critical genes of the O-glycosylation pathway. *PLoS genetics* **2017**, *13* (2), e1006609

(32) Ju, T.; Cummings, R. D. A unique molecular chaperone Cosmc required for activity of the mammalian core 1 β3-galactosyltransferase. *Proceedings of the national academy of sciences* **2002**, *99* (26), 16613-16618

(33) Allen, A.; Topham, P.; Harper, S.; Feehally, J. Leucocyte beta 1, 3 galactosyltransferase activity in IgA nephropathy. *Nephrology, dialysis, transplantation: official publication of the European Dialysis and Transplant Association-European Renal Association* **1997**, *12* (4), 701-706

(34) Suzuki, H.; Moldoveanu, Z.; Hall, S.; Brown, R.; Vu, H. L.; Novak, L.; Julian, B. A.; Tomana, M.; Wyatt, R. J.; Edberg, J. C. IgA1-secreting cell lines from patients with IgA nephropathy produce aberrantly glycosylated IgA1. *The Journal of clinical investigation* **2008**, *118* (2), 629-639

(35) Xing, Y.; Li, L.; Zhang, Y.; Wang, F.; He, D.; Liu, Y.; Jia, J.; Yan, T.; Lin, S. C1GALT1 expression is associated with galactosylation of IgA1 in peripheral B lymphocyte in immunoglobulin a nephropathy. *BMC nephrology* **2020**, *21*, 1-9

(36) Gale, D. P.; Molyneux, K.; Wimbury, D.; Higgins, P.; Levine, A. P.; Caplin, B.; Ferlin, A.; Yin, P.; Nelson, C. P.; Stanescu, H. Galactosylation of IgA1 is associated with common variation in C1GALT1. *Journal of the American Society of Nephrology: JASN* **2017**, *28* (7), 2158

(37) Wang, Y.-N.; Zhou, X.-J.; Chen, P.; Yu, G.-Z.; Zhang, X.; Hou, P.; Liu, L.-J.; Shi, S.-F.; Lv, J.-C.; Zhang, H. Interaction between GALNT12 and C1GALT1 associates with galactose-deficient IgA1 and IgA nephropathy. *Journal of the American Society of Nephrology: JASN* **2021**, *32* (3), 545

(38) Wang, C.; Ye, M.; Zhao, Q.; Xia, M.; Liu, D.; He, L.; Chen, G.; Peng, Y.; Liu, H. Loss of the Golgi matrix protein 130 cause aberrant IgA1 glycosylation in IgA nephropathy. *American Journal of Nephrology* **2019**, *49* (4), 307-316

(39) Hiki, Y.; Odani, H.; Takahashi, M.; Yasuda, Y.; Nishimoto, A.; Iwase, H.; Shinzato, T.; Kobayashi, Y.; Maeda, K. Mass spectrometry proves under-O-glycosylation of glomerular IgA1 in IgA nephropathy. *Kidney international* **2001**, *59* (3), 1077-1085

(40) Odani, H.; Hiki, Y.; Takahashi, M.; Nishimoto, A.; Yasuda, Y.; Iwase, H.; Shinzato, T.; Maeda, K. Direct evidence for decreased sialylation and galactosylation of human serum IgA1 Fc O-glycosylated hinge peptides in IgA nephropathy by mass spectrometry. *Biochem Bioph Res Co* **2000**, *271* (1), 268-274

(41) Suzuki, H.; Moldoveanu, Z.; Julian, B. A.; Wyatt, R. J.; Novak, J. Autoantibodies specific for galactose-deficient IgA1 in IgA vasculitis with nephritis. *Kidney international reports* **2019**, *4* (12), 1717-1724

(42) Liu, Y.; Wang, F.; Zhang, Y.; Jia, J.; Yan, T. ST6Gal1 is up-regulated and associated with aberrant IgA1 glycosylation in IgA nephropathy: An integrated analysis of the transcriptome. *Journal of Cellular and Molecular Medicine* **2020**, *24* (18), 10493-10500

(43) Baharaki, D.; Dueymes, M.; Perrichot, R.; Basset, C.; le Corre, R.; Cledes, J.; Youinou, P. Aberrant glycosylation of IgA from patients with IgA nephropathy. *Glycoconjugate J* **1996**, *13*, 505-511

(44) Knoppova, B.; Reily, C.; Maillard, N.; Rizk, D. V.; Moldoveanu, Z.; Mestecky, J.; Raska, M.; Renfrow, M. B.; Julian, B. A.; Novak, J. The origin and activities of IgA1-containing immune complexes in IgA nephropathy. *Frontiers in immunology* **2016**, *7*, 117

(45) Leung, J. C.; Tang, S. C.; Lam, M. F.; Chan, T. M.; Lai, K. N. Charge-dependent binding of polymeric IgA1 to human mesangial cells in IgA nephropathy. *Kidney international* **2001**, *59* (1), 277-285

(46) Lombana, T. N.; Rajan, S.; Zorn, J. A.; Mandikian, D.; Chen, E. C.; Estevez, A.; Yip, V.; Bravo, D. D.; Phung, W.; Farahi, F. Production, characterization, and in vivo half-life extension of polymeric IgA molecules in mice. In *MAbs*, 2019; Taylor & Francis: Vol. 11, pp 1122-1138.

(47) Oortwijn, B. D.; Roos, A.; Royle, L.; van Gijlswijk-Janssen, D. J.; Faber-Krol, M. C.; Eijgenraam, J.-W.; Dwek, R. A.; Daha, M. R.; Rudd, P. M.; van Kooten, C. Differential glycosylation of polymeric and monomeric IgA: a possible role in glomerular inflammation in IgA nephropathy. *Journal of the American Society of Nephrology* **2006**, *17* (12), 3529-3539

(48) Roos, A.; Bouwman, L. H.; van Gijlswijk-Janssen, D. J.; Faber-Krol, M. C.; Stahl, G. L.; Daha, M. R. Human IgA activates the complement system via the mannan-binding lectin pathway. *The Journal of Immunology* **2001**, *167* (5), 2861-2868

(49) Gao, Y.; Xu, L.; Zhang, J.; Zhang, Y.; Zhao, M.; Wang, H. Differential binding characteristics of native monomeric and polymeric immunoglobulin A1 (IgA1) on human mesangial cells and the influence of in vitro deglycosylation of IgA1 molecules. *Clinical & Experimental Immunology* **2007**, *148* (3), 507-514

(50) Li, M.; Foo, J.-N.; Wang, J.-Q.; Low, H.-Q.; Tang, X.-Q.; Toh, K.-Y.; Yin, P.-R.; Khor, C.-C.; Goh, Y.-F.; Irwan, I. D. Identification of new susceptibility loci for IgA nephropathy in Han Chinese. *Nature communications* **2015**, *6* (1), 7270

(51) Barrios, C.; Zierer, J.; Gudelj, I.; Štambuk, J.; Ugrina, I.; Rodríguez, E.; Soler, M. J.; Pavić, T.; Šimurina, M.; Keser, T. Glycosylation profile of IgG in moderate kidney dysfunction. *Journal of the American Society of Nephrology: JASN* **2016**, *27* (3), 933

(52) Bermingham, M. L.; Colombo, M.; McGurnaghan, S. J.; Blackbourn, L. A.; Vučković, F.; Pučić Baković, M.; Trbojević-Akmačić, I.; Lauc, G.; Agakov, F.; Agakova, A. S. N-glycan profile and kidney disease in type 1 diabetes. *Diabetes Care* **2018**, *41* (1), 79-87

(53) Barrios, C.; Zierer, J.; Gudelj, I.; Štambuk, J.; Ugrina, I.; Rodríguez, E.; Soler, M. J.; Pavić, T.; Šimurina, M.; Keser, T.; Pučić-Baković, M.; Mangino, M.; Pascual, J.; Spector, T. D.; Lauc, G.; Menni, C. Glycosylation Profile of IgG in Moderate Kidney Dysfunction. *Journal of the American Society of Nephrology : JASN* **2016**, *27* (3), 933-941

(54) Clerc, F.; Reiding, K. R.; Jansen, B. C.; Kammeijer, G. S.; Bondt, A.; Wuhrer, M. Human plasma protein N-glycosylation. *Glycoconj J* **2016**, *33* (3), 309-343

(55) Ceroni, A.; Maass, K.; Geyer, H.; Geyer, R.; Dell, A.; Haslam, S. M. GlycoWorkbench: A Tool for the Computer-Assisted Annotation of Mass Spectra of Glycans. *Journal of proteome research* **2008**, *7* (4), 1650-1659

Chapter 5

IgA Glycosylation Differs Between Crohn's Disease And Ulcerative Colitis

Immunoglobulin A Glycosylation Differs Between Crohn's Disease And Ulcerative Colitis

Florent Clerc[1], Karli R. Reiding[1,2,3], Noortje de Haan[1], Carolien A. M. Koeleman[1], Agnes L. Hipgrave Ederveen[1], Natalia Manetti[4,5], IBD-BIOM consortium, Viktoria Dotz[1#], Vito Annese[4,6,7], Manfred Wuhrer[1*]

[1]*Center for Proteomics and Metabolomics, Leiden University Medical Center (LUMC), Postbus 9600, 2300 RC Leiden, The Netherlands*

[2]*Biomolecular Mass Spectrometry and Proteomics, Bijvoet Center for Biomolecular Research and Utrecht Institute for Pharmaceutical Sciences, University of Utrecht, Padualaan 8, 3584 CH Utrecht, The Netherlands*

[3]*Netherlands Proteomics Center, Padualaan 8, 3584 CH Utrecht, The Netherlands.*

[4]*Unit of Gastroenterology SOD2 (Strutture Organizzative Dipartimentali), Azienda Ospedaliero Universitaria (AOU) Careggi, Florence, Italy.*

[5]*Gastroenterology Unit, San Jacopo Hospital, Pistoia, Italy*

[6]*Unit of Gastroenterology, IRCCS (Istituto di Ricovero e Cura a Carattere Scientifico–Casa Sollievo della Sofferenza) Hospital, San Giovanni Rotondo, Italy.*

[7]*Vita-Salute San Raffaele University Faculty of Medicine and Surgery, Milano, Italy7IRCCS Policlinico San Danato, San Donato Milanese, Italy*

#Current address: BioTherapeutics Analytical Development, Janssen Biologics BV, Einsteinweg 101, 2333 CB Leiden, The Netherlands

*Corresponding Author

e-mail: m.wuhrer@lumc.nl, Phone: +31-71-5266989.

Published in Journal of Proteome Research, 2023, 22 (10), 3213-3224.

DOI: 10.1021/acs.jproteome.3c00260.

Abstract

Inflammatory bowel diseases (IBD), such as Crohn's disease (CD) and ulcerative colitis (UC) are chronic and relapsing inflammations of the digestive tract with increasing prevalence, yet unknown origins or cure. CD and UC have similar symptoms but respond differently to surgery and medication. Current diagnostic tools often involve invasive procedures, while laboratory markers for patient stratification are lacking. Large glycomic studies of immunoglobulin G and total plasma glycosylation have shown biomarker potential in IBD and could help determine disease mechanisms and therapeutic treatment choice. Hitherto, the glycosylation signatures of plasma immunoglobulin A, an important immunoglobulin secreted into the intestinal mucin, have remained undetermined in the context of IBD.

Our study investigated the associations of immunoglobulin A1 and A2 glycosylation with IBD in 442 IBD cases (188 CD and 254 UC) and 120 healthy controls by reverse-phase liquid chromatography electrospray-ionization mass spectrometry of tryptic glycopeptides. Differences of IgA *O*- and *N*-glycosylation (including galactosylation, bisection, sialylation and antennarity) between patients groups were associated with the diseases and these findings led to the construction of a statistical model to predict the disease group of the patients without the need of invasive procedures. This study expands the current knowledge about CD and UC and could help the development of noninvasive biomarkers and better patient care.

Keywords: Inflammatory bowel disease, Crohn's Disease, ulceratives colitis, IgA1, glycosylation, biomarker

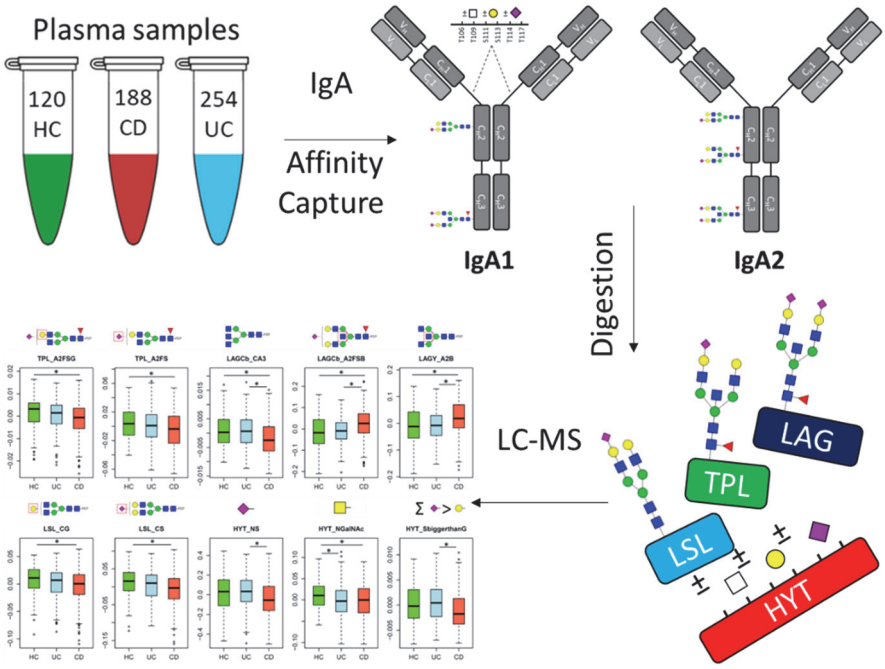
Plasma samples
120
HC
188
CD
254
UC
IgA
Affinity
Capture
IgA1
IgA2
Digestion
LC-MS
LAG
TPL
LSL
HYT

Introduction

Interest in large glycomics studies is rapidly increasing and associations of plasma protein glycosylation with disease have been demonstrated for cancers, autoimmune diseases and inflammatory bowel disease (IBD)[1-5].

IBD, comprising Crohn's disease (CD) and ulcerative colitis (UC) are lifelong, chronic and include relapsing inflammatory conditions of the digestive tract with yet unknown etiology [6]. CD and UC have similar symptoms but respond differently to medication and surgical treatments and the distinction between the two often requires invasive procedures which might include intestinal tissue sampling [7]. Early and non-invasive patient stratification from readily available body fluids is needed to best target therapy.

Immunoglobulin G (IgG) is of particular interest as an inflammatory marker in IBD because it is widely involved in autoimmunity. Having established the biomarker potential of the IgG glycosylation and total plasma *N*-glycome (TPNG) in IBD, IgA1 seemed to be an ideal additional candidate to receive attention due to its presence in mucosal fluids of the intestinal tract and its established role in immunological responses and mucosal protection against microorganisms such as bacteria and viruses. The latter happens by binding or agglutinating them, thus promoting clearance and preventing infections and inflammations[3, 4, 8-12]. However, the function of IgA glycosylation in health and disease is still an active area of research.

The *O*- and *N*-glycosylation of IgA1 and IgA2 have previously been monitored for 29 women during pregnancy and in the post-partum period using matrix-assisted laser desorption/ionization-Fourier-transform ion-cyclotron resonance (MALDI-FTICR)[13]. The same MALDI-FTICR method has again been used for the analysis of plasma IgA from 284 individuals comprising both rheumatoid arthritis (RA) patients and controls[14]. However, the complex and technically challenging sample handling used in these studies is an obstacle in large-scale clinical studies. Recently, an alternative LC-MS(/MS) approach with reduced benchwork sample preparation and a more streamlined workflow has been successfully applied to analyze IgA glycopeptides in a cohort of IgA nephropathy patients and healthy controls[15]. The same method was selected for this research.

Next to its important functions in intestine immunity, IgA was also implicated as potential target glycoprotein based on previous TPNG analysis. Specifically, the IgA glycans expectedly contribute to a large extent to specific plasma glycoforms affected by IBD, including elevated bisection levels of the diantennary fucosylated sialylated glycans[4, 16]. IgA1 and IgA2 glycoforms have previously been associated with CD, UC and IgA nephropathy (IgAN) where the general glycan size was reduced

(lower levels of sialylation, galactosylation and antennarity of *N*-glycans, and reduced sialylation and galactosylation of *O*-glycans) as well as with secondary IgA nephropathy where nephropathy follows CD, indicating the potential involvement of IgA in these diseases[15, 17-21]. Small-scale studies have also demonstrated changes in the *O*-glycosylation traits of IgA such as reduced levels of GalNAc in IBD[22, 23]. Still, the overall role of IgA glycosylation in disease remains largely unclear. It is mostly unexplored to which extent IgA glycosylation affects FcαR receptor binding triggering pro- or anti-inflammatory responses, or clearance from the circulation by the asialoglycoprotein receptor[16, 24, 25].

In this study, the IgA glycosylation profiles of 442 IBD patients and 120 healthy controls were analyzed by LC-MS/MS with glycosylation site-specificity. The main goal was to find associations between IgA glycosylation and IBD characteristics to discriminate CD, UC and HC, and subsequently, in a secondary analysis, to find associations with disease behavior, and surgical and medical treatments, for improved patient care.

Materials and methods

Clinical samples

The plasma samples used for this analysis were received from the University Hospital Careggi (Florence, Italy) and consisted of 442 IBD cases (188 CD and 254 UC) and 120 healthy controls (HC) as previously described[4, 26]. Written informed consent was obtained from the study participants and the ethical approval was obtained from the Ethics Review Board of the Casa Sollievo della Sofferenza Hospital (Italy). The clinical information of CD and UC patients was collected following the rules of the Montreal classification of inflammatory bowel disease[27]. The demographics of the individuals included in the statistical analysis are detailed in **Table 1**.

Table 1: Demographics of the individuals included for statistical analysis.

Sample numbers	HC	CD	UC
Total (males)	120 (72)	188 (110)	254 (159)
Age, mean ± SD			
Males	48.6 ± 16.1	36.0 ± 13.6	42.2 ± 16.1
Females	60.0 ± 17.8	37.3 ± 15.6	42.1 ± 16.7
All	53.2 ± 17.7	36.5 ± 14.4	42.1 ± 16.3
Patient information			
Disease group (counts (males))		CD	UC
Disease Location (CD)			
Illeum±UpperGI* (L1±L4)		65 (39) ± 1 (1)	
Colon±UpperGI (L2±L4)		67 (44) ± 6 (4)	
Illeum+Colon±UpperGI (L3±L4)		47 (20) ± 1 (1)	
Upper GI (L4)		8 (6)	
Disease Location (UC)			
Rectum (E1)			29 (15)
Sigmoid + Left colon (E2)			127 (79)
Entire colon (E3)			93 (61)
Disease behaviour (CD)			
Inflammatory (B1)		106 (64)	
Stenosing (B2)		55 (27)	
Fistulizing (B3)		26 (18)	
Surgery			
No		127 (74)	243 (151)
Before sample collection		49 (28)	8 (5)
After sample collection		8 (5)	2 (2)
Drugs			
Mesalazine		38 (19)	75 (46)
Steroids		42 (25)	79 (49)
Azathioprine/6-mercaptopurine		43 (26)	58 (38)
Anti-TNFα		51 (31)	22 (14)

*GI = Gastro-Intestinal (tract)

Glycoproteomics analysis

Capture of IgA

IgA1 and IgA2 were captured from five µL of plasma (containing approx. 350 µg total protein and 13µg IgA) with camelid antibodies domains immobilized on agarose beads (CaptureSelect IgA Affinity Matrix, Thermo Fisher Scientific, Waltham, MA) as previously described[13]. Ten µL of bead slurry were pipetted into each well of a 96-well Orochem filter plate (AcroPrep, Pall Corporation, Ann Arbor, MI, USA). The beads were washed three times with 200 µL ultrapure water (prepared at 18.2 MΩ with a Purelab Ultra, Veolia Water Technologies Netherlands B.V., Ede, The Netherlands). and three times with PBS 1x solution on vacuum manifold. Five µL of sample were added to 100 µL of PBS in each well and incubated with shaking for one hour at room temperature (RT). The beads were washed on vacuum manifold with 3x200 µL PBS 1x and three times 200 µL water. The captured IgA was released from the beads with 100 µL of 100 mM formic acid, eluted in PP V-bottom plates by centrifugation (1 min, 100 *g*), and dried at 50 °C in a vacuum centrifuge.

Trypsin digestion

The samples were reconstituted in 100 µL 20 mM ammonium bicarbonate buffer and reduced with 2 µL dithiothreitol (DTT) 125 mM for 30 min at 60 °C. 4µL of 125 mM of iodoacetamide (IAA) was added for alkylation and the samples incubated with shaking for 30 min at RT wrapped in aluminum foil. The alkylation was quenched by adding 2 µL 100 mM DTT. The digestion was performed overnight at 37 °C with 210 ng of TPCK-treated trypsin and the samples were frozen at -20°C until measurement.

RP-LC-ESI-MS(/MS)

Reverse-phase liquid chromatography electrospray-ionization mass spectrometry (RP-LC-ESI-MS) experiments were performed with an Ultimate 3000 RSLCnano system (Thermo Fisher Scientific) fitted with a Pepmap100 C18, 5 µm 0.3x5 mm precolumn and a custom-made Acquity BEH130 C18 75 um x 100 mm UPLC M-Class analytical column. This was coupled to a Maxis Impact HD quadrupole-time-of-flight (qTOF) mass spectrometer fitted with a captive spray nanoBooster (Capillary voltage: 1200V; nanoBooster pressure 0.2 bar; dry gas flow: 3.0 L/min; dry gas temperature: 180 °C) (Bruker Daltonics, Bremen, Germany). One µL of digested sample was injected, with a flow rate of 500 µL/min, eluted with the following gradient: 3% solvent B at 0 min, 30% B at 6.5 min, 95% B at 10 min, hold for two min, back to 3% B at 13 min, hold for eight min. Solvent A consisted of 0.1% TFA (v/v), solvent B of 95% ACN (v/v)). Mass spectra were recorded from 550 to 1800 Th with a frequency of 1 Hz.

To confirm the structures of certain analytes, high-resolution fragmentation spectra of selected glycopeptides were recorded on a different instrument. The material used for the MS/MS glycopeptide identification was a pooled sample of captured IgA taken from the first 96-well plate of the prepared samples including material from HC, CD, UC and control plasma (VisuconF, Affinity Biologicals, Canada). For this, a nanoLC (Thermo Fisher Scientific) was equipped with an Acclaim PepMap 100 trap column (100 µm × 20 mm, particle size 5 µm, Thermo Fisher Scientific) and an Acclaim PepMap RSLC C18 nano-column (75 µm × 150 mm, particle size 2 µm, Thermo Fisher Scientific). The separation gradient started from 97% solvent A (0.1% formic acid in water) and 3% solvent B (95% ACN) to 53% solvent B over 30 min, with a flow rate of 700 nL/min. The system was coupled to a maXis quadrupole time-of-flight-MS (q-TOF-MS; Bruker Daltonics) equipped with a nanoBooster (Bruker Daltonics). Ionization was enhanced by applying acetonitrile-enriched gas at 0.2 bar used as a dopant. The source parameters were set to a flow of nitrogen drying gas of 3.0 L/min at 180°C and a capillary voltage of 1200 V. The MS was operated in stepping-energy CID mode and acquired from m/z 50-2800 with the precursor selection above m/z value 680 as previously described[28].

Data processing

Raw LC-MS data were converted to mzXML with MSConvert. LacyTools[29] was used to align the retention time, calibrate the mass spectra, define time windows around each glycopeptide cluster extraction and for the integration of the sum spectra for a list of analytes determined by manual exploration of the data of each disease group using sum spectra and theoretical glycosylation sites based on the peptide sequence (Uniprot # P01876 for IgA1 and P01877 for IgA2). For time alignment, the most abundant glycopeptide of each cluster was used (search windows of 20 s) and the maximum mass error of the highest isotope ±0.15 Th. A time window of ± 8 s per cluster (10 s for the *O*-glycopeptide) was summed, and each extracted glycoform was reported as relative percentage per cluster. The optimal time windows for analyte extraction were determined for each cluster by monitoring the elution profile and retention time of all extracted analytes per glycopeptide cluster. The average retention time of the cluster was then calculated and the sum windows fixed to include all analytes. The extracted glycopeptide data was curated on average signal-to-noise ratio threshold >9, absolute error on exact mass <20 ppm, and deviation compared to the calculated isotopic pattern <0.2. This curation was applied for all detected charge states. Per sample, the data was kept when not more than one peptide cluster was rejected due to low-abundance of analytes. A final list of 51 glycopeptides was retained (26 *N*-linked and 25 *O*-linked glycopeptides (**Supplementary table 1, Supplementary table 2**) and from these, 45 derived traits were calculated (**Supplementary table 3**).

The identity of glycopeptides was verified by MS/MS using Byonic. The search parameters included the protein sequences of secreted IgA1 (P01876-1) and IgA2 (P01877-1) from Uniprot in FASTA format, cysteine alkylation as fixed peptide modification, two possible missed cleavages, and a semi-specific (N-ragged) digestion specificity. Furthermore, a list of 318 *N*-glycan compositions and 9 *O*-glycan compositions was included based on IgA glycoforms previously identified (based on monosaccharides HexNAc, Hex, Fuc, NeuAc and NeuGc)[15, 30, 31]. The precursor mass tolerance was set at 10 ppm, the fragment mass tolerance at 30 ppm. The results of the Byonic search were filtered based on the identification score (Pep2D) to be below 0.001, manually expected (at least one glycoform per peptide portion) and are reported in **Supplementary table 2** and **Supplementary Figure 1-4**. The identity of the IgA glycoforms that were not reported by Byonic were deduced by exact mass differences in the high-resolution MS1 data, including retention time and isotope pattern matching (**Supplementary Figures 5-9**).

Statistical analysis

The associations of the IgA glycopeptides and calculated derived traits with CD, UC, and IBD-specific clinical traits, *i.e.*, extent of the disease, drug intake and surgical intervention, were tested as previously described in the software R studio for R (Version 1.0.136)[4]. In short, the data was batch corrected (on logarithmically transformed data) to account for the different preparation days, position on row and column of the randomized samples on the 96-well plates. Associations with age and sex were determined in the three patient groups with linear and logistic regressions, included further as covariates in the logistic regression model. The associations of the IgA glycosylation with age, sex, Crohn's disease, ulcerative colitis and IBD-related parameters such as disease location, surgery and medication, were tested by linear and logistic regression on scaled data (subtraction of the mean and division by the SD). Age, sex and their interaction were included as covariates in the models for the disease-related tests. The odds ratios (OR) were calculated with their 95% confidence intervals (CI) assuming a Student's t-distribution, and are thus representative of single standard deviation increases in the tested traits.

For the receiver operating characteristic (ROC) analysis, the glycopeptides most significantly associated with IBD (*p*-values and effect sizes) were selected for the initial model. The ones found to not significantly contribute to the model were removed step-by-step considering similarities of derived traits (which can share effects in the model and lower their individual significance while only reflect a single biological trait) and percentage of effect on the prediction until only significant traits were left, thus achieving maximal prediction power with only the necessary selection of traits. The model was trained 20 times on a random selection of 75% of the

samples and the prediction was calculated for the respective 25% remaining. The standard error (SE) was also calculated for all predictions.

The Montreal classification of inflammatory bowel disease was followed to categorize disease localization, extent and behavior for CD and UC patients[27]. The different localization and extent of the disease were compared in CD patients affected either in the ileum (L1), the colon (L2), or both the ileocolon (L3) and in the upper gastro-intestinal (GI) tract (L4) (L1 *vs* L2 *vs* L3+L4). Association with disease behavior was tested by comparing the inflammatory (B1), the stenosing (B2), and the fistulizing variant (B3) (B1 *vs* B2 *vs* B3). In UC, the patients groups affected in the rectum + sigmoid + left colon (E1+E2) were compared to the ones affected in the entire colon (E3), (E1+E2 *vs* E3). The hypothesis tested here is that a more extensive or aggressive disease behavior would associate with more extreme glycosylation profiles compared to HC.

We also tested for association of profiles with surgery and medication. According to the guidelines of the respective countries to treat IBD diseases, patients were given mesalazine, steroids, azathioprine/6-mercaptopurine or anti-TNFα. Patients were stratified according to escalation of drug class used at the time of sample collection according to the practices of the medical center and the glycosylation profiles respective to each drug class were compared to each other[32, 33]. The hypothesis tested here is that patients suffering from more severe disease exhibit more extreme IgA glycosylation profiles and these patients can be identified based on their need to use more potent drugs. The groups of patients not requiring surgery were opposed to those who received surgery after sample collection, again using surgical intervention as a proxy for disease severity. Moreover, we compared the profiles of patients who received surgery before or after sample collection to evaluate the treatment effect.

The commonly accepted significance threshold of $\alpha = 0.05$ was adjusted for multiple testing with a Bonferroni correction when evaluating the associations with age, sex, CD and UC. As the relative intensities of the glycopeptide signals are intimately related, the number of tests performed on the derived traits was used as correction factor.

Results

Following site-specific IgA1/IgA2 glycosylation analysis by LC-MS/MS, a total of six *N*-linked glycoforms was characterized on Asn_{144}, eight on Asn_{205}, seven on Asn_{340}, five on the two different clusters of the truncated peptide containing Asn_{340}, and 25 *O*-linked glycoforms on the peptide portion containing $Ser_{89\text{-}126}$ (**Figure 1**, **Figure 2)**. Some glycopeptides similar to those found on Asn_{340} of IgA1 were observed on Asn_{327} of IgA2 (10x less abundant than IgA1) during the manual exploration of the data but the list of potential analytes did not pass the curation step during data extraction due to a low S/N ratio, also impacting their isotopic pattern match compared to the calculated pattern so they were rejected from the statistical analysis. No confident identifications for the IgA2 glycopeptides covering Asn_{327} were found starting with amino acids MAG instead of LAG (IgA2 isoform #P01877-1) in the Byonic workflow. No glycopeptides passing our quality criteria were observed for the theoretical glycosylation site of Asn_{47} of IgA2 nor for Asn_{92} of the low abundant allotype A2M of IgA2. Trace amounts of the what could be VFP glycopeptide (Asn_{47}) fragments with a different cleavage at the *N*-terminal of its sequence (SES) were detected, but not further evaluated due to their low abundance. For clarity of the discussion, the peptides will be referred to by the one-letter codes of the first three amino acids (and last for the peptides with a truncated variant); amino acid sequences are shown in **Figure 2**.

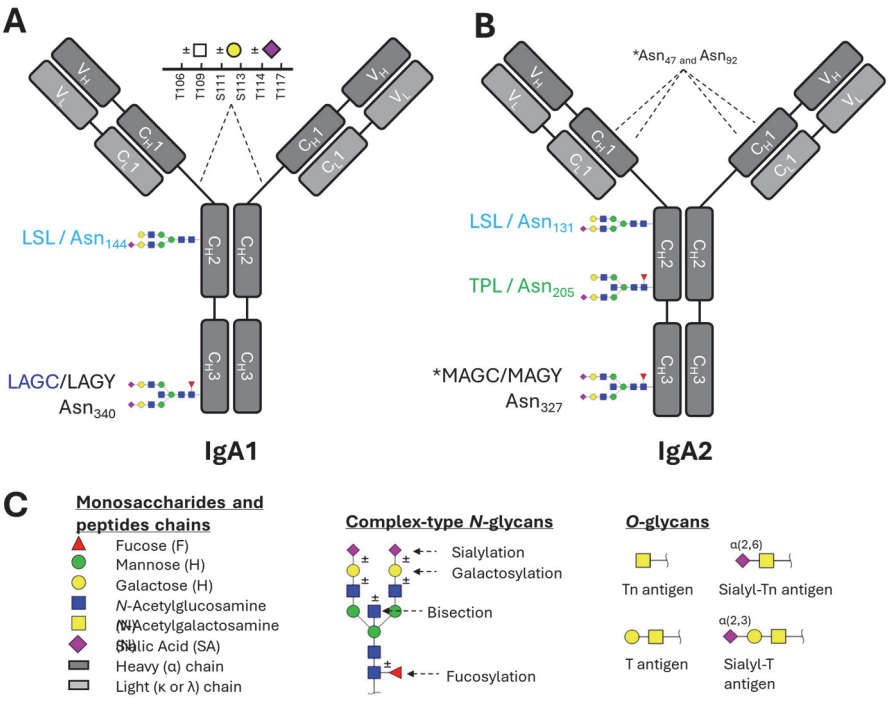

Figure 1: Symbolic representation of IgA1 and IgA2 glycosylation. *The acronyms HYT, LSL, TPL, LAG(C/Y) and MAG(C/Y), which are referring to the different glycopeptides, come from the first three amino acids of the corresponding tryptic digest sequence of IgA1 and IgA2. A) IgA1 has two N-glycosylation sites at Asn_{144} and Asn_{340} which are occupied by complex-type N-glycans. IgA1 also contains six O-glycosylation sites in the hinge region at Thr_{106}, Thr_{109}, Ser_{111}, Ser_{113}, Thr_{114} and Thr_{117}. The O-glycosylation of IgA1 is represented as one combined monosaccharide composition, as no information on specific glycan structures and attachment sites was obtained. B) The observed glycosylation sites of IgA2 at Asn_{131}, Asn_{205} and Asn_{327} are occupied with complex-type N-glycans. * The IgA2 glycosylation sites Asn_{47} and Asn_{92} and Asn_{327} did not pass quality curation criteria due the low intensity of analytes. C) Symbols used for representing the glycans and their general antennary structure (N-linked glycans) and example structures for the O-linked glycans.*

A)

IgA Type	Glycosylation site	Peptide name	Observed glycoforms	Peptide sequence
IgA1/2	Asn144 / Asn131	LSL	6	LSLHRPALEDLLLGSEANLTCTLTGLR
IgA2	Asn205	TPL	8	TPLTANITK
IgA1	Asn340	LAGY	7	LAGKPTHVNVSVVMAEVDGTCY
IgA1	Asn340-Y	LAGCa/b	5	LAGKPTHVNVSVVMAEVDGTC
IgA1	Ser89-126	HYT	25	HYTNPSQDVTVPCPVPSTPPTPSPSTPPTPSPSCCHPR
IgA2	Asn327	MAGY	Failed data curation	MAGKPTHVNVSVVMAEVDGTCY
IgA2	Asn47	VFP	Not observed	VFPLSLDSTPQDGNVVVACLVQGFFPQEPLSVTWSESGQNVTAR
IgA2 allotype A2M(2)	Asn92	HYT-2a	Not observed	HYTNSSQDVTVPCRVPPPPPCCHPR

B)

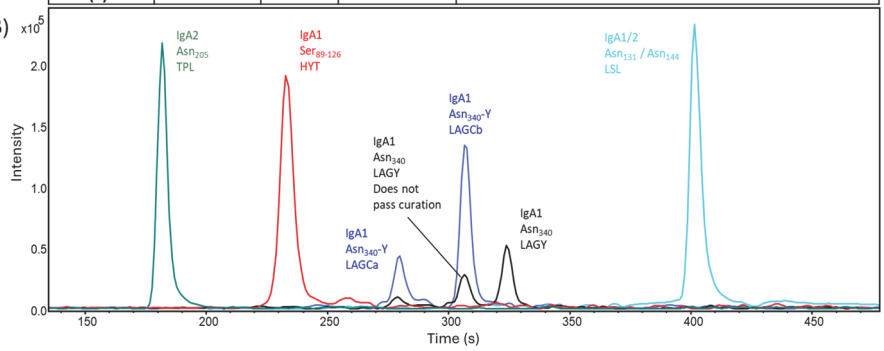

Figure 2: Description of the glycopeptide clusters. *A) IgA1 and IgA2 glycopeptides overview. Glycosylation sites, short peptide name, number of extracted glycoforms, and peptide sequence are given for each glycopeptide cluster. B) Extracted Ion Chromatograms (EIC) of one selected glycopeptide per cluster with representative retention time of the whole glycopeptide cluster.*

The identification of the glycoforms of the different detected peptides is depicted in **Figure 3**, **Figure 4** and in the **supplementary figures 1-9**. The peptide portion was annotated based on MS/MS data of high abundant parent ions as shown in ***the supplementary material***. The supplementary material is available at https://pubs.acs.org/doi/10.1021/acs.jproteome.3c00260.

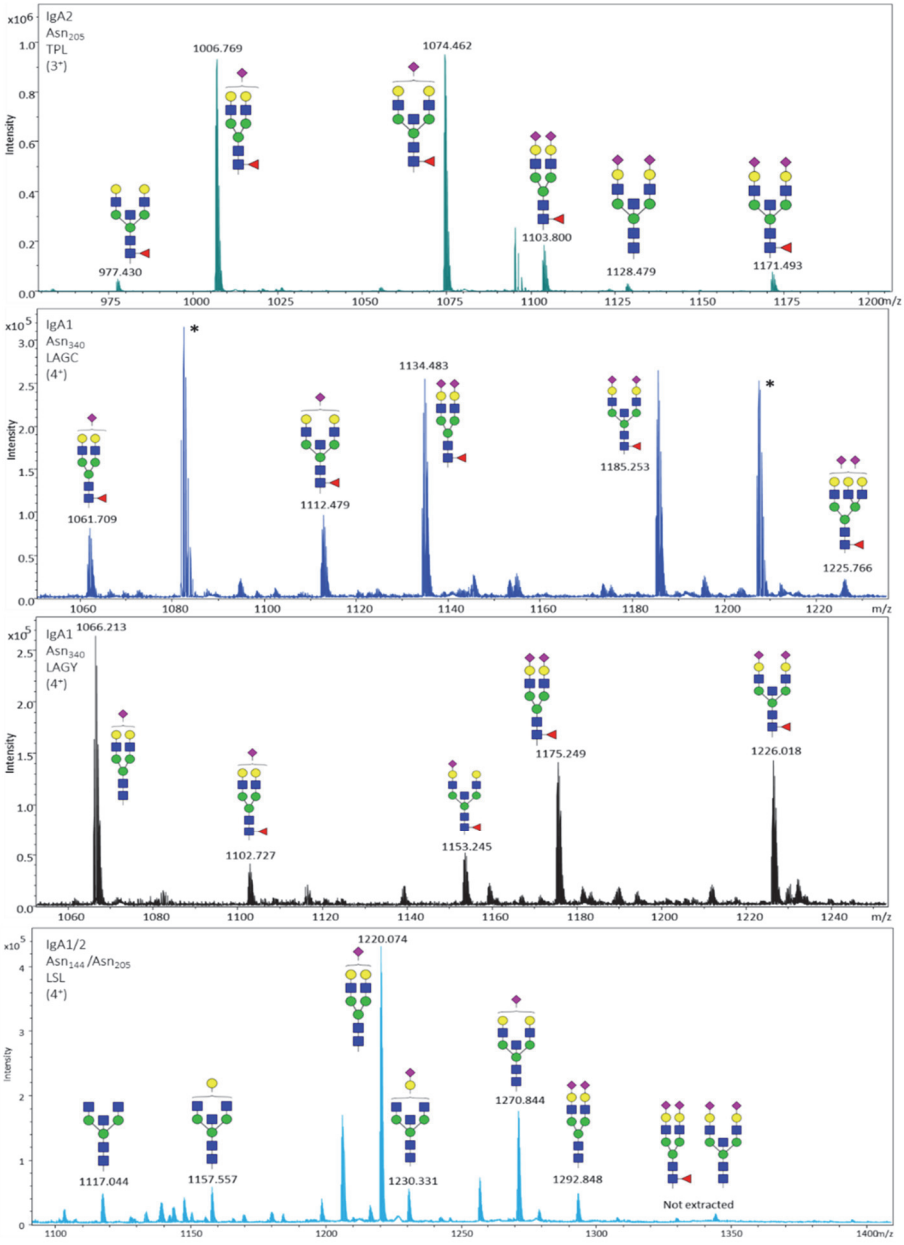

Figure 3: Assignment of the major *N*-glycoforms of IgA1 and IgA2. *A) Peptide cluster TPL at Asn_{205} of IgA2, zoom-in off the 3+ charged glycopeptides. B) Truncated peptide cluster LAGC at Asn_{340} of IgA1, zoom-in off the 4+ charged glycopeptides. The two peaks marked with an asterisk are residues from another peptide without glycan eluting at the same time and in charge state 2+. C) Peptide cluster LAGY at Asn_{340} of*

IgA1, zoom-in of the 4+ charged glycopeptides. D) Peptide cluster LSL at Asn_{144}/Asn_{205} of IgA1 and IgA2 and zoom-in of the 4+ charged glycopeptides. All the glycoforms are described in ***the supplementary material.***

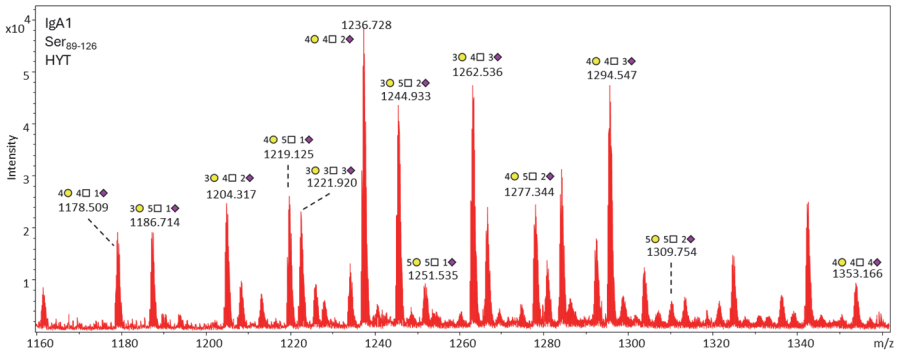

Figure 4: Assignment of O-glycoforms of peptide cluster HYT. *Assignment of O-glycoforms of peptide cluster HYT at Ser_{89-126} of IgA1 and zoom-in of the 5^+ charged glycopeptides. The pictograms represent the combined O-glycopeptide monosaccharide composition from all sites and does not convey information on specific glycan structures of attachment sites. Overall, the glycopeptides covered a wide range of compositions ($H_{3-5}N_{3-6}S_{1-5}$) containing up to 6N. Not all glycoforms are labeled on the figure as the complete list of the 25 IgA1 hinge region O-glycopeptide species identified and quantified is reported in* ***the supplementary material.***

IgA glycosylation is associated with age and sex in healthy controls and IBD patients

In HC, CD and UC, an increase of bisection, a decrease of galactosylation and sialylation per galactose were observed with age on all *N*-glycosylation sites (TPL, LAGY and the truncated LAGC glycopeptides) as reported in **Supplementary table 4**. A decrease of antennarity was observed in the glycans of the TPL peptide of HC and on the glycans of the LAGY peptide of HC and UC patients. No association between the *O*-glycans of the HYT peptide and age was found significant after correction for multiple testing.

The *N*-glycosylation of IgA was associated with sex, where a decrease of antennarity was observed on the TPL peptide in CD and UC males compared to the females **Supplementary table 4**. UC males had lower bisection levels than the females in all the *N*-glycopeptides clusters.

IgA glycosylation is associated with inflammatory bowel disease

Compared to HC, CD patients were found to have lower galactosylation and lower sialylation on LSL (Asn_{144})and TPL (Asn_{205})(**Figure 5** and **Supplementary table 5**). CD patients also showed lower levels of antennarity (lower CA3) and higher bisection on Asn_{340} and its truncated versions compared to HC and UC. CD and UC patients had a smaller amount of GalNAc on the *O*-glycans of the $Ser_{89\text{-}126}$-containing peptide than HC. In addition, the CD group was found to have a lower relative abundance of SA and lower ratio of SA per galactose in the *O*-linked glycans than in UC.

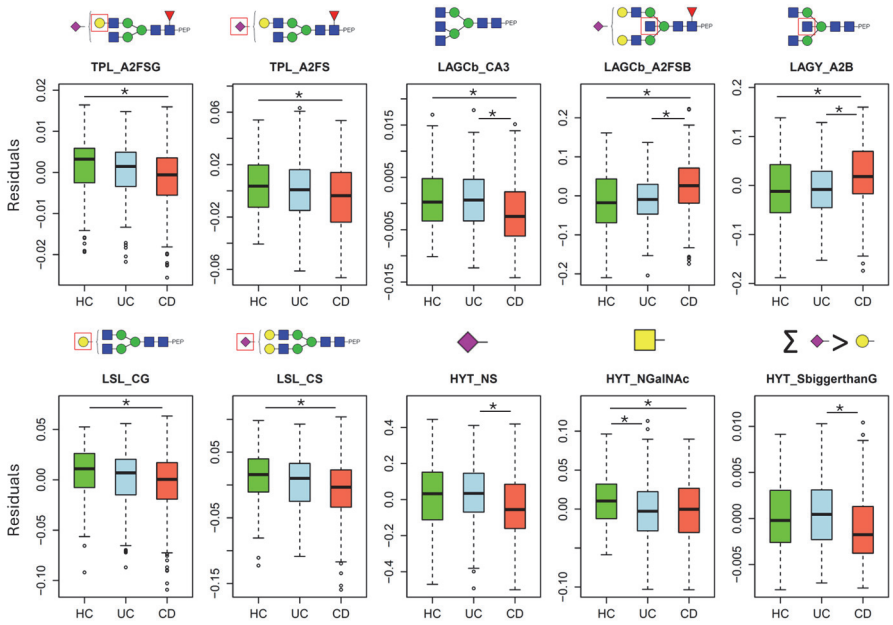

Figure 5: Main associations between IgA glycosylation derived traits and IBD per patient groups (HC = healthy controls, UC = ulcerative colitis, CD = Crohn's disease). *The derived traits were corrected age, sex and age*sex and are shown in boxplots. The 25th, 50th and 75th percentiles are represented in the boxes and the whiskers are at the 1st quartile – 1.5 * IQR (inter-quartile range) and at the 3rd quartile + 1.5 * IQR. P-values, ORs and confidence intervals are reported in* ***Supplementary Table 4****. Statistically significant associations (multiple testing corrected threshold* $3.70 \cdot 10^{-4}$ *as described in the supplementary tables) are marked with an asterisk.*

The ROC curves (**Figure 6**) that were calculated with a linear model based on the glycopeptides most significantly associated with IBD included age, sex and their interaction with the bisection and triantennarity of LAGC (LAGCb_CB, LAGCb_CA3),

the bisection of sialylated diantennary LAGY glycopeptides (LAGY_A2SB) and the sum of *O*-glycopeptides featuring higher number of SAs than galactoses (HYT_S>G). The prediction power for CD *vs* HC was good with an AUC of 0.790 ± 0.045. The power of the model was fair for predicting UC *vs* HC with an area under the curve (AUC) of 0.641 ± 0.052 SE and also fair for UC *vs* CD with an AUC of 0.674 ± 0.035.

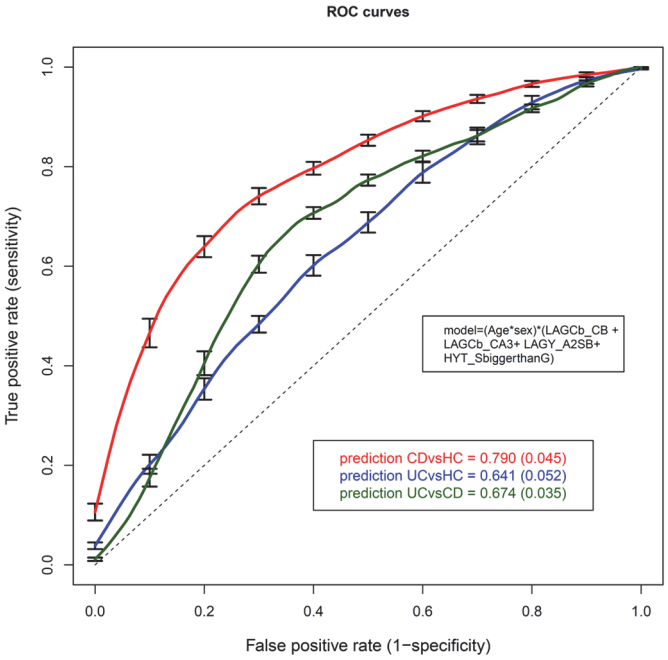

Figure 6: Receiver operating characteristic curves showing the power of selected glycans traits to predict CD and UC. *The mean and SE of 20 predictions are reported for the area under the curve. The prediction model included the interactions of age*sex *(LAGCb_CB + LAGCb_CA3 + LAGY_A2SB + HYT_S>G).*

Associations of IgA glycopeptides with CD and UC disease location and behavior were tested as previously described [3, 4] but no significant results were found in this study (**Supplementary table 6, Supplementary table 7 Supplementary table 8**). No significant associations were found between patients who received surgery *vs* non-surgery patients, and no associations were found in IgA glycosylation profiles of patients before and after surgery (**Supplementary table 9**).

When searching for associations of IgA glycosylation with the most potent drug administered to the patients, UC patients using AZT/6-MP were found to have lower galactosylation and lower sialylation of TPL and LSL peptides compared to UC mesalazine users (**Figure 7**).

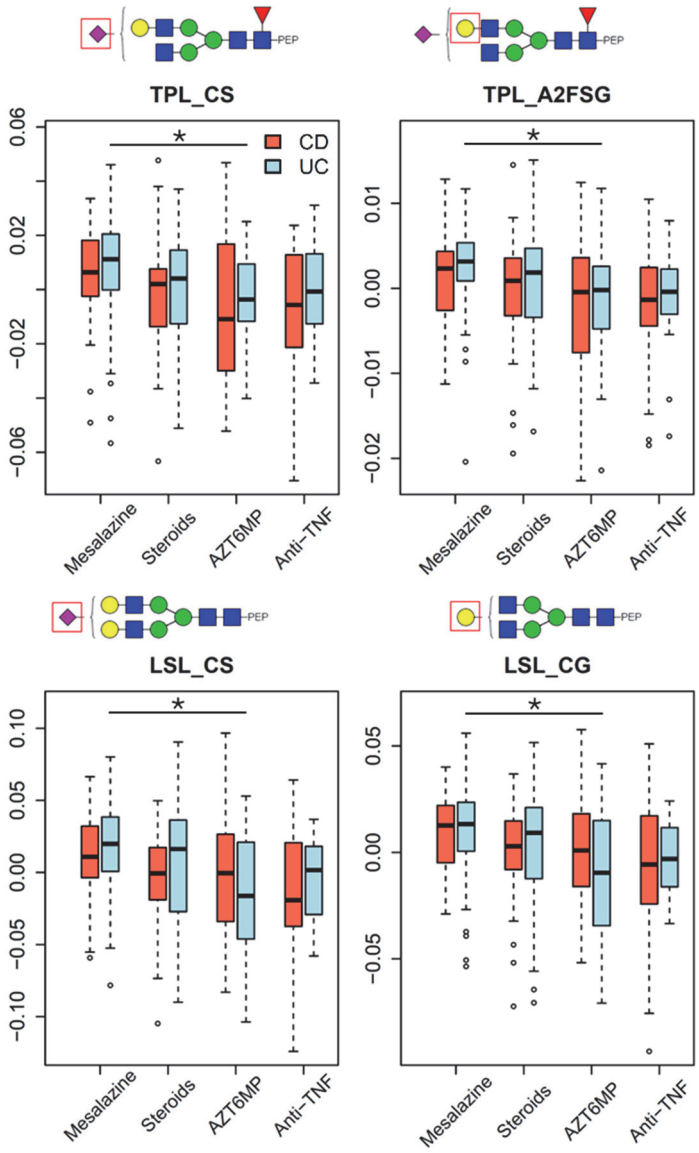

Figure 7: Main associations between IgA glycosylation derived traits and medication in CD and UC. *The derived traits were corrected age, sex and age*sex and are shown in boxplots. The 25th, 50th and 75th percentiles are represented in the boxes and the whiskers are at the 1st quartile – 1.5 * IQR (inter-quartile range) and at the 3rd quartile + 1.5 * IQR. P-values, ORs and confidence intervals are reported in* ***Supplementary Table 9****. Statistically significant associations (multiple testing corrected threshold 1.85·10-4 as described in the supplementary tables) are marked with an asterisk.*

Discussion

With our newly developed LC-MS/MS method, we could show that CD differed from HC in terms of IgA1 *O*-glycosylation as well as IgA1 and IgA2 *N*-glycosylation with regard to antennarity, bisection, galactosylation, and sialylation. In UC, mostly the *O*-glycosylation was altered compared to HC. Overall, for all associations of IgA glycosylation we found between IBD and HC, CD patients seemed to have the more extreme profile of inflammation-associated IgA glycosylation and UC is showing less extreme profiles, similarly to what has been found for the total plasma *N*-glycome and in an IgG-specific study [3, 4]. In the following, IgA glycosylation signatures of CD and UC will be discussed on the background of other cohort studies covering IgA glycosylation (**Figure 8**).

It is possible that with our analytical approach the changes in glycosylation observed in the IgA captured from serum reflects more global changes in glycosylation of immune system than what could be observed in localized tissue samples of the inflamed areas. However, sampling serum from patients is far less invasive than sampling tissue and is thus a more easily accessible biomarker specimen.

Antennarity and bisection

On the LAGY peptide comprising Asn_{340}, the glycosylation showed lower antennarity and elevated bisection in CD patients as compared to controls, parallel to what has been observed in other diseases such as RA and IgA nephropathy[14, 15]. In contrast, pregnancy has been found to be associated with lower bisection as well as with a concomitant improvement of the inflammation status in pregnant RA patients[34]. In other studies, a decrease of antennarity has been observed after delivery for both IgA and IgG[14, 34]. These two glycosylation traits were found to differ significantly between CD and UC, however, the functional role of these differences is not clear. These differences are also mainly IgA1 specific as IgA2 does not normally contain the LAGC/LAGY glycopeptide, but rather has a slightly different protein backbone MAGC/MAGY (in IgA2 isoform #P01877-1) that was not detected in our study. There could be an exception to this in the case of a rare mutation of the IgA2 Met_{319} which causes it to have to the same glycopeptide LAG as IgA1.

Galactosylation

In this study, a lower galactosylation in CD is reported on two glycosylation sites (TPL and LSL, **Supplementary table 1**), while a previous study reported no difference in IgA galactosylation in IBD *vs* HC[22]. This might be due to the increased performance of our newly developed analytical workflow enabling us to handle the larger number of cases analyzed here. Multiple studies have reported lower IgG galactosylation in

IBD patients and other diseases as non-specific inflammation marker and this appears to be in line with our findings for IgA, although with a less prominent effect size[3, 22, 35]. It is known that the clearance of IgA can be affected by its terminal *N*-glycosylation motifs and could thus be a factor of inflammation in IBD as well[36, 37]. The changes in galactosylation on TPL are IgA2-specific, while the changes observed on LSL are shared between IgA1 and IgA2 which could indicate a similar glycosylation mechanism for both sites and a more pronounced pro-inflammatory profile of IgA2[23].

Sialylation

The lower sialylation of *N*-glycans that was found on LSL and TPL glycopeptides of CD patients has also been found to be associated with other diseases such as IgA nephropathy and RA, and could be promoting the inflammation and, as discussed for galactosylation, could expose more galactose-terminated glycans and impact IgA clearance from the circulation[14, 15, 23]. The opposite effect has been observed during the late stage of pregnancy where elevated sialylation of LSL and LAGY/C glycopeptides were found before a return to normal levels post-delivery, suggesting an anti-inflammatory effect of higher sialylated *N*-glycans of IgA[13, 14].

O-Glycosylation

Overall, the *O*-glycopeptides covered a wide range of compositions ($H_{3-5}N_{3-6}S_{1-5}$) containing up to 6N e.g. H4N6S2 and H4N6S2, which is in accordance with literature data that indicates a variation in site occupancy from 3 to 6 sites with predominantly core 1 structures[31]. Our findings of lower number of GalNAcs on the IgA1 hinge-region *O*-glycopeptide of IBD patients are linked to increased disease activity and are in accordance with previous findings in IBD patients[22]. These results are also comparable to those found in IgA nephropathy and in RA (**Figure 8**)[22, 38-40]. The similarities of deficient *O*-glycosylation in IBD and other inflammatory diseases indicate a possible role in modulating IgA function which is however largely unexplored[41-45]. An exception to that would be the role of agalactosylated IgA1 hinge region *O*-glycans which has been reported to be a target of autoantibodies in IgA nephropathy[46].

Intervention and medication

The low number of significant associations found between IgA and treatments, whether surgical or medical, is most likely due to small effect size of the tested associations and the low statistical power possible in this study with the low number of patients in each category (Table 1) with the stringent Bonferroni correction with 270 tests performed (**Supplementary table 9**).

It is interesting to note that the significant traits of IgA glycosylation associated with medication found in this study are similar to what was previously reported with the analysis of the TPNG where lower galactosylation in UC patients was associated with the use of more potent drugs[4]. In a comparable study about IgAN, patients had lower levels of sialylation on the TPL and LSL glycopeptide compared to the controls[15]. Here, UC patients who were administered the more potent drugs similarly exhibited lower levels of sialylation on these two glycopeptide clusters.

Methodological considerations

While sialic acids usually have a strong effect on the retention time of glycopeptides in reverse-phase LC, as shown here for the MS2 identification data using a gradient containing formic acid, in our high resolution MS1 method used for the high-throughput measurements we optimized the LC conditions by adding TFA to the eluents to prevent this effect and to allow robust data processing as previously described[15, 47].

For the samples analyzed here, IgA concentration was not measured but it has previously been reported that IgA concentrations do not differ between IBD and HC[48]. The approach used for the sample preparation included an excess of immunoaffinity beads for capturing and total area normalization of the extracted glycans during data analysis enabled us to look at changes in the glycosylation profile of IgA without correction for IgA concentration.

The LC-MS method used here is not able to provide absolute quantitative results as no internal standard were included. However, when comparing different disease groups on the same analytes, it is possible to estimate if a cluster, *e.g.*, TPL (which is specific to IgA2), is elevated compared to the other groups. In this regard, as CD had a higher relative abundance of the TPL cluster (data not shown) compared to HC and UC, this could indicate that the ratio IgA1/IgA2 is decreased in CD, and that the difference in ratio could be associated with autoimmune diseases[23]. This could be further investigated by quantitative assays such as isotype-specific ELISAs or by adding isotopically labeled standards to the samples for MS analysis.

Similar studies

All the associations reported in this study were similarly reported for IgA and IgG in IBD, IgA nephropathy, and other autoimmune disease like RA, except for the sialylation of the *O*-glycans in RA and the bisection of IgG in CD *vs* HC (**Figure 8**)[3, 13-15, 22, 34, 38, 40, 45, 49]. The changes in IgA glycosylation with IBD were mostly opposite of the associations reported during pregnancy, similar to IgG where glycosylation

changes with inflammatory conditions were opposed to those occurring with pregnancy[13, 14, 34].

	Reference		This Study			Clerc 2021	Simurina 2018			Inoue 2012					Shinzaki 2013	Hiki 2001	Wada 2010		Bondt 2016	Bondt 2017		Bondt 2013		Field 1994	
	Immunoglobulin type (IgA / IgG)		IgA			IgA	IgG			IgG	IgA				IgG	IgA1	IgA		IgA	IgA		IgG		IgG	IgA
	IgA Type	Glycosylation site / Peptide	CD vs HC	UC vs HC	CD vs UC	IgAN vs HC	CD vs HC	UC vs HC	CD vs UC	IBD vs HC	CD vs HC	UC vs HC	CD vs UC	IgAN vs HC	CD vs HC	IgAN vs HC	IgAN vs HC	RA vs HC	Preg-nancy	Preg-nancy	RA	Preg-nancy	RA	RA	
N-glycosylation	IgA1 IgA2	Asn144 / Asn131 LSL	G↓ S↓	-	-	G↓ S↑ S/G↑ B↑	G↓ S↓ F↑ B↓	G↓ S↓ F↓ B↓	G↓ F↑ B↑	G↓	-			-	G↓	-	-	-	B↑ S↑	S↑ B↑	S↓ B↑	G↑ S↑ B↓ F↓	G↓ S↓ F↑	G↓	-
	IgA2	Asn205 TPL	G↓ S↓	-	-	G↓ S↓													-	-	-				
	IgA1	Asn340 LAGY	A↓ B↑	-	A↓ B↑	A↓													B↑ F↓ A↑	S↑ F↓ A↑	B↑				
	IgA1	Asn340-Y LAGC	A↓ B↑	-	A↓ B↑	A↓ F↑													B↑ F↓ A↑	B↑	-				
O-glycosylation	IgA1	Ser89-126 HYT	S↓ S/G↓ GN↓	GN↓		S↓ S/G↓ G↓ GN ↑ G/GN↓	-	-	-	-	GN ↓			GN↓ Gal↓	-	S↓ GN↓ G↓	G↓	GN↓	Gal↑ G/GN↑	GN↑ G↑ S↑ S/G↑ G/GN↑	S↑	-	-		

Figure 8: Comparison of associations found between IgA glycosylation and IBD in this study with IgA and IgG glycosylation associated with IBD, IgA Nephropathy, RA and pregnancy associated changes in recent literature. *A= Antennarity, B = Bisection, G= Galactosylation, GN= GalNAc, S= Sialylation. ↑ = Trait elevated in cases vs HC, ↓ = Trait lower in cases vs HC. In this study, the associations found between IgA glycosylation and IBD are marked in black. In the other studies, the color green indicates a significant association in the same direction (cases vs HC) as reported here, red indicates association in the opposite direction, and blue indicates reported associations that were not found in our study. The studies used for comparison are part of the bibliography cited in this article.*

Conclusion

In this study, we applied our recently developed IgA glycopeptide analytical workflow to a large number of samples and reported novel associations of IgA glycosylation with IBD. Our prediction model had a good performance to predict CD versus HC whilst the discrimination power for UC was lower. The possibility to detect IBD and discriminate CD from UC should be considered with using readily available biofluids as a first tentative approach for the early diagnostic of IBD before attempting invasive examination procedures for the comfort of the patients.

Authors

All authors had access to the study data and approved the final manuscript.

Acknowledgments

This work was supported by the European Commission (IBD-BIOM project, grant agreement 305479; GlycanTrigger, project 101093997). K.R.R. acknowledges NWO project number VI.Veni.192.058.

Raw Data

Mass spectrometry proteomics data raw mzXML datafiles have been deposited to the CMMS MassIVE archive [doi:10.25345/C5W08WS34] [dataset license: CC0 1.0 Universal (CC0 1.0)] at ftp://MSV000091731@massive.ucsd.edu (FTP download link) and ftp://massive.ucsd.edu/MSV000091731/ (public URL).

Supplementary Material

The supplementary material is available at https://pubs.acs.org/doi/10.1021/acs.jproteome.3c00260.

Supplementary table 1: Properties of analytes of IgA glycopeptides

Supplementary table 2: Byonic peptide fragmentation and identification

Supplementary table 3: Derived traits calculations

Supplementary table 4: Associations of IgA glycopeptides with age and sex

Supplementary table 5: Associations of IgA glycopeptides with IBD

Supplementary table 6: Associations of IgA glycopeptides with disease location in CD

Supplementary table 7: Associations of IgA glycopeptides with disease behavior in CD

Supplementary table 8: Associations of IgA glycopeptides with disease location in UC

Supplementary table 9: Associations of IgA glycopeptides with surgery

Supplementary table 10: Associations of IgA glycopeptides with drug strength

Supplementary Figure 1: Byonic identification of the glycopeptides TPL

Supplementary Figure 2: Byonic identification of the glycopeptides LAGC/Y

Supplementary Figure 3: Byonic identification of the glycopeptides LSL

Supplementary Figure 4: Byonic identification of the glycopeptides HYT

Supplementary Figure 5: Glycopeptide clusters and MS1 annotation of TPL

Supplementary Figure 6: Glycopeptide clusters and MS1 annotation of LAGC

Supplementary Figure 7: Glycopeptide clusters and MS1 annotation of LAGY

Supplementary Figure 8: Glycopeptide clusters and MS1 annotation of LSL

Supplementary Figure 9: Glycopeptide clusters and MS1 annotation of HYT

References

(1) Reily, C.; Stewart, T. J.; Renfrow, M. B.; Novak, J. Glycosylation in health and disease. *Nature Reviews Nephrology* **2019**, *15* (6), 346-366

(2) Dotz, V.; Wuhrer, M. N-glycome signatures in human plasma: associations with physiology and major diseases. *Febs Lett* **2019**, *593* (21), 2966-2976

(3) Simurina, M.; de Haan, N.; Vuckovic, F.; Kennedy, N. A.; Stambuk, J.; Falck, D.; Trbojevic-Akmacic, I.; Clerc, F.; Razdorov, G.; Khon, A.; Latiano, A.; D'Inca, R.; Danese, S.; Targan, S.; Landers, C.; Dubinsky, M.; Inflammatory Bowel Disease Biomarkers, C.; McGovern, D. P. B.; Annese, V.; Wuhrer, M.; Lauc, G. Glycosylation of Immunoglobulin G Associates With Clinical Features of Inflammatory Bowel Diseases. *Gastroenterology* **2018**, *154* (5), 1320-1333 e1310

(4) Clerc, F.; Novokmet, M.; Dotz, V.; Reiding, K. R.; de Haan, N.; Kammeijer, G. S. M.; Dalebout, H.; Bladergroen, M. R.; Vukovic, F.; Rapp, E.; Consortium, I.-B.; Targan, S. R.; Barron, G.; Manetti, N.; Latiano, A.; McGovern, D. P. B.; Annese, V.; Lauc, G.; Wuhrer, M. Plasma N-Glycan Signatures Are Associated With Features of Inflammatory Bowel Diseases. *Gastroenterology* **2018**, *155* (3), 829-843

(5) Trbojević-Akmačić, I.; Lageveen-Kammeijer, G. S.; Heijs, B.; Petrović, T.; Deris, H.; Wuhrer, M.; Lauc, G. High-throughput glycomic methods. *Chemical reviews* **2022**, *122* (20), 15865-15913

(6) Burisch, J.; Jess, T.; Martinato, M.; Lakatos, P. L.; EpiCom, E. The burden of inflammatory bowel disease in Europe. *Journal of Crohn's & colitis* **2013**, *7* (4), 322-337

(7) Annese, V.; Daperno, M.; Rutter, M. D.; Amiot, A.; Bossuyt, P.; East, J.; Ferrante, M.; Götz, M.; Katsanos, K. H.; Kießlich, R. European evidence based consensus for endoscopy in inflammatory bowel disease. *Journal of Crohn's and Colitis* **2013**, *7* (12), 982-1018

(8) Pezer, M. *Antibody Glycosylation*; Springer Cham, **2021**.

(9) Plomp, R.; Ruhaak, L. R.; Uh, H.-W.; Reiding, K. R.; Selman, M.; Houwing-Duistermaat, J. J.; Slagboom, P. E.; Beekman, M.; Wuhrer, M. Subclass-specific IgG glycosylation is associated with markers of inflammation and metabolic health. *Scientific reports* **2017**, *7* (1), 1-10

(10) Hansen, A. L.; Reily, C.; Novak, J.; Renfrow, M. B. Immunoglobulin A Glycosylation and Its Role in Disease. In *Antibody Glycosylation*, Pezer, M. Ed.; Springer International Publishing, **2021**; pp 433-477.

(11) Plomp, R.; de Haan, N.; Bondt, A.; Murli, J.; Dotz, V.; Wuhrer, M. Comparative Glycomics of Immunoglobulin A and G From Saliva and Plasma Reveals Biomarker Potential. *Front Immunol* **2018**, *9*, 2436

(12) Xue, J.; Zhu, L.-P.; Wei, Q. IgG-Fc N-glycosylation at Asn297 and IgA O-glycosylation in the hinge region in health and disease. *Glycoconjugate J* **2013**, *30* (8), 735-745

(13) Bondt, A.; Nicolardi, S.; Jansen, B. C.; Stavenhagen, K.; Blank, D.; Kammeijer, G. S.; Kozak, R. P.; Fernandes, D. L.; Hensbergen, P. J.; Hazes, J. M.; van der Burgt, Y. E.; Dolhain, R. J.; Wuhrer, M. Longitudinal monitoring of immunoglobulin A glycosylation during pregnancy by simultaneous MALDI-FTICR-MS analysis of N- and O-glycopeptides. *Sci Rep* **2016**, *6*, 27955

(14) Bondt, A.; Nicolardi, S.; Jansen, B. C.; Kuijper, T. M.; Hazes, J. M.; Van Der Burgt, Y. E.; Wuhrer, M.; Dolhain, R. J. IgA N-and O-glycosylation profiling reveals no association with the pregnancy-related improvement in rheumatoid arthritis. *Arthritis research & therapy* **2017**, *19* (1), 1-8

(15) Dotz, V.; Visconti, A.; Lomax-Browne, H.; Clerc, F.; Ederveen, A. H.; Medjeral-Thomas, N.; Cook, H. T.; Pickering, M.; Wuhrer, M.; Falchi, M. O-and N-Glycosylation of Serum Immunoglobulin A is Associated with IgA Nephropathy and Glomerular Function. *Journal of the American Society of Nephrology* **2021**, *32* (10), 2455-2465

(16) Clerc, F.; Reiding, K. R.; Jansen, B. C.; Kammeijer, G. S.; Bondt, A.; Wuhrer, M. Human plasma protein N-glycosylation. *Glycoconj J* **2016**, *33* (3), 309-343

(17) Trimarchi, H. M.; Iotti, A.; Iotti, R.; Freixas, E. A.; Peters, R. Immunoglobulin A nephropathy and ulcerative colitis. *American journal of nephrology* **2001**, *21* (5), 400-405

(18) Forshaw, M.; Guirguis, O.; Hennigan, T. IgA nephropathy in association with Crohn's disease. *International journal of colorectal disease* **2005**, *20* (5), 463-465

(19) Pouria, S.; Barratt, J. Secondary IgA nephropathy. In *Seminars in nephrology*, 2008; Elsevier: Vol. 28, pp 27-37.

(20) Wang, Y.-N.; Zhou, X.-J.; Chen, P.; Yu, G.-Z.; Zhang, X.; Hou, P.; Liu, L.-J.; Shi, S.-F.; Lv, J.-C.; Zhang, H. Interaction between GALNT12 and C1GALT1 associates with galactose-deficient IgA1 and IgA nephropathy. *Journal of the American Society of Nephrology* **2021**, *32* (3), 545-552

(21) Shi, D.; Zhong, Z.; Wang, M.; Cai, L.; Fu, D.; Peng, Y.; Guo, L.; Mao, H.; Yu, X.; Li, M. Identification of susceptibility locus shared by IgA nephropathy and inflammatory bowel disease in a Chinese Han population. *Journal of Human Genetics* **2020**, *65* (3), 241-249

(22) Inoue, T.; Iijima, H.; Tajiri, M.; Shinzaki, S.; Shiraishi, E.; Hiyama, S.; Mukai, A.; Nakajima, S.; Iwatani, H.; Nishida, T.; Mizushima, T.; Yasui, T.; Isaka, Y.; Kanto, T.; Tsujii, M.; Miyoshi, E.; Wada, Y.; Takehara, T. Deficiency of N-acetylgalactosamine in O-linked oligosaccharides of IgA is a novel biologic marker for Crohn's disease. *Inflamm Bowel Dis* **2012**, *18* (9), 1723-1734

(23) Steffen, U.; Koeleman, C. A.; Sokolova, M. V.; Bang, H.; Kleyer, A.; Rech, J.; Unterweger, H.; Schicht, M.; Garreis, F.; Hahn, J. IgA subclasses have different effector functions associated with distinct glycosylation profiles. *Nature communications* **2020**, *11* (1), 1-12

(24) Rouwendal, G. J.; van der Lee, M. M.; Meyer, S.; Reiding, K. R.; Schouten, J.; de Roo, G.; Egging, D. F.; Leusen, J. H.; Boross, P.; Wuhrer, M.; Verheijden, G. F.; Dokter, W. H.; Timmers, M.; Ubink, R. A comparison of anti-HER2 IgA and IgG1 in vivo efficacy is facilitated by high N-glycan sialylation of the IgA. *mAbs* **2016**, *8* (1), 74-86

(25) Ding, L.; Chen, X.; Cheng, H.; Zhang, T.; Li, Z. Advances in IgA glycosylation and its correlation with diseases. *Frontiers in Chemistry* **2022**, *10*,

(26) Latiano, A.; Palmieri, O.; Latiano, T.; Corritore, G.; Bossa, F.; Martino, G.; Biscaglia, G.; Scimeca, D.; Valvano, M. R.; Pastore, M.; Marseglia, A.; D'Incà, R.; Andriulli, A.; Annese, V. Investigation of Multiple Susceptibility Loci for Inflammatory Bowel Disease in an Italian Cohort of Patients. *Plos One* **2011**, *6* (7), e22688

(27) Satsangi, J.; Silverberg, M. S.; Vermeire, S.; Colombel, J. F. The Montreal classification of inflammatory bowel disease: controversies, consensus, and implications. *Gut* **2006**, *55* (6), 749-753

(28) Hinneburg, H.; Stavenhagen, K.; Schweiger-Hufnagel, U.; Pengelley, S.; Jabs, W.; Seeberger, P. H.; Silva, D. V.; Wuhrer, M.; Kolarich, D. The Art of Destruction: Optimizing Collision Energies in Quadrupole-Time of Flight (Q-TOF) Instruments for Glycopeptide-Based Glycoproteomics. *J Am Soc Mass Spectrom* **2016**, *27* (3), 507-519

(29) Jansen, B. C.; Falck, D.; de Haan, N.; Hipgrave Ederveen, A. L.; Razdorov, G.; Lauc, G.; Wuhrer, M. LaCyTools: A Targeted Liquid Chromatography-Mass Spectrometry Data Processing Package for Relative Quantitation of Glycopeptides. *Journal of proteome research* **2016**, *15* (7), 2198-2210

(30) Lippold, S.; de Ru, A. H.; Nouta, J.; van Veelen, P. A.; Palmblad, M.; Wuhrer, M.; de Haan, N. Semiautomated glycoproteomics data analysis workflow for maximized glycopeptide identification and reliable quantification. *Beilstein J Org Chem* **2020**, *16* (1), 3038-3051

(31) Momcilovic, A.; de Haan, N.; Hipgrave Ederveen, A. L.; Bondt, A.; Koeleman, C. A. M.; Falck, D.; de Neef, L. A.; Mesker, W. E.; Tollenaar, R.; de Ru, A.; van Veelen, P.; Wuhrer, M.; Dotz, V. Simultaneous Immunoglobulin A and G Glycopeptide Profiling for High-Throughput Applications. *Anal Chem* **2020**, *92* (6), 4518-4526

(32) Sandborn, W. J. The present and future of inflammatory bowel disease treatment. *Gastroenterology & Hepatology* **2016**, *12* (7), 438

(33) Raine, T.; Bonovas, S.; Burisch, J.; Kucharzik, T.; Adamina, M.; Annese, V.; Bachmann, O.; Bettenworth, D.; Chaparro, M.; Czuber-Dochan, W. ECCO guidelines

on therapeutics in ulcerative colitis: medical treatment. *Journal of Crohn's and Colitis* **2022**, *16* (1), 2-17

(34) Bondt, A.; Selman, M. H.; Deelder, A. M.; Hazes, J. M.; Willemsen, S. P.; Wuhrer, M.; Dolhain, R. J. Association between galactosylation of immunoglobulin G and improvement of rheumatoid arthritis during pregnancy is independent of sialylation. *Journal of proteome research* **2013**, *12* (10), 4522-4531

(35) Bohm, S.; Kao, D.; Nimmerjahn, F. Sweet and sour: the role of glycosylation for the anti-inflammatory activity of immunoglobulin G. *Current topics in microbiology and immunology* **2014**, *382*, 393-417

(36) Maverakis, E.; Kim, K.; Shimoda, M.; Gershwin, M. E.; Patel, F.; Wilken, R.; Raychaudhuri, S.; Ruhaak, L. R.; Lebrilla, C. B. Glycans in the immune system and The Altered Glycan Theory of Autoimmunity: A critical review. *Journal of Autoimmunity* **2015**, *57* (0), 1-13

(37) Basset, C.; Devauchelle, V.; Durand, V.; Jamin, C.; Pennec, Y.; Youinou, P.; Dueymes, M. Glycosylation of immunoglobulin A influences its receptor binding. *Scandinavian journal of immunology* **1999**, *50* (6), 572-579

(38) Hiki, Y.; Odani, H.; Takahashi, M.; Yasuda, Y.; Nishimoto, A.; Iwase, H.; Shinzato, T.; Kobayashi, Y.; Maeda, K. Mass spectrometry proves under-O-glycosylation of glomerular IgA1 in IgA nephropathy. *Kidney international* **2001**, *59* (3), 1077-1085

(39) Ohyama, Y.; Yamaguchi, H.; Nakajima, K.; Mizuno, T.; Fukamachi, Y.; Yokoi, Y.; Tsuboi, N.; Inaguma, D.; Hasegawa, M.; Renfrow, M. B.; Novak, J.; Yuzawa, Y.; Takahashi, K. Analysis of O-glycoforms of the IgA1 hinge region by sequential deglycosylation. *Scientific Reports* **2020**, *10* (1), 671

(40) Wada, Y.; Tajiri, M.; Ohshima, S. Quantitation of saccharide compositions of O-glycans by mass spectrometry of glycopeptides and its application to rheumatoid arthritis. *Journal of proteome research* **2010**, *9* (3), 1367-1373

(41) Ding, L.; Chen, X.; Cheng, H.; Zhang, T.; Li, Z. Advances in IgA glycosylation and its correlation with diseases. *Frontiers in Chemistry* **2022**, *10*, 974854

(42) Royle, L.; Roos, A.; Harvey, D. J.; Wormald, M. R.; van Gijlswijk-Janssen, D.; Redwan, E.-R. M.; Wilson, I. A.; Daha, M. R.; Dwek, R. A.; Rudd, P. M. Secretory IgA N-and O-glycans provide a link between the innate and adaptive immune systems. *J Biol Chem* **2003**, *278* (22), 20140-20153

(43) Kokubo, T.; Hiki, Y.; Iwase, H.; Tanaka, A.; Toma, K.; Hotta, K.; Kobayashi, Y. Protective role of IgA1 glycans against IgA1 self-aggregation and adhesion to extracellular matrix proteins. *Journal of the American Society of Nephrology* **1998**, *9* (11), 2048-2054

(44) Yan, Y.; Xu, L.; Zhang, J.; Zhang, Y.; Zhao, M. Self-aggregated deglycosylated IgA1 with or without IgG were associated with the development of IgA nephropathy. *Clinical & Experimental Immunology* **2006**, *144* (1), 17-24

(45) Field, M.; Amatayakul-Chantler, S.; Rademacher, T.; Rudd, P.; Dwek, R. Structural analysis of the N-glycans from human immunoglobulin A1: comparison of normal human serum immunoglobulin A1 with that isolated from patients with rheumatoid arthritis. *Biochem J* **1994**, *299* (1), 261-275

(46) Rudd, P.; Fortune, F.; Patel, T.; Parekh, R.; Dwek, R.; Lehner, T. A human T-cell receptor recognizes' O'-linked sugars from the hinge region of human IgA1 and IgD. *Immunology* **1994**, *83* (1), 99

(47) Falck, D.; Jansen, B. C.; de Haan, N.; Wuhrer, M. High-Throughput Analysis of IgG Fc Glycopeptides by LC-MS. In *High-Throughput Glycomics and Glycoproteomics: Methods and Protocols*, Lauc, G., Wuhrer, M. Eds.; Springer New York, **2017**; pp 31-47.

(48) Macpherson, A.; Khoo, U. Y.; Forgacs, I.; Philpott-Howard, J.; Bjarnason, I. Mucosal antibodies in inflammatory bowel disease are directed against intestinal bacteria. *Gut* **1996**, *38* (3), 365-375

(49) Shinzaki, S.; Kuroki, E.; Iijima, H.; Tatsunaka, N.; Ishii, M.; Fujii, H.; Kamada, Y.; Kobayashi, T.; Shibukawa, N.; Inoue, T. Lectin-based immunoassay for aberrant IgG glycosylation as the biomarker for Crohn's disease. *Inflammatory bowel diseases* **2013**, *19* (2), 321-331

Chapter 6

Discussion and Perspectives

Discussion and Perspectives

The work presented in this thesis has various innovative aspects. To my knowledge, the study presented in **chapter 3** is the largest analysis of the total plasma *N*-glycome (TPNG) in IBD patients, considering both the discovery and replication cohorts[1-3]. This research is novel, including sialic acid (SA) linkage-specific information in the TPNG and in IBD. We identified multiple associations of TPNG with Crohn's disease and ulcerative colitis, largely replicated in the second cohort. Differences in glycan complexity, fucosylation, bisection, galactosylation, and sialylation were found between IBD patients and healthy controls (HCs). Novel SA linkage data showed associations with age, sex, and IBD. Furthermore, our high-throughput method revealed differences within the CD and UC groups regarding surgery, medication response, and disease localization. Established inflammation markers, such as low galactosylation in IgG and higher sialylation in acute-phase proteins, were evident in CD and UC patients. The main findings about the glycosylation changes in antennarity, galactosylation, bisection, fucosylation and sialic acids were reproduced in a recent TSNG glycan study by UPLC using fluorescent procainamide labeling on released glycans[1]. That study did not include sialic acids linkage specific information like what is reported here in **chapter 3**, but they were able to report on a branching difference between CD and UC due to the different retention time observed with the α1,3 and α1,6-mannose arm-linked galactoses in their chromatography technique, which was not possible with our MALDI-TOF-MS approach. Looking ahead, a method that captures all these glycosylation features would be desirable, *i.e.*, resolving not only sialic acid linkage differences, but also branching differences. Combination of ion mobility with MS detection, eventually after sialic acid derivatization, may be an approach to achieve this goal. We also proposed specific proteins (e.g., IgA, haptoglobin, α1-acid-glycoprotein) as potential targets for future glycoproteomic studies to better understand IBD pathophysiology and develop therapeutic targets.

In **chapter 5**, we applied our IgA glycopeptide analytical workflow developed for IgAN analysis (**chapter 4** to a subset of the discovery cohort of IBD patients described in **chapter 3**, and report novel associations of IgA glycosylation with IBD. Our prediction model based on IgA glycopeptides effectively distinguished CD from HCs, whilst the model showed lower discrimination power for UC versus HCs. Plasma or serum glycomic analyses, using readily available biofluids, could aid early IBD diagnosis and differentiate CD from UC, reducing the need for invasive procedures. It is interesting to see that the changes reported in the TPNG for a few glycan traits like A2FS and A2FSB were potentially dominated by changes in IgA glycosylation as indicated by the relative contribution of each major plasma protein to specific glycoforms[4] (**Figure**

1). Indeed, these presumed associations between IgA glycosylation features and IBD were confirmed in the IBD IgA targeted study presented in **chapter 5.**

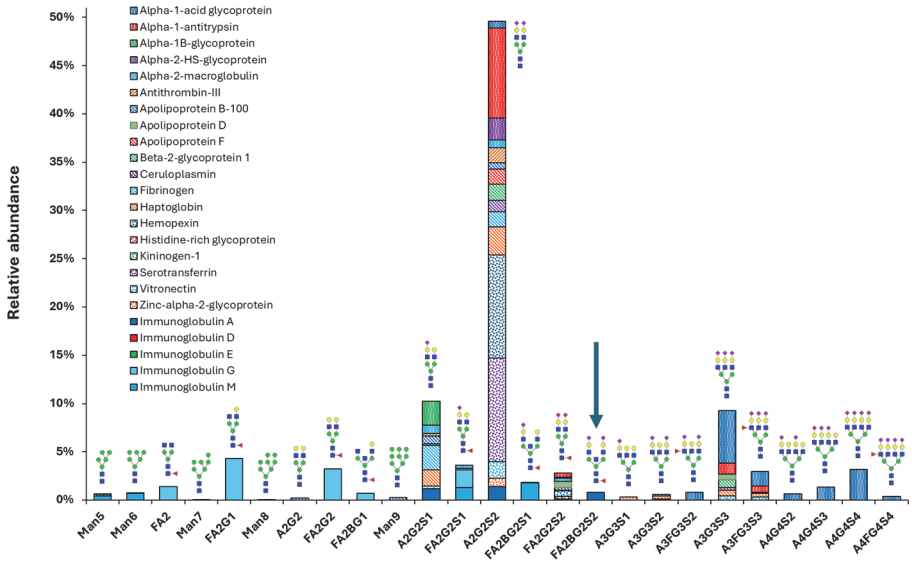

Figure 1: Estimated contribution of major blood glycoproteins to TPNG.

The contribution of IgA to FA2BG2S2 is highlighted with an arrow. The glycans contributing to FA2BG2S2 appear to be largely IgA-derived, making IgA a major contributor to the glycosylation traits A2FS and A2FSB, as postulated in the IgA specific chapters of the thesis. The figure is taken and modified from Chapter 2.

Confirming this predicted association made from findings in the non-targeted analysis of the TPNG with the targeted method on IgA shows the benefits of having a global overview of the glycosylation changes in serum, and proves the potential of TPNG analysis as starting point for biomarker research. Next to some of the IgA glycosylation changes in IBD, the well-known alterations in the high abundant IgG glycosylation with inflammation in general and specifically in IBD were also visible directly in the TPNG and confirmed in another study on the same IBD samples[5]. Unless specific proteins have already been proven to be the direct contributors or targets in specific diseases, using the TPNG analysis as starting point for investigations may be very informative.

Glycosylation's role in driving mucosal pathogenesis under chronic inflammation is an exciting and emerging research field. Current studies have shown that inflammation-induced changes in intestinal and immune cell glycosylation can produce potential prognostic biomarkers and targets for developing new therapies

to mitigate IBD-associated tissue damage. In a recent study on serum samples from IBD patients, the main glycosylation changes about antennarity, galactosylation, bisection, fucosylation and sialic acids were similarly to what is reported in **chapter 3** of this thesis[1]. Their analysis goes further in the search of predictive biomarkers for disease and treatment escalation and achieved great power in case vs controls prediction as well as in escalation of treatment in high-risk vs low risk patients[1].

The analysis of the TPNG is also aligning well with genomic studies, where the effects of alterations in glycosylation coding genes affects glycosylation profiles drawing a line from coding to expression[6-9]. Overall, we observe that the insights from the TPNG presented in **chapter 2** aid in the clinical interpretation of comprehensive plasma glycosylation analyses. This review highlights the critical need for further protein-specific glycosylation studies to address the significant gaps in our current understanding and is used as reference for glycosylation background in already more than 300 research articles (scopus, July 2024).

In this thesis, the detection of rather small differences in glycosylation between CD and UC was made possible thanks to the statistical power achieved with the large number of samples used in the discovery cohort with findings being replicated in another large replication cohort (**chapter 3**). A specific challenge addressed in this work was the logistical complexity of performing sample randomization, which led to the use of a robotic platform to handle the pipetting. This included optimizing the redistribution of samples from 25 donor-specific 96-well plates, originally sorted by disease status, into new receiver plates, while maintaining balanced distributions of cases, healthy controls, technical and biological controls, and blanks. Furthermore, special care was taken to limit each donor plate to a single thaw cycle and to minimize batch effects during sample processing, ensuring to retain optimal plasma quality. Following randomization, two batches of four 96-well plates each were prepared daily and spotted onto MALDI target plates for subsequent MALDI-TOF-MS analysis.

This study shows the potential and benefits of using a robotized platform for sample randomization and sialic acid derivatization with minimum effort compared to executing this protocol by hand, including the reduction of interday batch effects which are important when handling such large numbers of samples. This workflow has already been used and adapted for similar studies focused on other diseases[10-14]. As described in **chapter 3**, it was possible to apply batch correction (performed on logarithmically transformed data) to account for the different preparation days, as well as position on row and column of the randomized samples on the 96-well plates and to remove outliers from data analysis (**Figure 2** and **Figure 3**).

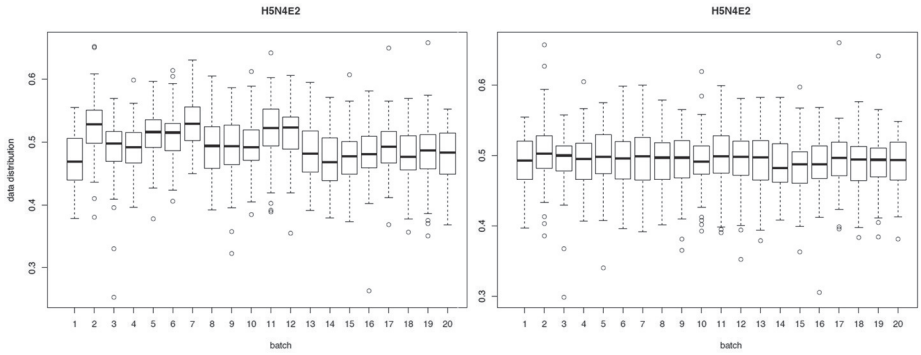

Figure 2: Batch correction applied to twenty plates of TPNG samples

Figure 2 *represents the effects of batch correction (before vs. after) on all plates of the TPNG samples analyzed in* ***chapter 3****. This batch correction considers sample position (row, column and plate). The mean and boxplot distribution of the major TPNG glycan H5N4E2 is represented. This batch correction method aims to model and remove the variability associated with batch preparation due to technical variations while retaining biologically meaningful differences.*

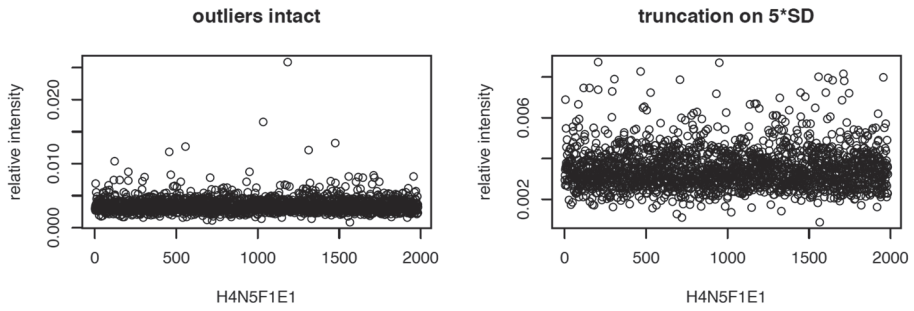

Figure 3: Outlier removal with a cut-off of 5x standard deviation

Figure 3 *visualizes the effect of removing data outliers of one extracted analyte (H4N5F1E1) with a cut-off at 5x standard deviation from the mean. It is assumed that biological differences between the groups are smaller than 5*SD and that these outliers are due to technical artefacts during sample preparation or analysis.*

A recent article expands the knowledge of blood protein *N*-glycosylation in a similar manner to **chapter 2,** highlighting the complexity of the *N*-glycome, its variation amongst different demographics, and its importance for understanding its variations in health and disease by comparing glycosylation changes in nine different diseases[14]. They showed that the glycosylation features found in IBD patients had

little resemblance to other diseases like breast, pancreatic and colorectal cancer or multiple myeloma while CD and UC exhibited rather similar glycosylation signatures (**Figure 4**).

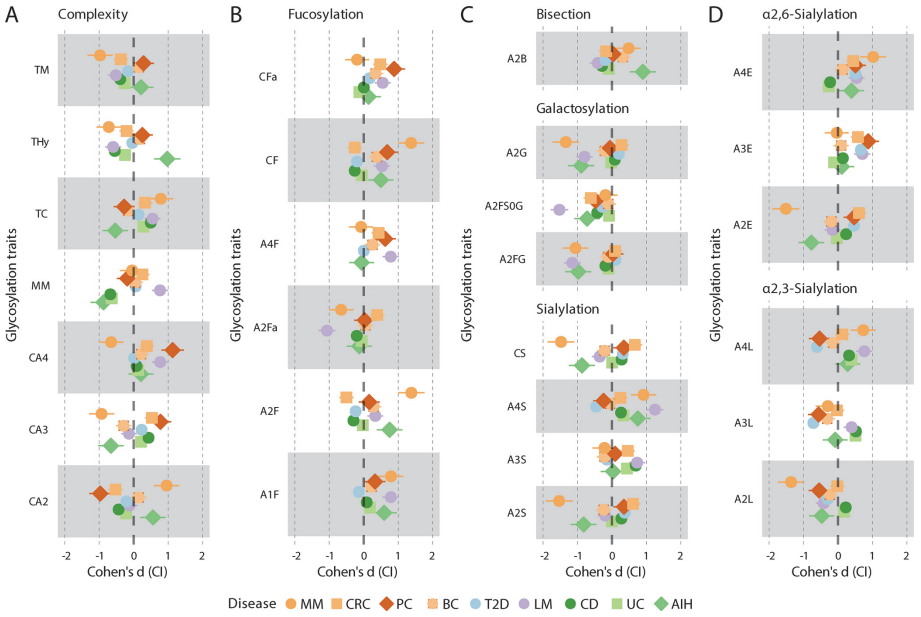

Figure 4: Forest plots visually illustrating the effect sizes of glycosylation traits observed in various diseases.

Taken from[14]*. The data and results from the studies on CD and UC reported in this thesis*[4] *was used by Pongracz et.al for comparison with the glycosylation changes generated on other diseases studied with similar methodological workflows and reported in their respective publications. Those studies were focused on multiple myeloma (MM)*[15]*, colorectal cancer (CRC)*[16]*, pancreatic cancer (PC)*[11]*, breast cancer (BC)*[17]*, type-2 diabetes (T2D)*[18]*, leishmaniasis (LM)*[19] *and autoimmune hepatitis (AIH)*[20]*.*

While these studies employed comparable methodologies, minor variations in sample preparation and data analysis may have introduced slight discrepancies in the results. Despite these differences, the most abundant glycosylation features (not the effect size or direction) remained consistent across all studies, whereas low-abundance analytes exhibited minor variability between individual investigations. Importantly, the use of glycosylation traits in all analyses effectively mitigated the impact of these inconsistencies. Importantly, glycosylation changes between healthy

controls and disease groups were consistently observed across studies, indicating that the cross-disease comparisons are valid and meaningful[14].

In IBD, comprising CD and UC, patients show a significant reduction in IgG *N*-glycan galactosylation and sialylation, correlating with disease severity and inflammation. Increased core fucosylation suggests an immune-modulatory role, similar to Rheumatoid Arthritis (RA), where IgG shows high core fucosylation. Galactose-deficient IgG is a key inflammatory marker linked to disease activity and often precedes clinical symptoms[21]. Compared to other inflammatory diseases, CD and UC generally show similar glycosylation trends but rarely exhibit the most extreme changes, except for α2,6-sialylation of tetra-antennary glycans (A4E) and α2,3-sialylation of bi- and tri-antennary glycans (A2L, A3L). They also display a distinct profile of multiple mannosidic structures (MM), comparable only to autoimmune hepatitis, while most other diseases show little or no MM variation—except visceral leishmaniasis (LM), which exhibits a marked increase. Notably, IBD has a relatively mild inflammatory glycosylation profile, with less pronounced IgG degalactosylation in di-antennary glycans (A2G) than e.g. LM[14].

IBD, including CD and UC, exhibit glycosylation changes that set it apart from other diseases, particularly cancers, autoimmune disorders, and metabolic conditions. Unlike Multiple Myeloma, which shows a strong skewing towards di-antennary glycosylation due to the secretion of large amounts of monoclonal immunoglobulins, IBD's glycosylation appear to involve IgG and IgA, with a consistent reduction in galactosylation and increase in sialylation. This pattern is indicative of chronic inflammation and shared with other inflammatory and autoimmune conditions, but distinct from cancer-related glycosylation alterations, which often involve increased branching (tri- and tetra-antennary glycans) and more enhanced sialylation. Pancreatic cancer (PC) and colorectal cancer (CRC) both exhibit a shift from di-antennary to more complex tri- and tetra-antennary glycans, alongside increased α2,6-sialylation and fucosylation, whereas IBD does not demonstrate such pronounced branching or elevated sialylation[14].

While both IBD and IgA Nephropathy (IgAN) involve altered IgA glycosylation, the signatures are distinct. IgAN is characterized by under-galactosylation of *O*-glycans in IgA1, which is thought to promote immune complex formation and kidney inflammation, whereas IBD shows more widespread glycosylation modifications affecting multiple glycoproteins in the circulation, including IgG and IgA. The systemic nature of IBD glycosylation alterations contrasts with the kidney-specific pathophysiology of IgAN. Similarly, autoimmune hepatitis (AIH) appeared to share some inflammatory glycosylation features with IBD, such as decreased galactosylation (more pronounced in AIH), but AIH also presents a marked increase in hybrid-type glycans and core fucosylation, a trait not prominently observed in IBD.

Moreover, AIH features a distinct reduction in di-antennary glycan sialylation and a significant decrease in oligomannosidic structures, whereas IBD's glycosylation changes are less pronounced in these areas[14].

Interestingly, although IBD manifests in the gastrointestinal tract as does colorectal cancer, their glycosylation profiles are rather different. While CRC shows a characteristic increase in tri- and tetra-antennary glycans, unlike IBD, suggesting distinct systemic effects. Moreover, in contrast to IBD, CRC exhibits reduced core fucosylation of di-antennary glycans[14].

Metabolic diseases such as Type 2 Diabetes (T2D) also share some glycosylation features with PC in terms of increased α2,6-sialylation of tri- and tetra-antennary glycans, a feature that is not prominent in IBD. This reinforces the idea that IBD's glycosylation changes are more aligned with chronic inflammatory processes rather than metabolic dysregulation. Additionally, while infections such as visceral leishmaniasis (LM) can induce strong glycosylation changes, including a marked reduction in galactosylation of IgG, IBD presents a more moderate and chronic version of this inflammatory glycosylation pattern rather than an acute immune response[14].

Overall, IBD's glycosylation signature is most similar to other inflammatory and autoimmune diseases, particularly in its reduction in galactosylation and sialylation, but it remains distinct from cancer-related glycosylation profiles that involve increased branching and sialylation. The ability of IBD glycosylation to predict treatment response, differentiates it from glycosylation signatures of other diseases[1].

In **chapter 4**, a new semi-automated sample preparation was developed to reduce benchtop errors during sample preparation for IgA capturing, digestion and glycopeptide purification and streamline glycopeptide analysis by reverse phase LC-MS. A previously published method described a workflow for capturing, purifying, and analyzing IgA glycopeptides using cotton-based HILIC extraction combined with MALDI-FTICR-MS [22]. Although this method provided excellent analytical performance, it was not easily scalable beyond a small number of samples due to the labor-intensive manual preparation of HILIC materials (cutting small cotton thread and immobilizing it inside pipette tips), the long pipetting sequence for the capturing and purification of the samples, and the complex data analysis required for MALDI-FTICR-MS datasets. In the research presented here, the core elements of the original method regarding specifically the IgA capture using camelid antibody domains immobilized on agarose beads and protein digestion with TPCK-treated trypsin are retained[22, 23]. However, significant changes were introduced for the purification and data acquisition steps to enable high-throughput analysis of hundreds of samples. In

this optimized workflow, IgA glycoprotein purification is performed using 96-well filtration plates, replacing the manual HILIC pipette-tip approach. Furthermore, mass spectrometric analysis was transitioned to an LC-MS platform, which resolved prior challenges in simultaneously detecting high- and low-mass analytes that complicated analysis with MALDI-FTICR-MS [22, 23]. To address the issue of sialic acid effects on glycopeptide retention in reverse-phase LC, optimized LC-MS conditions were developed by adding TFA to the eluents for the data acquisition, minimizing retention time shifts and enabling robust, high-throughput data processing, as described in two chapters of this thesis [24, 25].

Our novel approach for specific IgA glycosylation analysis provides detailed information on 69 measured IgA glycopeptides. Despite a small sample size limiting predictive model validation for IgAN, we demonstrated that IgA glycopeptides are better predictors of IgAN status and renal function than on lectin-based assays Gd-IgA levels and eGFR alone. Our findings suggest new opportunities for using glycopeptides as biomarkers for IgAN onset and progression.

After the publication of the manuscript presented in **chapter 4**, no other large glycomic studies have been performed in the context of IgA nephropathy with a similarly large number of glycans analyzed, most likely due to the technical challenges inherent to (*O*-)glycopeptide analysis mentioned in the discussion. This complicates the comparison of our findings with other research reports. A paper published one year after the manuscript of **chapter 4** was executed with a similar setup but based on an older protocol using desialylation of the *O*-glycans, allowing for simpler data analysis but lacking sialic acid information due to the neuraminidase treatment applied to their samples[26]. Nevertheless, their research confirmed the findings reported in this thesis except the ones about SA that were out of the scope of their research.

The sample preparation protocol that was previously used for the analysis of IgA in our research group was executed manually, including the affinity purification, and the samples were analyzed by MALDI-FTICR-MS (Fourier transform ion cyclotron resonance)[22]. One advantage of this previous method was the high resolution obtained from the FTICR-MS instrument used allowing for easy and highly confident identification of the analytes, and the relatively small size of the data generated compared to the LC-MS data presented here. Some of the drawbacks from the previous protocol were that the sample purification had to be performed manually with many pipetting steps for the HILIC purification, and that the analytes had to be measured in two parts to optimize their detection with the FTICR-MS, and then normalized together for the rest of the analysis. The very high resolution of the analytes obtained from their research, including the MS/MS experiments performed with direct infusion ESI-FTICR-MS allowed us to use it as a basis for the research of

the analytes present in the IgAN study presented here. The other approach chosen in the study of **chapter 4 and 5** with the 96-well plate sample preparation allowed all samples to be prepared in a single campaign. For the data acquisition, the use of exclusively LC-ESI-MS(/MS) enabled the analysis of all glycopeptides in a single run, with the only drawback of the large size of files generated which required a dedicated computer and a series of hard-drives to be used to process the data at once. Overall, this approach greatly improved the workflow for the analysis of IgA glycopeptides and allows this protocol to be used again more efficiently in future studies.

One point that was not discussed in both the IgA papers was the comparison of the relative intensity of the glycopeptide clusters (HYT, LSL, TPL, LAG(C/Y), and MAG(C/Y)).The variability of ionization efficiency of each glycopeptide, the different time windows used for the extraction of each peptide clusters, the different charge states and different number of analytes in each peptide in addition to the differences of glycans detected in HC vs patients renders a biologically meaningful and insightful comparison of the sum intensities of the glycopeptide clusters level challenging due to the many uncontrolled variables. Once the challenges are mastered, assessing the ratios of glycopeptide clusters could for example be used for investigating if there is a change of IgA1/IgA2 ratio in disease. This could potentially replace additional assays for measuring immunoglobulin isotype and subclass concentrations. While calculating a ratio of each cluster based on the non-normalized intensity of each individual glycopeptide is technically possible, it would be difficult to defend its use as clinical marker due to the lack of a proper way to normalize all the intensities of the individual glycopeptides. The perfect way to remedy this would be the use of isotopically labeled glycopeptides for each analyte present in the samples, spiked as reference in each sample. However, the costs in time and money spent to produce such standards may possibly outweigh the benefits of having them. Another possible way to still have a constant standard analyzed with each glycopeptide clusters would be to add a single reference standard either in one of the buffers or in a very small amount (not to disrupt too much the ionization efficiency of the sample's analytes) in the nano-booster solvent during the ESI to avoid gradient effects due to buffer composition change during the elution of the analytes, and to use this as reference to normalize the intensity of each glycopeptide cluster, then enabling their comparison directly based on the LC-MS data.

In our study in **chapter 4 and 5**, we analyzed the *O*-glycopeptide of IgA1 containing multiple glycosylation sites as a single block. In theory, its analysis with site-specific information would have been possible to achieve, but with much more time needed to prepare the samples and do the multiple enzymatic digestions necessary to cleave the peptides around the individual glycosylation sites. This would not have allowed

the use of the robotized platform in the way we intended. A recent paper reporting on a technique based on sequential deglycosylation of the IgA hinge region with site-specific information about the order of most occupied Gd-IgA1 glycosylation sites, could potentially be used on a sample set in the context of IgAN but has currently only been tested with the plasma of ten healthy individuals[27].

When trying to explain the origin of the gd-IgA, multiple reports exist about glycosylation enzymes and altered gene coding sequences for galactosyltransferases[28, 29]. Some heterogeneity in gd-IgA has also been observed amongst different populations although the glycosylation change with IgAN was similar in both populations[30]. The reported changes in the expression of glycosylation enzymes may explain the lower galactosylation of IgA observed in our paper. However, if this was the main cause of gd-IgA and/or nephropathy, there should be reports for other proteins showing deficiencies in galactosylation associated with "IgA"N, which is currently not the case[31-34]. A study investigated together the glycosylation changes of IgA and IgD in IgAN and while it confirmed the lower galactosylation of IgA, the contrary was observed for IgD, leaving more questions regarding the currently accepted explanation instead of confirming it. Although we have reported multiple glycosylation changes in the *N*-glycans of IgA1 and IgA2, most of the scientific reports seem to consider the *O*-glycosylation deficiency to be the main glycosylation cause of the harmful IgA complex formation, almost completely omitting the *N*-glycans from the equation[31]. However, these changes in *N*-glycosylation were found similarly in RA and IBD, giving hints that deregulated glycosylation may be shared between various inflammatory and autoimmune diseases.

The aberrant glycosylation of IgA appears central to the disease process, which leads to the formation of IgA self-aggregates which are then recognized by various ligands, triggering a cascade of inflammatory responses. Recent reports suggest that self-aggregation of IgA in Nephropathy patients could involve the cysteine-471 in the tailpiece of IgA1, although *O*-glycosylation deficiencies appear to promote nonspecific self-aggregation[35, 36]. Some other reports suggest that initial IgA aggregates that are recognized by IgG, IgM and C3 are then later forming multi-IgA aggregates and that these are the ones depositing in the kidneys[28, 30, 37]. It has been shown that the complement system can be triggered by multiple pathways in IgAN[38] and recent studies reports that the complement protein of the complement system plays a major role in the pathogenesis of IgAN, and that its presence in the IgA aggregates helps the diagnosis of IgAN from other glomerular IgA deposition[39, 40]. As much as researchers agree that the deposition of IgA complexes in the kidneys are an important factor for the destructive immune response occurring in IgAN, the exact mechanisms of the disease still remain unclear[41]. Researchers compared the

serum levels of IgA and glomerular levels of secretory IgA (SIgA) in a biopsy sample from the kidney of a nephropathy patient, and found values 120 times higher for the SIgA, indicating a very high accumulations of SIgA, but not of monomeric IgA, in the glomerular deposits[42]. They also compared the binding affinity of monomeric and polymeric IgA (pIgA) to the mesangial cells and found a stronger binding of pIgA compared to monomeric IgA, supporting theories that abnormally glycosylated IgA, which has a tendency to self-aggregate, and IgA complexes being involved in the inflammatory activation chain in IgAN. Some other recent reports detail how the aberrant glycosylation of IgA affects its binding with some of its receptors, and when IgA receptors on cell membrane are under expressed in IgAN, can slow down the clearance of IgA from circulation and favorize the formation of the inflammatory complexes[29]. A very interesting effect is also observed when IgA1 receptors like CD71 binding preferentially polymeric IgA1 (but not the monomeric IgA1/2), or integrin α2/β1 are found to be overexpressed in the mesangial cells of IgAN patients and could be potential targets of new treatments[29, 43, 44].

In theory, any of these steps mentioned above could be the target of novel treatments for IgAN, although most of recent developments seem to focus on the mediation of the inflammatory reaction chain and ligands recognizing the IgA complexes[45, 46]. Other current treatment candidates aim to reduce the production of pathogenic IgA in the gut or to target B cells to reduce the production of IgA, IgG and autoantibodies in general and to slow down the formation of the IgA-IgG-C3 complexes. There are also therapeutic strategies aimed at reducing the activation of the complement system, while others focus more on the mitigation of the effects by targeting a reduction of proteinuria to limit the damages to the kidneys and delay the progression of IgAN without actually treating the cause of the disease[47-54].

Even if the perfect approach to treat and possibly cure IgAN has not yet been proposed, it is important to see that there is a growing interest in understanding the disease and that developing therapeutics with multiple modes of actions could be envisaged and maybe combined for better results.

With the research presented in the different chapters of this thesis, it was encountered that previous glycomic studies often used small sample sets and various in-house methods, making comparisons difficult. Large-scale analyses have previously been hampered by traditional sample preparation methods and the lack of dedicated software. This thesis uses larger sample sets with streamlined sample preparation, enabled by robotized platforms and new software for analyte extraction and statistical analysis. Automated liquid handling robots improved sample preparation consistency and reduced human error. More than a thousand samples were included in a single glycomic study, allowing powerful statistical corrections. In-house software was used to process large LC-MS datasets, reducing

them from terabytes to megabytes of analyte-focused information, ready for statistical analysis. The sample preparation techniques avoided biases associated with glycan labeling and used protein capture based on peptide portions, reducing analyte bias. Analyzing relative intensities per glycoprotein cluster removed variability in protein concentration without needing an internal standard. This approach, along with derived traits grouping similar features of analytes, provided stronger insights into global glycosylation changes in diseases.

Overall, the analytical workflows presented in this thesis show the growing potential of glycomic analysis in the development of non-invasive biomarkers and shines light on the potential of robotized workflows to accelerate the research for new biomarkers and offer clinicians alternative tools for early diagnosis, patient stratification and personalized medicine based on easily accessible samples[12, 55-57].

References

(1) Shubhakar, A.; Jansen, B. C.; Adams, A. T.; Reiding, K. R.; Ventham, N. T.; Kalla, R.; Bergemalm, D.; Urbanowicz, P. A.; Gardner, R. A.; IBDBIOMConsortium; Wuhrer, M.; Halfvarson, J.; Satsangi, J.; Fernandes, D. L.; Spencer, D. I. R. Serum N-Glycomic Biomarkers Predict Treatment Escalation in Inflammatory Bowel Disease. *Journal of Crohn's & colitis* **2023**, *17* (6), 919-932

(2) Wu, Y.; Chen, Y.; Chen, H.; Yang, C.; Shen, X.; Deng, C.; Sun, N.; Wu, H. Probing serum N-glycan patterns for rapid and precise detection of Crohn's disease. *Chemical Communications* **2021**, *57* (86), 11362-11365

(3) Trbojevic-Akmacic, I.; Lageveen-Kammeijer, G. S. M.; Heijs, B.; Petrovic, T.; Deris, H.; Wuhrer, M.; Lauc, G. High-Throughput Glycomic Methods. *Chem Rev* **2022**, *122* (20), 15865-15913

(4) Clerc, F.; Novokmet, M.; Dotz, V.; Reiding, K. R.; de Haan, N.; Kammeijer, G. S. M.; Dalebout, H.; Bladergroen, M. R.; Vukovic, F.; Rapp, E.; Consortium, I.-B.; Targan, S. R.; Barron, G.; Manetti, N.; Latiano, A.; McGovern, D. P. B.; Annese, V.; Lauc, G.; Wuhrer, M. Plasma N-Glycan Signatures Are Associated With Features of Inflammatory Bowel Diseases. *Gastroenterology* **2018**, *155* (3), 829-843

(5) Simurina, M.; de Haan, N.; Vuckovic, F.; Kennedy, N. A.; Stambuk, J.; Falck, D.; Trbojevic-Akmacic, I.; Clerc, F.; Razdorov, G.; Khon, A.; Latiano, A.; D'Inca, R.; Danese, S.; Targan, S.; Landers, C.; Dubinsky, M.; Inflammatory Bowel Disease Biomarkers, C.; McGovern, D. P. B.; Annese, V.; Wuhrer, M.; Lauc, G. Glycosylation of Immunoglobulin G Associates With Clinical Features of Inflammatory Bowel Diseases. *Gastroenterology* **2018**, *154* (5), 1320-1333 e1310

(6) McGovern, D. P.; Jones, M. R.; Taylor, K. D.; Marciante, K.; Yan, X.; Dubinsky, M.; Ippoliti, A.; Vasiliauskas, E.; Berel, D.; Derkowski, C.; Dutridge, D.; Fleshner, P.; Shih, D. Q.; Melmed, G.; Mengesha, E.; King, L.; Pressman, S.; Haritunians, T.; Guo, X.; Targan, S. R.; Rotter, J. I.; International, I. B. D. G. C. Fucosyltransferase 2 (FUT2) non-secretor status is associated with Crohn's disease. *Human molecular genetics* **2010**, *19* (17), 3468-3476

(7) Ye, B. D.; McGovern, D. P. Genetic variation in IBD: progress, clues to pathogenesis and possible clinical utility. *Expert Rev Clin Immunol* **2016**, *12* (10), 1091-1107

(8) Štambuk, T.; Klasić, M.; Zoldoš, V.; Lauc, G. N-glycans as functional effectors of genetic and epigenetic disease risk. *Molecular aspects of medicine* **2021**, *79*, 100891

(9) Brazil, J. C.; Parkos, C. A. Finding the sweet spot: glycosylation mediated regulation of intestinal inflammation. *Mucosal Immunology* **2022**, *15* (2), 211-222

(10) Vreeker, G. C. M.; Nicolardi, S.; Bladergroen, M. R.; van der Plas, C. J.; Mesker, W. E.; Tollenaar, R.; van der Burgt, Y. E. M.; Wuhrer, M. Automated Plasma Glycomics

with Linkage-Specific Sialic Acid Esterification and Ultrahigh Resolution MS. *Anal Chem* **2018**, *90* (20), 11955-11961

(11) Vreeker, G. C.; Hanna-Sawires, R. G.; Mohammed, Y.; Bladergroen, M. R.; Nicolardi, S.; Dotz, V.; Nouta, J.; Bonsing, B. A.; Mesker, W. E.; van Der Burgt, Y. E. Serum N-glycome analysis reveals pancreatic cancer disease signatures. *Cancer Medicine* **2020**, *9* (22), 8519-8529

(12) de Haan, N.; Pučić-Baković, M.; Novokmet, M.; Falck, D.; Lageveen-Kammeijer, G.; Razdorov, G.; Vučković, F.; Trbojević-Akmačić, I.; Gornik, O.; Hanić, M. Developments and perspectives in high-throughput protein glycomics: enabling the analysis of thousands of samples. *Glycobiology* **2022**, *32* (8), 651-663

(13) Bladergroen, M. R.; Pongracz, T.; Wang, W.; Nicolardi, S.; Arbous, S. M.; Roukens, A.; Wuhrer, M. Total plasma N-glycomic signature of SARS-CoV-2 infection. *iScience* **2024**, *27* (7), 110374

(14) Pongracz, T.; Mayboroda, O. A.; Wuhrer, M. The Human Blood N-Glycome: Unraveling Disease Glycosylation Patterns. *JACS Au* **2024**, *4* (5), 1696-1708

(15) Zhang, Z.; Westhrin, M.; Bondt, A.; Wuhrer, M.; Standal, T.; Holst, S. Serum protein N-glycosylation changes in multiple myeloma. *Biochim Biophys Acta Gen Subj* **2019**, *1863* (5), 960-970

(16) de Vroome, S. W.; Holst, S.; Girondo, M. R.; van der Burgt, Y. E. M.; Mesker, W. E.; Tollenaar, R.; Wuhrer, M. Serum N-glycome alterations in colorectal cancer associate with survival. *Oncotarget* **2018**, *9* (55), 30610-30623

(17) Vreeker, G. C.; Vangangelt, K. M.; Bladergroen, M. R.; Nicolardi, S.; Mesker, W. E.; Wuhrer, M.; van der Burgt, Y. E.; Tollenaar, R. A. Serum N-glycan profiles differ for various breast cancer subtypes. *Glycoconjugate J* **2021**, *38*, 387-395

(18) Dotz, V.; Lemmers, R. F. H.; Reiding, K. R.; Hipgrave Ederveen, A. L.; Lieverse, A. G.; Mulder, M. T.; Sijbrands, E. J. G.; Wuhrer, M.; van Hoek, M. Plasma protein N-glycan signatures of type 2 diabetes. *Biochim Biophys Acta Gen Subj* **2018**, *1862* (12), 2613-2622

(19) Porcino, G. N.; Bladergroen, M. R.; Dotz, V.; Nicolardi, S.; Memarian, E.; Gardinassi, L. G.; Nery Costa, C. H.; Pacheco de Almeida, R.; Ferreira de Miranda Santos, I. K.; Wuhrer, M. Total serum N-glycans mark visceral leishmaniasis in human infections with Leishmania infantum. *iScience* **2023**, *26* (7), 107021

(20) Pongracz, T.; Biewenga, M.; Stoelinga, A. E. C.; Bladergroen, M. R.; Nicolardi, S.; Trouw, L. A.; Wuhrer, M.; de Haan, N.; van Hoek, B. Autoimmune hepatitis displays distinctively high multi-antennary sialylation on plasma N-glycans compared to other liver diseases. *J Transl Med* **2024**, *22* (1), 456

(21) Kissel, T.; Toes, R. E.; Huizinga, T. W.; Wuhrer, M. Glycobiology of rheumatic diseases. *Nature Reviews Rheumatology* **2023**, *19* (1), 28-43

(22) Bondt, A.; Nicolardi, S.; Jansen, B. C.; Stavenhagen, K.; Blank, D.; Kammeijer, G. S.; Kozak, R. P.; Fernandes, D. L.; Hensbergen, P. J.; Hazes, J. M.; van der Burgt, Y. E.; Dolhain, R. J.; Wuhrer, M. Longitudinal monitoring of immunoglobulin A glycosylation during pregnancy by simultaneous MALDI-FTICR-MS analysis of N- and O-glycopeptides. *Sci Rep* **2016**, *6*, 27955

(23) Bondt, A.; Nicolardi, S.; Jansen, B. C.; Kuijper, T. M.; Hazes, J. M.; Van Der Burgt, Y. E.; Wuhrer, M.; Dolhain, R. J. IgA N-and O-glycosylation profiling reveals no association with the pregnancy-related improvement in rheumatoid arthritis. *Arthritis research & therapy* **2017**, *19* (1), 1-8

(24) Dotz, V.; Visconti, A.; Lomax-Browne, H.; Clerc, F.; Ederveen, A. H.; Medjeral-Thomas, N.; Cook, H. T.; Pickering, M.; Wuhrer, M.; Falchi, M. O-and N-Glycosylation of Serum Immunoglobulin A is Associated with IgA Nephropathy and Glomerular Function. *Journal of the American Society of Nephrology* **2021**, *32* (10), 2455-2465

(25) Clerc, F.; Reiding, K. R.; de Haan, N.; Koeleman, C. A. M.; Hipgrave Ederveen, A. L.; Manetti, N.; Consortium, I.-B.; Dotz, V.; Annese, V.; Wuhrer, M. Immunoglobulin A Glycosylation Differs between Crohn's Disease and Ulcerative Colitis. *Journal of proteome research* **2023**, *22* (10), 3213-3224

(26) Zhang, S.; Sun, H.; Zhang, Z.; Li, M.; Guo, Z.; Ye, W.; Cai, G.; Sun, W.; Li, M. Diagnostic potential of plasma igA1 O-glycans in discriminating igA nephropathy from other glomerular diseases and healthy participants. *Frontiers in Molecular Biosciences* **2022**, *9*, 871615

(27) Ohyama, Y.; Yamaguchi, H.; Nakajima, K.; Mizuno, T.; Fukamachi, Y.; Yokoi, Y.; Tsuboi, N.; Inaguma, D.; Hasegawa, M.; Renfrow, M. B. Analysis of O-glycoforms of the IgA1 hinge region by sequential deglycosylation. *Scientific reports* **2020**, *10* (1), 671

(28) Novak, J.; King, R. G.; Yother, J.; Renfrow, M. B.; Green, T. J. O-glycosylation of IgA1 and the pathogenesis of an autoimmune disease IgA nephropathy. *Glycobiology* **2024**, *34* (11),

(29) Ohyama, Y.; Renfrow, M. B.; Novak, J.; Takahashi, K. Aberrantly Glycosylated IgA1 in IgA Nephropathy: What We Know and What We Don't Know. *Journal of Clinical Medicine* **2021**, *10* (16), 3467

(30) Ohyama, Y.; Yamaguchi, H.; Ogata, S.; Chiurlia, S.; Cox, S. N.; Kouri, N.-M.; Stangou, M. J.; Nakajima, K.; Hayashi, H.; Inaguma, D. Racial heterogeneity of IgA1 hinge-region O-glycoforms in patients with IgA nephropathy. *Iscience* **2022**, *25* (11),

(31) Sun, M.; Shi, G.; Zhang, X.; Kan, C.; Xie, S.; Peng, W.; Liu, W.; Wang, P.; Zhang, R. Deciphering roles of protein post-translational modifications in IgA nephropathy progression and potential therapy. *Aging* **2024**, *16* (1), 964

(32) Kouri, N. M.; Stangou, M.; Lioulios, G.; Mitsoglou, Z.; Serino, G.; Chiurlia, S.; Cox, S. N.; Stropou, P.; Schena, F. P.; Papagianni, A. Serum levels of miR-148b and let-7b

at diagnosis may have important impact in the response to treatment and long-term outcome in IgA nephropathy. *Journal of clinical medicine* **2021**, *10* (9), 1987

(33) Serino, G.; Sallustio, F.; Curci, C.; Cox, S. N.; Pesce, F.; De Palma, G.; Schena, F. P. Role of let-7b in the regulation of N-acetylgalactosaminyltransferase 2 in IgA nephropathy. *Nephrology Dialysis Transplantation* **2015**, *30* (7), 1132-1139

(34) Stamellou, E.; Seikrit, C.; Tang, S. C.; Boor, P.; Tesař, V.; Floege, J.; Barratt, J.; Kramann, R. IgA nephropathy. *Nature Reviews Disease Primers* **2023**, *9* (1), 67

(35) Xie, X.; Gao, L.; Liu, P.; Lv, J.; Lu, W.-H.; Zhang, H.; Jin, J. Propensity of IgA to self-aggregate via tailpiece cysteine-471 and treatment of IgA nephropathy using cysteamine. *JCI insight* **2021**, *6* (19),

(36) Hui, G. K.; Wright, D. W.; Vennard, O. L.; Rayner, L. E.; Pang, M.; Yeo, S. C.; Gor, J.; Molyneux, K.; Barratt, J.; Perkins, S. J. The solution structures of native and patient monomeric human IgA1 reveal asymmetric extended structures: implications for function and IgAN disease. *Biochem J* **2015**, *471* (2), 167-185

(37) Suzuki, H.; Fan, R.; Zhang, Z.; Brown, R.; Hall, S.; Julian, B. A.; Chatham, W. W.; Suzuki, Y.; Wyatt, R. J.; Moldoveanu, Z. Aberrantly glycosylated IgA1 in IgA nephropathy patients is recognized by IgG antibodies with restricted heterogeneity. *The Journal of clinical investigation* **2009**, *119* (6), 1668-1677

(38) Daha, M. R.; van Kooten, C. Role of complement in IgA nephropathy. *Journal of nephrology* **2016**, *29*, 1-4

(39) Rajasekaran, A.; Green, T. J.; Renfrow, M. B.; Julian, B. A.; Novak, J.; Rizk, D. V. Current Understanding of Complement Proteins as Therapeutic Targets for the Treatment of Immunoglobulin A Nephropathy. *Drugs* **2023**, *83* (16), 1475-1499

(40) Le Stang, M.-B.; Gleeson, P. J.; Daha, M. R.; Monteiro, R. C.; van Kooten, C. Is complement the main accomplice in IgA nephropathy? From initial observations to potential complement-targeted therapies. *Molecular Immunology* **2021**, *140*, 1-11

(41) Ding, L.; Chen, X.; Cheng, H.; Zhang, T.; Li, Z. Advances in IgA glycosylation and its correlation with diseases. *Frontiers in chemistry* **2022**, *10*, 974854

(42) Oortwijn, B. D.; van der Boog, P. J.; Roos, A.; Van der Geest, R.; De Fijter, J.; Daha, M.; Van Kooten, C. A pathogenic role for secretory IgA in IgA nephropathy. *Kidney international* **2006**, *69* (7), 1131-1138

(43) Haddad, E.; Moura, I. C.; Arcos-Fajardo, M.; Macher, M.-A.; Baudouin, V.; Alberti, C.; Loirat, C.; Monteiro, R. C.; Peuchmaur, M. Enhanced expression of the CD71 mesangial IgA1 receptor in Berger disease and Henoch-Schönlein nephritis: association between CD71 expression and IgA deposits. *Journal of the American Society of Nephrology* **2003**, *14* (2), 327-337

(44) Kaneko, Y.; Otsuka, T.; Tsuchida, Y.; Gejyo, F.; Narita, I. Integrin α1/β1 and α2/β1 as a receptor for IgA1 in human glomerular mesangial cells in IgA nephropathy. *International immunology* **2012**, *24* (4), 219-232

(45) El Karoui, K.; Fervenza, F. C.; De Vriese, A. S. Treatment of IgA Nephropathy: A Rapidly Evolving Field. *Journal of the American Society of Nephrology : JASN* **2024**, *35* (1), 103-116

(46) Selvaskandan, H.; Shi, S.; Twaij, S.; Cheung, C. K.; Barratt, J. Monitoring immune responses in IgA nephropathy: biomarkers to guide management. *Frontiers in immunology* **2020**, *11*, 572754

(47) Wimbury, D.; Muto, M.; Bhachu, J. S.; Scionti, K.; Brown, J.; Molyneux, K.; Seikrit, C.; Maixnerová, D.; Pérez-Alós, L.; Garred, P. Targeted-release budesonide modifies key pathogenic biomarkers in immunoglobulin A nephropathy: Insights from the NEFIGAN trial. *Kidney international* **2024**, *105* (2), 381-388

(48) Lafayette, R.; Kristensen, J.; Stone, A.; Floege, J.; Tesař, V.; Trimarchi, H.; Zhang, H.; Eren, N.; Paliege, A.; Reich, H. N. Efficacy and safety of a targeted-release formulation of budesonide in patients with primary IgA nephropathy (NefIgArd): 2-year results from a randomised phase 3 trial. *The Lancet* **2023**, *402* (10405), 859-870

(49) Barratt, J.; Tumlin, J.; Suzuki, Y.; Kao, A.; Aydemir, A.; Pudota, K.; Jin, H.; Gühring, H.; Appel, G.; investigators, J. s. Randomized phase II JANUS study of atacicept in patients with IgA nephropathy and persistent proteinuria. *Kidney international reports* **2022**, *7* (8), 1831-1841

(50) Maillard, N.; Wyatt, R. J.; Julian, B. A.; Kiryluk, K.; Gharavi, A.; Fremeaux-Bacchi, V.; Novak, J. Current understanding of the role of complement in IgA nephropathy. *Journal of the American Society of Nephrology* **2015**, *26* (7), 1503-1512

(51) Lafayette, R. A.; Rovin, B. H.; Reich, H. N.; Tumlin, J. A.; Floege, J.; Barratt, J. Safety, tolerability and efficacy of narsoplimab, a novel MASP-2 inhibitor for the treatment of IgA nephropathy. *Kidney international reports* **2020**, *5* (11), 2032-2041

(52) Zhang, H.; Rizk, D. V.; Perkovic, V.; Maes, B.; Kashihara, N.; Rovin, B.; Trimarchi, H.; Sprangers, B.; Meier, M.; Kollins, D. Results of a randomized double-blind placebo-controlled Phase 2 study propose iptacopan as an alternative complement pathway inhibitor for IgA nephropathy. *Kidney international* **2024**, *105* (1), 189-199

(53) Bruchfeld, A.; Magin, H.; Nachman, P.; Parikh, S.; Lafayette, R.; Potarca, A. C5a receptor inhibitor avacopan in immunoglobulin A nephropathy-an open-label pilot study. Clin Kidney J 15 (5): 922–928. 2022.

(54) Lim, R. S.; Yeo, S. C.; Barratt, J.; Rizk, D. V. An Update on Current Therapeutic Options in IgA Nephropathy. *Journal of Clinical Medicine* **2024**, *13* (4), 947

(55) Dotz, V.; Haselberg, R.; Shubhakar, A.; Kozak, R. P.; Falck, D.; Rombouts, Y.; Reusch, D.; Somsen, G. W.; Fernandes, D. L.; Wuhrer, M. Mass spectrometry for

glycosylation analysis of biopharmaceuticals. *TrAC trends in analytical chemistry* **2015**, *73*, 1-9

(56) van Duijl, T. T.; Ruhaak, L. R.; van Kooten, C.; de Fijter, J. W.; Cobbaert, C. M. Multiplex LC-MS/MS testing for early detection of kidney injury: a next-generation alternative to conventional immunoassays? *The Journal of Applied Laboratory Medicine* **2022**, *7* (4), 923-930

(57) de Haan, N.; Wuhrer, M.; Ruhaak, L. R. Mass spectrometry in clinical glycomics: The path from biomarker identification to clinical implementation. *Clin Mass Spectrom* **2020**, *18*, 1-12

Chapter 7

Thesis Summary

Thesis Summary

Protein glycosylation is a post-translational modification where carbohydrates (glycans) are attached to proteins, influencing their stability, function, and immune recognition as outlined in **chapter 1** of this thesis. This process plays a crucial role in cell signaling, inflammatory responses, and disease mechanisms. It offers great potential for disease biomarker discovery. By studying glycomic signatures in patient cohorts and comparing them with groups of healthy controls, the research presented in this thesis aims to enhance disease understanding, and provide leads for diagnostic tools and personalized treatment strategies. This thesis first provides an overview of the glycosylation of twenty-five highly abundant human plasma glycoproteins (**chapter 2**) and then investigates glycosylation changes in inflammatory bowel disease (IBD, **chapter 3** and **chapter 5**) and IgA nephropathy (IgAN, **chapter 4**).

The two major variants of IBD are Crohn's disease (CD) and ulcerative colitis (UC), both chronic inflammatory conditions of the intestinal tract. The exact causes of the diseases remain unknown, and despite available treatments, including medication and surgery, relapses are common, and early differential diagnosis between CD and UC remains challenging as their symptoms often overlap. The distinction between CD and UC is essential because the therapeutic approaches differ. UC is more localized, making surgical removal of the affected area more feasible, while CD can affect multiple areas of the intestine at the same time, limiting surgical treatment options. Current diagnostic techniques may take years to confirm a diagnosis, particularly in young patients, emphasizing the need for more precise and early biomarkers.

The research presented in this thesis focuses on plasma protein glycosylation (**chapter 3)** and immunoglobulin A (IgA) glycosylation (**chapter 5**) as potential biomarkers for distinguishing between these diseases and helping early patient stratification with non-invasive procedures. Lower galactosylation of immunoglobulin G (IgG) is a well-established marker of inflammation and has been strongly associated with both CD and UC. Moreover, alterations in fucosylation and sialylation patterns have been linked to disease severity and progression. Genome studies have also identified changes in genes related to glycosylation enzymes in IBD patients, further highlighting the connection between glycosylation and inflammation. The glycomic studies reported here reveal changes in sialylation, fucosylation, and branching patterns of plasma proteins in IBD patients, associating with disease severity and treatment response. By employing advanced mass spectrometry techniques and robust sample preparation methodology, the thesis

provides novel insights into how glycosylation patterns relate to disease pathophysiology, potentially leading to improved diagnostic tools.

Chapter 3 of the thesis employs high-throughput glycomic analysis using a robotic platform and MALDI-TOF-MS to analyze total plasma *N*-glycosylation in over 3,500 samples, identifying numerous associations with IBD. This large-scale study provides a robust dataset for future research and paves the way for personalized treatment strategies. The thesis then builds upon these findings by investigating glycosylation changes of IgA in IBD, due to its crucial role in mucosal immunity. **Chapter 5** reports new glycomic signatures that may serve as biomarkers for early disease detection and patient stratification.

Another disease approached in **chapter 4** of this thesis is IgA nephropathy. Also called Berger's disease, IgAN is a kidney disorder caused by abnormal glycosylation of IgA, leading to immune complex deposition in the kidneys' glomeruli and progressive renal damage. The disease progresses slowly, and patients may remain asymptomatic for years before experiencing kidney failure. Once kidney function deteriorates significantly, treatment options are limited to dialysis or transplantation. The underlying cause of IgAN remains poorly understood, but it is known that the immune system produces antibodies against abnormally glycosylated IgA, leading to immune complex formation and kidney inflammation. Current diagnostic tools, such as kidney biopsies, are invasive and not practical for routine screening, highlighting the need for non-invasive biomarkers. A major challenge for the clinicians is the lack of non-invasive biomarkers for early detection.

Glycosylation abnormalities in IgAN primarily involve under-galactosylation of IgA1, resulting in galactose-deficient IgA1 (Gd-IgA1), which promotes disease progression. Several lectin-based assays have been used to measure Gd-IgA1 levels, but they suffer from biases due to selective glycan affinities. This thesis addresses this limitation by developing a more precise and higher-resolution analytical method based on mass spectrometry. **Chapter 4** describes this approach, demonstrating that it shows better association with disease severity than the existing methods. This thesis investigates the previously reported glycosylation abnormalities in IgAN, particularly the reported under-galactosylation of *O*-glycans in IgA1, and reports novel *N*-glycosylation signatures of IgAN, with potential for improved IgAN diagnosis and prognosis.

Overall, the research conducted in this thesis employs high-end analytical techniques, including MALDI-TOF-MS (**chapter 3**) and LC-ESI-MS (**chapter 4 and 5**), to study glycosylation patterns in great detail and at a large scale. The automation of high-throughput glycan analysis enables the handling of thousands of patient samples, reducing bias and increasing reproducibility and statistical power, providing

deeper insights into disease mechanisms. A key innovation in this research is the automation of glycan sample preparation. Using robotic platforms, the study ensures consistent sample handling, minimizing technical variability and improving data reliability. For plasma *N*-glycan analysis, a chemical derivatization technique was applied to stabilize sialic acids, facilitating high-throughput analysis of up to 384 samples per MS run (**chapter 3)**. For IgA glycopeptide analysis, an optimized workflow using immobilized camelid antibody domains for IgA capture was developed (**chapter 4 and 5**). This method replaces manual lectin-based approaches, reducing bias and improving scalability.

The findings of this thesis have important biomedical and clinical implications as discussed in **chapter 6**. By mapping disease-specific glycosylation changes, the research contributes to the development of novel biomarkers for IBD and IgAN. The identification of specific glycosylation patterns associated with disease severity and treatment response could enable more precise patient stratification and personalized therapeutic approaches. Moreover, the high-throughput methodologies developed in this research set the stage for future large-scale glycomic studies, potentially leading to new discoveries in other immune-related diseases.

In conclusion, this thesis advances our understanding of glycosylation changes in IBD and IgAN, providing new insights into disease processes. The research highlights the potential of glycomic analysis for improved diagnosis and prognosis in immune-mediated diseases.

Nederlandse samenvatting

Eiwitglycosylering is een post-translationele modificatie waarbij koolhydraten (glycanen) worden gekoppeld aan eiwitten, wat hun stabiliteit, functie en herkenning beïnvloedt, zoals beschreven in **hoofdstuk 1** van dit proefschrift. Dit proces speelt een cruciale rol bij cel-cel communicatie, ontstekingsreacties en ziekteprocessen, en biedt aanzienlijke mogelijkheden voor de ontdekking van *biomarkers* voor ziekten. Door kenmerken van eiwitglycosylering in patiëntencohorten te bestuderen en deze te vergelijken met groepen van gezonde controles, beoogt het onderzoek in dit proefschrift het inzicht in ziekten te verbeteren teneinde aanknopingspunten te leveren voor diagnostische hulpmiddelen en gepersonaliseerde behandelingsstrategieën.

In dit proefschrift wordt een overzicht gegeven van de glycosylering van de vijfentwintig belangrijkste (meest abundante) humane plasma-glycoproteïnen (**hoofdstuk 2**). Vervolgens wordt onderzoek beschreven naar de veranderingen in glycosylering die worden waargenomen bij inflammatoire darmziekte (IBD, **hoofdstuk 3** en **hoofdstuk 5**) en IgA-nefropathie (IgAN, **hoofdstuk 4**). De twee belangrijkste varianten van IBD zijn de ziekte van Crohn (CD) en colitis ulcerosa (UC), beide chronische ontstekingsaandoeningen van het darmkanaal. De precieze oorzaken van deze ziekten zijn nog onbekend en ondanks beschikbare behandelingen, waaronder medicatie en chirurgie, komen terugvallen vaak voor. Bovendien is een vroege differentiële diagnose tussen CD en UC een uitdaging, aangezien de symptomen deels hetzelfde zijn. Het is van essentieel belang CD en UC te kunnen onderscheiden, omdat de therapeutische benaderingen verschillen. UC is meer lokaal, waardoor chirurgische verwijdering van het aangetaste gebied beter mogelijk is, terwijl CD meerdere gebieden van de darm tegelijkertijd kan aantasten, wat chirurgische behandelingen beperkt. De huidige diagnostische technieken zijn beperkt en het kan jaren duren voordat een diagnose is gesteld, vooral bij jonge patiënten, wat het belang benadrukt van preciezere en vroegtijdige *biomarkers*.

Het onderzoek dat in dit proefschrift wordt beschreven richt zich op plasma-eiwitglycosylering (**hoofdstuk 3**) en immunoglobuline A (IgA) glycosylering (**hoofdstuk 5**) als mogelijke *biomarkers* die onderscheid kunnen maken tussen deze ziekten en daarmee helpen bij vroege patiëntstratificatie via niet-invasieve procedures. Lagere galactosyleringsniveaus van immunoglobuline G (IgG) worden als marker van ontsteking toegepast bij zowel CD als UC. Bovendien zijn veranderingen in fucosylering- en sialyleringspatronen gekoppeld aan de ernst en progressie van de ziekte. Daarnaast zijn er in genoomstudies veranderingen geïdentificeerd in genen die coderen voor glycosyleringsenzymen bij IBD-patiënten, wat de verbinding tussen glycosylering en ontsteking verder benadrukt.

De eiwitglycosyleringsstudies die hier worden gerapporteerd onthullen veranderingen in sialylering, fucosylering en complexiteit in plasma-eiwitten bij IBD-patiënten, die verband houden met de ernst van de ziekte en de respons op behandeling. Door gebruik te maken van geavanceerde massaspectrometrie technologie en robuuste methoden voor monstervoorbewerking biedt dit onderzoek nieuwe inzichten in hoe glycosyleringspatronen verband houden met ziektefysiologie, wat kan leiden tot verbeterde diagnostische hulpmiddelen. **Hoofdstuk 3** van dit proefschrift maakt gebruik van *high-throughput* eiwitglycosyleringsanalyse met een robotplatform en een zogenaamde MALDI-TOF massaspectrometer om de totale plasma *N*-glycosylering in meer dan 3.500 monsters in kaart te brengen, waarbij talrijke associaties met IBD worden geïdentificeerd. Deze grootschalige studie biedt een robuuste dataset voor toekomstig onderzoek en effent het pad voor gepersonaliseerde behandelingsstrategieën.

Vervolgens worden deze resultaten verder geëvalueerd door glycosyleringsveranderingen van IgA bij IBD te onderzoeken, vanwege de cruciale rol van IgA in mucosale immuniteit. **Hoofdstuk 5** rapporteert nieuwe kenmerken van eiwitglycosylering die mogelijk kunnen dienen als *biomarkers* voor vroege ziektedetectie en patiëntstratificatie.

Een andere aandoening die in **hoofdstuk 4** van dit proefschrift wordt beschreven betreft IgA-nefropathie, ook bekend als de ziekte van Berger. IgAN is een nieraandoening die wordt veroorzaakt door abnormale glycosylering van IgA, wat leidt tot de vorming van immuuncomplexen in de glomeruli van de nieren en progressieve nierbeschadiging. De ziekte vordert langzaam, en patiënten kunnen jarenlang asymptomatisch blijven voordat ze nierfalen ervaren. Echter, wanneer de nierfunctie eenmaal verslechtert zijn de behandelingsopties beperkt tot dialyse of transplantatie. De onderliggende oorzaak van IgAN is slecht begrepen, maar het is bekend dat het afweersysteem antilichamen produceert tegen abnormaal geglycosyleerd IgA, wat leidt tot immuuncomplexvorming en nierontsteking.

Huidige diagnostische hulpmiddelen, zoals nierbiopten, zijn invasief en niet praktisch voor routinematige screening, wat de noodzaak benadrukt van niet-invasieve *biomarkers*. Het gebrek aan niet-invasieve biomarkers voor vroegdetectie vormt een belangrijke uitdaging voor clinici. Glycosyleringsafwijkingen bij IgAN betreffen voornamelijk lagere galactosyleringsniveaus van IgA1, wat resulteert in galactose-deficiënt IgA1 (Gd-IgA1), dat de ziekteprogressie bevordert. Verschillende lectine-gebaseerde assays zijn gebruikt om Gd-IgA1-niveaus te meten, echter zulke methoden zijn van beperkte waarde door selectieve glycaan-affiniteiten.

Dit proefschrift behandelt deze beperking door een nauwkeurigere en hoge-resolutie analytische methode te ontwikkelen op basis van massaspectrometrie. **Hoofdstuk 4** beschrijft deze aanpak en toont aan dat deze een betere associatie met de ernst van de ziekte vertoont dan de bestaande methoden. Dit proefschrift onderzoekt de eerder gerapporteerde glycosyleringsafwijkingen bij IgAN, met name de gerapporteerde verlaagde galactosyleringsniveaus van *O*-glycanen in IgA1, en rapporteert nieuwe *N*-glycosyleringskenmerken van IgAN, met mogelijkheden voor verbeterde diagnose en prognose van IgAN.

Over het algemeen wordt in het onderzoek dat in dit proefschrift wordt beschreven gebruik gemaakt van geavanceerde analytische technieken, waaronder MALDI-TOF-MS (**hoofdstuk 3**) en LC-ESI-MS (**hoofdstuk 4** en **hoofdstuk 5**), om glycosyleringspatronen op grote schaal te bestuderen. De automatisering van *high-throughput* glycaananalyse maakt de verwerking van duizenden patiëntmonsters mogelijk, vermindert bias, verhoogt de reproduceerbaarheid en statistische kracht, en biedt diepere inzichten in ziekteprocessen.

Een belangrijke innovatie in dit onderzoek is de automatisering van de voorbewerking van glycaanmonsters. De inzet van robotplatforms geeft deze studie een consistente monstervoorbewerking, wat technische variabiliteit minimaliseert en de betrouwbaarheid van gegevens verbetert. Voor plasma *N*-glycaananalyse wordt een chemische derivatisatietechniek toegepast die siaalzuren stabiliseert, waarmee analyse van maximaal 384 monsters per MS-run wordt vereenvoudigd (**hoofdstuk 3**). Voor IgA-glycopeptidenanalyse wordt een geoptimaliseerde workflow ontwikkeld met geïmmobiliseerde kameelachtige antilichaamdomeinen voor IgA-invang (**hoofdstuk 4** en **hoofdstuk 5**). Deze methode vervangt handmatige lectine-gebaseerde benaderingen, vermindert bias en verbetert schaalbaarheid.

De bevindingen beschreven in dit proefschrift hebben belangrijke biomedische en klinische implicaties, zoals besproken in **hoofdstuk 6**. Door ziekte-specifieke glycosyleringsveranderingen in kaart te brengen, draagt het onderzoek bij aan de ontwikkeling van nieuwe *biomarkers* voor IBD en IgAN. De identificatie van specifieke glycosyleringspatronen die verband houden met de ernst van de ziekte en de respons op behandeling kan meer precieze patiëntstratificatie en gepersonaliseerde therapeutische benaderingen mogelijk maken ("zorg op maat").

Bovendien vormen de ontwikkelde *high-throughput* methoden in dit onderzoek de basis voor toekomstige grootschalige eiwitglycosyleringsstudies, die mogelijk leiden tot nieuwe ontdekkingen bij andere immuun-gerelateerde aandoeningen.

Kortom, door het onderzoek dat is beschreven in dit proefschrift verbetert ons begrip van glycosyleringsveranderingen bij IBD en IgAN en worden nieuwe inzichten

in ziekteprocessen verkregen. De resultaten laten het potentieel zien van eiwitglycosyleringsanalyse voor verbeterde diagnostiek en prognose bij immunologische ziekten.

Chapter 8

Acknowledgements

Chapter 9

Curriculum Vitae

Chapter 10

Published Articles

Acknowledgements

I am deeply grateful to all those who contributed to the completion of this thesis. I could not have done it without you.

Manfred, I greatly appreciate your unwavering support over the years, including during the period when I was no longer at LUMC. Your persistence and encouragement were decisive in bringing this work to completion.

Viktoria, your critical perspective and insightful guidance greatly strengthened the scientific rigor and clarity of the articles included in this thesis. Your input was invaluable in shaping the outcome.

Karli, thank you. You played a key role in introducing me to the principles of coding for automated scientific data processing and for the many stimulating theoretical discussions we shared that sharpened my critical thinking. Those skills remained highly relevant in my personal and professional life.

Noortje, our collaboration on numerous projects combined with the enjoyable experiences at and outside the LUMC added both scientific and personal enrichment to this journey.

Agnes, Carolien, your expertise in operating instruments and generating essential data provided the foundation upon which this thesis was built. Your precision and reliability were indispensable.

Guinevere, Rosina, Bas, Albert, and David. I am thankful to you all for the time and effort you dedicated to working with me on all those projects. I greatly benefited from your unique expertise.

I am deeply grateful to my parents for their continuous support, especially during my move to the Netherlands. Your encouragement and trust have been essential to the completion of this PhD.

To everyone who played a part in this work and made this accomplishment possible, thank you.

Curriculum Vitae

My name is Florent Clerc, and I come from Geneva in Switzerland. I am an analytical scientist by training and mindset. In 2007, I completed my secondary education at Collège de Saussure in Geneva, specializing in chemistry and physics. Following this, I pursued a Bachelor's degree in chemistry and later a Master's degree focused on industrial processes, as well as analytical and computational chemistry at the University of Geneva. After completing my Master in 2012, I undertook two six-month internships at the University of Geneva's School of Pharmacy. These internships allowed me to deepen my expertise in mass spectrometry, which remains my preferred analytical technique.

In 2013, I embarked on a doctoral journey at Leiden University Medical Center in the Netherlands under the guidance of Professor Dr. Manfred Wuhrer and Dr. Viktoria Dotz. My PhD research concentrated on identifying biomarkers for inflammatory bowel disease and IgA nephropathy. After I completed the usual four-year duration for my thesis, several research articles remained unpublished. Subsequently, I worked at ThermoFisher as a GC-MS specialist and later joined International Flavors & Fragrances (IFF) as a research investigator in the perfume industry. At IFF, I applied various chromatography and mass spectrometry techniques to analyze and decode competitors' fragrances.

In 2020, I returned to Switzerland to take up a role at Biogen, where I currently work as an analytical expert. My responsibilities involve overseeing the analysis of raw materials and drug substances at the production facility in Solothurn. Concurrently, I have been steadily working to finalize and publish my remaining PhD research articles, in order to formally submit my thesis to the doctoral committee

.

Published Articles

*Clerc, F., Reiding, K. R., de Haan, N., Koeleman, C. A. M., Hipgrave Ederveen, A. L., Manetti, N., Dotz, V., Annese, V., Wuhrer, M., Immunoglobulin a Glycosylation Differs between Crohn's Disease and Ulcerative Colitis. *Journal of Proteome Research* **2023,** *22* (10), 3213-3224.

*Dotz, V.[†], Visconti, A.[†], Lomax-Browne, H.[†], Clerc, F.[†], Ederveen, A. H., Medjeral-Thomas, N., Cook, H. T., Pickering, M., Wuhrer, M., Falchi, M., *O*-and *N*-Glycosylation of Serum Immunoglobulin a Is Associated with IgA Nephropathy and Glomerular Function. *Journal of the American Society of Nephrology* **2021,** *32* (10), 2455-2465.

Šimurina, M.[†], de Haan, N.[†], Vučković, F.[†], Kennedy, N.A., Štambuk, J., Falck, D., Trbojević-Akmačić, I., Clerc, F., Razdorov, G., Khon, A., Latiano, A., D'Incà, R., Danese, S., Targan, S., Landers, C., Dubinsky, M., IBD-BIOM consortium, McGovern, D.P.B., Annese, V., Wuhrer, M., Lauc, G., Glycosylation of Immunoglobulin G Associates with Clinical Features of Inflammatory Bowel Diseases. *Gastroenterology* **2018,** *154* (5), 1320-1333.

*Clerc, F.[†], Novokmet, M.[†], Dotz, V.[†], Reiding, K. R., de Haan, N., Kammeijer, G. S., Dalebout, H., Bladergroen, M. R., Vukovic, F., Rapp, E., IBD-BIOM Consortium, Targan, S.R., Barron, G., Manetti, N., Latiano, A., McGovern, D.P.B., Annese, V., Lauc, G., Wuhrer, M., Plasma *N*-Glycan Signatures Are Associated with Features of Inflammatory Bowel Diseases. *Gastroenterology* **2018**, 155 (3), 829-843.

*Clerc, F., Reiding, K. R., Jansen, B. C., Kammeijer, G. S. M., Bondt, A., Wuhrer, M., Human Plasma Protein *N*-Glycosylation. *Glycoconjugate Journal* **2016**, 33 (3), 309-43.

Bladergroen, M. R., Reiding, K. R., Hipgrave-Ederveen, A. L., Vreeker, G. C., Clerc, F., Holst, S., Bondt, A., Wuhrer, M., van der Burgt, Y. E., Automation of High-Throughput Mass Spectrometry-Based Plasma *N*-Glycome Analysis with Linkage-Specific Sialic Acid Esterification. *Journal of Proteome Research* **2015**.

Porus, M., Clerc, F., Maroni, P. and Borkovec, M., Ion-Specific Responsiveness of Polyamidoamine (Pamam) Dendrimers Adsorbed on Silica Substrates. *Macromolecules* **2012**, 45 (9), 3919-3927.

*First authors and shared first author ([†]) articles used in the thesis manuscript *Glycomic Markers of Inflammatory Bowel Disease and IgA Nephropathy*